
TGF- β 1 and WNT5A Functional Crosstalk and its Role in Asthmatic Epithelial Repair

Thesis Submitted for the Degree of
Doctor of Philosophy
at the University of Leicester

by

Sheree Roberts

**Department of Respiratory Sciences,
University of Leicester
September 2021**

ABSTRACT

TGF- β 1 and WNT5A Functional Crosstalk and its Role in Asthmatic Epithelial Repair ~ Sheree Roberts

BACKGROUND

The epithelium is the first line of defence against inhaled pathogens, but it is found to be damaged and dysfunctional in asthma. This may predispose the airways to persistent inflammation that may drive airway remodelling. WNT5A and TGF- β 1 signalling are vital for lung development, and evidence suggests they may be reinstated in airway repair. Crosstalk between WNT5A and TGF- β 1 is evident in other cell types but is yet to be elucidated in the airway epithelium. Delineating this signalling crosstalk may further understanding of the repair process to provide tractable targets for new asthma therapies.

METHODS

This study sought to evaluate the impact of WNT5A and TGF- β 1 (alone or synergistic) on (1) epithelial repair in BEAS-2Bs and differentiated human bronchial epithelial cells (HBECs) and (2) epithelial-mesenchymal transition (EMT) induction and SMAD2/3 phosphorylation, which have been identified as WNT5A-TGF- β 1 crosstalk mechanisms in other cell types. The use of bulk transcriptional profiling in epithelial cells from moderate-severe asthmatic patients was used to identify potential mechanistic avenues to explore in the experimental *in vitro* models.

RESULTS

We found neither WNT5A nor TGF- β 1 stimulation alone had a significant effect on wound healing, however TGF- β 1 signalling was found to have a significant effect on WNT5A-mediated wound closure. Crosstalk however was not evident on EMT induction or SMAD2/3 phosphorylation. The bulk gene expression profiling analysis in moderate-severe asthmatic patients also failed to demonstrate an association between WNT and TGF- β signalling and airflow obstruction (a clinical surrogate marker of airway remodelling) in asthma.

DISCUSSION

This PhD does not support a role for WNT5A or TGF- β 1 in HBEC repair, but it does suggest that negative WNT5A-TGF- β 1 crosstalk may exist in HBECs. Further investigation is needed to confirm these findings.

STATEMENT OF WORK PERFORMED

Professor Salman Siddiqui, Professor Peter Bradding and the Biomedical Respiratory Centre nurses recruited and performed patient clinical assessments and bronchoscopies. Bronchoscopies were attended by me to assist in sample collection.

Dr Robert Hirst and his team cultured primary human bronchial epithelial cells to air-liquid interface on my behalf. All samples were transported by myself to their facility and all phenotyping experiments, TEER and functional experiments were performed by me.

Dr Matthew Richardson performed all advanced statistical tests requiring R. He therefore performed the two-way and three-way repeated measures Aligned ranks transformation ANOVA. Furthermore, Dr Matthew Richardson also assisted in the eigengene network analysis of the transcriptomics results chapter as detailed in section 3.12.4. All other statistical tests were performed by myself using Prism.

ACKNOWLEDGEMENTS

Firstly, I would like to thank my supervisors Professor Salman Siddiqui and Professor David Cousins for their support and guidance throughout my project. I would also like to thank Matt Richardson for all his stats advice and contribution to the data analysis when advanced statistics was required. Additionally, I would like to thank existing and past PhD students and Post docs for all their assistance and knowledge that has helped me in the acquisition of the data for this thesis (particularly Amanda, Ruth, Davinder, Adam, Michael, Kat and Jamie), including Tariq Daud, who was the predecessor for this project that was studied in epithelial cell lines. I want to personally thank my PRP panel members Yassine Amrani and Peter Bradding for their advice throughout this project, and everyone involved in arranging and providing me with bronchoscopy samples, with special thanks to Salman, Pete, Bev, Pam and Sue. A huge thank you to Rob Hirst and Gwyneth Williams for their help in providing me with cultured human bronchial epithelial cells and teaching me how to record ciliary beat frequency. Not worrying about culture success definitely took the pressure off and allowed me to focus on my functional experiments.

Last but not least, I owe thanks to my husband for supporting my ambitions and believing that I can achieve them, and for being understanding about all the late nights I spent in the lab. Sending love to my family for their unconditional love and support that kept me going when the going got tough.

PUBLICATIONS AND PRESENTATIONS SUBMITTED USING DATA FROM THIS THESIS

Publication: Tariq Daud*, **Sheree Roberts***, Amanda Sutcliffe, Matthew Richardson, Yassine Amrani, Peter Bradding, and Salman Siddiqui. The role of WNT5a and TGF- β 1 in asthmatic airway remodelling and epithelial repair (in preparation) *denotes equal first author contribution.

Abstract and Presentation: TGF- β and WNT5A crosstalk and its role in asthmatic epithelial repair

Sheree Roberts

11th Annual Postgraduate Student Conference, 1st April 2019, University of Leicester

Presentation: TGF- β and WNT5A crosstalk and its role in asthmatic epithelial repair

Sheree Roberts

Joint LISCB/LPMI-Respiratory Day, 4th April 2019, University of Leicester

CONTENTS

LIST OF TABLES.....	xiii
LIST OF FIGURES.....	xv
1 INTRODUCTION	1
1.1 What is Asthma?.....	1
1.2 Asthmatic Phenotypes	1
1.3 Asthmatic Endotypes	3
1.4 Managing Asthma According to International Guidelines.....	3
1.5 Asthma Treatments.....	4
1.6 Structure and Function of the Airways	5
1.7 The Bronchial Airway Epithelium	6
1.7.1 Physical Barrier Function of Airway Epithelium	7
1.7.2 Chemical Barrier Function of Airway Epithelium.....	8
1.7.3 Immunological Barrier Function of Airway Epithelium.....	10
1.8 Epithelial Barrier Repair in Allergy and Asthma	11
1.8.1 Epithelial Barrier Dysfunction and Airway Remodelling in Asthma	11
1.8.2 The Epithelial Mesenchymal Trophic Unit	15
1.8.3 Epithelial Damage and Dysregulated Repair in Asthma	16
1.9 Normal Airway Epithelial Repair.....	17
1.9.1 The Tissue-specific Stem Cell	17
1.9.2 Basal Cell Renewal and Proliferation	18
1.9.3 Basal Cell Differentiation	19
1.9.4 Cellular Migration into the Wound Bed	20
1.9.5 Summary of the Airway Wound Healing Process	21
1.10 Epithelial Repair Pathways	22
1.10.1 WNT Signalling.....	22

1.10.2	TGF- β Signalling	26
1.11	Evidence of WNT5A and TGF- β 1 Roles in Asthma Development and Repair	29
1.11.1	WNT5A and TGF- β 1 in Lung Development.....	29
1.11.2	Genetic Associations Between WNT5A, TGF- β 1 and Asthma Susceptibility.....	29
1.11.3	Associations Between WNT5A and Inflammatory Signatures in Asthma	30
1.11.4	Associations Between TGF- β 1 and Inflammatory Signatures in Asthma	31
1.11.5	Evidence of WNT5A in Epithelial Repair	31
1.11.6	Evidence of TGF- β 1 in Epithelial Repair.....	32
1.12	Evidence of WNT5A and TGF- β 1 Crosstalk	33
1.12.1	Dual Expression of WNT5A and TGF- β 1.....	33
1.12.2	TGF- β 1 Transcriptional Regulation of WNT5A Expression	33
1.12.3	Hypothetical WNT and TGF- β Crosstalk in Asthmatic Airway Epithelium.....	34
1.13	What is Signalling Crosstalk?	37
1.14	Therapies Targeting Airway Epithelial Repair.....	39
1.14.1	Effects of Conventional Asthma Therapeutics on Airway Epithelial Repair	39
1.14.2	WNT5A and TGF- β 1 Targeting Drugs on the Market or in the Pipeline which could be Repurposed as a Therapy for Airway Epithelial Repair	40
1.14.3	Effects of Conventional Asthma Therapeutics on WNT and TGF- β Signalling.....	41
1.15	Epithelial Cell Models	42
1.15.1	In Vivo	42
1.15.2	In Vitro.....	43

1.16	Hypothesis	47
1.17	Aims and Objectives	47
2	METHODS	48
2.1	Patient Clinical Characteristics.....	48
2.2	Bronchoscopy Sample Retrieval	48
2.3	Cell Culture	49
2.3.1	BEAS-2B Cells	49
2.3.2	Establishment of Human Bronchial Epithelial Cell ALI Cultures ...	49
2.3.3	Human Bronchial Epithelial Cell Culture	49
2.3.4	Immortalised Human Bronchial Epithelial Cell Culture	51
2.3.5	HEK293T Cell Culture	51
2.4	Transepithelial Electrical Resistance (TEER).....	51
2.5	Reconstituting BOX-5, Takinib and Recombinant Proteins for WNT5A and TGF- β 1	52
2.6	Selecting the Cell Signalling Pathway Inhibitors	53
2.6.1	BOX-5.....	53
2.6.2	Takinib.....	53
2.7	MTS	54
2.8	Development of ALI Scratch Wound Technique	56
2.9	Scratch Wound Assay Investigating the Effect of TGF- β 1 on Wound Healing.....	60
2.10	Scratch Wound Assay Investigating the Effect of TGF- β 1 and WNT5A With and Without the Presence of Inhibitors on Wound Healing	61
2.10.1	Scratch Wound Assay Analysis Plan.....	62
2.11	Transfection of ALI cultures and HEKS with Transfection Reagents	64
2.12	Transcriptomic Analysis	64
2.12.1	Cohort Discovery	64
2.12.2	Module Identification.....	65

2.12.3	Eigengene Network Analysis	68
2.12.4	Module Discovery Literature Review	68
2.12.5	How the Module Discovery Literature Review Shaped the Study Hypothesis.....	74
2.13	Gene Expression Analysis	75
2.13.1	BEAS-2B qRT-PCR.....	75
2.13.2	iHBEC qRT-PCR	76
2.13.3	PCR Data Analysis.....	78
2.14	Immunofluorescence	78
2.14.1	Image Analysis for Immunofluorescence	81
2.15	Developing the Flow Cytometry Panels	82
2.15.1	Selecting the Antibodies for the Basal Cell Antibody Panel.....	82
2.15.2	Antibody Titrations.....	87
2.15.3	Antibody Specificity Testing.....	90
2.16	Flow Cytometry.....	93
2.16.1	Preparing Single Cell Suspensions from Biopsies.....	93
2.16.2	Basal Cell Phenotyping	93
2.16.3	EMT Marker Expression With and Without Stimulation	94
2.16.4	WNT Receptor Phenotyping.....	96
2.16.5	pSMAD2/3 Expression	96
2.17	WNT5A Antibody Validation.....	97
2.17.1	Assessing the Literature for WNT5A Antibody Validation.....	97
2.17.2	Using Cloning to Produce a Positive Control.....	100
2.17.3	WNT5A Antibody Validation: Antibody Testing for Western Blot	120
2.17.4	WNT5A Antibody Validation: Antibody Testing for ICC	122
2.17.5	WNT5A Antibody Validation: Antibody Testing for Flow Cytometry	126

2.17.6	Antibody Validation Summary of Outcomes and Method Limitations	129
2.18	Analysis	130
3	ASSOCIATIONS BETWEEN WNT AND TGF- β TRANSCRIPTIONAL REPAIR MODULES, AIRFLOW OBSTRUCTION AND INFLAMMATORY PROFILES	131
3.1	Introduction	131
3.2	Methods	132
3.3	Results	132
3.3.1	The SARP and U-BIOPRED Cohorts	132
3.3.2	Correlation between FEV ₁ /FVC and TH Status and the Transcriptional Module Scores for the SARP and U-BIOPRED Cohorts .	133
3.4	Discussion.....	136
3.4.1	Transcriptional Module Association with Pre-BD FEV ₁ /FVC and TH Status	136
3.4.2	Limitations	137
4	EVALUATING WNT5A & TGF- β 1 WOUND HEALING IN DIFFERENTIATED HUMAN BRONCHIAL EPITHELIAL CELL CULTURES.....	139
4.1	Chapter Overview	139
4.2	Evaluating the Effects of WNT5A Inhibitor BOX-5 and Non-Canonical TGF- β Inhibitor Takinib on the Viability of Immortalised Human Bronchial Epithelial Cells	140
4.3	Assessing ALI Culture Wound Healing With and Without TGF- β 1 Stimulation	141
4.4	Assessing ALI Culture Wound Healing of TGF- β 1 Pre-Stimulated Cultures With and Without the Presence of Takinib.....	145
4.5	Assessing the Effect of WNT5A on ALI Culture Wound Healing With and Without TGF- β 1 Pre-Stimulation	149

4.6 Overall Effect of Takinib and TGF- β 1 on WNT5A-Mediated Wound Healing at 24 Hours	152
4.7 Overall Effect of All Stimulation Conditions on Wound Healing at 24 Hours	153
4.8 Exploring Transfection Efficiency of ALI Cultures	155
4.9 Summary.....	157
4.10 Discussion	158
4.10.1 The Wound Healing Response to WNT5A and TGF- β 1	158
4.10.2 The TEER Response to WNT5A and TGF- β 1	164
4.10.3 Limitations	166
5 INVESTIGATING SMAD2/3 AND TAK1 AS CROSSTALK INTERMEDIARIES BETWEEN TGF-β1 AND WNT5A IN EPITHELIAL WOUND HEALING AND EMT	169
5.1 Chapter Overview	169
5.2 Effect of TGF- β 1 Stimulation on WNT5A and TGF- β Associated Gene Expression in BEAS-2Bs and iHBECs.....	169
5.3 TGF- β 1 Stimulation Effect on WNT5A Receptor Expression in BEAS-2Bs and HBECs.....	173
5.4 Effect of TGF- β 1 and WNT5A Stimulation on EMT Induction in BEAS-2B Cells	174
5.5 Effect of TGF- β 1 and WNT5A Stimulation on EMT Induction in HBEC ALI Cultures	179
5.6 Effect of TGF- β 1 and WNT5A Stimulation on SMAD2/3 Phosphorylation in HBECs.....	182
5.7 Overall Effect of Takinib and TGF- β 1 on WNT5A-Mediated SMAD2/3 Phosphorylation	185
5.8 Overall Effect of TGF- β 1, WNT5A and Takinib on SMAD2/3 Phosphorylation	186
5.9 Summary.....	188

5.10	Discussion	188
5.10.1	TGF- β 1 Effect on WNT5A mRNA.....	188
5.10.2	TGF- β 1 Effect on WNT Receptor Expression.....	189
5.10.3	TGF- β 1 and WNT5A Effect on EMT in BEAS-2Bs and Differentiated HBECs.....	190
5.10.4	WNT5A Effect on SMAD2/3	193
6	OVERALL DISCUSSION	196
6.1	Further Work.....	198
6.2	Conclusion	200
7	APPENDIX.....	202
7.1	APPENDIX 1.....	202
7.2	APPENDIX 2.....	203
7.3	APPENDIX 3.....	204
7.4	APPENDIX 4.....	205
7.5	APPENDIX 5.....	231
7.6	APPENDIX 6.....	232
7.7	APPENDIX 7.....	233
7.8	APPENDIX 8.....	234
7.9	APPENDIX 9.....	235
8	REFERENCES	236

LIST OF TABLES

Table 2.1 Inhibitor Concentrations Tested in the MTS Assay	55
Table 2.2 Transcriptomic Module Analysis Gene Grouping	66
Table 2.3 Crosstalk Intermediaries Identified Between WNT, TGF-β and Notch Signalling	72
Table 2.4 Constituents of the WNT5A TaqMan Mastermix	78
Table 2.5 Immunofluorescence Antibody Concentration Table	80
Table 2.6 Antibody Panel List Used For Flow Cytometry	86
Table 2.7 List of Additional Flow Cytometry Reagents	86
Table 2.8 Basal Cell Phenotyping Antibody Panel	94
Table 2.9 EMT Phenotyping Antibody Panel	95
Table 2.10 WNT Receptor Phenotyping Antibody Panel	96
Table 2.11 Publications Containing WNT5A IHC Staining of Lung Tissue. Where information was not available in the literature, N/A is given. Discrepancy in information in literature to vendor website for the catalogue number given is shown in bold. The host is goat not rat on the Santa Cruz website.	98
Table 2.12 Primer Sequences Used For Amplifying the Plasmid Sequence	104
Table 2.13 Plasmid PCR Mastermix Constituents	105
Table 2.14 WNT5A Screening PCR Mastermix Constituents	111
Table 2.15 WNT5 Sequencing Primers	112
Table 2.16 WNT5A and WNT5B Plasmid DNA Nucleic Acid Concentrations	112
Table 2.17 Antibodies Used for Western Blot	121
Table 2.18 Antibodies Used for Immunohistochemistry. The greyed out 6F2 antibody concentration was used solely as a stock dilution and was not used for staining.	124
Table 3.1 Clinical Characteristics Table of the Transcriptional Cohorts. All characteristics are presented mean with standard deviation unless otherwise stated. With partial clinical information available for some characteristics, the number of patients contributing to the characteristic statistical analysis is presented as ⁽ⁿ⁾ . Lung function test results reported are pre-bronchodilator (Pre-BD). All tests were a Wilcoxon rank sum test, except for GINA treatment intensity and sex (a Chi-square test).	133
Table 3.2 Correlation of Transcriptomic Modular Scores With Pre-Bronchodilator FEV₁/FVC and TH Status. Pearson correlation, <i>r</i> , was assessed between pre-bronchodilator FEV ₁ /FVC ratio (%), TH2 and TH17 status and the modular scores of the six transcriptomic modules.	135
Table 4.1 Clinical Details of the Healthy Subjects Used in the TGF-β1 Stimulation Experiments.	142
Table 4.2 Clinical Details of the Asthmatic Subjects Used in the TGF-β1 and WNT5A Wounding Experiments. Data not available is indicated as N/A.	146

Table 5.1 ANOVA Summary Table for Basal Cell and EMT Marker Expression Before and After rhWNT5A and rhTGF-β1 Stimulation in ALI Cultures. Data summarised is n=4 (3 asthmatic, 1 healthy) for rhTGF- β 1 and n=3 for rhWNT5A (2 asthmatic, 1 healthy).	180
Table 7.1 List of Reagents Used for Cell Culture	202
Table 7.2 Transfection Methods for All Transfection Reagents Tested on ALI Cultures and HEK293T Cell Cultures	204
Table 7.3 Genes Included in the Canonical WNT Transcriptional Module, With Rationale of Inclusion in the Module	205
Table 7.4 Genes Included in the Non-Canonical WNT Transcriptional Module, With Rationale of Inclusion in the Module	209
Table 7.5 Genes Included in the Canonical TGF-β Transcriptional Module, With Rationale of Inclusion in the Module	213
Table 7.6 Genes Included in the Non-Canonical TGF-β Transcriptional Module, With Rationale of Inclusion in the Module	215
Table 7.7 Genes Included in the WNT TGF-β Overlap Transcriptional Module, With Rationale of Inclusion in the Module	218
Table 7.8 Genes Included in the WNT Notch TGF-β Overlap Transcriptional Module, with Rationale of Inclusion in the Module	226
Table 7.9 RT² Profiler PCR Array Gene List	231
Table 7.10 Constituents of the PCR Mastermix	232

LIST OF FIGURES

- Figure 1.1 Diagram of the Epithelial Cell-Cell Junctions.** Created with BioRender.com 8
- Figure 1.2 Structural Changes Within the Bronchial Airways Between Asthma and Health**
Created with BioRender.com 13
- Figure 1.3 The Airway Wound Healing Response Labelled with Key Epithelial Repair Pathways Roles.** Following wounding to the airway epithelium, TGF- β activation induces fibroblast secretion of ECM and induces cells proximal to the wound edge to dedifferentiate and undergo EMT. The newly synthesised ECM provides a matrix for the cells to migrate into the wound bed, however, the ECM may also need to be degraded en route to the area of repair. The gene transcription of MMPs and plasminogen, ECM proteolytic enzymes, are regulated by noncanonical WNT signalling. Noncanonical WNT PCP signalling also mediates the polarised migration of the cells into the wound bed. Once the wound bed is fully covered, the basal cells, the known progenitor cell of the tracheobronchial epithelium, can regenerate the luminal cells that were shed or destroyed by inflammation. Basal cell renewal and proliferation appears to be regulated by β -catenin dependent canonical WNT signalling, and cell differentiation is mediated by Notch. A sustained notch signal promotes differentiation into secretory cells, whereas reduced notch signalling induces differentiation into a ciliated cell fate. The newly synthesised and differentiated daughter cells can then form cell-cell adhesion junctions with neighbouring epithelial cells to restore epithelial barrier function. Created with BioRender.com. 22
- Figure 1.4 WNT Signalling Pathways.** Created with BioRender.com. 25
- Figure 1.5 TGF- β Signalling Pathways.** Created with BioRender.com. 28
- Figure 1.6 TGF- β -TAK1 Induced WNT5A Expression in Airway Smooth Muscle Cells.**
Created with BioRender.com 35
- Figure 1.7 Wounding to the Epithelium Initiates Numerous Cell Signalling Cascades.** Severing of integrins (through mechanical stress) activates and initiates latent TGF- β proximal to the wound site. Disruption of adherens junctions leads to a β -catenin feed into the canonical WNT pathway, and exposure of basal cells to air initiates Notch signalling (and thus cellular differentiation). TGF- β 1 sequesters canonical WNT signalling via NLK but promotes transcription of noncanonical WNT WNT5A directly through canonical TGF- β -SMAD signalling and indirectly through noncanonical TGF- β -TAK1 signalling. Whilst doing this, TGF- β induces EMT in the proximal cells. The induced WNT5A promotes cellular migration and organisation of the regenerating epithelium. Through signalling through PKC, WNT5A can sequester canonical WNT signalling (through phosphorylation of β -catenin). Created with BioRender.com 36
- Figure 1.8 Hypothetical WNT5A and TGF- β 1 Signalling Crosstalk** 38
- Figure 2.1 Culturing to ALI Methodology.** Cells are first expanded in flasks, then seeded in transwells and left overnight to adhere and then the apical fluid is removed exposing the cells to an air-liquid interface. 51

Figure 2.2 Effects of Takinib (A) and BOX-5 (B) Comparative to Basal Conditions on Metabolic Activity in Immortalised Human Bronchial Epithelial Cells. Stimulants were applied for 48 hours. Data is n=3 and presented as mean with standard deviation. *p < 0.05 by One-way ANOVA with Dunnett's post hoc test for intergroup comparisons. **** is p-value of <0.0001.	56
Figure 2.3 Transwell Scratch Wound Assay Optimisation with BEAS-2Bs Cultured on the Transwell Membrane. (A-B) Representative BEAS-2B scratch wound images at 0 (A) and 37 hours (B) for the same condition. (C) Summary figure of BEAS-2B optimisation scratch wound assay without stimulation and following stimulation with both rhTGF- β 1 (10ng/ml) and rhWNT5A (1 μ g/ml) alone and in combination. Data is n=3, and presented mean with standard deviation. Data was acquired over 37 hours, but data is only shown for every 4 hours post-wounding so error bars could be visibly differentiated.	57
Figure 2.4 Macro Selection of a Representative BEAS-2B Scratch Wound Assay Image.	58
Figure 2.5 Scratch Wound Assay Experimental Plan Showing Group Comparisons For Each Assay Objective.	63
Figure 2.6 Venn Diagram Depicting Gene Overlap Between the Module Groupings. There are four signalling pathway modules, one central module (WNT5A and TGF- β overlap), and one outer Notch, WNT and TGF- β . The numbers represent the number of genes common to the two or three overlapping pathways.	67
Figure 2.7 Potential Crosstalk Intermediaries to Investigate Between the WNT, TGF-β and Notch Signalling Pathways. Created with BioRender.com.	71
Figure 2.8 Example of BEAS-2B Cell Elongation Image Analysis	82
Figure 2.9 Separation Index Graphs of Antibodies Using FMO Controls (n=1)	89
Figure 2.10 Separation Index Graphs of Antibodies Using Isotype Controls (n=1)	90
Figure 2.11 Cytokeratin-5 Staining in Fibroblasts. The fibroblast population was selected, and the dead cells and doublets removed. CK5 gating was established using an FMO control (termed without CK5 in the gating strategy). Experiment is n=1.	90
Figure 2.12 BEAS-2B Basal Cell Gating Strategy. Cell population was gated, and single cells selected. Alive cells were then selected based on live dead staining. To test population gating strategy, CD166+ CD326- (top left quadrant), CD166+ CD326+ dual positive cells (top right quadrant) and the CD326+ CD166+ gated population within quadrant 2 were investigated for basal cells markers – CD49F, NGFR, CK5 and CD44. The CD326+ CD166+ gated population within quadrant 2 appears more basal cell like as these cells express the highest percentages of basal cell markers compared to the other two populations.	92
Figure 2.13 Submerged Human Bronchial Epithelial Cell Gating on Epithelial and Basal Cell Markers	93
Figure 2.14 Plasmid Map of Active WNT5A-V5 (Addgene Plasmid Number 43813)	102
Figure 2.15 Plasmid Map of Active WNT5B-V5 (Addgene Plasmid Number 43814)	103

Figure 2.16 Verification of the Linearised Expression Plasmid Backbone and WNT5 Insert on a 1% Agarose Gel	106
Figure 2.17 Plasmid Map of the Empty Vector (the plasmid without the WNT5A/B insert) After The Infusion Reaction	108
Figure 2.18 Plasmid Map of the WNT5A Plasmid After The Infusion Reaction	109
Figure 2.19 Plasmid Map of the WNT5B Plasmid After The Infusion Reaction	110
Figure 2.20 Colony Screening for WNT5A (top row) and WNT5B Inserts (bottom row)	113
Figure 2.21 Colony A13 Forward Sequencing Results Aligned With the Expected WNT5A Insertion Site. The WNT5A sequence lies within base region 93-1299. The miss-call of a base insertion is highlighted in the boxed region of the WNT5A sequence alignments. FinchTV view of the electropherogram of this region is shown to confirm the miss-call.	115
Figure 2.22 Colony A13 Reverse Sequencing Results Aligned With the Expected WNT5A Insertion Site. The WNT5A sequence lies within base region 125-1338.	116
Figure 2.23 Colony B14 Forward Sequencing Results Aligned With the Expected WNT5B Insertion Site. The WNT5B sequence lies within base region 93-1235.	117
Figure 2.24 Colony B14 Reverse Sequencing Results Aligned With the Expected WNT5B Insertion Site. The WNT5B sequence lies within base region 124-1267. The miss-call of a base insertion is highlighted in the boxed region of the WNT5B sequence alignments. FinchTV view of the electropherogram of this region is shown to confirm the miss-call.	118
Figure 2.25 Validation of Negative and Positive Control Cells. (A) RFP reporter expression of the RFP EV, WNT5A and WNT5B transfected cells used in the RT-qPCR experiment. (B) Image of the non-denatured agarose gel with the extracted HEK293T RNA from the cells shown in (A). (C) Relative expression of WNT5A mRNA between the untransfected, and RFP EV, WNT5A and WNT5B transfected HEK293T cells shown in (A), n=1.	119
Figure 2.26 WNT5A Protein Expression in Overexpressed HEK293T Cells. Bands were detectable for WNT5A antibody clone 6F2 (A) and 3A4 (B- left hand side). No band was detected for clone A-5 (B-right hand side). To confirm protein loading for 3A4 and A-5, the membrane in B was stained with house-keeping gene β -actin to confirm protein loading (C).	122
Figure 2.27 Immunocytochemistry Staining for WNT5A Protein Expression in Overexpressed HEK293T Cells. Paraffin embedded cell pellets of transiently transfected HEK293T cells (RFP empty vector, WNT5A and WNT5B) were stained with WNT5A antibody clones A-5, 6F2 or 3A4. Relevant isotype controls matched for clonality and antibody concentration (where possible) for each clone are also shown.	126
Figure 2.28 Assessment of the WNT5A mAb Clone 6F2 for Flow Cytometry Application. HEK293T without plasmid transfection and HEK293T cells transiently transfected with an RFP empty vector, WNT5A or WNT5B were stained with WNT5A antibody clone 6F2 to assess suitability for the application of flow cytometry.	128
Figure 2.29 Assessment of the WNT5A mAb Clone 3A4 for Flow Cytometry Application. HEK293T without plasmid transfection and HEK293T cells transiently transfected with an	

RFP empty vector, WNT5A or WNT5B were stained with WNT5A antibody clone 3A4 to assess suitability for the application of flow cytometry. 128

Figure 4.1 Effects of Takinib (A) and BOX-5 (B) Comparative to Basal Conditions on Metabolic Activity In Immortalised Human Bronchial Epithelial Cells. Stimulants were applied for 48 hours. Data is n=3 and presented as mean with standard deviation. *p < 0.05 by One-way ANOVA with Dunnett's post hoc test for intergroup comparisons. **** is p-value of <0.0001. 141

Figure 4.2 The Effect of TGF- β 1 Pre-Stimulation on TEER Prior to Wounding. (A-B) Summary figure of the effect of a 24-hour (A) and 48-hour pre-stimulation (B) on TEER prior to wounding. Data is n of 3 and presented mean with standard deviation. *p < 0.05 by paired t-test. 143

Figure 4.3 The Effect of TGF- β 1 Pre-Stimulation Duration on ALI Culture Wound Healing. (A) Representative images of the ALI culture scratch wound healing assay immediately after wound induction and after 8 hours of healing, with and without a 48-hour 10ng/ml rhTGF- β 1 stimulation. This donor had enhanced wound healing in response to TGF- β 1 stimulation. (B-C) Summary figure of the 24-hour (B) and 48-hour (C) 10ng/ml rhTGF- β 1 stimulation wound healing assay. Four time points were investigated – 0h, 4h, 8h and 24h. Data is n of 3, and presented mean with standard deviation. *p < 0.05 by two-way repeated measures (of both factors) ANOVA. (D-E) Summary figure of the 24-hour (D) and 48-hour (E) pre-stimulation. TEER results during the scratch wound healing assay. 3 time points were investigated – immediately before wounding, immediately after wounding and 24 hours post-wounding. Data is n of 2, and presented mean with standard deviation. 144

Figure 4.4 The Effect of TGF- β 1 Pre-Stimulation With and Without TAK1 Inhibition on TEER Prior to Wounding. (A-B) Summary figures of the effect of 48-hour 20ng/ml TGF- β 1 pre-stimulation without TAK1 inhibition (A), and with TAK1 inhibition (B) using Takinib on TEER prior to wounding. Data is n of 9 and presented mean with standard deviation. *p < 0.05 by paired t-test. 147

Figure 4.5 The Effect of TGF- β 1 Pre-Stimulation With and Without Inhibition With Takinib on Wound Healing and TEER. (A-B) Summary figure of the effect of a 48-hour 20ng/ml TGF- β 1 pre-stimulation on wound healing (A) and TEER (B). Data is n of 8 (as unpaired data excluded) and presented mean with standard deviation. *p < 0.05 by Wilcoxon matched-pairs signed rank test for wound healing and a paired t-test for TEER at 24 hours. (C-D) Summary figure of Takinib inhibition of TGF- β 1 on wound healing (C) and TEER (D). Takinib (8.4nM) was added 30 minutes prior to TGF- β 1 stimulation. Data is n of 9 and presented mean with standard deviation. *p < 0.05 by Wilcoxon matched-pairs signed rank test for wound healing and a paired t-test for TEER at 24 hours 148

Figure 4.6 The Effect of WNT5A Stimulation With and Without Signalling Inhibitor BOX-5 on Wound Healing and TEER. (A-B) Summary figures comparing the impact of WNT5A stimulation (1 μ g/ml) against basal on wound healing (A) and TEER (B). WNT5A was added after wounding following a 30-minute incubation with BOX-5 or vehicle control, and

the effect on wound healing observed at 4-, 8- and 24-hours post-wounding. Data is n of 8 (as unpaired data was excluded). (C-D) Summary figures comparing BOX-5 inhibition of WNT5A on wound healing. BOX-5 (500 μ M) was added 30 minutes prior to WNT5A stimulation. Data is n of 9. All data is presented mean with standard deviation. 24-hour time points were used for statistical analysis. * $p < 0.05$ by Wilcoxon matched-pairs signed rank test for wound healing and a paired t-test for TEER. All p-values were adjusted to account for multiple comparisons. 150

Figure 4.7 The Effect of a 48-Hour TGF- β 1 Pre-Stimulation on WNT5A-Mediated Wound Healing and TEER. (A-B) Summary figures comparing the impact of WNT5A stimulation (1 μ g/ml) against basal conditions on wound healing (A) and TEER (B) following a 20ng/ml 48-hour TGF- β 1 pre-stimulation. (C-D) Summary figures assessing the impact of TAK1 inhibition (8.4nM Takinib) on 48-hour TGF- β 1 pre-stimulation on wound healing (C) and TEER (D) of WNT5A stimulated cultures. Data is n of 9 and presented mean with standard deviation. * $p < 0.05$ by Wilcoxon matched-pairs signed rank test for wound healing and paired t-test for TEER. 151

Figure 4.8 The Effect of Takinib and TGF- β 1 Pre-Stimulation on WNT5A-Mediated Wound Healing and TEER. Summary figure comparing the impact of Takinib and TGF- β 1 stimulation on WNT5A stimulated cultures 24 hours post-wounding on wound closure (A) and TEER (B). Data is n of 9 and presented mean with standard deviation for B and C. * $p < 0.05$ by two-way repeated measures (by both factors) Aligned ranks transformation ANOVA for wound healing and two-way repeated measures (by both factors) ANOVA for TEER. 152

Figure 4.9 The Effect of Takinib, TGF- β 1 and WNT5A Stimulation on Wound Healing and TEER. Summary figure comparing the impact of Takinib and rhTGF- β 1 and rhWNT5A stimulation on all conditions 24 hours post-wounding on percentage culture wound closure and TEER. Data is n of 9 and presented mean with standard deviation. * $p < 0.05$ by three-way repeated measures (by all three factors) Aligned Ranks ANOVA for wound healing and a three-way repeated measures (by all three factors) mixed-effect model for TEER. 154

Figure 4.10 Exploring Transfection Efficiency of ALI Cultures in Comparison to HEK293T Cells Using Numerous Transfection Reagents. The efficiency of Lipofectamine 2000, Viromer Blue, Viromer Green and Interferin was tested on ALI cultures (top row) and HEK293T cells (bottom row). Experiment is n=1. 156

Figure 5.1 Assessing RNA Quality Prior to RT-qPCR. (A) Bioanalyser profiles of the BEAS-2B samples. Eleven out of twelve samples were tested on this chip. (B) Non-denatured Agarose gel results of the iHBEC RNA. The 28S band and peak widths for all samples are 2-2.7 times larger than those of 18S indicating intact RNA. 170

Figure 5.2 RT-qPCR Analysis of WNT5A and TGF- β 1 Pathway Signalling Effectors in BEAS-2Bs and iHBECs. (A-B) The log₂ fold change of 16 WNT5A and TGF- β 1 related genes in individual BEAS-2B passages are depicted in these heatmaps following a 30-

minute (A) and 4-hour (B) 10ng/ml rhTGF- β 1 stimulation. The mean log₂(FC) and statistical significance are indicated (n=4). Statistical significance was calculated using a paired t-test on the $\Delta\Delta$ CT of each gene. (C) Graph comparing the 30-minute and 4-hour log₂FC. Statistical comparisons were made between the 30-minute and 4-hour stimulations using a paired t-test for each gene. Data is presented mean with standard deviation. (D) Relative expression of WNT5A mRNA between non-stimulated iHBEC cells (which received vehicle control) and cells stimulated with 48-hours 10ng/ml TGF- β 1. Data is n=3 and presented mean with standard deviation. *p < 0.05 by paired t-test. **172**

Figure 5.3 BEAS-2B ROR2 and FZD4 Expression Before and After TGF- β 1 Stimulation.

Flow cytometry summary figures of percentage expression of ROR2 in EpCAM- (A) and EpCAM+ (B) and FZD4 in EpCAM- (C) and EpCAM+ (D) BEAS-2B populations before and after a 48-hour stimulation with 10ng/ml rhTGF- β 1, n=3. *p < 0.05 by Wilcoxon matched-pairs signed rank test. **173**

Figure 5.4 HBEC ROR2 and FZD4 Expression Before and After TGF- β 1 Stimulation. (A)

Summary figure of ROR2 and FZD4 percentage expression on HBECs retrieved from bronchial brushings. Data is presented mean with standard deviation. (B) Summary figures of ROR2 and FZD4 percentage expression on ALI cultures before and after a 48-hour stimulation with 10ng/ml rhTGF- β 1, n=3. *p < 0.05 by Wilcoxon matched-pairs signed rank test. **174**

Figure 5.5 BEAS-2B Cytokeratin-5, COL1A1 and Vimentin Expression Before and After 48-Hour 10ng/ml rhTGF- β 1 Stimulation.

Images are representative of four independent passages. All images taken at x200 magnification. **175**

Figure 5.6 BEAS-2B Cytokeratin-5, COL1A1 and Vimentin Expression Before and After 48-Hour 1 μ g/ml rhWNT5A Stimulation.

Images are representative of three independent passages. All images taken at x200 magnification. **176**

Figure 5.7 BEAS-2B Cytokeratin-5, COL1A1 and Vimentin Expression Before and After rhTGF- β 1 and rhWNT5A Stimulation.

Summary figures of CK5 (A, D), COL1A1 (B, E) and Vimentin (C, F) immunofluorescence staining following a 48-hour 10ng/ml rhTGF- β 1 (top row A-C), n=4, and 1 μ g/ml rhWNT5A (bottom row D-F) stimulation compared to vehicle control (basal). n=3, *p < 0.05 by paired t-test. **177**

Figure 5.8 BEAS-2B Cellular Elongation Before and After rhTGF- β 1 and rhWNT5A Stimulation.

Summary figures of cellular elongation assessed by measuring vimentin stained cells with and without a 48-hour 10ng/ml rhTGF- β 1 (A), n=4, or 1 μ g/ml rhWNT5A (B) stimulation, n=3, compared to vehicle control (basal). *p < 0.05 by paired t-test. **177**

Figure 5.9 Geometric Mean Fluorescence Intensity of Basal Cell and EMT Marker Expression Before and After rhTGF- β 1 Stimulation in BEAS-2B Cells.

Summary figures of geometric mean fluorescence intensity (GMFI) of basal cell and EMT markers with and without a 48-hour 10ng/ml rhTGF- β 1 stimulation compared to vehicle control (basal) for BEAS-2B EpCAM- (A) and EpCAM+ (B) populations, n=5. *p < 0.05 by paired

t-test. A single t-test was conducted for each protein per population, and p values adjusted using the Holm-Sidak method ($\alpha=0.05$). 179

Figure 5.10 Geometric Mean Fluorescence Intensity of Basal Cell and EMT Marker

Expression Before and After rhWNT5A and rhTGF- β 1 Stimulation in ALI Cultures.

Gating strategy used to select each population is shown. A-C represent geometric mean fluorescence intensity (GMFI) summary figures of basal cell and EMT marker expression after a 48-hour 10ng/ml rhTGF- β 1 or 1 μ g/ml rhWNT5A stimulation compared to vehicle control (basal) for EpCAM- (A), EpCAM+ (B) and basal cell populations (C). Data is n=4 (3 asthmatic, 1 healthy) for rhTGF- β 1 and n=3 for rhWNT5A (2 asthmatic, 1 healthy). *p < 0.05 by one-way repeated measures ANOVA with Dunnett's multiple comparison post hoc test. Significance testing shown is between each stimulation compared to vehicle control rather than across all groups. A single one-way ANOVA was conducted for each protein per population, and ANOVA summary p values adjusted using the Holm-Sidak method ($\alpha=0.05$). Post hoc analysis p values were adjusted for multiplicity within each ANOVA. 181

Figure 5.11 The Effect of rhTGF- β 1 Stimulation With and Without TAK1 Inhibition on

SMAD2/3 Phosphorylation of ALI Cultures. (A) EpCAM and NGFR population gating

applied to ALI cultures following cellular debris, dead cell and doublet exclusion. (B)

Summary figure of the effect of a 30-minute 10ng/ml rhTGF- β 1 stimulation compared to

basal on phosphorylated SMAD2/3 expression. (C) Summary figure of the effect of Takinib

on ALI cultures stimulated with 10ng/ml rhTGF- β 1 for 30 minutes. Data is presented mean

with standard deviation, n=4. *p < 0.05 by Wilcoxon matched-pairs signed rank test. All p-

values were adjusted to account for multiple comparisons. 183

Figure 5.12 The Effect of WNT5A Stimulation With and Without Receptor Inhibition on

SMAD2/3 Phosphorylation of ALI Cultures. (A) Summary figure comparing the impact

of a 30-minute 1 μ g/ml WNT5A stimulation (1 μ g/ml) against basal. (B) Summary figure

comparing BOX-5 inhibition of WNT5A on phosphorylated SMAD2/3 expression. BOX-5

was added 30 minutes prior to WNT5A stimulation. Data is presented mean with standard

deviation, n=4. *p < 0.05 by Wilcoxon matched-pairs signed rank test. All p-values were

adjusted to account for multiple comparisons. 184

Figure 5.13 The Effect of WNT5A and TGF- β 1 Dual Stimulation With and Without

Receptor Inhibition on SMAD2/3 Phosphorylation of ALI Cultures. (A) Summary figure

comparing the impact of a 30-minute 1 μ g/ml rhWNT5A and 10ng/ml rhTGF- β 1 dual

stimulation against rhTGF- β 1 alone. (B) Summary figure comparing TAK1 inhibition on

WNT5A phosphorylated SMAD2/3 expression. Takinib was added 30 minutes prior to dual

stimulation. Data is presented mean with standard deviation, n=4. *p < 0.05 by Wilcoxon

matched-pairs signed rank test. All p-values were adjusted to account for multiple

comparisons. 185

Figure 5.14 The Effect of WNT5A Stimulation With and Without Takinib Inhibition on

SMAD2/3 Phosphorylation. Summary figures of phosphorylated SMAD2/3 expression

following a 30-minute 1 μ g/ml rhWNT5A stimulation without (A) and with Takinib inhibition

- (B) for the three populations present within ALI cultures, which are categorised by their EpCAM and NGFR dual expression. Data is presented mean with standard deviation, n=4. *p < 0.05 by two-way repeated measures Aligned ranks transformation ANOVA. **186**
- Figure 5.15 The Effect of Takinib, TGF- β 1 and WNT5A Stimulation on SMAD2/3 Phosphorylation.** Summary figures of phosphorylated SMAD2/3 expression comparing the impact of Takinib and rhTGF- β 1 and rhWNT5A stimulation on all conditions for the three populations present within ALI cultures, as categorised by their EpCAM and NGFR dual expression. Data is presented mean with standard deviation, n=4. *p < 0.05 by three-way repeated measures (by all three factors) Aligned Ranks ANOVA. **187**
- Figure 6.1 Summary of WNT5A and TGF- β 1 Crosstalk Results** **197**
- Figure 7.1 rhWNT5A Proteomic Results.** The first 3 protein hits were for Serum albumin (Bos Taurus), ALB protein (Bos Taurus) and Serum albumin (homo-sapiens). Hits for both homo-sapien WNT5A and WNT5B were then observed. **203**
- Figure 7.2. Selecting Antibody Panel Fluorochromes.** (Top panel) shows the BD Biosciences spectra viewer prediction of spectral spillovers between potential fluorochromes. (Bottom panel) shows the compensation matrix of potential fluorochromes using compensation beads run on the Attune. **233**
- Figure 7.3 The Effect of TGF- β 1 Pre-Stimulation With and Without Inhibition With Takinib on Wound Healing and TEER in GINA2-4 Patients.** (A-B) Summary figure of the effect of a 48-hour 20ng/ml rhTGF- β 1 pre-stimulation on wound healing (A) and TEER (B). Data is n of 5 and presented mean with standard deviation. *p < 0.05 by Wilcoxon matched-pairs signed rank test for wound healing and a paired t-test for TEER at 24 hours. (C-D) Summary figure of Takinib inhibition of TGF- β 1 on wound healing (C) and TEER (D). Takinib (8.4nM) was added 30 minutes prior to TGF- β 1 stimulation. Data is n of 5 and presented mean with standard deviation. *p < 0.05 by Wilcoxon matched-pairs signed rank test for wound healing and a paired t-test for TEER at 24 hours. **234**
- Figure 7.4 The Effect of TGF- β 1 Pre-Stimulation With and Without Inhibition With Takinib on Wound Healing and TEER in GINA5 Patients.** (A-B) Summary figure of the effect of 48-hour 20ng/ml TGF- β 1 pre-stimulation on wound healing (A) and TEER (B). Data is n of 3 (as unpaired data excluded) and presented mean with standard deviation. *p < 0.05 by Wilcoxon matched-pairs signed rank test for wound healing and a paired t-test for TEER at 24 hours. (C-D) Summary figure of Takinib inhibition of TGF- β 1 on wound healing (C) and TEER (D). Takinib (8.4nM) was added 30 minutes prior to TGF- β 1 stimulation. Data is n of 4 and presented mean with standard deviation. *p < 0.05 by Wilcoxon matched-pairs signed rank test for wound healing and a paired t-test for TEER at 24 hours. **235**

LIST OF ABBREVIATIONS

5ZO	(5Z)-7-oxozeaenol
ALI	Air-liquid-interface
AEC	Airway epithelial cells
AJC	Apical junction complex
ASL	Airway surface liquid
ASM	Airway Smooth Muscle
BAL	Bronchoalveolar lavage
CamKII	Ca ²⁺ /calmodulin-dependent protein kinase 2
CBF	Cilia beat frequency
CDC42	Cell division cycle 42 protein
CDHR3	Cadherin-related family member 3
CK5	Cytokeratin-5
COPD	Chronic obstructive pulmonary disease
CRP	C-reactive protein
CRTH2	Chemoattractant receptor–homologous molecule expressed on type 2 cells
CysLT	Cysteinyl leukotrienes
DAAM1	DVL-associated activator of morphogenesis 1
DAMP	Danger associated molecular patterns
DKK	Dickkopf
DVL	Dishevelled

ECM	Extracellular matrix
EGF	Epidermal growth factor
ELISA	Enzyme-linked immunosorbent assay
EpCAM	Epithelial cell adhesion molecule
EMT	Epithelial–mesenchymal transition
EMTU	Epithelial mesenchymal trophic unit
FEV ₁	Forced expiratory volume in 1 second
FVC	Forced vital capacity
FGF	Fibroblast growth factor
FGFR	Fibroblast growth factor receptor
FZD	Frizzled receptor
GINA	Global Initiative for Asthma
GLI	Glioma-associated transcription factors
GMA	Glycol methanlacrylate acrylic resin
GM-CSF	Granulocyte-macrophage colony-stimulating factor
GSK-3 β	Glycogen synthase kinase 3 beta
GWAS	Genome wide association studies
HBEC	Human bronchial epithelial cells
ICS	Inhaled corticosteroid
IFN- γ , - β , - λ	Interferon $\gamma/\beta/\lambda$
IgA, IgM, IgE	Immunoglobulin A/M/E
IHC	Immunohistochemistry
IL-1 β , -4, -5, -10, -13, -17A and -33	Interleukin-1 β /4/5/10/13/17A/33

IL1RL1	Interleukin 1 receptor-like 1 interleukin 1 receptor-like 1
IL18R1	Interleukin 18 receptor 1
ILCs	Innate lymphoid cells
IPF	Idiopathic pulmonary fibrosis
IMS	Industrial methylated spirit
JNK	c-Jun kinases
LABA	Long-acting β -agonist
Ultra LABA	Ultra long-acting β -agonist
LAP	Latency-associated peptide
LAMA	Long-acting muscarinic antagonist
LPS	Lipopolysaccharide
LRI	Leicester Royal Infirmary
LRP	Low-density lipoprotein receptor-related protein
LTA4, LTB4, LTC4, LTD4 and LTE4	Leukotriene A4/B4/C4/D4/E4
LTBP	Latent TGF- β -binding protein
LTRA	Leukotriene receptor antagonists
MMP	Matrix metalloproteinases
NBF	Neutral buffered formalin
NGFR	Nerve Growth Factor Receptor
NICD	Notch intracellular domain
NLK	Nemo-like kinase
OCS	Oral corticosteroid
ORMDL3	Orosomucoid-like 3

PAMP	Pathogen associated molecular patterns
PBMCs	Peripheral blood mononuclear cells
PCDH1	Protocadherin-1
PCL	Periciliary liquid
PCLS	Precision-cut lung slices
PCP	Planar cell polarity
PKC α	Protein kinase C α
PLC	Phospholipase C
Rac1	Ras-related C3 botulinum toxin substrate 1
RhoA	Ras-homologous A
ROCK	Rho-associated kinase
ROR2	Receptor tyrosine kinase like Orphan Receptor 2
ROS	Reactive oxygen species
SABA	Short-acting β 2 agonist
SARP	Severe Asthma Research Program
SI	Sensitivity Index
TAC	Transit-amplifying cell
TAK1	TGF- β 1 activated kinase 1
TEER	Transepithelial electrical resistance
TGF- α	Transforming growth factor-alpha
TGF- β	Transforming growth factor-beta
TGF- β 1	Transforming growth factor-beta 1
TGF- β R1/2	Transforming growth factor beta receptor 1/2

TH2	T-helper type 2
TIMP	Tissue inhibitors of metalloproteinases
TLR	Toll-like receptors
TNF (- α)	Tumour necrosis factor (-alpha)
TSC	Tissue-specific stem cell
TSLP	Thymic stromal lymphopoietin
U-BIOPRED	Unbiased Biomarkers for the Prediction of Respiratory Disease Outcomes
WNT	Wingless/integrase
WNT5A	Wingless/integrase (Wnt) family member 5A
ZO-1, ZO-2, ZO-3	Zonula occluden -1/-2/-3

1 INTRODUCTION

1.1 What is Asthma?

Asthma is a chronic inflammatory disease of the airways, that clinically presents as periodic episodes of dyspnoea (shortness of breath), chest tightness, wheeze and recurrent cough (GINA 2020: A, p20). Asthma is diagnosed based on the patient's history of the respiratory symptoms previously listed along with a combination of: the absence of symptoms associated with an alternative diagnosis and the patient presenting with variable expiratory airflow limitation using spirometry or peak expiratory flow (SIGN/BTS 2019). The pattern of symptoms and post-bronchodilator spirometry is vital for supporting an asthma diagnosis and ruling out other acute or chronic conditions which present similarly to asthma (Larsson *et al.* 2020). The following symptom patterns are supportive of an asthma diagnosis: symptoms being variable over time, appearing worse at night or on waking, and if symptoms are triggered by exercise, allergies, viral infections, cold weather, or irritants such as smoke, exhaust fumes or strong smells (GINA 2020: A, p21).

The prevalence of asthma varies worldwide, with asthma prevalence varying from 1-18% between different countries (GINA 2020: A, p20). It is estimated that 300 million people are affected worldwide (GINA 2020: B, p9). Approximately 3.7% of asthmatics have severe asthma; these patients have poor symptom control despite maximal therapy, and good adherence and inhaler technique (GINA, 2020: A, p95).

1.2 Asthmatic Phenotypes

Asthma is a complex disease with patients presenting with different underlying pathophysiologies, of which there are several genes associated with its manifestation (Moffatt *et al.* 2010). A phenotype, such as the exercise-induced or obesity-related asthma, is defined as the observable characteristics of an organism, which results through the interaction between the organism's genetics and its environment (Ray, Oriss and Wenzel 2015). Originally, asthmatics were

grouped into phenotypes according to clinical presentation (e.g. age of onset, treatment resistance/asthma severity), and symptomatic associated triggers, which can be either allergic (dust, pet dander) or non-allergic (such as aspirin sensitive, obesity-related and exercise induced asthma) (Wenzel 2006). An alternative clinical approach utilising cluster analysis identified several different asthmatic phenotypes (Haldar *et al.* 2008) (Moore *et al.* 2010). Unfortunately, grouping patients this way was not informative enough to identify patients by specific pathophysiologies and therefore did not improve treatment outcome (Ray, Oriss and Wenzel 2015). However, the study by Moore *et al.* (2010) did establish that airflow obstruction is an important phenotypic feature of severe asthma, but to date, the pathophysiology of airflow obstruction (which likely includes airway and cellular remodelling) is not fully understood.

Classifying asthma heterogeneity has since progressed from phenotyping patients by clinical and molecular phenotypes, instead patients are now identified by endotypes underpinning the pathobiologic and genetic processes associated with the presentation of specific clinical characteristics (Anderson 2008). Investigating cellular inflammation of the asthmatic lung identified four inflammatory profile phenotypes: eosinophilic, neutrophilic, mixed granulocytic (neutrophilic and eosinophilic) and paucigranulocytic (where both eosinophils and neutrophils are within normal range) (Robinson *et al.* 2017). Eosinophilia is associated with type 2 airway inflammation, deemed TH2 high asthma, which is mainly mediated by eosinophils, mast cells, T-helper type 2 (TH2) cells, innate lymphoid cells type 2 (ILC2s) and IgE-producing B cells (Fahy, 2015). Non-type 2 (TH2-low) asthma, however, is not associated with type 2 inflammation and includes the paucigranulocytic and neutrophilic phenotypes mentioned previously (Ray, Oriss and Wenzel 2015). Neutrophilic asthma is often determined by eosinophil sputum counts of <2% and neutrophil sputum counts $\geq 61\%$ (Pembrey *et al.* 2018). Neutrophilic asthma is associated with more severe disease and steroid-resistance and is mediated mainly by TH17 cells (Lambrecht and Hammad 2015).

1.3 Asthmatic Endotypes

The asthmatic endotype proposed in 2008 by Anderson and later refined by Lötvall *et al.* (2011), categorises asthmatics based on the distinct pathophysiological mechanism driving their asthmatic phenotype and treatment response. Lötvall *et al.* (2011) suggested that there are six asthmatic endotypes, but at present the concept remains largely hypothetical with little evidence supporting their identification by the defined biomarkers and pathophysiological mechanisms (Wenzel 2012). Endotyping patients to take into account asthma's heterogeneity, however, is still a top priority of clinical practitioners as it will open up the possibility of personalised medicine (Belgrave *et al.* 2017).

1.4 Managing Asthma According to International Guidelines

Well managed asthma achieves good control of symptoms so that normal activity levels can be maintained with minimal risk of exacerbations, persistent airflow obstruction and asthma-related death (GINA 2020: A, p42). To attempt to achieve well managed asthma for each patient, Global Initiative for Asthma (GINA) guidelines implement a cycle of three continuous steps which involve assessing, treating and reviewing the patient to ensure an effective, appropriate level of treatment is provided at a minimal effective dose (GINA 2020: A, p44-47).

There are three main categories of asthma medications listed by GINA in their 2020 report: controller medications, reliever medications and add-on therapies. Controller medications aim to control symptoms, reduce airway inflammation and reduce the risk of complications, whereas, reliever medications relieve symptoms in time of exacerbation or periodic episodes of worsening, and add-on therapies (long-acting muscarinic antagonists, leukotriene receptor antagonists and biologics) are provided to moderate-severe asthmatics where exacerbations and symptoms are uncontrollable despite optimised controller treatment (GINA 2020: A, p47-51).

1.5 Asthma Treatments

All marketed asthma therapies target airway inflammation. Inhaled corticosteroids (ICS) are the most effective controller medication for asthma, with GINA now recommending all asthmatic adults and adolescents receive ICS-containing controller treatment (GINA 2020: A). Their mechanism of action, through binding to glucocorticoid receptors, is to suppress inflammation by reversing histone acetylation, which consequently reduces inflammatory gene activation (Barnes, Adcock and Ito 2005). Inflammatory cytokines that are reduced include TH2 cytokines interleukin-4, -5 and -13 (IL-4/-5/-13) and Granulocyte-macrophage colony-stimulating factor (GM-CSF) (Barnes 2010). Symptoms are reported to be reduced along with hyperresponsiveness (Barnes 2010), frequency and severity of exacerbations (Pauwels *et al.* 2003), and asthma mortality (Suissa *et al.* 2000). Corticosteroids can be inhaled (ICS) or oral (OCS); taken orally, corticosteroids are more potent, however, they also have a higher risk of side effects (Kim, Song and Cho 2016). Localised side effects, which are reported at higher ICS doses, include oral candidiasis, a hoarse voice and cough, whereas, systemic side effects include growth and adrenal suppression, bruising, glaucoma, osteoporosis, cataracts, metabolic abnormalities and psychiatric disturbances (Barnes 2010). A recent study also suggests OCS are associated with higher risk of fracture, sepsis and venous thromboembolism (Waljee *et al.* 2017).

Corticosteroids upregulate Beta-2 (β 2)-adrenergic receptors in the human lung (Mak, Nishikawa and Barnes 1995). β 2 agonists bind to β 2 adrenergic receptors on airway smooth muscle (ASM) to induce relaxation and therefore bronchodilation (Billington, Penn and Hall 2017). Corticosteroids therefore protect against β 2-receptor downregulation after long-term use (Mak *et al.* 1995), explaining their frequently administered combination therapy. There are three types of β 2-agonist therapies, short-acting and long-acting (termed SABA and LABA respectively) and ultra-long-acting (ultra-LABA) (Kim, Song and Cho 2016). If used alone, SABA and LABAs promote eosinophilic airway inflammation (Gauvreau *et al.* 1997), resulting in uncontrolled asthma and increased risk of mortality (Spitzer *et al.* 1992) (Salpeter *et al.* 2006) (Nelson *et al.* 2006). In the

National Review of Asthma Deaths 2014 report, of 192 asthma deaths recorded in the UK in 2012, 39% of patients were over reliant on SABAs, using over 12 inhalers in the year prior to death (Royal College of Physicians 2014). Both SABAs and LABAs are therefore now only advised to be taken as needed alongside ICSs as a controller medication in the current GINA guidelines.

Other available asthma medications include the long-acting muscarinic antagonist (LAMA), leukotriene receptor antagonist (LTRA) and biologics. The LAMA tiotropium bromide inhibits one of three muscarinic receptors present in the bronchial airways to regulate mucus secretion and ASM contraction (Gosens *et al.* 2006) (Kaplan and Chang 2020). LTRAs Montelukast and Zafirlukast both target the cysteinyl leukotriene (CysLT) receptor CysLT1 to reduce bronchoconstriction. The CysLTs are synthesised by activated leukocytes (Lynch *et al.* 1999). (Kanaoka and Austen 2019). There are also several monoclonal antibodies on the market targeting type 2 inflammation, including Omalizumab, an anti-IgE, Mepolizumab and Reslizumab, both anti-IL-5, Benralizumab, an anti-IL-5R α , and Dupilumab, which is an anti-IL-4R α and so blocks IL-4 and IL-13 signalling (O'Byrne *et al.* 2019). A raised blood or sputum eosinophilic count, serum IgE or fractional exhaled nitric oxide are biomarkers for predicting the efficacy of the biologics in GINA treatment intensity step 5 patients (O'Byrne *et al.* 2019) (McGregor *et al.* 2019).

1.6 Structure and Function of the Airways

In humans, the airways consist of two sections: the conducting airways and the respiratory airways. The conducting airways consist of the nose, trachea and bronchi, whereas, the respiratory consists of the respiratory bronchioles and alveoli (Hollenhorst, Richter and Fronius 2011). The conducting zone is responsible for preparing the air by warming it and removing pathogens that may have entered the airways on inhalation, and for transporting the air to the respiratory zone; the respiratory zone, as the name suggests, mediates gaseous exchange of respiration (Hollenhorst, Richter and Fronius 2011). All parts of the airway are lined with epithelium, of which forms a barrier between the external

environment and the host, preventing free exchange between the two (Hollenhorst, Richter and Fronius 2011). The composition of the airways differs across the upper, lower and alveolar airways; the upper airways is a pseudostratified columnar epithelium, transitioning into cuboidal epithelial cells in the bronchioles, followed by a single-cell thick, flat-shaped alveolar epithelium with cuboidal-shaped alveolar type II progenitor cells (Heijink *et al.* 2020).

1.7 The Bronchial Airway Epithelium

The bronchial airways are lined with a pseudostratified epithelium that contains four main cell types; these are: secretory (containing 2 subtypes: goblet and club cells), ciliated cells, basal cells and undifferentiated intermediate cells (Tilley *et al.* 2015). There are also numerous rarer cell populations such as the neuroendocrine cells, ionocytes and solitary chemosensory (tuft) cells, each of which have differing roles in epithelial barrier function (Hellings and Steelant 2020) (Montoro *et al.* 2018). The airway epithelium is the initial line of defence that protects the lungs from environmental agents (such as allergens, pathogens and pollutants) present in the air (Gohy *et al.* 2020). To prevent access of these inflammatory stimuli into the lung, and to maintain lung tissue homeostasis, the epithelial cells have an elaborate number of cell-cell adhesive complexes that allow them to form a selectively permeable sheet-like structure (Davies 2014). This structure provides a physical barrier, preventing access of inhaled materials into the lung tissue, as well as a chemical barrier, through mucus secretion which traps inhaled particles (Hellings and Steelant 2020). Ciliated cells then waft the mucous up and out of the airways to the mouth for disposal; this process of particulate matter removal from the respiratory tract is called the mucociliary escalator (Davies 2014). The combination and effectiveness of these barrier functions in the airways ensure that most environmental challenges that enter the airway are overcome without the need to initiate an inflammatory response (Davies 2014).

1.7.1 Physical Barrier Function of Airway Epithelium

The epithelial cell-cell adhesion junctions that are involved in forming the epithelial barrier include: tight junctions, adherens junctions and desmosomes (Gohy *et al.* 2020). The tight junctions and adherens junctions are located in the apical junction complex (AJC), closest to the airway lumen (Loxham, Davies and Blume 2014). The tight junctions regulate the paracellular passage of ions and molecules across the epithelia, essentially allowing the epithelium to function as a selectively permeable barrier; whereas the adherens junction, along with desmosomes, are critical for providing an adhesive force between neighbouring epithelial cells (Loxham, Davies and Blume 2014) (Davies 2014). These three cell-cell junctions link adjacent epithelial cells together. Hemidesmosomes, however, anchor the epithelial cells to the basement membrane, and are thus located on the basolateral membrane of epithelial cells (Loxham, Davies and Blume 2014).

Looking into the function of these epithelial junctions in more depth, the adherens junctions are comprised of E-cadherin and an α - and β -catenin adapter complex, which links the actin cytoskeleton of neighbouring cells (Heijink *et al.* 2020). They are the first junctions which form between epithelial cells, and they appear to be essential for other cell-cell junction formations, and therefore epithelial layer development (Davies 2014). The tight junction, which is also located in the AJC, consist of transmembrane proteins (such as occludin and the claudin family), intracellular proteins (such as the zonula occluden proteins ZO-1, ZO-2 and ZO-3), which link transmembrane proteins to the cytoskeleton, and regulatory proteins (RP), which can modify the transmembrane-intracellular links (Loxham, Davies and Blume 2014). Tight junctions form around the entire perimeter of each epithelial cell, binding adjacent epithelial cells together, thereby allowing a selectively permeable barrier to form between the airways and the underlying basal membrane, whilst also providing epithelial polarity (Davies 2014). A pictorial version of these cell-cell junctions is shown in **Figure 1.1**.

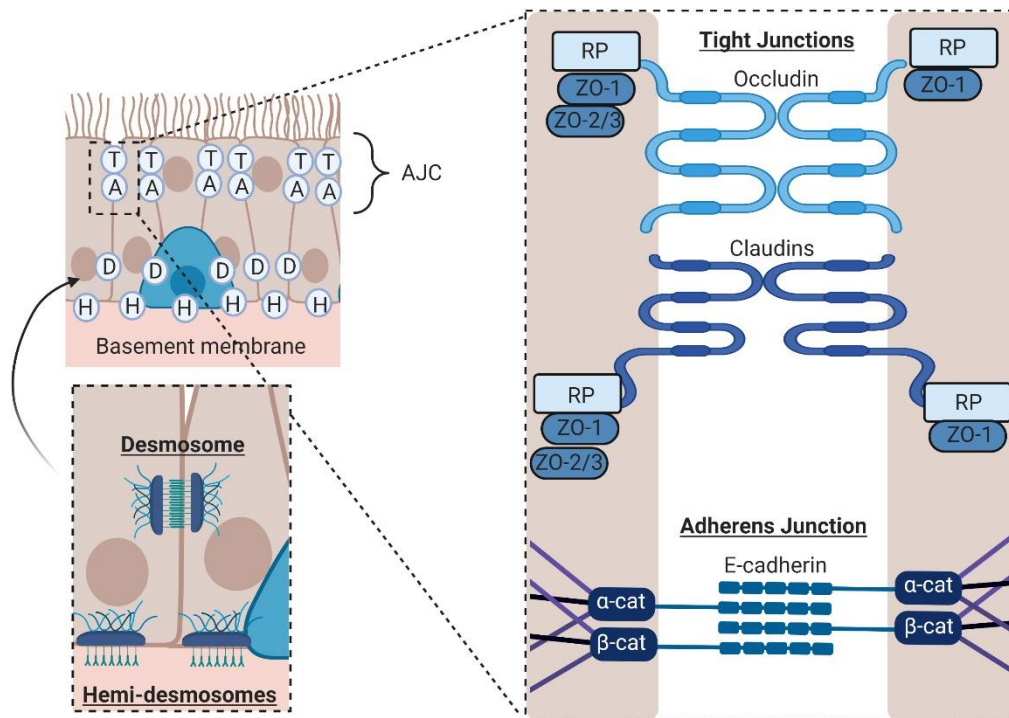


Figure 1.1 Diagram of the Epithelial Cell-Cell Junctions. Created with BioRender.com

1.7.2 Chemical Barrier Function of Airway Epithelium

In conjunction with submucosal gland secretion, goblet cells produce and secrete mucus consisting of hydrated gel-forming mucins, salts, lipids and antimicrobial molecules (Frey *et al.* 2020). These mucus components act as a chemical barrier, trapping and inactivating inhaled agents; the clearance of these agents is then facilitated by the epithelial mucociliary escalator (Davies 2014). There are multiple secretory mucins: MUC2, MUC5B, MUC5AC and MUC19, but MUC5AC and MUC5B are the most abundantly secreted in the airways (Frey *et al.* 2020). MUC5AC is primarily produced by goblet cells in the airways, and its production is predominantly upregulated in asthmatics, with mucus hypersecretion and goblet cell hyperplasia being a characteristic feature of asthma (Loxham, Davies and Blume 2014). MUC5B, however, is produced by the submucosal glands, and under normal healthy airway conditions is the principal mucin found in the airways (Frey *et al.* 2020).

The protective features of mucus rely on mucin glycoprotein cross-linking, which produces a mucin mesh thought to prevent dehydration of the epithelial barrier, and limit pathogen aggregation, pathogenic binding and penetration through the epithelium (Loxham, Davies and Blume 2014). For clearance of this mucus gel, the ciliated cells that line the airways must have coordinated directional movement (Gohy *et al.* 2020). The cilia tips enter the mucus layer only on the forward motion to propel the mucus, whereas, on the reverse stroke, the cilia shaft bends causing the tip to pass underneath the mucus layer; by doing so, mucus is propelled in one direction - up and out of the airway (Vanaki *et al.* 2020). Each ciliated columnar cell contains approximately 300+ motile cilia (Gohy *et al.* 2020). The beat frequency of cilia is dependent on multiple signalling molecules: Ca^{2+} (Schmid and Salathe 2011), cAMP (Joskova, Mokry and Franova 2020) (Kogiso *et al.* 2017), nitric oxide (Jiao *et al.* 2011) and progesterone (Jain *et al.* 2012). Additionally, mechanical stress can also stimulate ATP release to increase cilia beat frequency (CBF) (Button and Boucher 2008). The effectiveness of the mucociliary escalator therefore depends on numerous factors, including mucin production and its hydration, cilia structure and length, coordinated cilia movement and CBF (Tilley *et al.* 2015).

In addition to the aforementioned, ion transport also plays a fundamental part in mucociliary clearance. The ion transport of ciliated cells controls transepithelial water flow (through altering the osmotic gradient), therefore regulating the periciliary liquid (PCL) volume and depth (Bustamante-Marin and Ostrowski 2017). The PCL along with the mucus layer forms the airway surface liquid (ASL) (Lewis, Patial and Saini 2019). The PCL lubricates the airway epithelium and facilitates ciliary beating for effective mucociliary clearance (Bustamante-Marin and Ostrowski 2017). It also provides a media for immunomodulatory proteins (for example leukotrienes, prostaglandins and lipoxins), antimicrobials (e.g. lysozyme and lactoferrin) and chemotactic agents such as: eotaxin which recruits eosinophils, CXCL8 which recruits neutrophils, and CXCL10 which attracts numerous cell types (Gohy *et al.* 2020). When ion transportation malfunctions, as seen in cystic fibrosis patients, the ASL volume is depleted resulting in impaired ciliary function and accumulation of mucus within the airways, which

increases the risk of infection (Lewis, Patial and Saini 2019). This stresses the importance of ciliary function in the innate defence against pathogens (Hollenhorst, Richter and Fronius 2011).

1.7.3 Immunological Barrier Function of Airway Epithelium

In addition to the physical and chemical barrier functions, the airway epithelium also provides an immunological barrier against inhaled pathogens and particles not removed by mucociliary clearance (Loxham, Davies and Blume 2014). Epithelial cells produce lysozyme to break down bacterial capsules, defensins to perforate the bacterial cell membrane, and lactoferrin and transferrin to deplete iron ions required by self-replicating organoids for growth (Frey *et al.* 2020). The epithelium is also able to transport and lumenally release immunoglobulins, Immunoglobulin A and M (IgA and IgM), that possess a joining-chain via their poly Ig receptor that can bind to airway pathogens (Frey *et al.* 2020).

Epithelial cells can also recognise inhaled pathogens using pattern recognition receptors such as NOD like receptors (NLR) and transmembrane toll-like receptors (TLRs); these receptors recognise pathogen associated molecular patterns (PAMPs) which are expressed by pathogens and toxins, and danger associated molecular patterns (DAMPs) which are molecules released by injured cells (Frey *et al.* 2020). DAMPs and PAMPs initiate cellular signalling that result in cytokine and chemokine production, which recruit immune cells into the airways (Heijink *et al.* 2020). This cytokine and chemokine production is rapid; the cytokine and chemokines secreted include Interleukin-1 β (IL-1 β), IL-6, tumour necrosis factor (TNF), CXCL8, CXCL11 and CXCL20, which recruit dendritic cells, T cells, B cells, eosinophils and neutrophils into the airways (Frey *et al.* 2020). This cellular recruitment into the airways can enhance profibrotic cytokine expression such as transforming growth factor- β (TGF- β) within the airways by providing an additional cytokine source or via inducing resident airway cell TGF- β production to promote remodelling (Boxall, Holgate and Davies 2006). For example, eosinophils are a major source of TGF- β 1 in the airway mucosa,

but they also indirectly induce ASM secretion of TGF- β 1 (Halwani *et al.* 2011) (Januskevicius *et al.* 2016).

Airway epithelial cells can also skew the type of inflammatory response, promoting TH2 inflammation through the secretion of alarmins, thymic stromal lymphopoietin (TSLP), IL-25 and IL-33 in allergic asthma (Gohy *et al.* 2020). On exposure to allergen proteases, IL-33 is cleaved, consequently activating type 2 cytokine production (Cayrol *et al.* 2018). Therefore, airway epithelia can orchestrate the type of local inflammatory response.

1.8 Epithelial Barrier Repair in Allergy and Asthma

1.8.1 Epithelial Barrier Dysfunction and Airway Remodelling in Asthma

Inflammatory cytokines TNF- α , IFN- γ , IL-13 and IL-4 have been shown to disrupt airway epithelial barrier function, as evident by reduced transepithelial electrical resistance (TEER) and junctional adhesion protein expression/assembly, and increased permeability to ions and macromolecules (Georas and Rezaee 2014) (Wawrzyniak *et al.* 2017). The immune-regulatory cytokine IL-10, which inhibits effector cell activity, is also significantly lower in asthmatic bronchoalveolar lavage (BAL) fluid and plasma compared to healthy control subjects (Borish *et al.* 1996) (Huang *et al.* 2016). The IL-10 producing cell count, which includes T regulatory (Treg) cells, monocytes and B cells, is also lower in asthma than health (Tomiita *et al.* 2015). Through diminished levels of IL-10 production, the balance between the IL-10 and type 2 cytokine ratio could be disturbed resulting in reduced suppression of the type 2 inflammatory response. Consequently, asthmatics have increased pro-inflammatory cytokine production which promotes a persistent and severe inflammatory response (Trifunović *et al.* 2015).

Airway remodelling and dysfunction was initially thought to be a consequence of chronic inflammation in asthmatics, but it has recently been discovered that the reticular basement membrane is thickened in children with confirmed wheeze and paediatric asthma (Saglani *et al.* 2007) (Payne *et al.* 2003), suggesting that

epithelium dysfunction occurs before the inflammatory process and may be fundamental for pathogenesis through increasing allergen barrier penetration and sensitisation (Bergeron, Tulic and Hamid 2010).

Persistent inflammation, damage and synthesis of growth factors, such as Transforming growth factor- β (TGF- β), can result in aberrant tissue repair to cause airway remodelling (Hough *et al.* 2020). In addition to the thickening of the basement membrane, there is also increased ASM content, extracellular matrix (ECM) protein deposition and increased vascularity in asthmatic airways (Siddiqui *et al.* 2007) (Bergeron, Al-Ramli and Hamid 2009)(Liu *et al.* 2017). Consequently, the airway wall is thickened (Niimi *et al.* 2000) (Asker, Asker and Ozbay 2014) (Siddiqui *et al.* 2009), and the airway lumen diameter is reduced (Gupta *et al.* 2014), which is thought to contribute to fixed airflow obstruction. Overproduction of the protein collagen, the most abundant ECM protein, also results in airway wall stiffness (Hough *et al.* 2020), which determines ASM strain and impacts airway hyperresponsiveness (Noble, McFawn and Mitchell 2007).

Increased airway wall thickening correlates with asthma severity, with fatal asthma showing over a 200% increase in wall thickness compared to non-respiratory cause of death controls (James *et al.* 2002); of which the extent of subepithelial fibrosis correlates with fibroblast (Hoshino, Nakamura and Sim 1998) and myofibroblast cell frequencies (Brewster *et al.* 1990) (Jendzjowsky and Kelly 2019). These extra myofibroblast frequencies, alongside reduced ECM degradation, leads to overproduction of ECM and subsequently fibrosis (Jendzjowsky and Kelly 2019). ECM degradation is regulated by matrix metalloproteinases (MMPs) and tissue inhibitors of metalloproteinases (TIMPs); MMPs break down ECM proteins, whereas TIMPs inhibit MMP enzymatic activity (Chung *et al.* 2019). In asthma, the balance of MMPs and TIMPs are disturbed, which skews ECM in favour of increased matrix deposition (Vignola *et al.* 1998) (Al-Muhsen, Johnson and Hamid 2011).

The vital function of the airway epithelium is dependent on the proper distribution, proportion and functional ability of the differentiated cells that are present within the epithelium (Rock *et al.* 2011). Within asthmatics, there is enlargement of epithelial cells, termed epithelial hypertrophy, and the composition of the epithelium is altered (Erle and Sheppard 2014). There is also increased epithelial shedding, with epithelial clumps commonly being found within BAL fluid and sputum of asthmatic patients, suggesting loss of attachment to the basement membrane (Barnes 1996). This damage and shedding may lead to an increase in allergen barrier penetration and sensitisation. There is also an increase in mucin expression and goblet cell frequencies (termed goblet hyperplasia) (Lambrecht and Hammad 2012), which is reported to be influenced by IL-4 and IL-13 cytokines during cellular differentiation (Atherton, Jones and Danahay 2003). This increase in goblet cell frequency disrupts the ratio of ciliated to secretory cell frequencies, which alongside mucus hypersecretion and ciliary dysfunction, impairs the effectiveness of mucociliary escalator clearance (Whitsett 2018). The changes in the epithelium between asthma and health is shown pictorially in **Figure 1.2**.

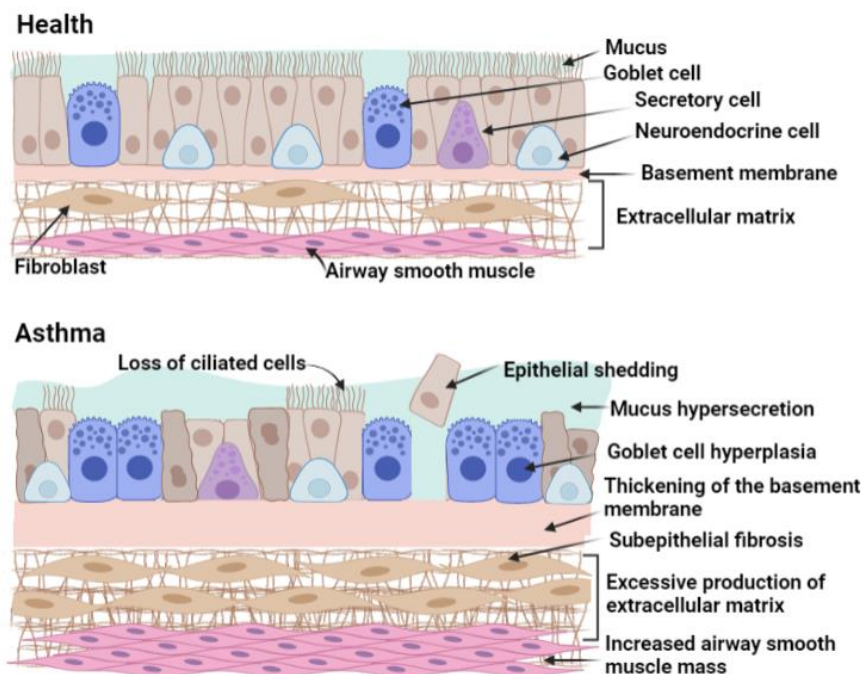


Figure 1.2 Structural Changes Within the Bronchial Airways Between Asthma and Health Created with BioRender.com

Mucus composition is also altered in asthma, with increased MUC5AC production (over MUC5B) associated with type 2 airway inflammation (Lachowicz-Scroggins *et al.* 2016) and increased mucus viscosity so it is more difficult to clear from the airways (Hellings and Steelant 2020). Further disturbing mucociliary clearance, ciliated cell function is also impaired with asthmatic cilia demonstrating abnormal CBF and dyskinesia (abnormal cilia movement) that worsens with disease severity (Thomas *et al.* 2010). With impaired mucociliary clearance, asthmatics have a build-up of mucus within the airways leading to mucus plugging that obstructs the movement of air in and out of the airways (Dunican, Watchorn and Fahy 2018). Consequently, autopsies of asthmatic patients who died due to a fatal asthma attack reveal mucus plugging within the large proximal airways (Dunican, Watchorn and Fahy 2018). Dunican *et al.* (2018) suggest airway eosinophilia and type 2 cytokine gene expression in sputum are associated with mucus plugging in asthma.

Not only is the cellular composition altered, but cellular interactions are also reduced. Tight junction and adheren junction protein immunohistochemistry show patchy localisation in asthmatics compared to healthy controls, which have continuous staining throughout the epithelium (de Boer *et al.* 2008) (Xiao *et al.* 2011). By reducing cell-cell adhesion, the ability of the epithelium to function as a barrier is compromised (Davies 2014). Loss of function mutations in Filaggrin, an important barrier protein which contributes to barrier formation, is also reported to confer major susceptibility to atopic diseases including atopic asthma (Palmer *et al.* 2007) (Basu *et al.* 2008) (Rodriguez *et al.* 2009) (Irvine, McLean and Leung 2011). Epithelial barrier dysfunction is supported by evidence indicating asthmatics have reduced TEER and increased permeability to macromolecules compared to healthy individuals (Xiao *et al.* 2011). Additionally, asthmatic epithelial cells are also found to produce lower amounts of interferon-beta and -lambda (IFN- β and λ), which may partly explain why asthmatics have increased viral infection susceptibility (Kelly and Busse 2008).

To reverse these abnormalities, and effectively reduce the symptoms of asthma, the epithelium will need to undergo efficient repair. In order to achieve this theoretically it would be beneficial to reduce inflammation first and then target epithelial repair, as exposure of the repairing epithelium to inflammatory cytokines such as IL-4 and IL-13 can drive goblet cell differentiation; which would disrupt mucociliary escalator function in the regenerated area of the airway. By taking anti-inflammatories (to reduce systemic inflammation), the self-perpetuating, persistent inflammatory response in the airways may be halted to prevent hinderance of the repair process. The restored epithelial barrier function (due to appropriate cellular frequencies) will then reduce allergen barrier penetration and sensitisation, to ultimately improve asthma symptoms.

1.8.2 The Epithelial Mesenchymal Trophic Unit

The pathological changes of airway remodelling are orchestrated by the numerous cell types present within the airway wall and submucosa (Hough *et al.* 2020). The submucosa, which is located beneath the mucosal layer consisting of the epithelium, basement membrane and collagen layer, is a fibroblast and proteoglycan layer which is embedded in collagen and elastin (Eskandari, Pfaller and Kuhl 2013). The interaction between the epithelium and the underlying mesenchymal cells in asthma is thought to reactivate the epithelial mesenchymal trophic unit (EMTU), which is associated with lung morphogenesis during lung development, to drive airway remodelling (Holgate *et al.* 2004). Conceptually, the reactivation occurs because the EMTU is abnormally sensitive to environmental agents due to genetic and environmental factors, such as cigarette smoke exposure during foetal development, which predisposes the airways into developing asthma (Henderson and Warner 2012).

The EMTU consists of the epithelial and mesenchymal layer, with the basement membrane (containing ECM proteins and nerves) interfacing between the two (Evans *et al.* 1999). The EMTU model proposes that a defective epithelium consequently leads to repetitive environmental challenge that drives airway inflammation and pathological remodelling (Shifren *et al.* 2012). Supportive

evidence of the EMTU concept is mainly derived from findings of conditioned media exposure experiments, epithelial and mesenchymal coculture experiments or ECM co-culture models (Osei, Booth and Hackett 2020).

1.8.3 Epithelial Damage and Dysregulated Repair in Asthma

The bulk of evidence indicating airway epithelium damage occurs in asthmatics comes from investigating the upregulation of markers of repair, such as cell adhesion molecule CD44 (Holgate 2000) (Lackie *et al.* 1997) (Leir *et al.* 2000). Epigenetic regulation of epithelial gene expression is also explored, with connexin37 (*GJA4*), cadherin-26 (*CDH26*) and cadherin-related family member 3 (*CDHR3*) being reported as linked to asthma susceptibility and the altered biology and function of the airway epithelium in asthmatics (Heijink *et al.* 2020). Expression quantitative trait loci studies highlight numerous genes involved in epithelial function, such as interleukin 1 receptor-like 1 (*IL1RL1*), thymic stromal lymphopoietin (*TSLP*) and *CDHR3* as risk alleles for asthma development, supporting the role of the epithelium in asthma pathogenesis (Heijink *et al.* 2020).

Genome-wide association studies (GWAS) have also identified numerous epithelial susceptibility genes, including epithelial derived cytokines *IL1RL1*, interleukin 18 receptor 1 (*IL18R1*), interleukin-33 (*IL-33*) and *TSLP*, and numerous genes that have a role in regulating epithelial e.g. protocadherin-1 (*PCDH1*), *CDHR3* and orosomucoid-like 3 (*ORMDL3*) (Loxham and Davies 2017). *PCDH1* is reported to regulate epithelial function (Faura Tellez *et al.* 2016) and canonical transforming growth factor- β (TGF- β) signalling (Faura Tellez *et al.* 2015), whereas, *CDHR3* is involved in cellular interactions and the polarity of the epithelium (Heijink *et al.* 2020). Mucociliary clearance genes such as mucin *MUC5AC*, and *KIF3A* and *EFHC1* involved in ciliary function are also implicated (Heijink *et al.* 2020).

ORMDL3, the most well-known asthmatic epithelial-associated GWAS signal, is associated with increased asthma development risk through altering the cellular stress level response of the epithelium, and thus its damage response. GWAS

comparing asthmatics and non-asthmatics highlighted that single nucleotide polymorphisms within the *ORMDL3* gene is associated with childhood onset of asthma (Moffatt *et al.* 2010). *ORMDL3* regulates endoplasmic reticulum calcium signalling through reducing sarco-endoplasmic reticulum calcium ATPase (SERCA) activity, a calcium pump that returns calcium to the ER resulting in reduced ER calcium levels (James, Milstien and Spiegel 2019). Low ER calcium levels increase cellular stress levels through facilitating the levels of misfolded and unfolded proteins within the ER; this activates the unfolded protein response which will either repair the damage or induce apoptosis depending on severity of the cellular damage caused (Cantero-Recasens *et al.* 2010) (Miller *et al.* 2014). To add to this increased damage susceptibility, the asthmatic bronchial airways also display decreased ki67, p27 and increased cell cycle inhibitor p21^{waf}, which suggests that the epithelium will have a reduced ability to repair following damage (Puddicombe *et al.* 2003) (Fedorov *et al.* 2005) (Semlali *et al.* 2010). This is supported by the report that airway epithelial cells from asthmatic children take a significantly longer time to repair than healthy controls (Stevens *et al.* 2008).

1.9 Normal Airway Epithelial Repair

1.9.1 The Tissue-specific Stem Cell

Terminally differentiated airway cells (ciliated and mucus secreting cells) are incapable of self-renewal, and the loss of these airway luminal cells due to inflammation or injury must be replaced by multipotent cells (Tilley *et al.* 2015) (Rock *et al.* 2011). These cells include local tissue-specific stem cells (TSCs), their direct descendent the transit-amplifying cell (TAC), which can rapidly proliferate but only possess the ability to differentiate into a luminal cell fate, and progenitor cells, which are also limited to a basal or luminal cell fate (Reynolds *et al.* 2012). The TSC is defined as a cell capable of self-renewal as well as differentiation into all the different mature cells located within the local tissue environment (Loeffler and Roeder 2002).

Cell turnover in the airways is usually slow however, in response to injury, the epithelium undergoes rapid proliferation of surviving cells to restore barrier

function (Crystal *et al.* 2008). The airway epithelial lining can be divided into three regions: the tracheobronchial, the bronchiolar and the alveolar airways, of which each region has a TSC capable of restoring the epithelium; club cells do so in the bronchiolar region, type II cells in the alveolar region and basal cells within the tracheobronchial region (Carraro and Stripp 2015). Multiple studies support that basal cells are the source of tissue-specific stem cell responsible for repair within the tracheobronchial airways (Rock *et al.* 2009) (Brechbuhl *et al.* 2011) (Teixeira *et al.* 2013).

1.9.2 Basal Cell Renewal and Proliferation

Teixeira *et al.* (2013) state basal cell division must be precisely shaped to meet homeostatic and regenerative needs; in order to provide this, the basal population frequencies must remain fairly constant. To conserve their numbers, stem cells on average must produce one basal cell and one differentiated cell; this asymmetric division can be either on a single cell basis or as a population on a whole (Simons and Clevers 2011). On a population as a whole, stochastic division (a random determination of cell fate) would mean that there are three possible fate outcomes: two symmetric cell duplications (two stem cells produced), asymmetric division (one stem cell and one differentiated cell produced) or terminal division (where both cells undergo differentiation) (Teixeira *et al.* 2013). The canonical Wingless/integrase (WNT) 1 pathway is thought to regulate basal cell renewal and proliferation (Brechbuhl *et al.* 2011) (Habib *et al.* 2013).

The canonical WNT pathway promotes the long-term renewal of stem cells, and controls asymmetric stem cell differentiation (Okuchi *et al.* 2020). During stem cell proliferation, a spatially localised WNT signal orients the mitotic division plane of stem cells, so that WNT signalling components are distributed asymmetrically; in doing so the cell closest to the WNT signal maintains a stem cell, whereas the distal cell differentiates (Habib *et al.* 2013) (Okuchi *et al.* 2020)

Through inhibiting the canonical WNT pathway, the noncanonical WNT pathway can regulate stem cell proliferation. WNT5A has been shown to inhibit rat adipose-derived stem cell (Tang *et al.* 2018), haematopoietic stem cell (Povinelli and Nemeth 2014) and human umbilical vein endothelial cell (Cheng *et al.* 2008) proliferation. Miyoshi *et al.* (2012) investigated WNT signalling in intestinal stem cells during colonic crypt repair. They found that WNT5A was highly expressed in the colonic wound bed compared to uninjured adjacent mucosa, and that this localisation was not associated with canonical WNT-active, proliferative epithelial cells. Miyoshi *et al.* (2012) demonstrated that WNT5A-ROR2 signalling decreased intestinal epithelial cell proliferation driven by canonical WNT signalling through activation of the TGF- β R, which initiated the TGF- β -SMAD dependent cascade. Miyoshi *et al.* (2012) therefore concluded that crypt formation occurs through WNT5A locally inhibiting proliferation of stem cells within the wound channel to ensure correct organisation of the regenerating epithelium.

These papers highlight the potential of noncanonical and canonical WNT signalling intersecting. Canonical WNT signalling appears to regulate basal cell renewal and proliferation, and consequently differentiation through asymmetric division, whereas, noncanonical WNT signalling appears to be responsible for the spatial designation of the daughter cells to ensure correct epithelial architecture is maintained.

1.9.3 Basal Cell Differentiation

The differentiation of basal cells into luminal cells is highly Notch dependent (Carraro and Stripp 2015), and Notch inhibition reduces basal cell differentiation, instead promoting self-renewal and survival of irradiated basal cells (Giuranno *et al.* 2020). There are four Notch paralogue transcripts (Notch 1-4), however, Notch-1 is enriched within the basal cell population (Rock *et al.* 2011). During cellular differentiation of p63+ basal cells, the level of Notch present dictates the lineage acquired, with sustained Notch activity promoting differentiation into a secretory lineage (either Club cells or Goblet cells), and low Notch activity into a

ciliated cell fate (Rock *et al.* 2011) (Pardo-Saganta *et al.* 2015). Further research into airway epithelial lineage hierarchy have identified that there are multiple intermediary progenitor cell populations throughout this process (Pardo-Saganta *et al.* 2015) (Pan *et al.* 2014).

One mechanism which controls Notch levels within the airways is oxygen availability, as basal cell differentiation into ciliated cells is inhibited in *in vitro* submerged cultures. This mechanism was identified by Gerovac *et al.* (2014), who showed that the volume of transwell apical fluid altered ciliogenesis in rat tracheal epithelial cells, and that this inhibition of ciliated cell differentiation is determined by oxygen availability (determined by levels of hypoxia markers HIF-1 α and HIF-2 α). Through using the Notch γ -secretase inhibitor, ciliated cell differentiation was restored in submerged, hypoxic conditions similar to the levels seen at ALI.

The level of Notch signalling throughout repair is important in determining stem cell renewal and daughter cell fate. As asthmatics have an increase in goblet cell frequencies, disrupting the ratio of secretory to ciliated cells in the mucociliary escalator, mucus plugging of the airways is increased; it is therefore important to understand how to manipulate basal cell differentiation into a ciliated fate in order to restore mucociliary escalator function. The cilia on these cells also need to be functional, with a normal CBF, to effectively move mucus out of the airways.

1.9.4 Cellular Migration into the Wound Bed

For epithelial cells to migrate to a site of damage, they must undergo epithelial-mesenchymal transition (EMT). The EMT process involves loss in cell polarity and an increase in migratory ability (Xu, Lamouille and Derynck 2009). EMT can be induced *in vitro* by TGF- β 1-SMAD3 signalling in human airway epithelial cells (Hackett *et al.* 2009). During the EMT process, there is a loss of epithelial markers and an increase of mesenchymal markers (Rout-Pitt *et al.* 2018). This mesenchymal transition increases the cells migratory ability and invasiveness, allowing the cell to downregulate key epithelial cell-cell adhesion proteins, such

as E-cadherin, to leave the epithelial barrier it was a component of and relocate to the damaged area for replication (Kalluri and Weinberg 2009).

For migration to occur, the cell must also be able to remodel the provisional ECM in order to degrade cell-ECM contacts en route to the site of damage (Legrand *et al.* 1999). This is achieved via MMPs, which are regulated by WNT signalling (Pongracz and Stockley 2006). Additionally, migrating cells need to induce planar cell polarity (PCP) signalling to regulate actin polarisation and microtubule cytoskeletal dynamics required for directional cellular movement; this is thought to be mediated by the noncanonical WNT-PCP pathway, but current evidence has not established whether the role of WNTs are instructive or permissive in PCP operations (Vladar and Königshoff 2020). However, with a strong association with PCP signalling, a role in mediating ECM degradation and an ability to direct cells to maintain correct tissue architecture during organogenesis or repair, noncanonical WNT signalling appears vital for cellular migration in repair (alongside the TGF- β pathway which induces EMT).

1.9.5 Summary of the Airway Wound Healing Process

Following wounding, cells at the edge of the wound bed begin to spread, dedifferentiate and undertake epithelial-mesenchymal transition (EMT) to migrate into the wound bed and lay down a provisional matrix to rapidly restore some barrier protection (Grainge and Davies 2013). The basal cells then undergo proliferation and differentiation to restore the luminal cells that were shed or destroyed by inflammation (Iosifidis *et al.* 2020). This process is shown in **Figure 1.3**. The fibroblasts underlying the epithelium are also induced to proliferate, and differentiate into myofibroblasts, to secrete ECM proteins that provide a scaffold for cellular migration across the basement membrane (Grainge and Davies 2013).

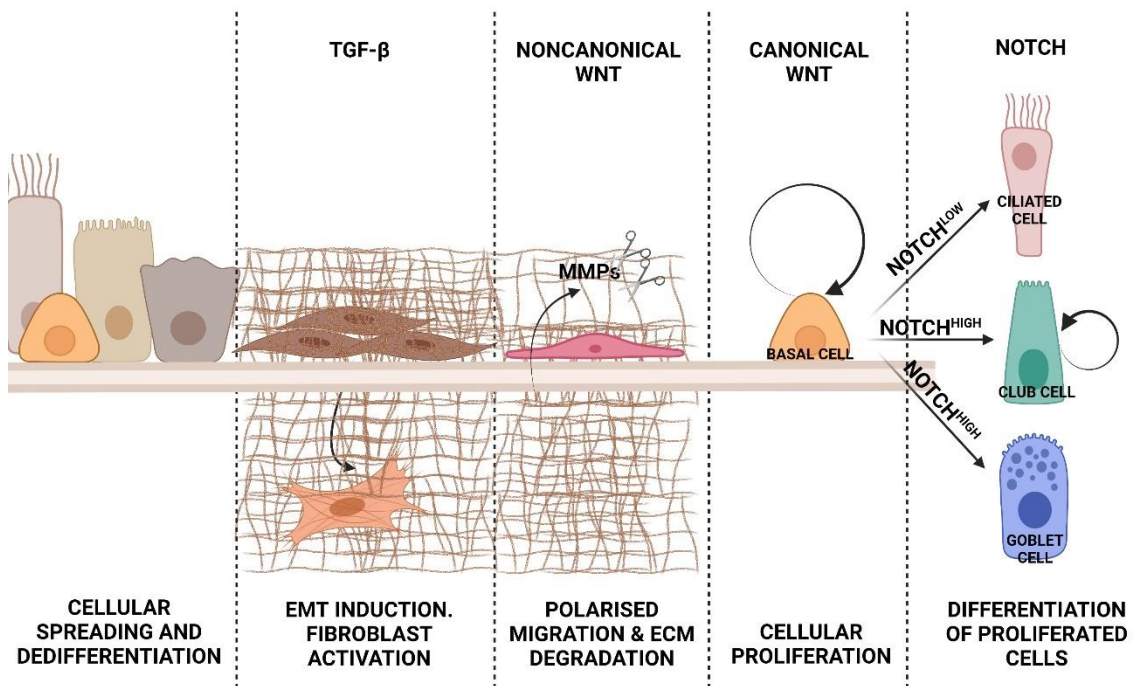


Figure 1.3 The Airway Wound Healing Response Labelled with Key Epithelial Repair Pathways Roles. Following wounding to the airway epithelium, TGF- β activation induces fibroblast secretion of ECM and induces cells proximal to the wound edge to dedifferentiate and undergo EMT. The newly synthesised ECM provides a matrix for the cells to migrate into the wound bed, however, the ECM may also need to be degraded en route to the area of repair. The gene transcription of MMPs and plasminogen, ECM proteolytic enzymes, are regulated by noncanonical WNT signalling. Noncanonical WNT PCP signalling also mediates the polarised migration of the cells into the wound bed. Once the wound bed is fully covered, the basal cells, the known progenitor cell of the tracheobronchial epithelium, can regenerate the luminal cells that were shed or destroyed by inflammation. Basal cell renewal and proliferation appears to be regulated by β -catenin dependent canonical WNT signalling, and cell differentiation is mediated by Notch. A sustained notch signal promotes differentiation into secretory cells, whereas reduced notch signalling induces differentiation into a ciliated cell fate. The newly synthesised and differentiated daughter cells can then form cell-cell adhesion junctions with neighbouring epithelial cells to restore epithelial barrier function. Created with BioRender.com.

1.10 Epithelial Repair Pathways

1.10.1 WNT Signalling

WNT signalling is vital for lung development, with homozygous knock out studies in mice highlighting that total loss of function of WNT ligands, receptors and WNT-associated proteins results in foetal death or death at birth, as summarised by Hussain *et al.* (2017: A). Other than embryogenesis, WNT signalling is known to play roles in stem cell self-renewal, specification of cell fate, and cell proliferation,

polarity, migration and survival (Koopmans and Gosens 2018). WNT signalling is associated with the pathogenesis and the progression of numerous chronic lung diseases, including idiopathic pulmonary fibrosis (IPF), asthma and chronic obstructive pulmonary disease (COPD) (Baarsma and Königshoff 2017).

In humans to date there are 19 currently known WNT ligands, which bind to several membrane-bound receptors (Kumawat and Gosens 2016). In primary lung tissue samples and cell lines, the WNT ligands WNT1, WNT3, WNT3A, WNT4, WNT5A, WNT5B, WNT7A, WNT7B and WNT10B are expressed (Winn *et al.* 2005) (Königshoff *et al.* 2008) (Heijink *et al.* 2013). The WNT ligands are secreted proteins which undergo post-translational modifications palmitoylation (in order to activate cellular signalling on receptor binding) and glycosylation (to permit secretion) (Kurayoshi *et al.* 2007). The WNT receptors include 10 class Frizzled (FZD) receptors, multiple non-class Frizzled receptors (such as RYK, PTK7, ROR1 and ROR2) and low-density lipoprotein receptor-related protein (LRP) 5/6 co-receptors (Green, Nusse and Amerongen 2014) (Hussain *et al.* 2017: A). On receptor binding, there are two branches of intracellular WNT signalling that are initiated: the canonical β -catenin dependent pathway and the non-canonical β -catenin independent pathways (Li *et al.* 2015). WNT ligands therefore have typically been grouped as either canonical or noncanonical pathway activators however, under certain conditions, some WNT ligands can stimulate activation of both the noncanonical and canonical pathway; WNT5A, for example, is typically a noncanonical activator, but is also able to activate the canonical pathway in the presence of LRP5 and FZD4 (Mikels and Nusse 2006).

The canonical WNT β -catenin pathway is activated by WNT ligand binding to a FZD receptor and LRP5/6 co-receptor (Kumawat and Gosens 2016). In the absence of WNT ligand binding, β -catenin is phosphorylated by a destruction complex consisting of glycogen synthase kinase 3 β (GSK3 β), adenomatous polyposis coli (APC), Axis inhibition protein (AXIN) and casein kinase 1 (CK1 α), which results in its ubiquitination and subsequent proteasome degradation by E3-ubiquitin ligases (Sharma and Pruitt 2020). Upon ligand binding, however,

dishevelled (DVL) is recruited and the destruction complex is disabled, so β -catenin is free to accumulate and translocate into the nucleus to bind to the LEF/TCF transcription factor complex, to regulate gene expression associated with stem cell renewal, cell fate, and cell proliferation and differentiation (Skronska-Wasek *et al.* 2018) (Li *et al.* 2015). In addition to mediating canonical WNT transcriptional activity, β -catenin is also a component of the adherens junction (alongside E-cadherin); of which the conformation of β -catenin specifies its function rather than competitive binding between E-cadherin and TCF/LEF (Brembeck, Rosario and Birchmeier 2006).

The two best characterised non-canonical pathways include the WNT/ Ca^{2+} and WNT/planar cell polarity (PCP) pathway (Kumawat and Gosens 2016). The WNT/ Ca^{2+} pathway, via a WNT-FZD-ROR2 complex, triggers phospholipase C (PLC) activity that leads to the generation of DAG and IP_3 , that elevates intracellular calcium ion concentration to activate protein kinase C ($\text{PKC}\alpha$) and subsequently cell division cycle 42 protein (CDC42), calcineurin and Ca^{2+} /calmodulin-dependent protein kinase 2 (CaMKII) cellular signalling cascades, that regulate cell adhesion and migration (Sharma and Pruitt 2020) (Semenov *et al.* 2007). CaMKII can also activate TGF- β activated kinase 1 (TAK1) and subsequently Nemo-like kinase (NLK), which can inhibit β -catenin gene transcription (Semenov *et al.* 2007). The PCP pathway, however, recruits DVL to a FZD and co-receptor complex, which interacts with Ras-related C3 botulinum toxin substrate 1 (Rac1) and DVL-associated activator of morphogenesis 1 (DAAM1), to subsequently activate c-Jun kinases (JNK) and Ras-homologous A (RhoA) respectively, of which RhoA further activates ROCK (Sharma and Pruitt 2020) (Semenov *et al.* 2007). ROCK regulates cytoskeletal dynamic processes such as cell polarity, migration and asymmetric cell division (Vladar and Königshoff 2020). An illustration of the WNT signalling pathways are shown in **Figure 1.4**.

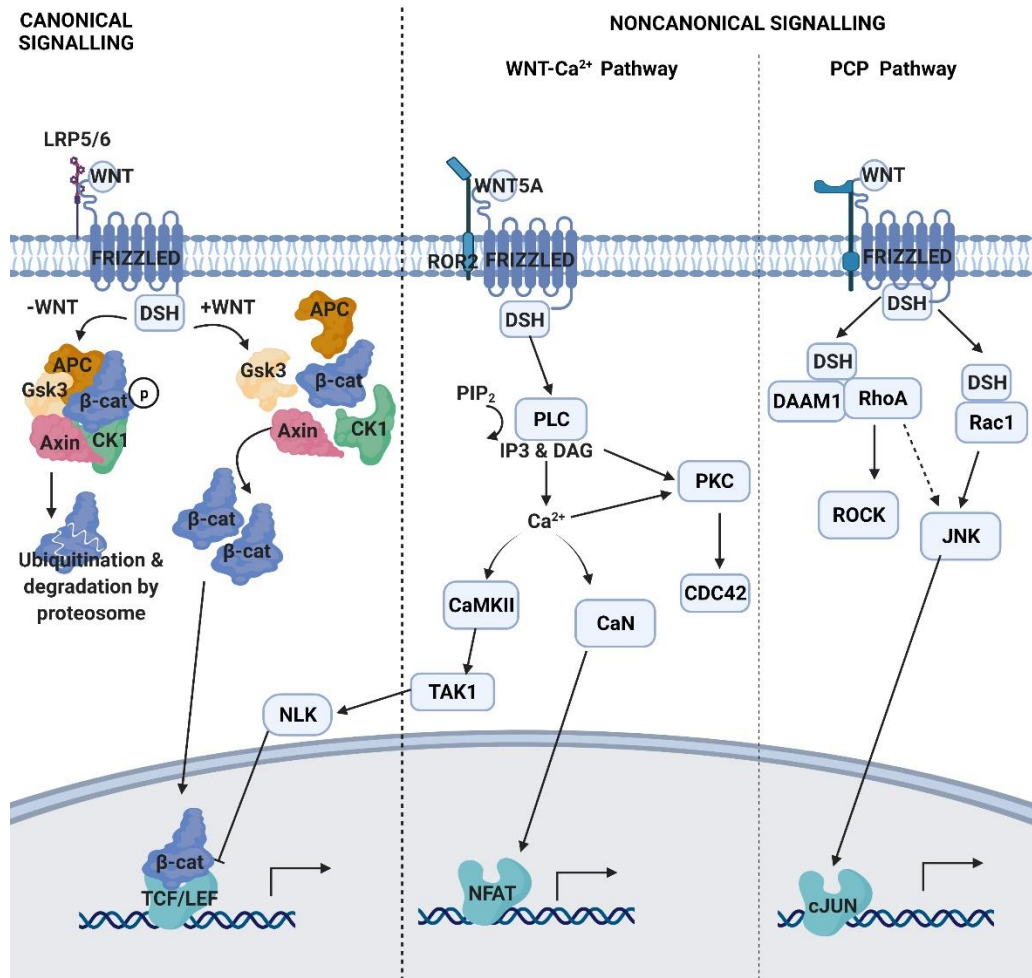


Figure 1.4 WNT Signalling Pathways. Created with BioRender.com.

WNT5A is the most extensively studied noncanonical WNT ligand. WNT5A has two isoforms, WNT5A-L and WNT5A-S, which are composed of 380 and 365 amino acids respectively (Kumawat and Gosens 2016). WNT5A can signal through numerous receptors, including FZD2-8, ROR2, RYK and CD146 (Kumawat and Gosens 2016). ROR2 and WNT5A gene knockout in the lung however display a similar phenotype, suggesting an important role for WNT5A ROR2 signalling in lung development (Oishi *et al.* 2003).

Adding to the complexity of WNT signalling, there is coordinated interplay between the canonical and noncanonical pathways of WNT signalling (Sharma and Pruitt 2020). This can be achieved at the receptor level through competing for receptor binding (Grumolato *et al.* 2010) or via downstream signalling

crosstalk mechanisms such as TAK1 and PKC (Ishitani *et al.* 2003) (Gwak *et al.* 2006) (Baarsma *et al.* 2017) (Lee *et al.* 2010).

1.10.2 TGF- β Signalling

TGF- β is involved in numerous biological processes including cell proliferation, death and differentiation, specification of cell fate, ECM synthesis, organogenesis, tissue regeneration and the immune response (Saito, Horie and Nagase 2018), and is considered a key player in airway remodelling (Murdoch and Lloyd 2010). TGF- β has three isoforms: TGF- β 1, TGF- β 2 and TGF- β 3 (Michalik *et al.* 2018). Both TGF- β 1 and TGF- β 2 are differentially expressed during wound healing (Ito *et al.* 2011), however, TGF- β 1 is more widely studied for its role in asthma; a meta-analysis study suggests that polymorphisms within the *TGFB1* gene are associated with an increased risk of asthma development (Yao *et al.* 2016). TGF- β 1 can alter mesenchymal cell proliferation (Khalil *et al.* 2005)(Xiao *et al.* 2012), induce fibroblast secretion of ECM proteins (such as collagens I and III, fibronectin and proteoglycan) (Halwani *et al.* 2011), and promote differentiation of fibroblasts into myofibroblasts, which have high ECM synthesis activity (Batra *et al.* 2004). TGF- β 1 can also induce EMT, further contributing to fibroblast cell numbers within the airways; of which asthmatics are reported to undergo more extensive EMT in response to TGF- β than healthy individuals (Hackett *et al.* 2009).

TGF- β 1 can influence expression of MMPs and TIMPs, which alongside increasing mesenchymal frequencies and ECM synthesis through the numerous means listed can induce ECM deposition within the airways (Zhou *et al.* 2007) (Ye *et al.* 2011) (Lechapt-Zalcman *et al.* 2006). TGF- β 1 can also induce angiogenesis, another characteristic feature of airway remodelling (Viñals and Pouysségur 2001). Predictably, TGF- β 1 expression correlates with airway wall thickening (Boxall, Holgate and Davies 2006), and is linked to bleomycin-induced pulmonary fibrotic changes and IPF (Higashiyama *et al.* 2007) (Khalil *et al.* 1996) (Khalil *et al.* 2001).

TGF- β is synthesised and secreted bound to latency-associated peptide (LAP), which prevents TGF- β receptor binding (Bauché and Marie 2017). The LAP-TGF- β complex can covalently associate with Latent TGF- β -binding protein (LTBP) to form a large latent complex, that on association determines TGF- β storage localisation within the ECM and its potential activation (Worthington, Klementowicz and Travis 2011). TGF- β needs to be activated in order to bind to its receptor and initiate a signalling cascade that modulates gene transcription (Saito, Horie and Nagase 2018). The TGF- β isoforms have been proposed to be activated by numerous physiological situations, including reactive oxygen species (ROS) (Krstić *et al.* 2015), acidic pH (Lawrence, Pircher and Jullien 1985), multiple proteases (Yu and Stamenkovic 2000) (Sato and Rifken 1989), heat (Yang *et al.* 1999), mechanical stress (Wells 2013) and the membrane glycoprotein thrombospondin-1 (Crawford *et al.* 1998). The main activator, however, is thought to be the integrins (Nolte and Margadant 2020). Of the twenty-four integrin receptors, six have been reported to bind and activate latent TGF- β ($\alpha\beta3$, $\alpha\beta5$, $\alpha\beta6$, $\alpha\beta8$, $\alpha\beta1$, $\alpha8\beta1$), however, only four are suggested to have demonstrated the release of the activated TGF- β form following binding; these four integrins are: $\alpha\beta3$, $\alpha\beta5$, $\alpha\beta6$ and $\alpha\beta8$ (Worthington, Klementowicz and Travis 2011) (Nolte and Margadant 2020).

Upon activation, TGF- β can bind to the TGF- β RII homodimer of the TGF- β receptor (TGF- β R), which then phosphorylates the TGF- β RI homodimer (Aschner and Downey 2016). In the canonical TGF- β pathway, SMAD2/3 are recruited to the receptor and phosphorylated (Saito, Horie and Nagase 2018). Phosphorylated SMAD2 or SMAD3 can then bind to SMAD4 or TIF1 γ (also called TRIM33) to form a complex that can translocate into the nucleus to activate or repress gene transcription (Bauché and Marie 2017). Inhibitory SMADs, e.g. SMAD7, can inhibit this downstream signalling through numerous mechanisms, including competing with SMAD2/3 for TGF- β RI binding, promoting degradation of TGF- β RI and preventing SMAD2/3/4 complex formation and therefore transcriptional activity (Miyazawa and Miyazono 2017).

However, TGF- β R signalling can also directly activate non-SMAD mediated pathways, such as PI3K, JNK, ERK and p38 (Aschner and Downey 2016). TGF- β receptor signalling can signal through TRAF6 and TAK1, that activates MKK3/6 and MKK4 to activate p38 and JNK respectively, and via ShcA to activate Erk signalling (Zhang 2017). Through TAK1 activation of NLK, TGF- β can inhibit β -catenin-dependent WNT signalling and transcriptional activity (Ishitani *et al.* 1999). SMAD7, rather than inhibiting as it does with SMAD2/3 signalling, enhances activation of the TAK1-p38-JNK pathway (Miyazawa and Miyazono 2017). TGF- β can also signal directly via PI3K and CDC42, and RhoA and ROCK (Zhang 2017). The cell signalling pathway that results after TGF- β R binding appears to depend on the cell type, the cellular condition and the cellular microenvironment of which the receptor is located (Makinde, Murphy and Agrawal 2007). Both the SMAD-mediated and non-SMAD mediated TGF- β pathways are displayed pictorially in **Figure 1.5**.

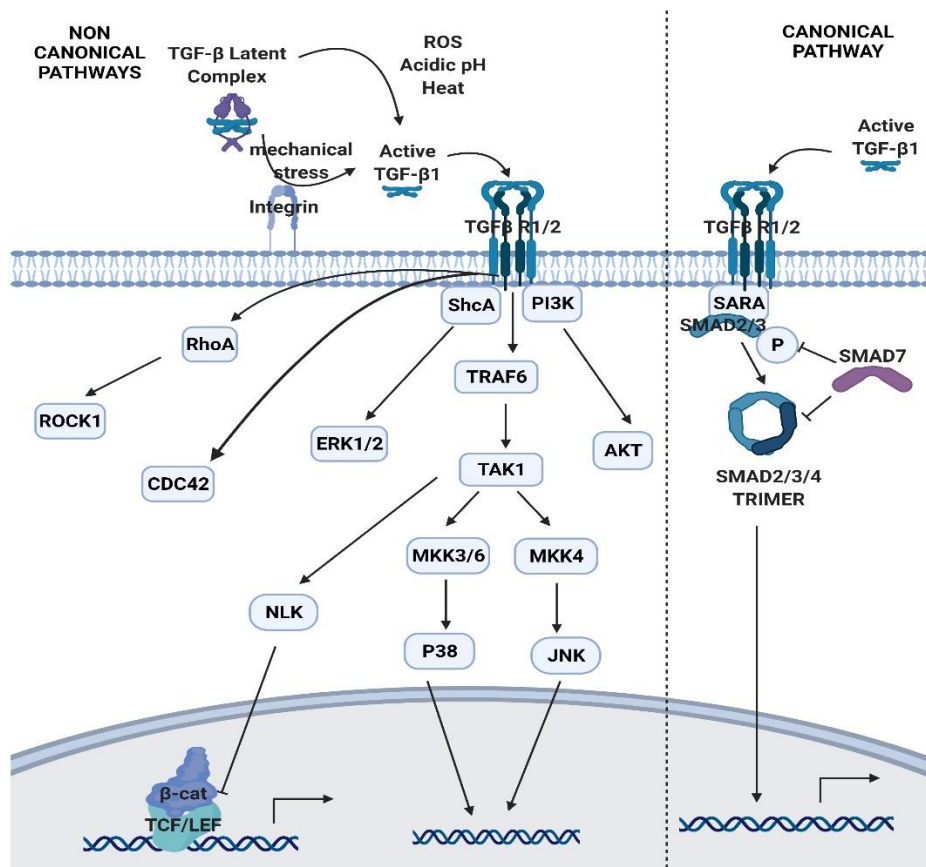


Figure 1.5 TGF- β Signalling Pathways. Created with BioRender.com.

1.11 Evidence of WNT5A and TGF- β 1 Roles in Asthma Development and Repair

1.11.1 WNT5A and TGF- β 1 in Lung Development

Both WNT5A and TGF- β 1 play a vital role in lung development. WNT5A knockout mice die shortly after birth due to what appears to be respiratory failure, and on examination of the lungs a truncated trachea and increased airway branching is observed (Li *et al.* 2002). Embryonic mouse lungs excised at day 11 and exposed to varying doses of TGF- β 1 also display reduced branching (Zhao *et al.* 1996). This suggests that WNT5A and TGF- β 1 have parallel roles in mediating branching morphogenesis in the lung. Similarly, TGF- β 1 and WNT5A have similar effects on mammary gland development; this is because TGF- β 1 regulates WNT5A expression, which partly mediates TGF- β 1 effects on branching inhibition (Roarty and Serra 2007). Suppression of WNT5A or TGF- β increases the activity of the β -catenin dependent WNT pathway in mammary epithelium, suggesting a dual role of WNT5A and TGF- β in inhibiting β -catenin signalling (Roarty *et al.* 2009). Airway branching may also exhibit a similar functional interaction between WNT5A, TGF- β 1 and β -catenin.

1.11.2 Genetic Associations Between WNT5A, TGF- β 1 and Asthma Susceptibility

Several GWAS have highlighted genetic links between *TGFB1*, *WNT5A* and asthma risk. A C-509T polymorphism in the *TGFB1* promoter region (Silverman *et al.* 2004) and numerous *TGFB1* polymorphisms have been identified, both of which are reported to contribute to asthma pathogenesis (Sharma *et al.* 2009) (Sharma *et al.* 2012) (Li *et al.* 2007) (Zhang *et al.* 2010). Additionally, *SMAD3* and *SMAD3* promoter methylation have also been implicated in contributing to asthma susceptibility in numerous genetic studies of asthma, suggesting a strong link between TGF- β signalling and asthma (Shrine *et al.* 2019) (Barreto-Luis *et al.* 2017) (Torgerson *et al.* 2011) (Moffatt *et al.* 2010) (Lund *et al.* 2018) (DeVries *et al.* 2017).

Similarly, WNT5A also displays a strong association with asthma, with both *SMAD3* and *WNT5A* being highlighted as differentially expressed between asthmatic and healthy subjects in the peripheral airways (Singhania *et al.* 2017). *WNT5A* and *SMAD3* were also significantly associated with asthma susceptibility in a study by Barreto-Luis and colleagues (2017). This study by Barreto-Luis *et al.* (2017) identified the WNT signalling pathway as enriched in asthma GWAS data, with 152 WNT-associated genes being highlighted as differentially expressed between asthmatic subjects and controls, but that polymorphisms in the WNT5A receptors *FZD3* and *FZD6* were particularly associated with asthma risk (Barreto-Luis *et al.* 2017).

1.11.3 Associations Between WNT5A and Inflammatory Signatures in Asthma

WNT5A is correlated with a positive TH2 signature in mild-moderate asthmatic bronchial biopsy tissue, and its receptor *FZD5* associates with TH2-high asthma (Choy *et al.* 2011), suggesting a link between WNT5A and asthma. IL-13 stimulation has also been shown to increase *WNT5A* mRNA and protein expression a dose-dependent manner in human nasal epithelial cells, however on the contrary to Choy *et al.* (2011), *FZD5* mRNA and protein expression was decreased in a dose dependent manner following IL-13 administration suggesting an inverse relationship with a TH2 asthmatic signature (Shi *et al.* 2021). This is supported further by a study by Syed *et al.* (2007) which revealed *WNT5A* is increased in peripheral blood mononuclear cells (PBMCs) following treatment with TH2 cytokines IL-4 and IL-13. On the contrary, DNA methylation of the *WNT5A* receptor *ROR2* in peripheral blood monocytes has been reported to be associated with neutrophilic asthma (Gunawardhana *et al.* 2014). TH17 cells are reported to promote airway neutrophilia both directly and indirectly (Pelletier *et al.* 2010). Supporting the link between WNT5A and TH17 status, *WNT5A* has a chemotactic effect on neutrophils and so can induce neutrophilic infiltration (Jung *et al.* 2013). *WNT5A* expression has also been reported to induce the TH17 cytokine IL-17 (Liu *et al.* 2019: B) (Tian, Mauro and Li 2019).

1.11.4 Associations Between TGF- β 1 and Inflammatory Signatures in Asthma

TGF- β 1 stimulation in combination with IL-6 can induce naïve T cell differentiation into TH17 cells through the induction of STAT3 and the lineage-determining transcription factor ROR γ t (Bettelli *et al.* 2006) (Choi *et al.* 2021). However, Das *et al.* (2009) report that TGF- β indirectly promotes differentiation into a TH17 cell fate through suppressing TH1 and TH2 cellular differentiation transcription factors STAT4 and GATA-3. On the contrary to this, Smeltz *et al.* (2005) found that TGF- β only inhibited TH2 differentiation via GATA-3 reduction in murine T cells but that TH1 cell frequencies were enhanced. Similarly, knockdown of TAK1 is reported to induce TH2 cytokine production (Vink *et al.* 2013), and its inhibition is reported to exhibit a TH1 to TH2 cytokine shift in T lymphocytes (Cao *et al.* 2015). This supports that in addition to promoting TH17 differentiation, TGF- β 1 may also enhance TH1 differentiation in certain cells as reported by Smeltz *et al.* (2005). Courties *et al.* (2010), however, report that TAK1 silencing decreases both TH1 and TH17 cell frequencies. This is in line with the earlier mentioned studies in that reduced noncanonical TGF- β -TAK1 signalling skews inflammation towards a TH2 driven response. Canonical TGF- β signalling may also contribute to TGF- β mediated TH17 differentiation as SMAD2/3 double knockout abolishes TGF- β dependent induction into a TH17 cell fate; this occurs as the knockout increases IL-2 production, which partially represses TH17 development (Takimoto *et al.* 2010). Tanaka *et al.* (2018) also identified that SMAD2 can bind to Trim33 to regulate *IL17A* and *IL10* transcription indicating SMAD2 also plays a more direct role in TH17 differentiation.

1.11.5 Evidence of WNT5A in Epithelial Repair

WNT5A expression is increased following lung injury (Villar *et al.* 2011: A) (Villar *et al.* 2014) and is upregulated in asthmatic mouse (Kwak *et al.* 2015) and IPF lung tissue (Newman *et al.* 2016), suggestive of a role in repair. One study in murine lung epithelial cells indicates that WNT5A stimulation does increase wound healing, but the effect is not significant, and that it also diminishes WNT3A-mediated wound healing (Baarsma *et al.* 2017). However, as the

incidence of chronic lung disease increases with age (Lehmann, Baarsma and Königshoff 2016), and WNT5A expression in human lung tissue also increases with age (Kovacs *et al.* 2014) (Baarsma *et al.* 2017), one may postulate that WNT5A may be a potential regulator of repair. This increased WNT5A expression coincides with a decrease in canonical WNT signalling, supporting reciprocal WNT regulation exists between noncanonical and canonical WNT signalling (Baarsma *et al.* 2017).

1.11.6 Evidence of TGF- β 1 in Epithelial Repair

The reported expression of TGF- β protein in the epithelium of asthmatic bronchial biopsy tissue varies across the literature, and whether its expression correlates with asthma severity is controversial (Vignola *et al.* 1997) (Redington *et al.* 1998) (Hoshino, Nakamura and Sim 1998) (Chakir *et al.* 2003). Redington *et al.* (1998) and Hoshino, Nakamura and Sim (1998) both report that TGF- β 1 pattern of expression does not differ between asthma and health, whereas Minshall *et al.* (1997) and Chakir *et al.* (2003) suggest immunoreactivity for TGF- β 1 increases with asthma severity in bronchial biopsies. Phosphorylated SMAD2 expression, a marker of active canonical TGF- β signalling, is also reported to correlate with basement membrane thickness in asthmatic bronchial biopsy tissue (Sagara *et al.* 2002). Both inflammatory and structural cells produce TGF- β 1, with the major source of TGF- β in the airway mucosa being the eosinophils through their direct production of TGF- β 1, and indirect induction of ASM TGF- β 1 (Halwani *et al.* 2011) (Januskevicius *et al.* 2016). AA study conducted by Ling *et al.* (2016) report that that *TGFB1* expression is increased in non-asthmatic primary airway epithelial cells (AECs) compared to those of asthmatics, and that non-asthmatics have a higher fold increase in TGF- β 1 gene and protein expression post-wounding. Knocking out TGF- β 1 in asthmatic AECs reduced healing further compared to non-asthmatic controls (Ling *et al.* 2016). In line with this, TGF- β stimulation enhances wound healing in undifferentiated HBEC cultures (Kaur *et al.* 2020) (Ito *et al.* 2011) and differentiated human nasal epithelial cell (HNEC) cultures (Lechapt-Zalcman *et al.* 2006). TGF- β 1 also promotes wound healing in alveolar epithelial type 2 cells (Buckley *et al.* 2008), and intestinal epithelial cells (Anzai *et al.* 2020). However, there are also reports that TGF- β has a diminishing

effect on repair in bovine and human bronchial epithelial cell cultures (Spurzem *et al.* 1993) (Neurohr, Nishimura and Sheppard 2006). This effect does not appear to be concentration dependent as both Neurohr, Nishimura and Sheppard (2006) and Kaur *et al.* (2020) exposed HBEC cultures to 10ng/ml rTGF- β 1.

1.12 Evidence of WNT5A and TGF- β 1 Crosstalk

1.12.1 Dual Expression of WNT5A and TGF- β 1

Immunohistochemistry staining of human asthmatic lungs show WNT5A and TGF- β 1 are both highly expressed in asthmatic epithelium compared to healthy control subjects; the positive staining seen was constrained mainly to the basal epithelium, with dual-positive staining and a strong correlation identified between WNT5A and TGF- β 1 (Daud 2017). As mentioned previously, *SMAD3* and *WNT5A* gene expression is also significantly expressed in the peripheral airways of asthmatics, reinforcing further that crosstalk may exist between WNT5A and TGF- β 1 signalling (Singhania *et al.* 2017).

1.12.2 TGF- β 1 Transcriptional Regulation of WNT5A Expression

Within the lung, TGF- β 1 can induce WNT5A expression in fibroblasts (Newman *et al.* 2016) (Baarsma *et al.* 2017) (Contreras *et al.* 2020), and ASM cells (Kumawat *et al.* 2014) (Newman *et al.* 2016). HBECs have not yet been investigated. Other cell types of the body which also increase WNT5A in response to TGF- β 1 include cardiac fibroblasts (Contreras *et al.* 2020), aortic smooth muscle cells (Shi *et al.* 2014) (DiRenzo *et al.* 2016), LX-2 cells (Beljaars *et al.* 2017), basal tumour-initiating cells (Borcherding *et al.* 2015), mammary epithelial cells and fibroblasts (Roarty and Serra 2007), and the KM101 marrow stromal cell line (Zhou, Eid and Glowacki 2004). There are also reports that WNT5A can increase TGF- β 1 expression. In hepatic stellate LX2 cells, WNT5A knockdown downregulated TGF- β 1 and collagen expression (Xiong *et al.* 2012). Beljaars *et al.* (2017), however, also report that TGF- β induces WNT5A expression in LX-2 cells, suggesting that a WNT5A positive feedback mechanism may exist to potentiate TGF- β signalling effects in this cell type. The induced WNT5A was shown to play an important role in TGF- β -induced regulation of EMT

markers fibronectin, vimentin and col1a1, with WNT5A knockdown significantly reducing their induced gene expression by TGF- β (Beljaars *et al.* 2017).

Other than LX-2 cells, TGF- β has been reported to induce WNT5A expression to potentiate its own actions in a few other cellular systems. In mammary gland development, WNT5A mediates TGF- β 1 inhibition of ductal growth (as previously mentioned) (Roarty and Serra 2007), and in human lung fibroblasts, WNT5A-FZD7 signalling regulates TGF- β 1-mediated ECM synthesis (Guan and Zhou 2017). Conversely, Spanjer *et al.* (2016) report that WNT5B-FZD8 signalling (rather than WNT5A-FZD7) mediates TGF- β 1-induced ECM synthesis in human lung fibroblasts. WNT5A has also been shown to potentiate TGF- β signalling during colonic crypt regeneration by decreasing proliferation of intestinal epithelial stem cells; WNT5A-TGF- β 1 crosstalk was shown to occur through TGF- β R1 as TGF- β R1 inhibitor, SB431542, suppressed the inhibitory effect of WNT5A on cell growth (Miyoshi *et al.* 2012). WNT5A is also reported to induce SMAD2/3 phosphorylation, characteristic of the canonical TGF- β pathway (Miyoshi *et al.* 2012) (Daud 2016) (Borcherding *et al.* 2015), further supporting WNT5A-TGF- β 1 pathway crosstalk. On the contrary, WNT5A-ROR2 signalling can also reverse TGF- β 1-induced remodelling effects in mouse peritoneum through blocking the WNT/ β -catenin pathway, which potentiated TGF- β -induced fibrosis and angiogenesis (Padwal, Liu and Margetts 2020). With numerous crosstalk mechanisms being identified, this suggests WNT5A-TGF- β 1 crosstalk differs depending on the cell type being investigated.

1.12.3 Hypothetical WNT and TGF- β Crosstalk in Asthmatic Airway Epithelium

Referring back to the lung and asthma pathogenesis, eosinophils from asthmatic subjects are reported to induce *WNT5A* and *TGFB1* expression in ASM (Januskevicius *et al.*, 2016). In immortalised ASM cell lines, Kumawat *et al.* (2014) reports that TGF- β 1 signalling induces WNT5A transcription through the non-canonical TGF- β -TAK1 pathway via the transcription factor Sp1; whereas, the canonical SMAD pathway was reported to negatively regulate WNT5A

transcription in ASM, as SMAD3 inhibition significantly increased WNT5A mRNA. To support TGF- β 1-induced WNT5A transcription, TGF- β also increased β -catenin, which functioned as a co-activator of Sp1 (Kumawat *et al.* 2014). **Figure 1.6** visually summarises TGF- β 1-induced WNT5A transcription in ASM as deduced from research conducted by Kumawat *et al.* (2014). With ASM also being within the lung environment, perhaps a similar crosstalk mechanism will be utilised by airway epithelial cells during repair.

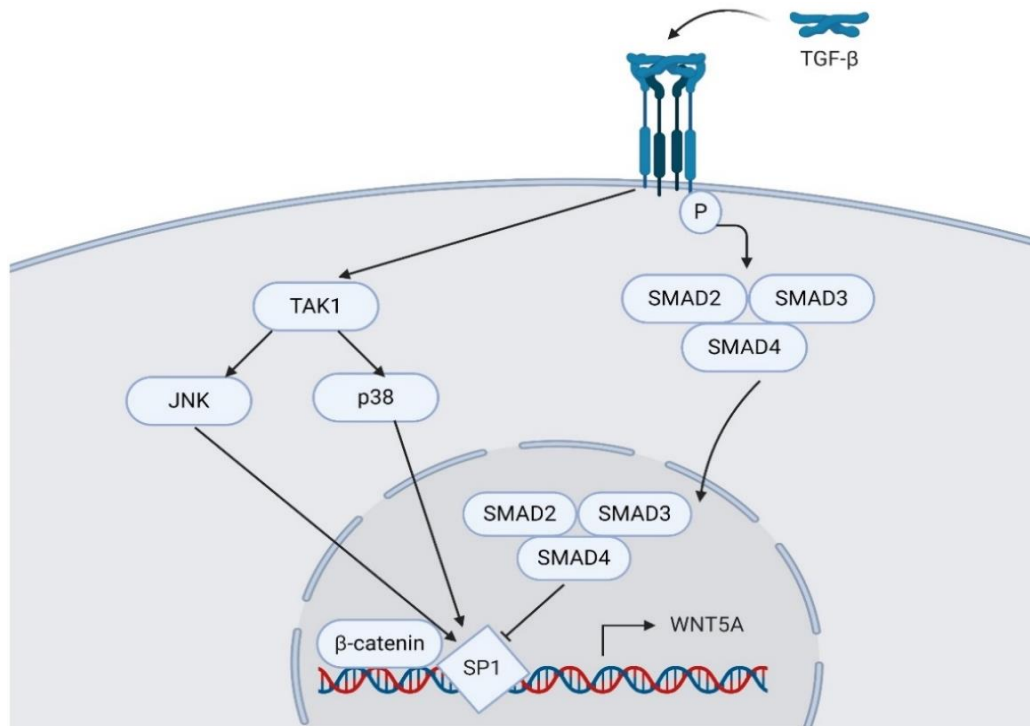


Figure 1.6 TGF- β -TAK1 Induced WNT5A Expression in Airway Smooth Muscle Cells. Created with BioRender.com

There is a wealth of literature supporting a role for TGF- β and WNT β -catenin dependent and independent signalling in airway restitution. Airway remodelling is associated with aberrant repair. TGF- β 1 has been identified as a key player in airway remodelling, yet TGF- β targeted therapeutics thus far have been unsuccessful at clinical trials. As evidence suggests TGF- β 1 signalling exhibits crosstalk with WNT5A to potentiate TGF- β 1 mediated effects, targeting the TGF- β 1 pathway indirectly through a crosstalk intermediary may provide an alternative approach to enhance wound healing. TGF- β 1 is reported to induce WNT5A transcription directly through SMAD signalling and indirectly through TAK1 (Katoh and Katoh 2009). As TAK1 can inhibit β -catenin transcriptional activity

through NLK, TGF- β 1 may promote the noncanonical WNT axis to further skew WNT signalling in its favour.

I hypothesise that TGF- β 1 promotes WNT5A signalling, through either SMAD-dependent or SMAD-independent TAK1 signalling, to potentiate TGF- β 1-mediated cellular migration in human bronchial epithelial cell wound repair. This hypothesis can be visualised in **Figure 1.7**.

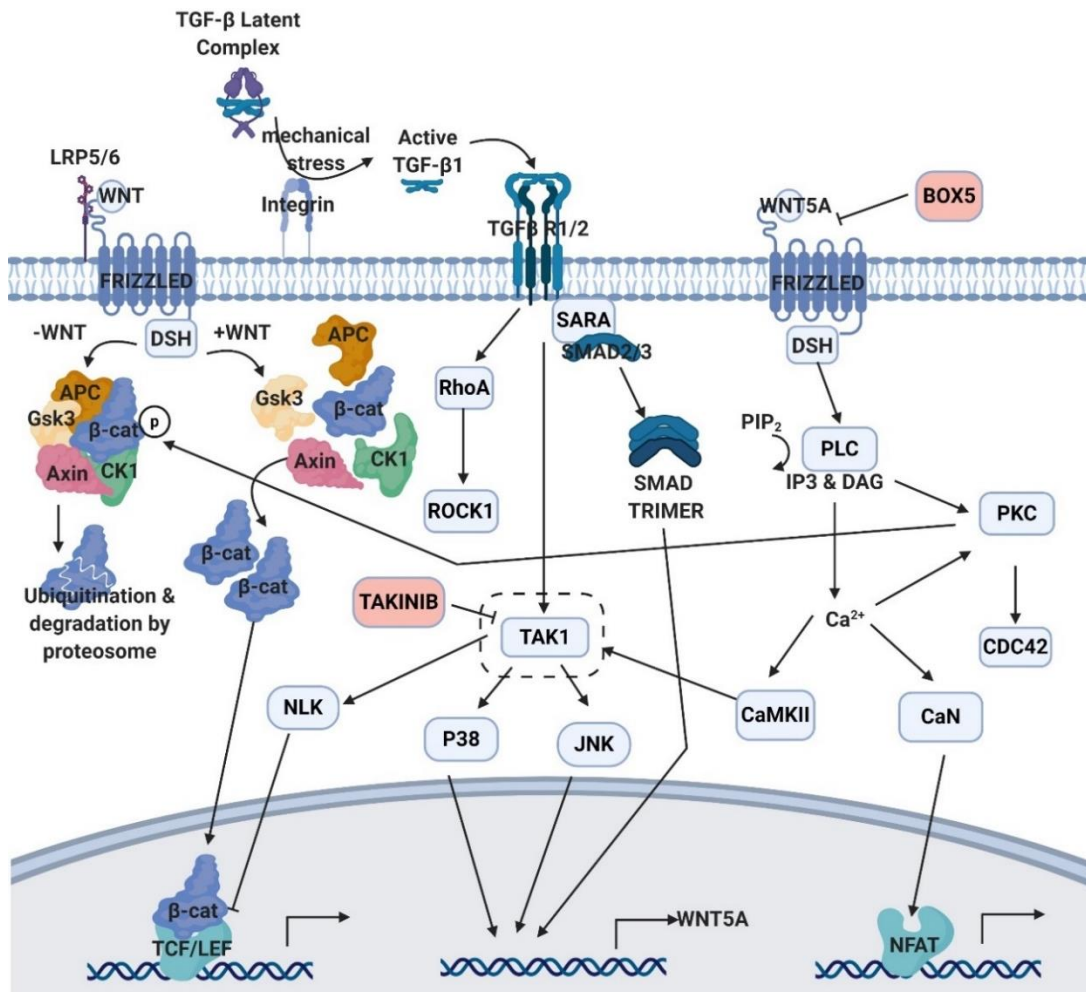


Figure 1.7 Wounding to the Epithelium Initiates Numerous Cell Signalling Cascades. Severing of integrins (through mechanical stress) activates and initiates latent TGF- β proximal to the wound site. Disruption of adherens junctions leads to a β -catenin feed into the canonical WNT pathway, and exposure of basal cells to air initiates Notch signalling (and thus cellular differentiation). TGF- β 1 sequesters canonical WNT signalling via NLK but promotes transcription of noncanonical WNT WNT5A directly through canonical TGF- β -SMAD signalling and indirectly through noncanonical TGF- β -TAK1 signalling. Whilst doing this, TGF- β induces EMT in the proximal cells. The induced WNT5A promotes cellular migration and organisation of the regenerating epithelium. Through signalling through PKC, WNT5A can sequester canonical WNT signalling (through phosphorylation of β -catenin). Created with BioRender.com

1.13 What is Signalling Crosstalk?

Multiple signalling pathways share core signalling proteins. Current models of signalling do not fully elucidate the level of which inter-pathway connections exist, which as suggested by Coster *et al.* (2017) could be:

1. **Through regulation of receptor signal transduction of the second signalling pathway.** This could be a direct mechanism such as ligand synthesis or receptor expression, or indirect through inhibitor/dummy receptor synthesis, both of which would mediate ligand-receptor binding. For example, TGF- β 1 is reported to induce WNT5A transcription (Kumawat *et al.* 2014).
2. **Through cytoplasmic downstream signalling events** common to both pathways. For example, WNT5A- and TGF- β 1-mediated TAK1 signalling is reported to downregulate transcriptional activity of β -catenin (Ishitani *et al.* 1999) (Li *et al.* 2010) (Ota *et al.* 2012) (Ishitani *et al.* 2003).
3. **Through regulating transcriptional activity of the second signalling pathway,** for example, TGF- β -SMAD3 signalling can interact directly with the NICD during Notch signalling in order to regulate CSL transcriptional activity (Blokzijl *et al.* 2003).
4. **Through post-transcriptional regulation of the second signalling pathway,** such as controlling post-translational modifications and secretion of a protein. For example, WNT5A-PKC α signalling can mediate phosphorylation of β -catenin, resulting in its degradation (Gwak *et al.* 2006) (Baarsma *et al.* 2017).

To clarify further, just because two pathways have the same end point, e.g that both TGF- β 1 and WNT5A induce TAK1 signalling (as detailed in section 1.12), doesn't mean crosstalk has occurred. They may independently induce TAK1, and the downstream signalling events used to do this are separate. However, there may be instances where signalling pathways recruit the same transcription factors or signalling components to reach the same end goal, be it to positively or negatively regulate the end signal strength, which is TAK1 signalling in this example. However, for this to be considered crosstalk, my interpretation is that one pathway (TGF- β 1 signalling) must affect the transcriptional activity of the

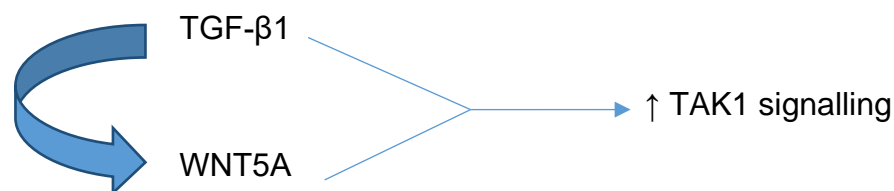
other (WNT5A signalling) pathway to control a common end point (SMAD2/3). If the second pathway is regulated by the first to amplify a common end goal, I would consider this positive crosstalk. If the second pathway is regulated by the first pathway to reduce the end signal strength, I would consider this negative crosstalk. This definition of negative crosstalk is similar to negative feedback but acts across signalling pathways rather than within a single pathway. Crosstalk by this definition would be measured by the ability of the one signal transduction pathway to positively or negatively regulate another to regulate a common downstream signalling component, thereby impacting a specific cellular outcome or response e.g. TGF- β 1 inducing WNT5A transcription to promote TAK1 signalling as shown as an example in **Figure 1.8**.

Not Crosstalk

TGF- β 1 ————— \uparrow TAK1 signalling

WNT5A ————— \uparrow Ca² signalling/CaMKII ————— \uparrow TAK1 signalling

Positive Crosstalk



Negative Crosstalk

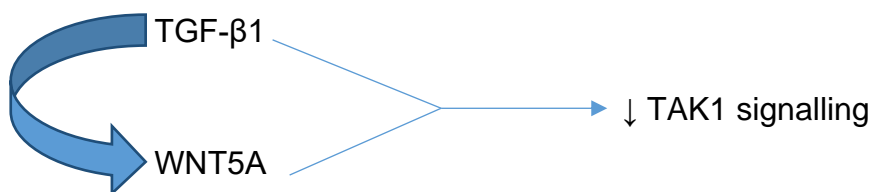


Figure 1.8 Hypothetical WNT5A and TGF- β 1 Signalling Crosstalk

In the context of this study, the effect of rhTGF- β 1 on WNT5A transcription was investigated, alongside WNT5A receptor expression. The end point investigated was wound healing, with shared crosstalk intermediary TAK1 being manipulated

to investigate TAK1 effects for both pathways. Due to research conducted on WNT5A and TGF- β 1 crosstalk in BEAS-2Bs by Daud (2017), and supportive evidence in the literature in ASM cell lines outlined in chapter 1.12, SMAD2/3 was also investigated as a potential WNT5A-TGF- β 1 crosstalk intermediary.

1.14 Therapies Targeting Airway Epithelial Repair

Considering the many roles of the airway epithelium in defending against respiratory insult listed in section 1.7, and the evidence of aberrant repair detailed in section 1.8, manipulating the wound healing response to efficiently repair airway damage and reduce airway remodelling is clinically attractive. Yet there is limited, and non-definitive evidence into the effects of therapies on airway epithelial restitution (Heijink *et al.* 2020).

1.14.1 Effects of Conventional Asthma Therapeutics on Airway Epithelial Repair

The β -agonists Salbutamol and Isoproterenol have been shown to attenuate epithelial wound healing (Schnackenberg *et al.* 2006)(Wadsworth, Nijmeh and Hall 2006). Corticosteroids, however, have conflicting outcomes on wound healing. Some report corticosteroids inhibit epithelial repair (Yu, Jiang and Sun 2020) (Li *et al.* 2020) (Liu *et al.* 2013), whereas, others report they reverse EMT (Doerner and Zuraw 2009) and restore barrier function following oxidative stress (Heijink *et al.* 2014). Interestingly, Wadsworth and colleagues (2006) report Dexamethasone initially inhibits the healing response, but that it extends the lifespan of ALI cultures subjected to repeat damage, suggestive of prolonged basal cell proliferative capacity and perhaps altered β -catenin WNT signalling.

If wound healing is indeed impaired by these medications, long-term use may contribute to airway remodelling rather than hinder it. The asthmatic epithelium is also reported to be less responsive to ICS (Heijink *et al.* 2014), suggesting that if ICS do confer a beneficial effect on repair that this will only offer partial restoration. As conventional treatments do not confer adequate asthma control

in severe asthmatics, this highlights the need for new epithelial repair targeted treatment strategies.

1.14.2 WNT5A and TGF- β 1 Targeting Drugs on the Market or in the Pipeline which could be Repurposed as a Therapy for Airway Epithelial Repair

As WNT5A and TGF- β display a strong association with asthma susceptibility in GWAS studies, and numerous studies provide evidence for WNT5A and TGF- β in repair, drugs on the market or in clinical trials currently targeting either pathway could be repurposed to treat airway epithelial repair.

Targeting TGF- β at the ligand/receptor level has raised numerous safety concerns, and so TGF- β targeting drugs in clinical trials generally interfere with downstream signalling of TGF- β or TGF- β mediated responses (Györfi, Matei and Distler 2018). However, there are two drugs which target the ligand-receptor signal transmission: TRK-250 and Gallunisertib. TRK-250 is an siRNA-based therapy, currently in stage I clinical trials, designed to silence TGF- β 1 mRNA expression to inhibit pulmonary fibrosis in IPF patients (Shibata *et al.* 2019). Whereas Gallunisertib, which is in ongoing clinical trials for numerous solid tumour cancers, targets TGF- β R tyrosine kinase activity (Roane, Arend and Birrer 2019). Abituzumab, which targets α V integrin, and IVA337, which targets PPAR, are also reported to interfere with TGF- β signalling (Györfi, Matei and Distler 2018). There are also two therapeutics authorised for treatment of IPF, Pirfenidone and Nintedanib, which are known to counteract TGF- β induced effects (such as collagen fibril assembly), but their mechanisms of action are currently unknown (Knüppel *et al.* 2017).

Many of the WNT signalling targeting drugs currently in clinical trials are being evaluated as therapies for cancer. Of these drugs the majority modulate the WNT negative regulator dickkopf (DKK) and β -catenin (Lu *et al.* 2016). As DKK binds to LRP5/6 to prevent ligand-receptor complex formation, and LRP5/6 is essential for WNT/ β -catenin signal transduction, these therapies are mainly focussed on

targeting the canonical WNT axis (Semënov *et al.* 2001) (Skronska-Wasek *et al.* 2018). There are two WNT5A specific modulators, BOX-5 and FOXY-5, which are respectively in preclinical testing and phase II clinical trials (WntResearch n.d.). Both are WNT5A-derived hexapeptides, but BOX-5 is a WNT5A antagonist and FOXY-5 is a WNT5A agonist (Yuan *et al.* 2015). Other than mimicking WNT5A structural attributes to manipulate activity, WNT5A function can be modulated through blocking receptor signal transduction; Vantictumab, a human monoclonal antibody which targets FZD-1, 2, 5, 7 and 8 (all known WNT5A FZD receptors), was terminated in phase 1b clinical trials due to safety concerns over bone related toxicities (Davis *et al.* 2020). Ipafricept, a FZD8 decoy receptor, was also terminated early in phase 1b clinical trials for the same reason (Moore *et al.* 2019). There are also multiple porcupine inhibitors (LGK974, CGX1321 and ETC-1922159) currently in phase 1 testing in clinical trials, which prevent palmitoylation and secretion of all WNTs (Davis *et al.* 2020). Manipulation of the WNT5A signalling pathway is also being investigated through combination-therapy of Cyclosporin A, a marketed calcineurin inhibitor (which inhibits the noncanonical WNT-Ca²⁺ pathway), and the MEK inhibitor Selumetinib (Kim *et al.* 2012) (Krishnamurthy *et al.* 2018).

1.14.3 Effects of Conventional Asthma Therapeutics on WNT and TGF- β Signalling

Interestingly, corticosteroids are reported to regulate WNT signalling, which is one of the potentially causal mechanisms for Dexamethasone-induced osteoporosis (Li *et al.* 2013). Dexamethasone has been reported to reduce bronchial/tracheal proliferation and repair; mechanistically, this is reported to be achieved through activating WNT β -catenin signalling in airway epithelial cells (Yu, Jiang and Sun 2020) (Liu *et al.* 2013). On the contrary Hu *et al.* (2013) report that Dexamethasone inhibits WNT- β -catenin signalling to reduce cellular proliferation and apoptosis of the craniofacial epithelium to result in cleft palate. Similarly, Dexamethasone reduced proliferation of rat neural precursor cells through enhancing GSK-3 β activity that ultimately controls β -catenin proteasomal degradation (Boku *et al.* 2009). From these studies, it can be deduced that corticosteroids do modify canonical WNT β -catenin signalling, and that due to the

coordinated interplay between the canonical and noncanonical signalling axis, corticosteroids may have a knock-on effect on noncanonical WNT signalling. Additionally, corticosteroids are also reported to rescue TGF- β 1 induced cAMP levels and gene expression (Chung *et al.* 2020), and partly prevent TGF- β 1 induced EMT (Doerner and Zuraw 2009). TGF- β is reported to be reduced in lung tissue of mice administered with β -catenin siRNA, suggesting β -catenin signalling modifies TGF- β synthesis (Kwak *et al.* 2015). TGF- β and β -catenin signalling crosstalk is also documented in other epithelial cell types (Nlandu-Khodo *et al.* 2017) (Sun *et al.* 2015). This highlights that corticosteroids may also indirectly modulate TGF- β signalling.

1.15 Epithelial Cell Models

Epithelial dysfunction is evident in asthma, but at present there are limited therapeutics which target epithelial wound repair. To assess epithelial reparation, an appropriate epithelial cell model needs to be selected to be able to investigate cell signalling pathway manipulation on the wound healing response. A brief explanation of the available models are therefore provided and benefits and disadvantages discussed in relation to assessing wound repair.

1.15.1 In Vivo

Animal models are used to create disease models. The application of the model depends on how well the model reflects the human disease (Shapiro 2008). BALB/c mice are usually used to model the allergic response in asthma as this animal model is more prone to developing a type 2 inflammatory response following bronchial challenge or allergic sensitisation (Sagar, Akbarshahi and Uller 2015). Utilising transgenic or gene knockout technique allows the investigation of a specific molecule or proteins role in a hypothesised pathological mechanism (Bucchieri *et al.* 2017). However, these models cannot always be translated to human disease due to genetic and physiological differences between animals and humans (Barré-Sinoussi and Montagutelli 2015). To increase translatability to human disease, xenograft systems have been utilised to integrate normal and asthmatic human bronchial epithelium onto

decellularized rat tracheas, which are ligated to plastic cassettes and grafted into immunocompromised murine hosts (Hackett *et al.* 2017). In the study by Hackett *et al.* (2017), the asthmatic xenograft failed to recapitulate goblet cell hyperplasia present in human asthmatic airways, but reduced junctional proteins were evident. As these animal models are limited in translatability, *in vitro* human cell-based models of the airways are thought to more accurately recapitulate the human airways (Bucchieri *et al.* 2017).

1.15.2 In Vitro

There are numerous *in vitro* models which offer an alternative to animal models. This includes cell line culture, submerged and undifferentiated primary human bronchial epithelial cell (HBEC) culture, air-liquid interface (ALI) cell culture, epithelial/fibroblast coculture, organoids, *ex vivo* transplants, precision cut lung slices, and the lung on a chip model.

1.15.2.1 Organoids

Organoids are organ specific multicellular 3D structures which within the lung are produced from isolated basal cells (Shrestha *et al.* 2020). Organoids derived from tracheal basal cells are termed tracheospheres, and from the bronchi bronchospheres (Barkauskas *et al.* 2017). This is a desirable model but wounding the epithelium would be difficult to achieve in organoids because the differentiated cells are luminal (Barkauskas *et al.* 2017).

1.15.2.2 Organ-on-a-chip

An organ-on-a-chip is a microfluidic cell culture device which replicates the 3D microenvironment by layering cells similarly to the *in vivo* environment to produce better organ functionality than other model systems (Bhatia and Ingber 2014). The layers are separated by a porous membrane, of which the epithelial layer can be exposed to air to induce differentiation, whilst the bottom layer consists of pulmonary vascular endothelial cells that are maintained by continuous circulation of culture media to mimic blood flow (Shrestha *et al.* 2020). The barrier between the epithelial-vascular compartments is also mechanically stretched to

imitate physiological breathing motions (Shrestha *et al.* 2020). This model offers the best recapitulation of the airway epithelium, but costs were too high to render this a feasible option for this project.

1.15.2.3 Precision-cut Lung Slices

Precision-cut lung slices (PCLS) can be cultured for up to 14 days from explanted asthmatic and healthy human or animal lung (Liu *et al.* 2019: A). To prevent airway collapse, the tissue is injected with agarose solution and solidified rapidly in ice-cold buffer before precision slicing (Liu *et al.* 2019: A). For this reason, functional experiments on the epithelium is therefore not desirable, and this model is better suited for organ specific toxicology testing and response to inflammatory stimuli or infection. Tissue explants similarly to PCLS offer the advantage of retaining the *in vivo* cellular architecture, however, they also cannot be used to model an intact epithelial barrier, so instead air-liquid interface (ALI) cultures are generally utilised in these studies (Bucchieri *et al.* 2017).

1.15.2.4 Cell Line Culture

There are numerous bronchial airway epithelial cell lines, including BEAS-2B, 16HBE σ - and Calu-3, available to model the human airway. Cell lines are easily accessible and more economical than *in vivo* experiments and offer the ability to conduct reproducible and high throughput experiments (Forbes 2000). The Calu-3 cell line is derived from human bronchial adenocarcinoma cells, whereas BEAS-2Bs are immortalised normal, human bronchial epithelial cells. BEAS-2Bs do not form tight junctions as readily as 16HBE14 σ - and Calu-3 cells (Stewart *et al.* 2012: B) (Wan *et al.* 2000), however, BEAS-2Bs do respond to TGF- β 1 in a similar manner to primary HBECs as indicated by the paper by Doerner and Zuraw (2009), which is why they were selected as the initial cell model in this thesis.

Immortalised human bronchial epithelial cells (iHBECs) were utilised for gene expression analysis and for the MTS assay for identifying the appropriate concentrations of BOX-5 and Takinib. These cells were utilised instead of BEAS-

2Bs as on phenotyping the BEAS-2Bs by flow cytometry, the BEAS-2Bs displayed a more mesenchymal than epithelial phenotype. This observation is also reported by Han *et al.* (2020). The iHBECs were chosen over alternative cell lines as human *BMI-1* extends the proliferative ability of the cells whilst retaining the ability to fully differentiate; the cilia beat frequency is also within normal range of normal respiratory cilia (Munye *et al.* 2016).

1.15.2.5 Primary HBEC Cultures – Monolayer, ALI and HBEC-Fibroblast Co-Culture

HBEC cultures cultured at the ALI form pseudostratified cell layers which form tight junctions and contain all airway differentiated cell subtypes, therefore forming a functional epithelium similar to the *in vivo* airways (Liu *et al.* 2019: A). In this way, it surpasses undifferentiated monolayer cell culture systems consisting solely of undifferentiated cells. Conversely, ALI cultures possess higher basal cell frequencies than uncultured HBECs (potentially affecting observations on repair), however, this does not affect gene expression and a close correlation is seen between the two (Dvorak *et al.* 2011). Additionally, ALI cultures do not consider the complex cell-cell and cell-matrix interactions that are present in the *in vivo* environment (Bucchieri *et al.* 2017).

ALI co-cultures, containing epithelial cells and fibroblasts, on the other hand do offer cell-cell and cell-matrix interactions, which increase the differentiation and apoptosis of basal cells thereby improving epithelial functionality (Liu *et al.* 2012). ALI cocultures can be achieved by numerous methods; both epithelial and fibroblasts can be cultured separately before combining together, cultured together in transwells but with a porous support separating the two, or epithelial cells can be cultured atop a collagen gel with fibroblasts embedded (Choe, Sporn and Swartz 2003). Through mimicking the EMTU physiological environment, ALI cocultures can be used in functional experiments such as wound healing assays to assess the impact of epithelial-mesenchymal crosstalk (Osei, Booth and Hackett 2020). Beneficially, co-culturing can prolong the life and differentiation potential of primary cells (Liu *et al.* 2012).

1.15.2.6 Models Selected for Experimental Designs

ALI cultures were chosen as the model for assessing wound healing because ALI cultures contain the differentiated cell types present in the airway and permit the evaluation of disease impact on wound healing. It would also allow the course of repair to be visually assessed over time, which may have been difficult to achieve in all the other models. As ALI culturing had not yet been set up at Glenfield, achieving a co-culture system would have been too time consuming to optimise within the PhD timeframe. However, ultimately it would be the long-term goal in assessing the role of WNT5A and TGF- β 1 in airway wound healing. A similar study to Thompson *et al.* (2006) or Semlali *et al.* (2010) would be performed. Alternatively, the lung-on-a-chip would offer better physiological complexity in mimicking the EMTU, however, the extra cost compared to coculture models would need to be justified.

1.16 Hypothesis

I hypothesise that TGF- β 1 and WNT5A may have either independent or synergistic effects on epithelial wound healing and epithelial-mesenchymal transition in asthma.

1.17 Aims and Objectives

AIM 1. To investigate epithelial WNT and TGF- β individual and crosstalk transcriptional repair modules and their association with inflammatory signatures and airflow obstruction (as a surrogate of airway remodelling) in moderate to severe asthma.

AIM 2. To evaluate the impact of TGF- β 1 and WNT5A on wound healing in BEAS-2B and scratch wound primary airway epithelial cell air-liquid interface (ALI) model systems.

AIM 3: To investigate the role of Smad2/3 and TAK1 as crosstalk intermediaries between TGF- β 1 and WNT5A in the context of epithelial wound healing and EMT.

Objectives:

My objectives are to test the hypothesis aims 1,2 and 3 using a combination of experimental methodologies, specifically; (I) BEAS-2B and primary HBEC ALI wound healing models, (II) flow cytometry to characterise epithelial cells subtypes undergoing EMT and (iii) airway epithelial gene expression from well characterised moderate-to severe asthma patient to identify potentially relevant transcriptional repair modules associated with airflow obstruction and airway inflammation.

2 METHODS

2.1 Patient Clinical Characteristics

Asthmatic patients and healthy control subjects were recruited from Glenfield Hospital, Leicester. Healthy control subjects recruited had normal spirometry results with no prior history of respiratory disease. All asthmatic patients were current non-smokers, with previous history of 10 pack years or less, and met one or more of the following diagnostic criteria for variable airflow obstruction: methacholine airway hyperresponsiveness (provocation concentration resulted in 20% drop in forced expiratory volume in 1 second (FEV₁), PC₂₀ ≤8mg/ml), bronchodilator reversibility of ≥12% and 200mls following inhaled salbutamol, or peak flow variation of ≥20% from twice-daily peak expiratory flow measurements over a 2 week period. Asthma severity was classified according to Global Initiative for Asthma (GINA) treatment intensity, with GINA 1 being mild, GINA 2-3 moderate and GINA 4-5 as severe (Global Initiative for Asthma 2020). The studies were approved by the Leicestershire Research Ethics Committee (REC numbers: 08/H0406/189, 16/EM/0260 and 04/Q2502/74). Informed consent was retrieved from all participants prior to bronchoscopy.

2.2 Bronchoscopy Sample Retrieval

Bronchoscopies were performed by Professor Salman Siddiqui and Professor Peter Bradding. Bronchial biopsies were retrieved from patients using standard single-use 2.8mm Radial Jaw 4 biopsy forceps (Boston Scientific cat no M00513380). Bronchial biopsies were either added to DMEM for flow cytometric analysis or 10% neutral buffered formalin for immunohistochemistry paraffin fixation. A bronchial cytology brush with a 3mm brush diameter (1.8mm x 120cm length) (TeleMed cat no 3104) was used for obtaining bronchial brushings. Bronchial brushes were retrieved from the patient and submerged into a 15ml falcon containing 3ml Pneumacult™ Expansion Plus Media (Stemcell cat no 05040) (max of 2 brushes per 15ml falcon). The brushings were used for cell culture and flow cytometric analysis.

2.3 Cell Culture

The reagents used for cell culture are listed in **Appendix 1**.

2.3.1 BEAS-2B Cells

BEAS-2B cells were seeded onto tissue culture vessels coated with a 1% (vol/vol) 3mg/ml bovine collagen solution (Advanced BioMatrix) in phosphate-buffered saline (PBS). BEAS-2Bs were cultured in Bronchial Epithelial Growth Media (Lonza) supplemented with 5ml antibiotic/antimycotic solution (Gibco) and 1.5ml Fungizone (Gibco) for immunofluorescence and BEAS-2B PCR array experiments. Due to supplier demand issues, BEAS-2Bs were cultured in LHC-9 in later experiments (with the same antibiotic/antimycotic and Fungizone supplementation as BEGM).

2.3.2 Establishment of Human Bronchial Epithelial Cell ALI Cultures

Growing human bronchial epithelial cells is notoriously difficult. These cells require very high humidity - a standard sized cell culture incubator requires two-three 3L water baths. Without a dedicated cell culture facility at Glenfield hospital, and a lack of regular bronchoscopies (resulting in cell culture reagent expiry), a decision to culture the cells at the Leicester Royal Infirmary (LRI) was made to increase culturing success. The LRI, as part of the National Primary Ciliary Dyskinesia Centre, were already successfully culturing human nasal epithelial cell cultures and so this mitigated further cell culture loss.. A collaboration with Dr Robert Hirst and Professor Chris O'Calloghan was formed where his lab cultured the HBECs on my behalf at the LRI, preventing me from having to buy in cultures from suppliers such as Epithelix where donor clinical information would not have been provided, and the cost implication would have restricted the number of experiments I could have achieved with my bench fee account.

2.3.3 Human Bronchial Epithelial Cell Culture

Bronchial brush samples in 3ml PneumaCult™-Ex Plus media (Stemcell) were transferred on ice to the LRI for culture in Dr Robert Hirst's lab. To prevent media

wastage, I aliquoted the 50x supplement and hydrocortisone stock solution for storage at -20°C and made-up small volumes of media for sample collection as and when needed. Dr Robert Hirst and Gwyneth Williams kindly cultured the cells on my behalf. Complete PneumaCult™-Ex Plus media was made up according to manufacturer's recommendations, with 5ml penicillin-streptomycin (Sigma) and 5ml Fungizone (Gibco) added to reduce infection. Complete basal media was used up to 4 weeks and ALI media up to 3 weeks post-preparation.

Human airway epithelial cells were isolated from 3mm bronchial brushes by shaking the cells off the brush vigorously. Two brushings were generally seeded into two 1% PureCol (Advanced BioMatrix) coated T80 flasks. Plasticware was coated with 1% PureCol in sterile water, rinsed off with sterile water and then stored in the dark at room temperature until use. The batch of PureCol was changed when nearing expiry to prevent poor cell culture to plasticware adhesion. Media was changed every two to three days until confluent. The cells were then trypsinised with Trypsin-EDTA (Sigma) at 37°C and over-seeded into twelve 12mm 0.4µm pore polyester transwells (Corning). The media was removed the following day and replaced with PneumaCult™-ALI media (Stemcell) in the basal chamber only. This process is explained pictorially in **Figure 2.1**. PneumaCult™-ALI media was made according to manufacturer's instructions with 5ml penicillin-streptomycin (Sigma) and 5ml Fungizone (Gibco) added (as added to the expansion media). Cultures were fed every two days - 850µl of media in the week and 900µl on the weekend. Apical surfaces were washed with PBS for the first time after a week of seeding at ALI, and then every two days when being fed to remove excess mucus. Cilia appeared within two-four weeks of culturing at ALI.

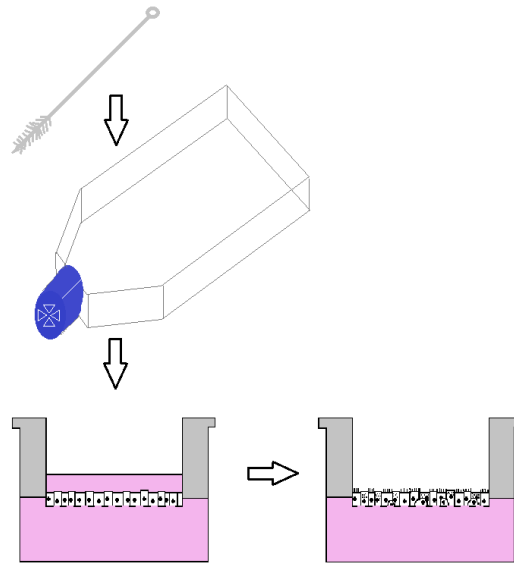


Figure 2.1 Culturing to ALI Methodology. Cells are first expanded in flasks, then seeded in transwells and left overnight to adhere and then the apical fluid is removed exposing the cells to an air-liquid interface.

2.3.4 Immortalised Human Bronchial Epithelial Cell Culture

Immortalised human bronchial epithelial cells (iHBECs) were gifted from Dr Robert Hirst. They were cultured in the same as human bronchial epithelial cells cultured from bronchial brushings. They were expanded in PneumaCult™-Ex Plus Media and cultured at ALI with PneumaCult™-ALI Media. Cultures remained at ALI for two-four weeks until cilia became apparent.

2.3.5 HEK293T Cell Culture

HEK293T cells used for WNT5 antibody validation were seeded at 2.5-3 million cells per uncoated 10cm petri dish. Cells were fed 10ml complete DMEM containing 10% FBS and 1% Penicillin and Streptomycin. Media was changed every two days. As HEK293T cells are weakly adherent, during media changes, the media was gently aspirated and pipetted to prevent cell detachment.

2.4 Transepithelial Electrical Resistance (TEER)

To assess the integrity of the epithelial barrier, TEER measurements were taken for each culture before and after wounding using an EvomX and STX2 electrode chopsticks (WPI, cat no STX2). The electrodes were sterilised by immersing the

electrodes in 70% ethanol for 15 minutes, then air drying them for 15 seconds. Excess mucus was always removed by washing the cultures twice with warm sterile PBS prior to taking resistance readings. 800µl of PBS was added basally and 500µl apically to the ALI cultures, and three resistance readings taken per culture to account for tissue monolayer uniformity variation, and an average taken. The blank resistance reading was taken every time the EVOM was used. TEER results were always taken in the same order and as quickly as possible to avoid deviations due to temperature. TEER was calculated using the following equation (where R stands for resistance):

$$R(\text{TISSUE}) (\Omega) = R(\text{TOTAL}) - R(\text{BLANK})$$

$$\text{TEER} (\Omega \cdot \text{cm}^2) = R(\text{TISSUE}) \times \text{Effective Membrane Area} (\text{cm}^2)$$

As the ALI cultures were always seeded into 12-well transwells, the effective membrane area was always 1.12cm². The average R(BLANK) value was 174.4Ω.

2.5 Reconstituting BOX-5, Takinib and Recombinant Proteins for WNT5A and TGF-β1

10mg BOX-5 (Merck Chemicals Ltd, cat no 681673-10MG) was reconstituted in 260.8µl DMSO to get a stock concentration of 50mM, which was stored at -20°C. It is stable for 6 months at this temperature according to the supplier.

5g Takinib (Sigma Aldrich, cat no SML2216-5MG) was solubilised with 1.551ml DMSO to get a 10mM stock concentration, which was stored at -80°C. It is stable for 6 months at this temperature according to the supplier.

Recombinant human TGF-β1 (Bio-technie, cat no 240-B-002), rhTGF-β1, was reconstituted in 1mg/ml BSA in water with 4mM hydrochloric acid (HCl) solution to 2µg/ml. Recombinant human WNT5A (Bio-technie, cat no 645-WN-010), rhWNT5A, was reconstituted in 0.1% BSA PBS solution to 100µg/ml. BSA, 1M HCl and sterile PBS were purchased from Sigma Aldrich (cat no A7906, H9892 and D8662 respectively). Both were always reconstituted to 100µl and filtered

with a 0.2µm acrodisc before storage at -20°C, where they should be stable for 3 months according to the supplier.

To assess if the rhWNT5A also contained rhWNT5B, the recombinant protein was run on a 12% polyacrylamide monomer gel. The bands were excised and sent for proteomic analysis at the Protein Nucleic Acid Chemistry Laboratory (PNAACL), based at the University of Leicester. Hits returned for both WNT5A and WNT5B protein. Results are shown in **Appendix 2**.

2.6 Selecting the Cell Signalling Pathway Inhibitors

2.6.1 BOX-5

To inhibit WNT5A signalling, there was a choice between WNT5A siRNA or WNT5A inhibitor BOX-5 (whose precise mechanism of action is yet to be determined). As siRNA transfection can be difficult to achieve in fully differentiated primary epithelial cell cultures (Xie *et al.* 2015), BOX-5 was chosen. BOX-5 is a *t*-butyloxycarbonyl-modified WNT5A-derived hexapeptide (Prasad, Mohapatra and Andersson 2015). Proteomic profiling of A2058, a melanoma cell line, identified that 0.2µg/ml rhWNT5A treatment altered expression of 174 proteins, which could be inhibited with 100µM BOX-5 (Sherwood *et al.* 2014). BOX-5 has been shown to inhibit the effects of WNT5A stimulated cellular effects (Sherwood *et al.* 2014) (Yuan *et al.* 2015), including cellular migration in A2058 and HTB63 melanoma cell line wound healing assays (Jenei *et al.* 2009). In the A2058 cell line, BOX-5 inhibited WNT5A-induced cellular migration through directly antagonising WNT-Ca²⁺ and PKC signalling (Jenei *et al.* 2009). As this project also incorporated a wound healing assay, this strengthened the resolve to utilise BOX-5 to delineate the impact of WNT5A signalling on primary HBEC wound healing.

2.6.2 Takinib

TGF-β1 has been reported by Katoh and Katoh (2009) to induce WNT5A transcription directly via SMAD signalling, and indirectly via TAK1 and NFκB. The

noncanonical WNT-Ca²⁺ pathway also signals through TAK1, which may be fundamental in the crosstalk signal in HBEC repair. An inhibitor targeting the potential crosstalk intermediary TAK1 was therefore selected. There were numerous inhibitors for TAK1 available. The most popular identified was (5Z)-7-oxozeaenol (5ZO). Takinib, another TAK1 inhibitor identified, however is reported to have higher selectivity than 5ZO with less off target effects (Totzke *et al.* 2017). Takinib was therefore selected to prevent off target effects through other MAP2K and MAP3K family members.

2.7 MTS

Prior to use in crosstalk studies, Takinib and BOX-5 needed to be tested for cellular toxicity on epithelial cells, so appropriate concentrations could be selected for these functional assays. To do this, an MTS assay was performed which assesses metabolic activity of cells. The negative charge of the MTS tetrazolium prevents cellular permeability into the cells, but through the use of intermediate electron acceptors (which can penetrate and exit the cells), the electron acceptors can reduce the MTS tetrazolium compound into a soluble, purple coloured formazan dye (Riss *et al.* 2016); the principal is that the enzymatic activity is related to the number of viable cells, and so it can be used to assess proliferation or cytotoxicity in response to cell treatment (Wang, Henning and Heber 2010). An MTS assay was conducted because the detection sensitivity is high, whilst producing fast and repeatable results. Due to the potentially toxic nature of the intermediate electron acceptor, the absorbance could be read periodically (as the formazan dye is already solubilised unlike with the MTT assay), to aid assay optimisation (Riss *et al.* 2016). The MTS assay also offers a safer alternative to the radioactive tritiated thymidine ([³H]) proliferation assay, where level of radioactive signal is proportional to cellular proliferation (Riss *et al.* 2016).

Immortalised human bronchial epithelial cells were seeded onto 1% PureCol coated 24-well plates at 25,000 cells per well and left to adhere overnight in an incubator. The concentration of Takinib and BOX-5 shown in **Table 2.1** along

with equivalent vehicle controls for each concentration were added to triplicate wells and incubated for 48 hours. Media only wells and 1µM staurosporine were used as negative and positive controls. A 1:5 CellTiter 96 AQueous One solution reagent (containing the tetrazolium compound 3-(4,5-dimethylthiazol-2-yl)-5-(3-carboxymethoxyphenyl)-2-(4-sulfophenyl)-2H-tetrazolium, which is also known as MTS) (Promega, cat no G3580) to PneumaCult™-Ex Plus Media (Stemcell, cat no 05040) solution was prepared, of which 240µl was added per well. The plates were then left to incubate at 37°C for 3 hours, before the absorbance was read at 490nm using an Enspire plate reader.

Table 2.1 Inhibitor Concentrations Tested in the MTS Assay

Inhibitor	Concentration range tested					
Takinib	100nM	50nM	10nM	7.5nM	5nM	2.5nM
BOX-5	500µM	250µM	50µM	5µM		

Summary results for the MTS assay are shown in **Figure 2.2**. For Takinib, concentrations 10nM and above significantly increased cell viability, indicative of enhanced cellular proliferation. 7.5nM was therefore chosen as the concentration to use for the crosstalk studies to remain as physiologically relevant as possible. For BOX-5, none of the tested concentrations had a significant effect on cell viability, although, at 500µM the cell viability trended towards significance ($p=0.0713$). 250µM BOX-5 was therefore used in future experimentation to inhibit WNT5A as effectively as possible without reducing cell viability.

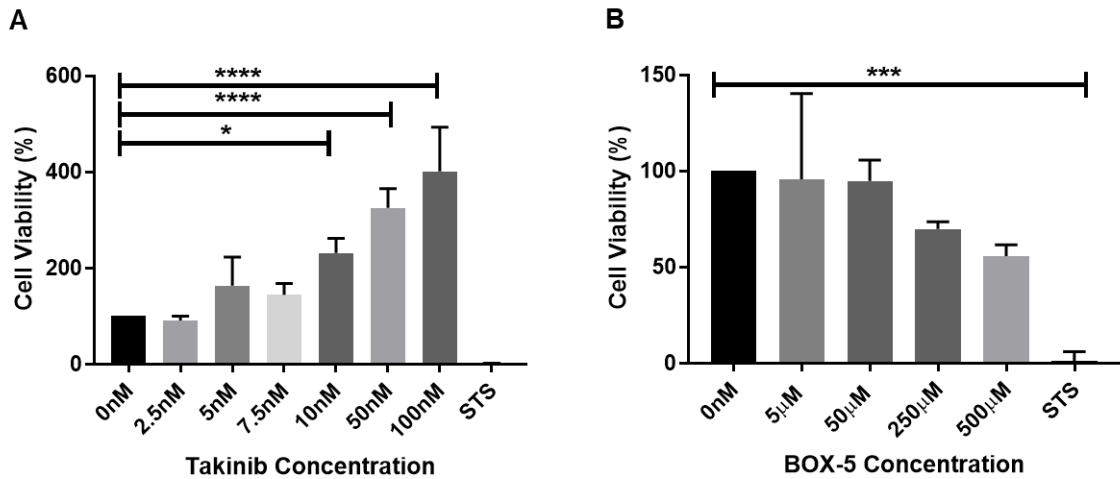


Figure 2.2 Effects of Takinib (A) and BOX-5 (B) Comparative to Basal Conditions on Metabolic Activity in Immortalised Human Bronchial Epithelial Cells. Stimulants were applied for 48 hours. Data is $n=3$ and presented as mean with standard deviation. $*p < 0.05$ by One-way ANOVA with Dunnett's post hoc test for intergroup comparisons. **** is p -value of <0.0001 .

2.8 Development of ALI Scratch Wound Technique

To initially see if scratch wounding on transwells were feasible, a preliminary study was performed to look at BEAS-2B repair on transwell membranes using a JuLI stage real-time cell history recorder (NanoEnTek). The JuLI was on loan, so was only available for this experiment. Three independent passages of BEAS-2Bs were overseeded into four transwells of a 12-well plate. I wounded the cultures, washed them once with PBS (as excess washing detached BEAS-2B cells from the membrane), and set the JuLI to acquire images every hour. As the JuLI is placed within the incubator, the cultures did not need to be removed from the incubator at any time.

The BEAS-2Bs did not show signs of healing with or without stimulation of rhWNT5A or rhTGF- β 1, as shown in representative images in **Figure 2.3A-B**, and in fact stimulation appeared to decrease confluency from basal. The summary of the results are shown in **Figure 2.3C**.

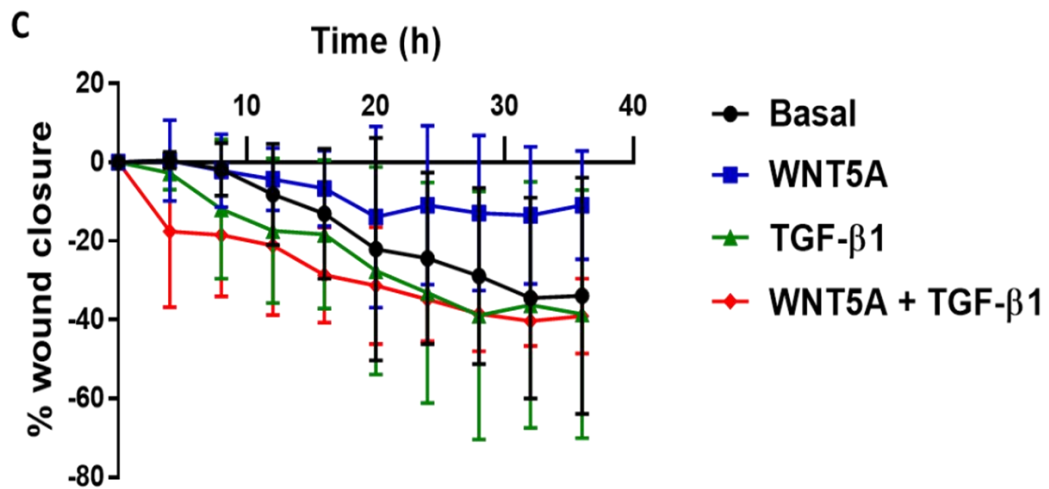
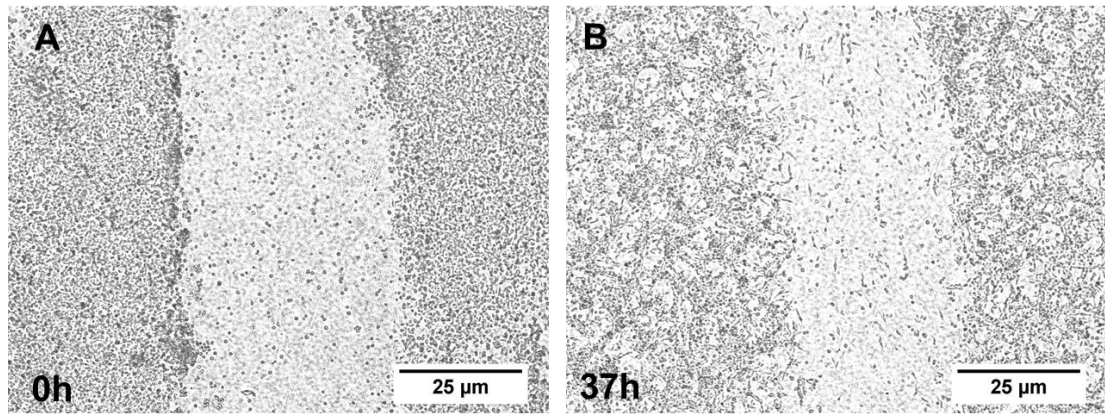


Figure 2.3 Transwell Scratch Wound Assay Optimisation with BEAS-2Bs Cultured on the Transwell Membrane. (A-B) Representative BEAS-2B scratch wound images at 0 (A) and 37 hours (B) for the same condition. (C) Summary figure of BEAS-2B optimisation scratch wound assay without stimulation and following stimulation with both rhTGF- β 1 (10ng/ml) and rhWNT5A (1 μ g/ml) alone and in combination. Data is n=3, and presented mean with standard deviation. Data was acquired over 37 hours, but data is only shown for every 4 hours post-wounding so error bars could be visibly differentiated.

To analyse the images, I used a macro sourced from a paper by Nunes and Dias (2017). The macro calculates percentage surface area covered by cells. **Figure 2.4** shows how the macro selects the areas. On interpretation of the images, the macro was fairly successful at determining between the membrane pores and cells and selected the cells appropriately as long as shading and bubbles were not present in the image. To save time and effort in manual measurement of the wound bed, it was decided that the macro would be used for future analysis.

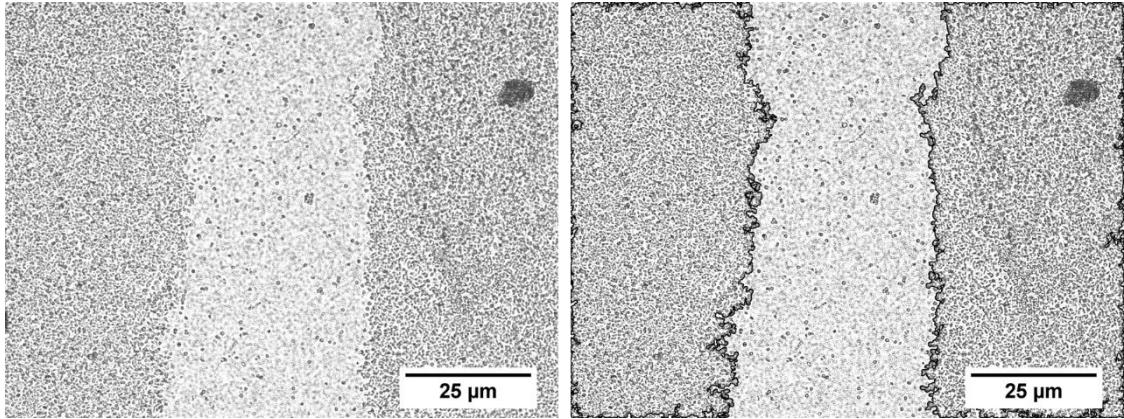


Figure 2.4 Macro Selection of a Representative BEAS-2B Scratch Wound Assay Image.

From this preliminary experiment, it was discovered that it is feasible to wound cultures without tearing the membrane. BEAS-2Bs did not show signs of healing over 37 hours but did show signs of migration. This could be because BEAS-2Bs do not develop tight junctions, so perhaps are easier to detach from the membrane (Stewart *et al.* 2012: B). They also express lower amounts of the epithelial cell adhesion molecule (EpCAM), which was evident by staining the BEAS-2B cells for basal cell markers for flow cytometric analysis. Additionally, TGF- β 1 stimulation may also have induced EMT, propagating further detachment.

Scratch wounding of HBECs on membranes have been reported, and healing observed (Carlsson 2013) (Milara *et al.* 2010). I therefore progressed to attempt scratch wounding on differentiated HBECs. To optimise the scratch wound assay, I evaluated which instrument is best to wound with, whether it was better to wound with the apical surface dry or submerged, and how to improve wound regularity (to use a ruler or not, and which direction across the transwell I should wound).

As the transwell does not have a continuous rim that anchors the transwell, I found it was easier to wound from the gap in the rim down. This was beneficial for two reasons. The first being, it allowed me to orientate the transwell so I could always identify where the wound would be, and the second in that it prevented

the transwell from tipping during wounding, which compromised wound regularity and increased the chance of puncturing the membrane.

In addition to wounding away from the gap in the rim, using a sterilised ruler helped prevent the well from tipping. It also steadied my hand to ensure wounds were straight and consistent. When assessing the wounding instrument, I originally tested two brands of 200µl pipette tips (VWR and Starlab TipOne). With plastic pipette tips, in a fraction of the cultures, I encountered cell banking either side of the wound, and cells remained behind in the wound bed. To circumvent this, I tried glass Pasteur pipettes as used by Carlsson (2013) in his ALI scratch wound assays. The glass pipettes did remedy the cell banking, however, the wound beds became inconsistent due to the inadequate application of wounding pressure used to avoid puncturing the membrane. The glass pipettes also visually damaged the membrane, which supports what Carlsson (2013) reported. I therefore switched back to the more rigid 200µl VWR pipette tip for the optimised assay design, which provided me with the best consistency but did not damage the membrane. To minimise the issue of cell banking, I switched to wounding the cultures submerged in PBS. This was to encourage any lifted cells/cell sheet to float rather than bank, thereby preventing reattachment and in theory aiding cell removal.

With the scratch wound assay, I had to refer back to the area of the wound I had acquired pictures of; I had two options, to draw on the bottom of the 12-well plate and use the lines to orientate myself to the original scratch wound picture destination, or use a microscope with a motorised stage. For the first proposed method, this highlighted the need for orientating the transwell. Due to ease, and the fact that the microscope had an environmental test chamber that could maintain a temperature of 37°C, I chose to use the microscope with the automated stage. In later experiments the test chamber was removed due to maintenance problems and wasn't replaced as the humidity in the chamber appeared to affect the xy coordination of the stage motor. For this reason, all scratch wound assays performed after the maintenance tended to include

landmark features in the images to help orientate myself back to the same location if the motor should stall or fail, to safeguard against acquiring incorrect follow-up images.

2.9 Scratch Wound Assay Investigating the Effect of TGF- β 1 on Wound Healing

ALI Cultures were washed twice with warm PBS and assessed for TEER (the 'before wounding TEER' as referenced in Chapter 4). PBS was then removed and 800 μ l 10ng/ml rhTGF- β 1 in PneumaCult ALI Media was added basally. After a 24- or 48-hour incubation, the basal media was removed, the apical surface of the culture washed twice with warm PBS and TEER recorded (this is the 'immediately before wounding' TEER referenced in Chapter 4). Please refer to the TEER method for further information on how this was conducted. The cultures were then wounded once vertically through the centre of the membrane using a sterile 200 μ l VWR pipette tip. The 200 μ l tip was inserted into a 1ml pipette tip to increase wounding tool length and therefore decrease contamination risk. The cultures were washed again a further two times before further TEER analysis (this is the 'immediately after wounding' TEER as referenced in Chapter 4). The cultures were then fed 800 μ l PneumaCult ALI media basally.

Pictures were acquired at 10x magnification at 0h, 4h, 8h and 24h with NIS-Elements AR 3.0 using a Nikon Eclipse TE2000-U inverted microscope with motorised stage. After the 24-hour image was acquired, the basal media was removed the apical surface of the culture washed twice with warm PBS and the TEER recorded one final time (the 24-hours post wounding' TEER as referenced in Chapter 4). Two images were taken per well, with attention to acquiring images for wound beds of similar width. The images were analysed for percentage wound healing using a macro in ImageJ. The macro used was sourced from a paper by Nunes and Dias (2017) as mentioned in the section on optimisation of this method. The macro calculates percentage surface area covered by cells.

2.10 Scratch Wound Assay Investigating the Effect of TGF- β 1 and WNT5A With and Without the Presence of Inhibitors on Wound Healing

Prior to stimulation, ALI Cultures were washed with warm PBS twice and assessed for TEER. Please refer to the TEER method for further information on how this was conducted. PBS was then removed and 700 μ l of 7.5nM Takinib or DMSO control in Stemcell PneumaCult ALI Media was added within the basal chamber and left to incubate for 30 minutes at 37°C prior to rhTGF- β 1 stimulation. A 100 μ l ALI media supplement containing rhTGF- β 1 and Takinib, or vehicle control equivalents, was then added basally to give an overall concentration of 20ng/ml rhTGF- β 1 and 8.4nM Takinib in the 800 μ l volume.

After a 48-hour incubation at 37°C, the ALI cultures were washed twice with warm PBS and assessed for TEER prior to wounding (the 'immediately before wounding TEER' as referenced in Chapter 4). The cultures were then wounded once vertically through the centre of the membrane using a sterile 200 μ l VWR pipette tip. The 200 μ l tip was inserted into a 1ml pipette tip to increase wounding tool length and therefore decrease contamination risk. The cultures were washed again a further two times before further TEER analysis (this is the 'immediately after wounding' TEER as referenced in Chapter 4). Then 700 μ l of 500 μ M BOX-5 Stemcell PneumaCult ALI Media was added basally and left to incubate for 30 minutes at 37°C before the addition of a 100 μ l supplement with rhWNT5A, a BOX-5 top-up or vehicle control, to give an overall concentration of 1 μ g/ml rhWNT5A and 500 μ M BOX-5 within the 800 μ l basal chamber.

Pictures were acquired at 10x magnification at 0h, 4h, 8h and 24h with NIS-Elements AR 3.0 using a Nikon Eclipse TE2000-U inverted microscope with motorised stage. After the 24-hour image was acquired, the basal media was removed, the apical surface of the culture washed twice with warm PBS and the TEER recorded one final time (the 24-hours post wounding' TEER as referenced in Chapter 4). Two images were taken per well, with attention to acquiring images for wound beds of similar width. The images were analysed for percentage

wound healing using a macro in ImageJ. The macro used was sourced from a paper by Nunes and Dias (2017) as mentioned in the section on optimisation of this method. The macro calculates percentage surface area covered by cells.

2.10.1 Scratch Wound Assay Analysis Plan

The scratch wound assay contained 12 conditions, of which cultures were cultured with and without rhTGF- β 1 and rhWNT5A, and with or without inhibitors Takinib and BOX-5. The experiment was designed in this way to minimise the number of bronchoscopy procedures required, and therefore improve efficiency, whilst also answering the assay objectives, which were:

- 1) Does rhTGF- β 1 stimulation enhance wound healing?
- 2) Does Takinib reverse any effect induced by rhTGF- β 1 stimulation on wound healing?
- 3) Does rhWNT5A stimulation enhance wound healing?
- 4) Does BOX-5 inhibition of rhWNT5A stimulation affect the wound healing response?
- 5) Does rhTGF- β 1 pre-stimulation enhance rhWNT5A stimulated wound healing?
- 6) Does Takinib reverse the rhTGF- β 1 pre-stimulation effect on rhWNT5A stimulated wound healing?
- 7) Does dual Takinib and rhTGF- β 1 pre-stimulation affect rhWNT5A wound healing?
- 8) What is the overall effect of Takinib, rhTGF- β 1 and rhWNT5A on wound healing?

The breakdown of the conditions used to answer each objective is shown in **Figure 2.5**. Each number corresponds to the eight previously listed objectives of the assay.

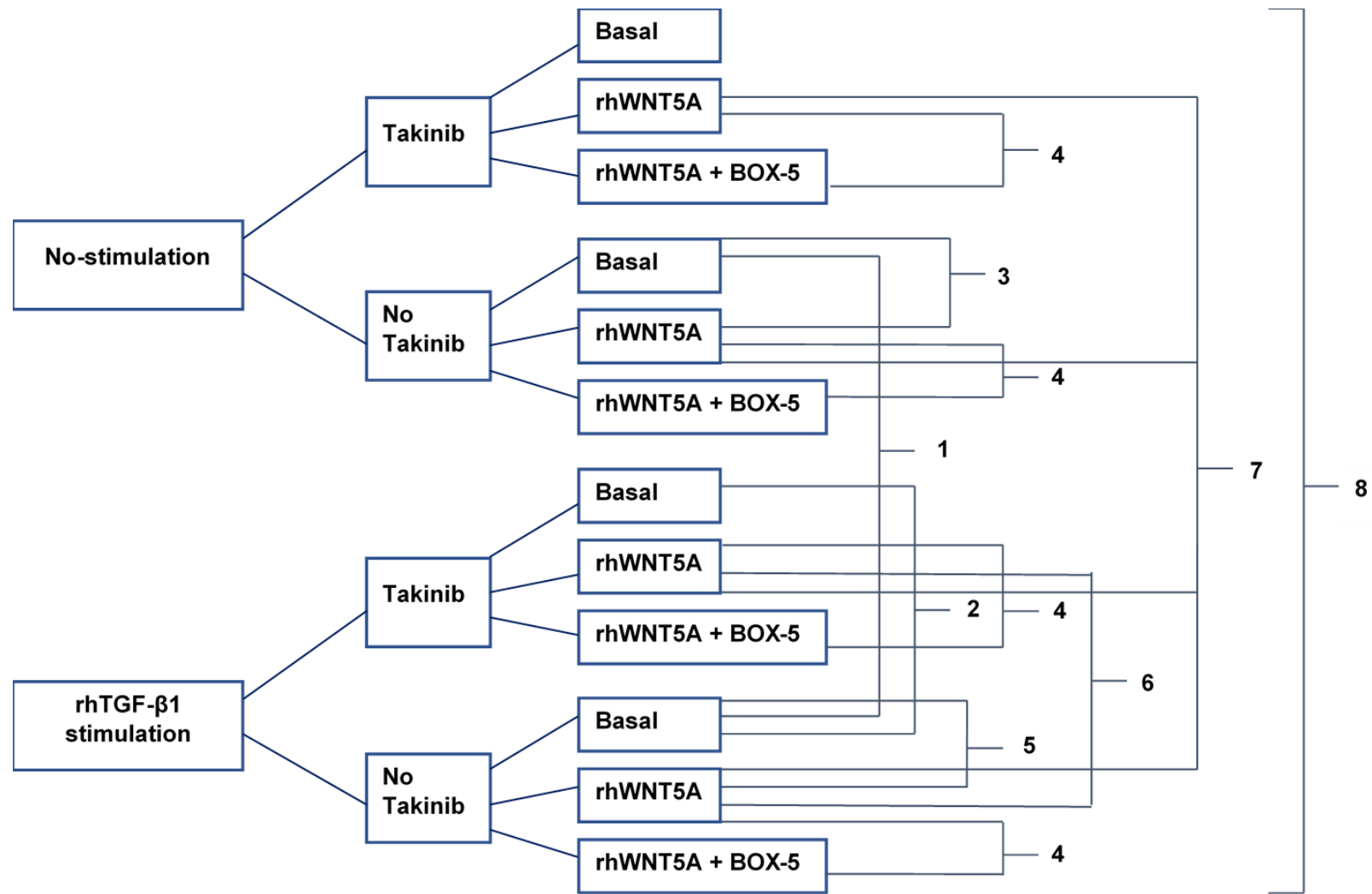


Figure 2.5 Scratch Wound Assay Experimental Plan Showing Group Comparisons For Each Assay Objective.

2.11 Transfection of ALI cultures and HEKS with Transfection Reagents

INTERFERin, Viromer Blue, Viromer Green and Lipofectamine was tested for transfection efficiency on ALI cultures using a fluorescently labelled GAPDH siRNA. FAP siRNA (Thermofisher, cat no AM4620) was re-suspended in 500 μ l RNA free H₂O to give a 10 μ M stock concentration. For experiments investigating transfection reagents on ALI cultures, Stemcell PneumaCult Basal Media without antibiotics was used. For HEK transfection, Opti-mem with reduced serum (Thermofisher, cat no 31985070) and no antibiotics was used. The protocol shown in **Appendix 3** details the transfection method for each transfection reagent used. After a 5- hour incubation, the cells were washed with PBS, and either trypsinised for 10 minutes at 37°C for ALI cultures, or detached using PBS if HEK293T. The cells were delegated into tubes and run instantly on the Attune NxT Flow Cytometer (Thermofisher).

2.12 Transcriptomic Analysis

2.12.1 Cohort Discovery

The Severe Asthma Research Program (SARP) discovery population consisted of 69 severe asthmatic patients. All severe asthmatics identified within the SARP were subjected to comprehensive phenotypic characterisation to further understanding of pathophysiological mechanisms in severe asthma. This previously published epithelial brush microarray data (Moore *et al.* 2010) (Modena *et al.* 2014) was generated using the following microarray plate: GPL6480 Agilent-014850 Whole Human Genome Microarray 4x44K G4112F (Probe Name version). A second replication cohort was also identified to confirm whether the findings were reproducible: Unbiased Biomarkers for the Prediction of Respiratory Disease Outcomes (U-BIOPRED). The U-BIOPRED study brush microarray data was generated using a GeneChip® Human Genome U133 Plus 2.0 microarray plate (Kuo *et al.* 2017: A). U-BIOPRED also focused on enhancing understanding of different asthma phenotypes but this was investigated in both adults and children, and therefore only adults with severe asthma were included in the comparative analysis. The U-BIOPRED replication cohort (Bel *et al.* 2011)

(Shaw *et al.* 2015) (Bigler *et al.* 2017) (Kuo *et al.* 2017: B) consisted of 49 severe asthmatic patients.

2.12.2 Module Identification

The gene modules were derived from the pathway gene lists for each signal transduction Kyoto Encyclopedia of Genes and Genomes (KEGG) signalling pathway. The following KEGG pathway maps were used to generate the gene lists: map04350 (TGF- β), map04310 (WNT), map04330 (Notch) and map04010 (MAPK signalling). As transcriptomic data sets have high dimensionality, a pathway gene set analysis method was applied to continuously link the epithelial repair pathway transcriptomic genes into a single transcriptional module that could then be condensed into a single gene expression pattern profile representative of module expression.

Four signalling pathway modules (canonical and noncanonical WNT and TGF- β) and two signalling overlap modules (WNT5A and TGF- β 1, and WNT, TGF- β 1 and Notch) were identified based on their role in epithelial repair, which may be responsible for asthmatic airway remodelling if gone awry. The overlapping gene modules were derived based on hypothetical crosstalk between signalling pathways. To identify if WNT and TGF- β 1 signalling collaborate in epithelial repair as hypothesised, a WNT and TGF- β 1 transcriptional module was assessed. To assess a link between goblet cell hyperplasia and WNT-TGF- β 1 signalling in epithelial repair, a transcriptional module linking Notch, WNT and TGF- β 1 was also evaluated. The genes included in each module are shown in **Table 2.2**, and the rationale for their module inclusion is given in **Appendix 4**. The gene overlap between these modules are shown in **Figure 2.6**.

Table 2.2 Transcriptomic Module Analysis Gene Grouping

<p>Canonical WNT Signalling</p>	<p>CDH1, CAPN1, WNT1, WNT2, WNT2B, WNT3, WNT3A, WNT5A, WNT8A, WNT8B, WNT9A, WNT9B, WNT10A, WNT10B, WNT11, WNT16, NDP, FZD1, FZD2, FZD3, FZD4, FZD5, FZD6, FZD7, FZD8, FZD9, FZD10, LRP5, LRP6, RSPO1, RSPO2, RSPO3, RSPO4, LGR4, LGR5, LGR6, PORCN, NOTUM, GPC4, INVS, WIF1, DKK1, DKK2, DKK4, KREMEN1, KREMEN2, SERPINF1, SOST, SOSTDC1, BAMBI, SFRP1, SFRP2, SFRP4, SFRP5, CSNK1E, DVL1, DVL2, DVL3, NKD1, NKD2, FRAT1, FRAT2, CSNK2A1, CSNK2A2, CSNK2B, CSNK2A3, GSK3B, AXIN, AXIN2, APC, APC2, CSNK1A1, CSNK1A1L, CTNNB1, CTNNBIP1, CHD8, PSEN1, PRKACA, PRKACB, PRKACG, CREBBP, MAP3K7, NLK, TLE1, TCF7, TCF7L1, TCF7L2, LEF1, MYC, JUN</p>
<p>Noncanonical WNT Signalling</p>	<p>NFKB1, TLE1, CUX1, FOXA2, SP1, MYB, PAX2, WNT2B, WNT4, WNT5A, WNT5B, WNT6, WNT7A, WNT7B, WNT9A, WNT9B, WNT11, WNT16, NDP, FZD1, FZD2, FZD3, FZD4, FZD5, FZD6, FZD7, FZD8, FZD9, FZD10, ROR1, ROR2, RYK, MCAM, RSPO1, RSPO2, RSPO3, RSPO4, LGR4, LGR5, LGR6, PORCN, NOTUM, GPC4, INVS, WIF1, DVL1, DVL2, DVL3, NKD1, NKD2, SFRP1, SFRP2, SFRP4, SFRP5, VANGL1, VANGL2, PLCB1, PLCB2, PLCB3, PLCB4, PRKCA, PRKCB, PRKCG, CDC42, MAP2K7, CAMK2A, CAMK2B, CAMK2D, CAMK2G, MAP3K7, DAAM1, DAAM2, RHOA, ROCK2, RAC1, RAC2, RAC3, FLNA, CAPN1, MAPK8, MAPK9, MAPK10, MAPK11, MAPK12, MAPK13, MAPK14, PPM1A, PPP3CA, PPP3CB, PPP3CC, PPP3R2, PPP3R1, NLK, NFATC1, NFATC2, NFATC3, NFATC4, RUNX2, CREBBP, EP300</p>
<p>Canonical TGF-β Signalling</p>	<p>TLE1, ITGA6, THBS1, DCN, RUNX2, TCF4, TGFB1, TGFBR1, TGFBR2, TGFBR3, BAMBI, SMURF1, SMURF2, SMAD2, SMAD3, SMAD4, SMAD6, SMAD7, SMAD9, ZFYVE9, ZFYVE16, TGIF1, TGIF2, PMEPAI, SKIL, CREBBP, EP300, SP1, MYC, CDKN2B</p>
<p>Non-canonical TGF-β Signalling</p>	<p>ITGA6, THBS1, DCN, RUNX2, TCF4, TGFB1, TGFBR1, TGFBR2, TGFBR3, BAMBI, MAP3K7, NLK, MAP3K14, CHUK, IKBKB, IKBKG, NFKB1, NFKB2, RELA, RELB, NFKB1A, TLE1, MAP2K4, MAP2K7, MAPK8, MAPK9, MAPK10, NFATC1, NFATC3, DAXX, MAP3K5, MAP2K3, MAP2K6, TRAF2, TRAF6, MAPK11, MAPK12, MAPK13, MAPK14, RHOA, ROCK1, RAC1, RAC2, RAC3, CDC42, PRKCA, PRKCB, PRKCG, PRKACA, PRKACB, PRKACG, RAF1, MAP2K1, MAP2K2, MAPK1, MAPK3, MYC, ATF4</p>

WNT-TGF- β Overlap	CUX1, FOXA2, SP1, MYB, PAX2, PORCN, NOTUM, GPC4, INVS, WIF1, WNT5A, ITGA6, LTBP1, THBS1, DCN, ROR2, RYK, MCAM, FZD2, FZD3, FZD4, FZD5, FZD6, FZD7, FZD8, LRP5, RSPO1, RSPO2, RSPO3, RSPO4, LGR4, LGR5, LGR6, RUNX2, TCF4, TGFB1, TGFB1, TGFB2, TGFB3, BAMBI, SMURF1, SMURF2, SMAD2, SMAD3, SMAD4, SMAD6, SMAD7, ZFYVE9, ZFYVE16, TGIF1, TGIF2, PMEPAI, SKIL, SKI, MAP2K4, MAP2K7, MAPK8, MAPK9, MAPK10, NFATC1, NFATC3, DAXX, TRAF6, MAP3K7, PRKACA, PRKACB, PRKACG, CREBBP, MAPK11, MAPK12, MAPK13, MAPK14, NLK, RHOA, RAC1, RAC2, RAC3, PRKCA, PRKCB, PRKCG, CDC42, MAP3K5, MAP2K3, MAP2K6, MAP3K14, CHUK, IKBKB, IKBKG, NFKB1A, NFKB1, NFKB2, RELA, RELB, TLE1, RAF1, MAP2K1, MAP2K2, MAPK1, MAPK3, MYC, ATF4
WNT-Notch-TGF- β Overlap	NOTCH1, DLL1, DLL3, DLL4, JAG1, JAG2, ADAM17, LFNG, MFNG, RFNG, DVL1, DVL2, DVL3, NUMB, NUMBL, PSEN1, PSEN2, NCOR2, HIF1A, MAML1, MAML2, MAML3, RBPJ, RBPJL, GSK3B, TGFB1, SMAD3, SMAD4, CTNNB1, TLE1, LEF1, TCF7, TCF7L1, TCF7L2, HEY1, HES1

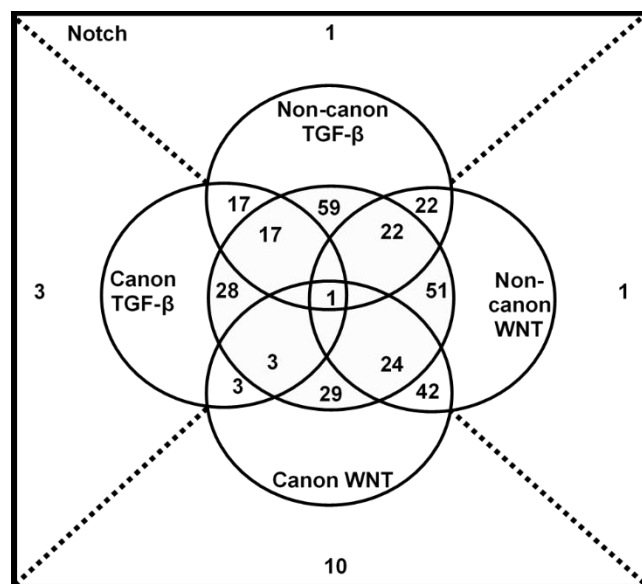


Figure 2.6 Venn Diagram Depicting Gene Overlap Between the Module Groupings. There are four signalling pathway modules, one central module (*WNT5A* and TGF- β overlap), and one outer Notch, WNT and TGF- β . The numbers represent the number of genes common to the two or three overlapping pathways.

Multiple genes were present across the four main pathways, with one key central overlapping pathway module (WNT and TGF- β). **Figure 2.6** depicts the number of overlapping genes between each signalling pathway and the central WNT/TGF- β transcriptional overlap pathway module. For example, non-canonical TGF- β shares 59 genes in common with the central overlap module, 17 genes with both the canonical TGF- β and central WNT- TGF- β overlap module, 17 genes with canonical TGF- β alone, and 1 gene with the Notch, WNT and TGF- β overlap module. Those 17 genes are common across all three modules. There was 1 hub gene which presented in all the transcriptional group modules – TLE1 (Transducin-like enhancer protein 1).

2.12.3 Eigengene Network Analysis

Following the previously described pathway gene set analysis method used to define the transcriptional modules specified in table 2.3, data dimensionality was reduced into a single gene expression pattern profile representative of module expression. This linear single gene expression pattern profile explains the modular expression variance and is termed the module's eigengene. The eigengene is defined as the first principal component of the module expression matrix, and allows the association with a given trait, such as FEV₁/FVC, to be studied with co-regulated module gene expression rather than the gene expression of a single gene within a module; thereby reducing the number of necessary comparisons required to investigate a specific hypothesis. In this study, the association between the module eigengene expression and pre-bronchodilator ratio of FEV₁ to forced vital capacity (FVC), which is termed the FEV₁/FVC ratio, and TH status was investigated, of which the summary data of the associations are given for each of the transcriptional modules for both the SARP and UBIOPRED cohort. This analysis was performed by Dr Matt Richardson (Leicester NIHR BRC statistician) using R (3.6.0).

2.12.4 Module Discovery Literature Review

To identify relationships between epithelial repair pathways and FEV₁/FVC ratio, a crude marker of airflow obstruction associated with airway remodelling in

asthma, and TH2 and TH17 inflammatory transcriptional signatures previously defined by Choy *et al.* (2015), a literature review was conducted to investigate the cell signalling pathways associated with epithelial repair, which may be responsible for asthmatic airway remodelling if gone awry. Sections 2.12.4.1 to 2.12.4.4 explain the role of each signalling pathway in the context of epithelial repair.

2.12.4.1 Canonical and Noncanonical TGF- β Signalling

Following wounding, cells closest to the wound begin to spread, and undergo EMT to migrate into the wound bed. TGF- β signalling can induce EMT via the SMAD3 axis to promote cellular migration (Hackett *et al.* 2009), stimulate fibroblast secretion of ECM (Halwani *et al.* 2011), and influence expression of ECM regulators MMPs and TIMPs (Zhou *et al.* 2007) (Ye *et al.* 2011) (Lechapt-Zalcman *et al.* 2006). By doing so, it promotes secretion of a provisional ECM which provides cellular anchorage points for cells to exert traction on (Atkinson *et al.* 2008) (Legrand *et al.* 1999). TGF- β can also signal through non-SMAD pathways such as TRAF6-TAK1-p38/JNK and Shc-Erk signalling to regulate EMT, and PI3K-CDC42 and RhoA-ROCK to induce actin polymerisation and the dissolution of tight junctions during EMT (Zhang 2017).

2.12.4.2 Canonical and Noncanonical WNT Signalling

Like TGF- β signalling, noncanonical WNT signalling is also involved in cellular migration - WNT/Ca²⁺ signalling regulates cell adhesion and migration (Sharma and Pruitt 2020) (Semenov *et al.* 2007), and the PCP pathway governs cytoskeletal dynamic processes such as cellular polarity, migration, and asymmetric cell division (Vladar and Königshoff 2020). The role of noncanonical WNT signalling in asymmetric division interplays with canonical WNT signalling in controlling basal cell proliferation during repair to ensure regenerative needs are met but basal cell frequencies maintained (Teixeira *et al.* 2013). Canonical WNT signalling is reported to be a key regulator of stemness and differentiation, promoting long-term renewal of stem cells (Brechbuhl *et al.* 2011) (Habib *et al.* 2013). This is supported by an association between canonical WNT signalling

and basal cell hyperproliferation in lung malignancy (Aros *et al.* 2020). The role of noncanonical WNT in basal cell division, however, is thought to be vital for spatial patterning, as during murine and avian lung development WNT5A knockout results in increased cellular proliferation and airway branching (Li *et al.* 2002) (Li *et al.* 2015), whereas, WNT5A overexpression results in reduced airway formation (Loscertales *et al.* 2008). This is supported by a study into colonic wound repair which showed noncanonical WNT5A signalling inhibits canonical WNT proliferation to organise the regenerating epithelium and restore crypt formation (Miyoshi *et al.* 2012).

2.12.4.3 WNT, TGF- β 1 and Notch

After basal cell division and migration to the site of repair, the daughter cell(s) then need to undergo differentiation to the correct proportion of goblet to ciliary fate to restore the mucociliary escalator. As mentioned previously, a localised canonical WNT signal drives asymmetric division (Habib *et al.* 2013), but Notch signalling is responsible for basal cell differentiation into luminal epithelial cells (Rock *et al.* 2011). TGF- β signalling can influence the transcriptional activity of both canonical WNT signalling via TAK1-NLK signalling (Ishitani *et al.* 1999), and Notch signalling via SMAD3 (Blokzijl *et al.* 2003), to potentially mediate differentiation during repair.

2.12.4.4 WNT and TGF- β 1

Considering the interplay between the canonical and noncanonical WNT pathways, and the identified role of TAK1-NLK in downregulating β -catenin transcriptional activity, TGF- β 1 and noncanonical WNT signalling may exhibit crosstalk to inhibit canonical WNT signalling activity to potentiate a common end goal.

To further understanding of the crosstalk between these three signalling pathways, the numerous crosstalk mechanisms identified by extensive literature review are listed in **Table 2.3.** and displayed pictorially in **Figure 2.7.** There are at least 10 crosstalk mechanisms that could have been investigated.

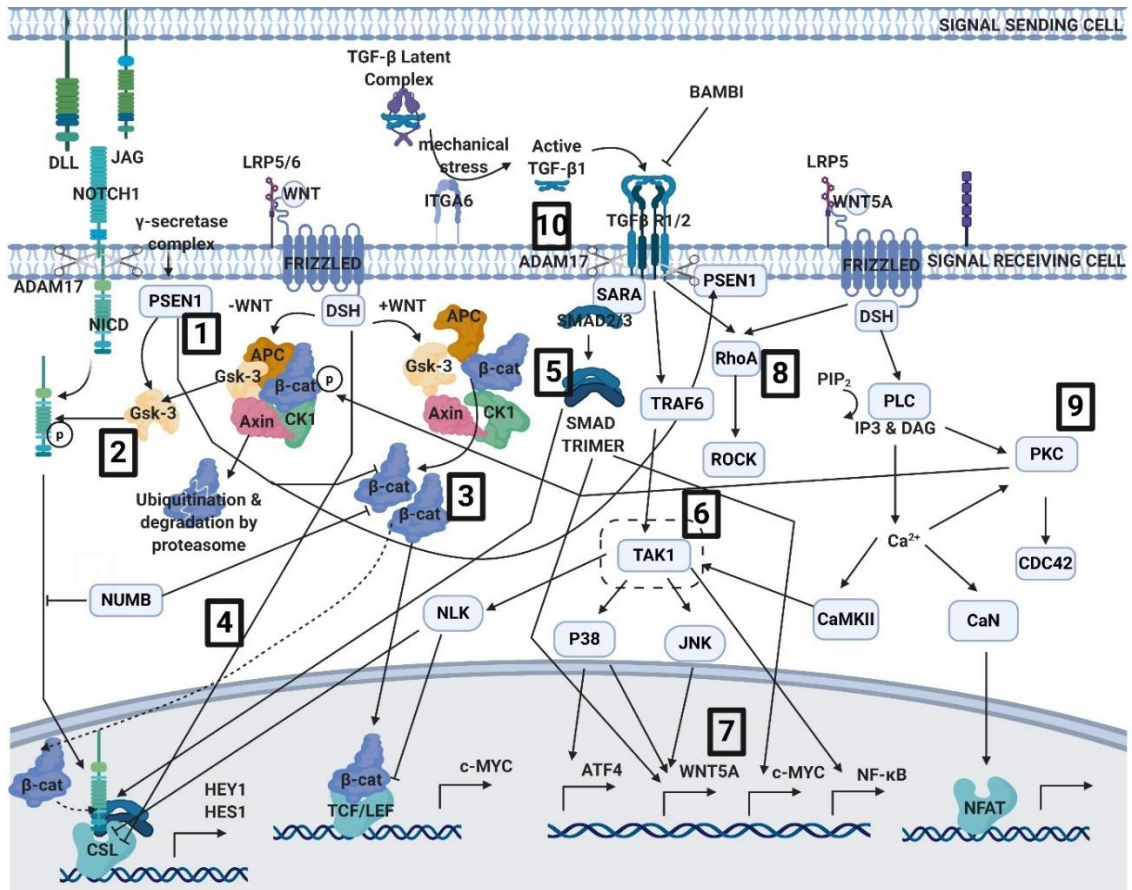


Figure 2.7 Potential Crosstalk Intermediaries to Investigate Between the WNT, TGF- β and Notch Signalling Pathways. Created with BioRender.com.

Table 2.3 Crosstalk Intermediaries Identified Between WNT, TGF- β and Notch Signalling

Crosstalk Intermediary	Signalling Overlap Module	Roles in each pathway of the Signalling Overlap Module	References
Presenilin 1	WNT, TGF- β 1 and Notch	<p>Notch: Forms part of the γ-secretase complex that cleaves Notch thereby releasing its NICD to activate signalling.</p> <p>TGF-β: Can be induced by TGF-β signalling and recruited by Traf6 to cleave the TGF-βR.</p> <p>WNT: Can inhibit canonical WNT signalling through altering GSK-3β activity.</p>	Gudey <i>et al.</i> 2014 Dobrowolski <i>et al.</i> 2012 Van Gassen <i>et al.</i> 2000
GSK-3 β	WNT, TGF- β 1 and Notch	<p>WNT: Forms part of the β-catenin destruction complex.</p> <p>Notch: GSK-3β can positively or negatively regulate Notch signalling</p> <p>TGF-β: GSK-3β also negatively regulates EMT protein SNAIL-1 which is induced through TGF-β signalling. SNAIL-1 then inactivates GSK-3β to provide a form of negative feedback.</p>	Guha <i>et al.</i> 2011 Foltz <i>et al.</i> 2002 Zheng and Conner 2018 Jin <i>et al.</i> 2009: B Polimeni <i>et al.</i> 2016 Matsumoto <i>et al.</i> 2018 Yu, Jiang and Zhang 2018
β -catenin	WNT, TGF- β 1 and Notch	<p>WNT: a key downstream effector of canonical WNT signalling.</p> <p>WNT/Notch: interacts with the NICD promoting NICD transcriptional activity on CSL and HES1. Notch signalling, however, negatively regulates canonical WNT signalling through regulating active β-catenin levels, and through forming a Notch- β-catenin complex which induces β-catenin degradation.</p>	Jin <i>et al.</i> 2009: A Yamamizu <i>et al.</i> 2010 Acosta <i>et al.</i> 2011 Kwon <i>et al.</i> 2011 Hayward <i>et al.</i> 2005
Dishevelled	WNT, TGF- β 1 and Notch	<p>WNT: acts directly downstream of WNT Frizzled receptor signalling.</p> <p>WNT/Notch: DVL2 inhibits Notch signalling through binding to RBPJK reducing its transcriptional activity.</p>	Collu <i>et al.</i> 2012
SMAD3	WNT, TGF- β 1 and Notch	Notch/TGF-β: SMAD3 can interact directly with the NICD to regulate Notch transcriptional activity via CSL.	Blokzijl <i>et al.</i> 2003
WNT5A transcription	WNT and TGF- β 1	WNT/TGF-β: TGF- β signalling can directly and indirectly influence WNT5A transcription via SMAD signalling and TAK1.	Katoh and Katoh 2009 Kumawat <i>et al.</i> 2014
TAK1	WNT and TGF- β 1	WNT/TGF-β: TGF-TAK1-NLK signalling downregulates canonical WNT β -catenin transcriptional activity through TCF/LEF. This is cell	Ishitani <i>et al.</i> 1999 Li <i>et al.</i> 2010 Ota <i>et al.</i> 2012

		<p>context dependent, however, as NLK can also positively regulate WNT β-catenin signalling.</p> <p>WNT: Noncanonical WNT WNT5A has also been reported to induce TAK1-NLK signalling to antagonise the canonical WNT pathway. This is controversial however, with conflicting reports evident in the literature.</p> <p>Notch: TAK1 represses Notch1 transcriptional activity via NLK. TAK1 deficiency also increases notch inhibitor, NUMBL, to downregulate Notch transcriptional activity.</p>	<p>Ishitani <i>et al.</i> 2003 Baarsma <i>et al.</i> 2017 Smit <i>et al.</i> 2004 Ishitani <i>et al.</i> 2010 Swarnkar <i>et al.</i> 2015</p>
RhoA	WNT and TGF- β 1	<p>WNT/TGF-β: Both TGF-β and WNT5 signal through RhoA-ROCK to induce EMT that is evidenced through adheren junction disruption, actin cytoskeletal reorganisation and cell migration.</p>	<p>Bhowmick <i>et al.</i> 2001 Korol, Taiyab and West-Mays 2016 Zhu <i>et al.</i> 2006 Linke <i>et al.</i> 2017 Wang <i>et al.</i> 2013</p>
PKC α	WNT and TGF- β 1	<p>WNT: WNT5A signalling sequesters the canonical WNT pathway directly through PKCα-mediated phosphorylation of β-catenin resulting in its degradation, and indirectly via PKCα phosphorylation of RORα which facilitates its binding to β-catenin to repress its transcriptional activity.</p>	<p>Gwak <i>et al.</i> 2006 Baarsma <i>et al.</i> 2017 Lee <i>et al.</i> 2010</p>
Adam17	WNT, TGF- β 1 and Notch	<p>Notch: Initiates Notch signalling through S2 cleavage (which breaks ligand-receptor bonds).</p> <p>TGF-β: Following MAPK signalling activation, ADAM17 cleaves TGF-βR1, thereby reducing its expression.</p>	<p>Jia <i>et al.</i> 2019 Liu <i>et al.</i> 2009 Mu <i>et al.</i> 2011</p>

2.12.5 How the Module Discovery Literature Review Shaped the Study Hypothesis

Signalling pathways are depicted as linear pathways in KEGG diagrams. This overly simplistic approach, as mentioned by Moon and Gough (2016), inadequately considers spatial localisation and other dynamics that shape the pursuant cell signalling response following pathway activation. **Figure 2.7** highlights the difficulty in adequately representing pathway crosstalk, with a strenuous effort required to express how signal transduction may flow through a pathway whilst incorporating crosstalk from neighbouring influential cell pathways. The ten crosstalk mechanisms highlighted in **Table 2.3** are likely to contribute to the net balance of signals to determine the cellular healing response.

Van Amerongen and Nusse (2009) stresses the need to consider integration of numerous WNT pathways to determine cell response, of which is effectually determined by receptor binding and the downstream intracellular response. Noncanonical and canonical WNT can exert reciprocal pathway inhibition at the receptor level by competitive FZD receptor binding (Grumolato *et al.* 2010), as well as through the downstream signalling crosstalk mechanisms listed previously via TAK1 and PKC α . Pathway activation and the functional response that pursues is also dependent on the cellular context as receptor expression and ligand-receptor binding can initiate canonical and noncanonical WNT signalling via different receptor/co-receptors (Kikuchi, Yamamoto and Sato 2009).

TAK1 appears pivotal in the net balance of signals between the canonical and noncanonical WNT signalling axis, although TAK1 may or may not be involved in WNT5A antagonism of the canonical WNT signalling pathway. TGF- β TAK1 signalling may skew the WNT response in favour of the noncanonical axis through increasing WNT5A transcription directly through TAK1 or indirectly through TAK1-mediated NF- κ B (Katoh and Katoh 2009). Through increasing WNT5A expression, TGF- β can indirectly inhibit the canonical WNT axis through noncanonical inhibition of the canonical pathway, and directly through TAK1-NLK

inhibition of β -catenin transcriptional activity. TAK1 was therefore chosen as the crosstalk intermediary to investigate.

2.13 Gene Expression Analysis

2.13.1 BEAS-2B qRT-PCR

2.13.1.1 RNA Extraction

BEAS-2B cells were seeded (at 500,000 cells/dish) into four 10cm diameter petri dishes coated with 1% PureCol (Advanced BioMatrix, 5005-100ml) PBS, and fed every two days with 5ml BEGM until achieving or nearing full confluence. They were then stimulated for either 30 minutes or 4 hours with 10ng/ml rhTGF- β 1 or vehicle control (1mg/ml BSA with 4mM HCl solution) in BEGM. RNA was extracted using a Total RNA Safety Line Kit (cat no 732-2870, VWR) according to manufacturer's instructions. The RNA concentration was determined using a Nanodrop 2000 (Thermo Scientific), and the RNA frozen down at -80°C for later conversion to mRNA.

2.13.1.2 Assessing RNA Quality

RNA quality and integrity following freezing at -80°C was assessed using an Agilent RNA 6000 Pico kit (Agilent, cat no 5067-1513) as per the manufacturer's instructions. 5000pg of total RNA was analysed per sample. Data was acquired and assessed on the Agilent 2100 Bioanalyser, using 2100 Expert software.

2.13.1.3 cDNA Synthesis

The RNA extracted for the four conditions above was converted to cDNA using a Qiagen RT2 First Strand Kit (Qiagen, cat no 330404) according to manufacturer's instructions. The RNA concentration converted was 0.5 μ g, as recommended by the supplier for first time users.

2.13.1.4 PCR of the Array Plates

The PCR plates used were custom made RT² Profiler PCR Arrays (CAPH13484A) purchased from Qiagen. A complete gene list can be viewed in **Appendix 5**. All four stimulation conditions were run on a single 96-well plate. As such, the PCR component mastermix was produced as shown in **Appendix 6**. The SYBR Green mastermix was first diluted and divided equally into four aliquots, of which per aliquot 25.5µl of cDNA synthesis reaction was added to form the PCR mastermix. Each well of the PCR plate then received 25µl of PCR component mix, and the plates were centrifuged for 5 minutes at 1000G at room temperature (15-25°C) to remove bubbles. The qRT-PCR was performed using a Stratagene Mx3000P and MxPro software v4.10. The thermal profile used contained an initial 10-minute cycle at 95°C to activate the Hot-Start Taq DNA polymerase, followed by 40 cycles at 95°C for 15s (denaturation) and 1 minute at 60°C (annealing/extension).

2.13.2 iHBEC qRT-PCR

1.1.1.1 iHBEC RNA Extraction

Cells were seeded into 10cm diameter petri dishes coated with 1% PureCol (Advanced BioMatrix, 5005) PBS and fed every two days with 5ml PneumaCult™-Ex Plus Media until achieving or nearing full confluence. They were then stimulated for 48 hours with 10ng/ml rhTGF-β1 or vehicle control (1mg/ml BSA with 4mM HCl solution). RNA was extracted using the Total RNA Safety Line Kit (cat no 732-2870, VWR) according to the manufacturer's instructions. The RNA concentration was determined using a Nanodrop 2000 (Thermo Scientific), and the RNA frozen down at -80°C for later conversion to mRNA.

2.13.2.1 Assessing RNA Quality

A 1% agarose gel was used to check integrity rather than using a bioanalyser chip assay due to lack of samples to justify kit purchase. GelRed (Biotium® cat no 41003) was added to the agarose gel (1:10000 dilution). GelRed was chosen

as the gel stain as it was readily available and is reported to be safer and have a higher sensitivity than Ethidium Bromide.

5µl of 500ng RNA was loaded per sample well with 5µl 2x loading dye (New England Biolabs, cat no B0363S). A ssRNA ladder (New England Biolabs, cat no N0362S) was loaded as a size standard. The sample and ladder were heated for 2.5 minutes then placed on ice for 2 minutes before loading into the gel. The gel was run at 60V and visualised using a Syngene Gene Genius Bio Imaging System with 40ms exposure.

2.13.2.2 RNA Clean-up of Samples

10µg of RNA was purified using a Monarch RNA Clean-up kit (New England Biolabs, cat no T2040) in accordance with manufacturer's instructions, and RNA concentration was assessed using a Nanodrop 2000. All samples had a 260/280 ratio of approximately 2.0 suggesting high quality RNA.

2.13.2.3 cDNA Synthesis

cDNA was prepared with a LunaScript RT Supermix Kit (New England BioLabs, cat no E3010S) according to manufacturer's instructions with 1µg RNA input into the synthesis reaction. In triplicate no template controls were synthesised alongside no-RT control reactions for each sample. cDNA was stored at -20°C.

2.13.2.4 TaqMan PCR

4µl of diluted cDNA (1µg diluted to 250ng using ultrapure water) and 6µl of PCR mastermix was added per well of a 384-well plate (Thermofisher, cat no 4309849) and sealed with MicroAmp Optical Adhesive Film (Thermofisher, cat no 4311971). The mastermix was formulated according to **Table 2.4**. All samples were performed in triplicate. The WNT5A probe was labelled with FAM, and 18S with VIC. 18S was selected as a housekeeping control because of its invariable expression across various tissues and treatments. This is evident in the literature

but was also supported by my earlier customised PCR plate analysis where stimulation with rhTGF- β 1 decreased stability of other reference genes.

Table 2.4 Constituents of the WNT5A TaqMan Mastermix

Component	Volume per reaction (μl)
TaqMan® Fast Advanced Master Mix (2X) - Fisher Scientific Cat no 13428456	5
TaqMan® WNT5A FAM Assay (20X) - Thermofisher Scientific Cat no 4453320 (Hs00998537_m1 WNT5A Taqman Assay)	0.5
18S rRNA VIC Assay (20X) - Applied Biosystems Cat no 4319413E	0.5
TOTAL VOLUME	6

The plate was briefly centrifuged for 1 minute at 1000rpm prior to loading into the QuantStudio5. The thermal profile used was according to manufacturer's recommendations: hold for 2 minutes at 50°C, then hold for 2 minutes at 95°C to activate the polymerase, followed by 40 cycles of 95°C for 1 second (denaturation) and 60°C for 20 seconds (annealing/extension).

2.13.3 PCR Data Analysis

The relative BEAS-2B RNA expression level, corrected using the reference dye ROX and normalized to the average of 18s rRNA and β -actin expression, was calculated by $2^{-\Delta\Delta C_t}$. Relative HBEC RNA expression was analysed using the same method but was normalised to 18s rRNA only.

2.14 Immunofluorescence

BEAS-2Bs were seeded into 1% PureCol coated Permax plastic 8-well chamber slides (Fisher Scientific, cat no 10098850) at 40,000 cells per well. The following day, the cells were stimulated for 48 hours with 300 μ l BEGM containing either 10ng/ml rhTGF- β 1, 1ng/ml rhWNT5A or vehicle control. Four conditions were investigated per stimulation with either rhTGF- β 1 or rhWNT5A: no stimulation stained with isotype control, no stimulation stained with target

antibody, stimulation stained with isotype control and stimulation stained with target antibody. Each condition was performed in duplicate.

Following 48-hours stimulation, the 8-well chamber slides were washed with PBS (without magnesium and calcium) and fixed on ice with methanol for 20 minutes. The slides were then air dried for 10 minutes at room temperature, washed with PBS, and non-specific antibody binding blocked with 3% BSA solution for 1 hour at room temperature before primary antibody staining for 90 minutes on ice. Antibody concentrations are shown in **Table 2.5**. The chamber slides were washed three times using 0.05% Tween 20 diluted in distilled water, and the secondary FITC-conjugated antibody added for 90 minutes on ice. The slides were washed three times with 0.05% Tween 20 PBS and three times with 1x PBS before nuclei staining with 0.1µg/ml DAPI per well for 45 seconds at room temperature. The slides were washed a final six times with 1x PBS, the plastic chambers removed, and 4 drops of prolong gold (Invitrogen, P36930) added to each slide prior to coverslipping.

Table 2.5 Immunofluorescence Antibody Concentration Table

Primary Antibody	Clonality	Clone Name	Supplier	Catalogue Number	Working concentration of antibody (µg/ml)
Vimentin	Monoclonal	V9	Sigma Aldrich	V6389	5
COL1A1	Polyclonal	N/A	Merck Millipore	Ab745	5
Cytokeratin-5	Monoclonal	RCK103	Santa Cruz	Sc-32721	4
Mouse IgG1	Monoclonal	DAK-GO1	Agilent	X0931	4
Rabbit IgG1	Polyclonal	RUO	BD Biosciences	550875	5
Secondary Antibody	Clonality	Clone Name	Supplier	Catalogue Number	Working concentration of antibody (µg/ml)
Rabbit anti Mouse FITC Secondary	Polyclonal	--	Agilent	F0313	7.2
Goat anti Rabbit Col1A1 FITC Secondary	Polyclonal	--	Sigma	F0382	1 in 20 dilution. Concentration not given

2.14.1 Image Analysis for Immunofluorescence

The Zeiss Axio Imager.Z2 AX10 was used to attain all images. All images were taken within 48 hours of staining completion. The exposure time applied was 1 second for FITC, and 400ms for DAPI. Three images were taken for each condition across two duplicate wells. To eliminate bias, pictures were acquired by identifying wells based on their position on the 8-well chamber slide and on DAPI staining. The FITC staining was not seen until the picture was acquired.

FITC fluorescence intensity was quantified using Zen 2 software image analysis. The sum of channel FITC parameter was selected as the measure of FITC staining. The isotype control images were used to retract background staining (in the FITC channel) through determining the average FITC threshold low level to select. To consider confluency in FITC fluorescence intensity, the fluorescence intensity was divided by the number of nuclei per image to give fluorescence intensity per cell. The average across all images acquired per condition was taken as the reportable result. The nuclei count was performed using the perimeter count of DAPI staining to give an estimation of nuclei per image. To retract any background noise, any DAPI perimeter smaller or equal to 0.01mm was retracted. Additionally, each image was inspected for overlapping nuclei, and the cell count adjusted if any cells were not counted as individual cells.

To measure cell elongation, ten vimentin positive selected cells were measured for height and width. Four cells were strategically selected by being the nearest visibly whole cell to the corners of each image. The remaining six cells were randomly selected based on their position (evenly spread across the entire image). An example of how the cells were selected is shown in **Figure 2.8**.

In the early stages of developing my panel, I collated a list of which target antigens I wanted to include based on a bronchial epithelium basal cell literature review. These were EpCAM, pan-cytokeratin, CD49F (which is also known as Integrin $\alpha 6$) and Nerve Growth Factor Receptor (NGFR). Later, two additional markers were added: CD166 and CD44. EpCAM and pan-cytokeratin dual-staining was reported as a novel gating strategy for defining epithelial cells by flow cytometry (Maestre-Batlle *et al.* 2017). I would have purchased the pan-cytokeratin antibody in that paper, but it was discontinued, suggesting it perhaps wasn't specific. Tariq Daud, however, did use a cytokeratin-5 (CK5) antibody for staining BEAS-2B cells in his thesis (Daud, 2017), and so I used the same antibody and clone as a substitute. However, this antibody was also found to be non-specific for the application of flow cytometry and was dropped from the panel, which is discussed in the next flow cytometry optimising sub-section(s).

NGFR and CD49F were initially chosen as my basal cell markers based on a paper by Rock *et al.* (2009), which identified the markers via transcriptomic analysis of mouse basal cells. To confirm their ability to identify the basal cell population, bronchial airway tissue was sorted for NGFR+CD49F+ expression which were cultured in matrigel for their ability to differentiate and form bronchospheres, of which they did. To help identify epithelial cells further, as the majority of BEAS-2Bs (which were the only epithelial cells I had available at the time) did not express those epithelial cell markers, I selected an additional two markers: CD166 (expressed by all epithelial cells) and CD44 (expressed basally only). These markers were identified from basal cell transcriptomic and surface marker profiling papers by Van De Laar *et al.* (2014) and Hackett *et al.* (2011). Scouring the literature further for evidence of these markers in bronchial epithelium, I discovered CD166 was also used for flow cytometry alongside CD49F and EpCAM to identify subsets of epithelial cells in human lung (Weeden *et al.* 2017), and that CD44 is highly expressed by BEAS-2B cells (Atsuta *et al.* 1997). Hackett *et al.* (2011) also reported CD44 as being upregulated during repair and affiliated with airway remodelling. This consolidated the decision to include it within the panel.

I then researched the different clones and their available conjugations for each antibody suitable for the application of flow cytometry to see if there were any antibodies which would be restrictive in which channel they had to be on. I then sought to establish which fluorochromes offer the least spectral overlap to produce as low a compensation matrix as possible.

As my panel contained intracellular proteins, a fixable viability dye was required. I decided on Fixable Viability Dye eFluor 780 (Fisher Scientific, cat no 13539140). This was a good choice because the RL3 channel has spectral overlap with a few other channels, but any positive staining (aka dead cells) would be gated out negating the false positives seen in the channels it leaks into. As I needed to ensure all red blood cells would be removed from my epithelial cell gating, I added CD45 into the same channel to produce a dump channel.

Using a spectra viewer provided online by BD Biosciences, I established which fluorochromes had the least spectral overlap, and the percentage of leakage from one channel to another. The results are shown in **Appendix 7 (top panel)**. To confirm the expected leakage based on the bandpass filters, I stained beads with different fluorescently labelled antibodies to confirm the best fluorochrome set possible. The resulting compensation matrix is shown in **Appendix 7 (bottom panel)**. By doing this, I discovered BV605 spills over into too many channels, and that AF647 and AF700, and PE, PE-dazzle and PECF-594 were not great combinations (YL1 and YL2 overlap and RL1 and RL2 overlap). As I needed seven channels for my biggest panel, I chose to use BV421, BV785, AF488, PerCP, AF647, Live/dead in the RL3 channel (which is equivalent to APC-Cy7) and PE.

For my pSMAD2/3 Phosflow intracellular staining protocol, a harsh permeabilisation method (Phosflow perm buffer III) was required which can degrade fluorochromes. Small non-protein fluorophores such as AF647 and AF488 are not as susceptible to this degradation, and therefore I chose to reduce my basal cell panel to incorporate only these fluorochromes. I chose to have

NGFR on AF647 and EpCAM on AF488. As the pSMAD2/3 antibody was available on AF647, PECE-594 and PE, I had to choose between PECE-594 or PE conjugation. I chose PECE-594 as it had a larger emission shift.

The antibodies and reagents used for flow cytometry are summarised in **Table 2.6 and 2.7** respectively.

Table 2.6 Antibody Panel List Used For Flow Cytometry

	Epitope	Clone	Fluorochrome conjugate	Supplier	Catalogue number
Basal cell panel	EpCAM	9C4	BV785	Biolegend	324238
	CD166	3A6	PE	Biolegend	343904
	CD49F	GoH3	BV421	Biolegend	313624
	NGFR	ME20.4	AF647	Biolegend	345114
	CD44	IM7	PerCP	Biolegend	103036
	CD45	2D1	APC/Fire ⁷⁵⁰	Biolegend	368518
	CK5	RCK103	AF647	Santa-Cruz	Sc-32721
EMT marker panel	EpCAM	9C4	BV785	Biolegend	324238
	CD49F	GoH3	BV421	Biolegend	313624
	NGFR	ME20.4	AF647	Biolegend	345110
	CD44	IM7	PerCP	Biolegend	103036
	CD45	2D1	APC/Fire ⁷⁵⁰	Biolegend	368518
	Vimentin	RV202	AF488	BD Biosciences	562338
	E-cadherin	67A4	PE	Biolegend	324106
WNT receptor panel	EpCAM	9C4	BV785	Biolegend	324238
	NGFR	ME20.4	AF647	Biolegend	345110
	CD45	2D1	APC/Fire ⁷⁵⁰	Biolegend	368518
	ROR2	Ror2	PE	BD Biosciences	565551
	FZD4	CH3A4A7	APC	Miltenyi Biotec	130-106-571
pSMAD2/3 panel	EpCAM	9C4	AF488	Biolegend	324210
	CD49F	GoH3	BV421	Biolegend	313624
	pSMAD2/3	O72-670	PE-CF594	BD Biosciences	562697
WNT5A antibody validation	V5 Tag	SV5-PK1	FITC	Fisher Scientific	11585432
	IgG1	RMG1-1	AF647	Biolegend	406617
	IgG2a	RMG2a-62	AF647	Biolegend	407115
	WNT5A	6F2	N/A	Insight Biotechnology	GTX83127
	WNT5A	3A4	N/A	Bio-technne	H00007474-M04

Table 2.7 List of Additional Flow Cytometry Reagents

Reagent Name	Supplier	Catalogue Number
UltraComp eBeads	Fisher Scientific	01-2222-42
Fixable Viability Dye eFluor 780	Fisher Scientific	13539140
Human TruStain FcX	Biolegend	422302
Perm Buffer III	BD Biosciences	558050
Ebioscience fix and perm kit	Fisher Scientific	88-8824-00
Cytofix	BD Biosciences	554655
Lightning-link Conjugation kit	Expedeon	332-0030
GentleMACS C tubes	Miltenyi Biotec	130-093-237
Tumour Dissociation Kit	Miltenyi Biotec	130-095-929

2.15.2 Antibody Titrations

To avoid off target binding caused by excessive antibody concentrations, all basal cell and EMT flow cytometry antibodies were titrated in BEAS-2B cells. It would have been ideal to have titrated the antibodies in primary HBECs, but as primary HBECs were difficult to culture they were considered too precious to use for optimisation and so optimisation was performed on BEAS-2Bs, a HBEC cell line.

The sensitivity index (SI) was calculated using the following equation proposed by Telford *et al.* (2009). The numerator is the difference between the median fluorescence intensity of the positive and negative population. The denominator of this equation can be calculated in FlowJo using the robust standard deviation. This SI calculation indicates which titration of the antibody achieves optimal staining.

$$\text{Sensitivity Index} = \frac{\text{Med}_{\text{pos}} - \text{Med}_{\text{neg}}}{[(84\%_{\text{neg}} - \text{Med}_{\text{neg}})/0.995]}$$

Of the eight antibodies originally tested, only four reached saturation- EpCAM, CD49F, Vimentin and CD166. CK5, NGFR on PECy7 and AF647, and CD44 did not saturate. I originally purchased NGFR on PECy7 but switched to AF647 due to my pSMAD2/3 panel. The antibody volume recommended for all antibodies was 5µl per 1million cells, however, some antibodies saturated above this, such as vimentin and EpCAM. **Figure 2.9** shows the SI graphs of those 6 antibodies. The solid arrow indicates the antibody saturation volume, and the dotted line represents the manufacturer's recommended volume.

To see if the channel has high background (which could be preventing saturation), I used an isotype control as the negative population rather than a fluorescence full minus one (FMO). An FMO contains all the fluorochromes in the panel except the one of interest. This control allows you to properly interpret multicolour flow cytometry data because it ensures the spread of the data seen by adding the antibody of interest is due to binding, rather than spread of other

fluorochromes into that channel. An isotype, however, is used to identify the background signal caused by nonspecific binding of immunoglobulins to Fc receptors present on the cell surface. Using isotype controls, I found the median negative fluorescence intensity increased with increasing concentrations of isotype antibody, suggesting high background in these channels. The SI graphs using isotype controls are shown in **Figure 2.10**.

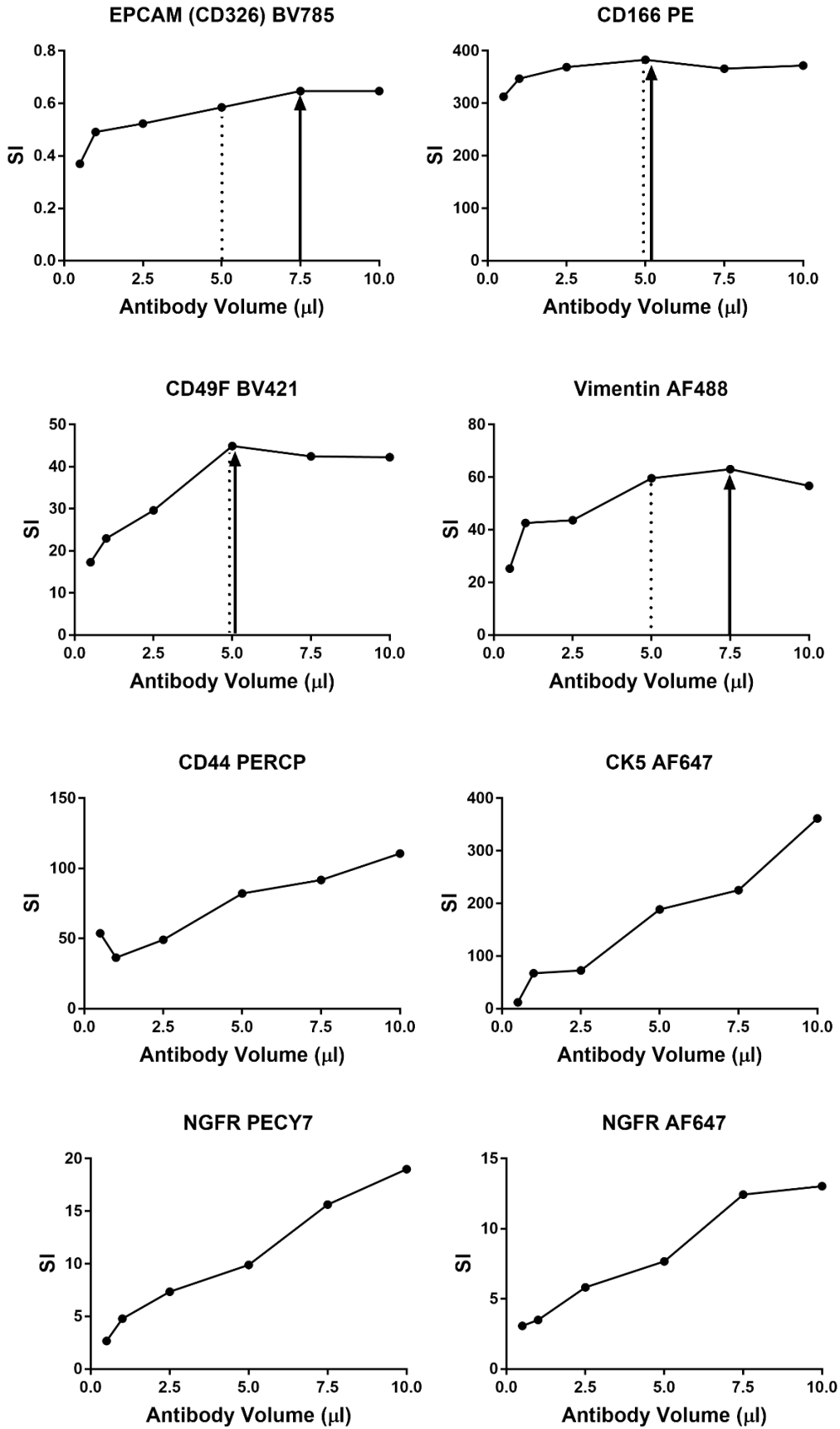


Figure 2.9 Separation Index Graphs of Antibodies Using FMO Controls (n=1)

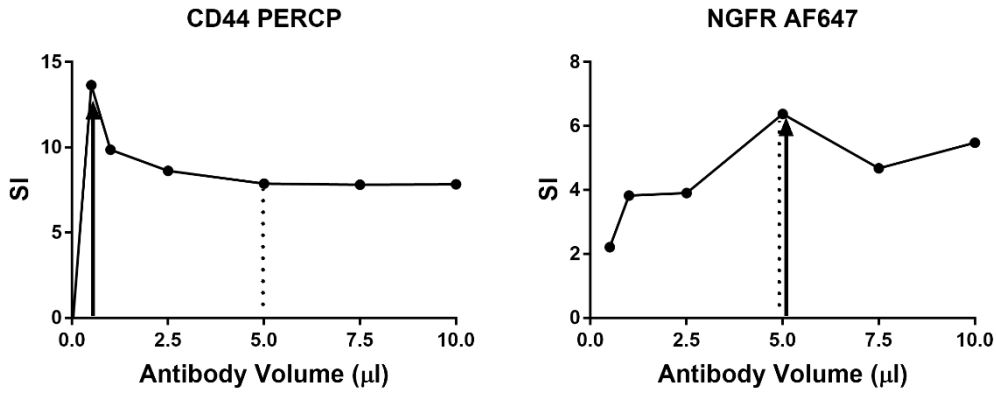


Figure 2.10 Separation Index Graphs of Antibodies Using Isotype Controls (n=1)

2.15.3 Antibody Specificity Testing

As some of the antibodies didn't saturate, I wanted to confirm antibody specificity using biological controls. I stained fibroblasts for CK5 and blood for CD44. CK5 was found to be expressed on all fibroblasts although fibroblasts are a biological negative control, suggesting the antibody is non-specifically binding. The flow cytometry gating strategy is shown in **Figure 2.11**. CD44 was found to be expressed on memory CD4+ and CD8+ T cells as expected (data not shown).

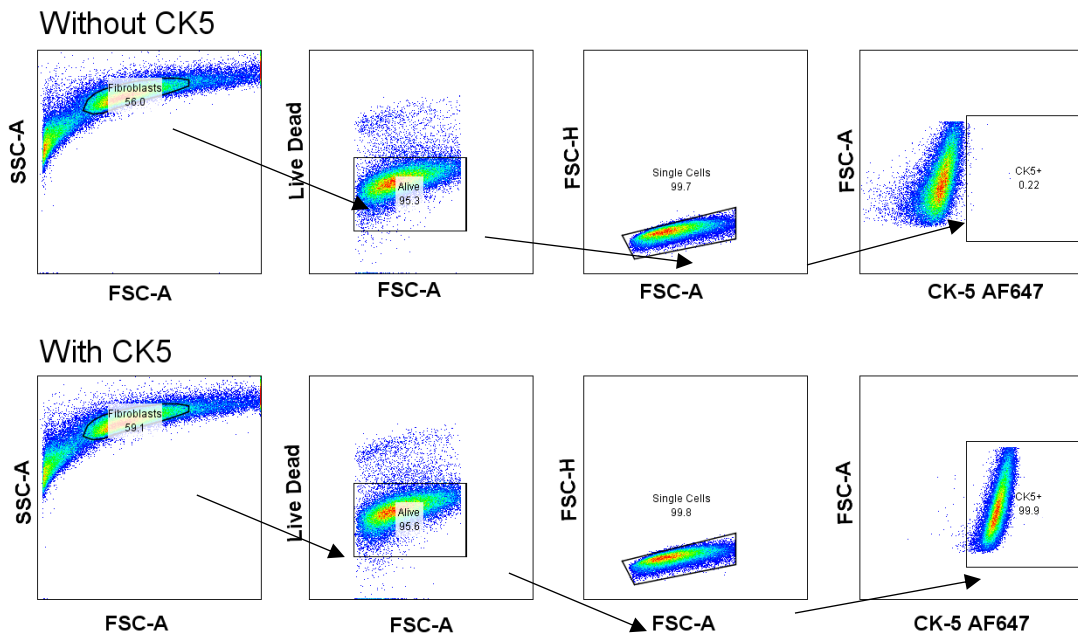


Figure 2.11 Cytokeratin-5 Staining in Fibroblasts. The fibroblast population was selected, and the dead cells and doublets removed. CK5 gating was established using an FMO control (termed without CK5 in the gating strategy). Experiment is n=1.

The antibodies were tested in BEAS-2Bs and submerged HBECs. The BEAS-2B gating strategy is shown in **Figure 2.12**. Two subpopulations are prominent in BEAS-2Bs, one of which appears basal like expressing EpCAM, NGFR and CD49F. These cells only account for roughly 2-5% of the entire population though. When investigating these markers in submerged HBECs, all cells were EpCAM, NGFR and CD49F positive, supportive of these markers defining basal cells (for clarification: submerged cultures are not differentiated at ALI yet so they should be basal). They were also 100% positive for CD166, and high CD44 expression was also found. This data is shown in **Figure 2.13**. To note, CK5 was also investigated here, and NGFR was fluorescently labelled with PECy7, as these experiments were conducted prior to panel changes.

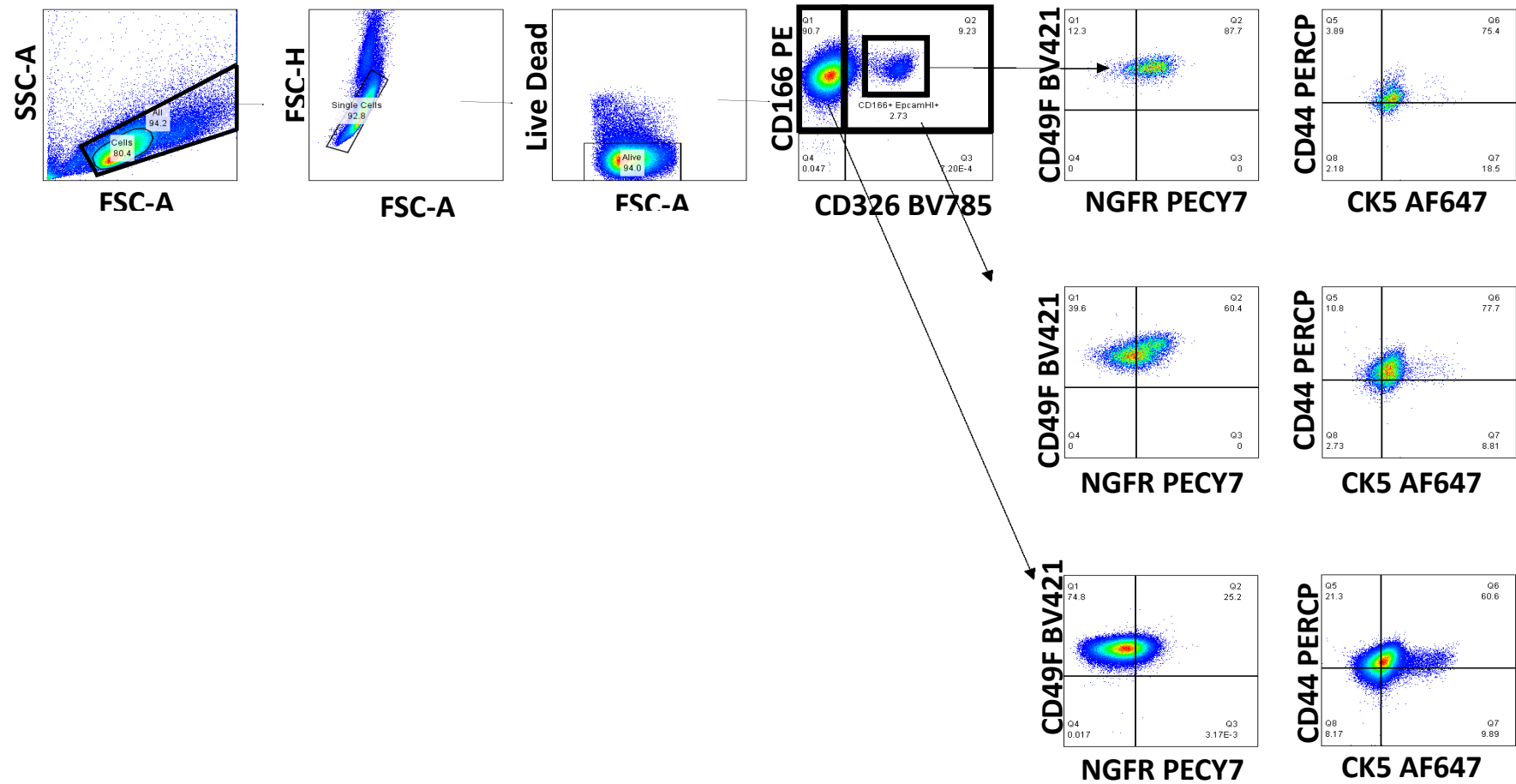


Figure 2.12 BEAS-2B Basal Cell Gating Strategy. Cell population was gated, and single cells selected. Live cells were then selected based on live dead staining. To test population gating strategy, CD166+ CD326- (top left quadrant), CD166+ CD326+ dual positive cells (top right quadrant) and the CD326+ CD166+ gated population within quadrant 2 were investigated for basal cells markers – CD49F, NGFR, CK5 and CD44. The CD326+ CD166+ gated population within quadrant 2 appears more basal cell like as these cells express the highest percentages of basal cell markers compared to the other two populations.

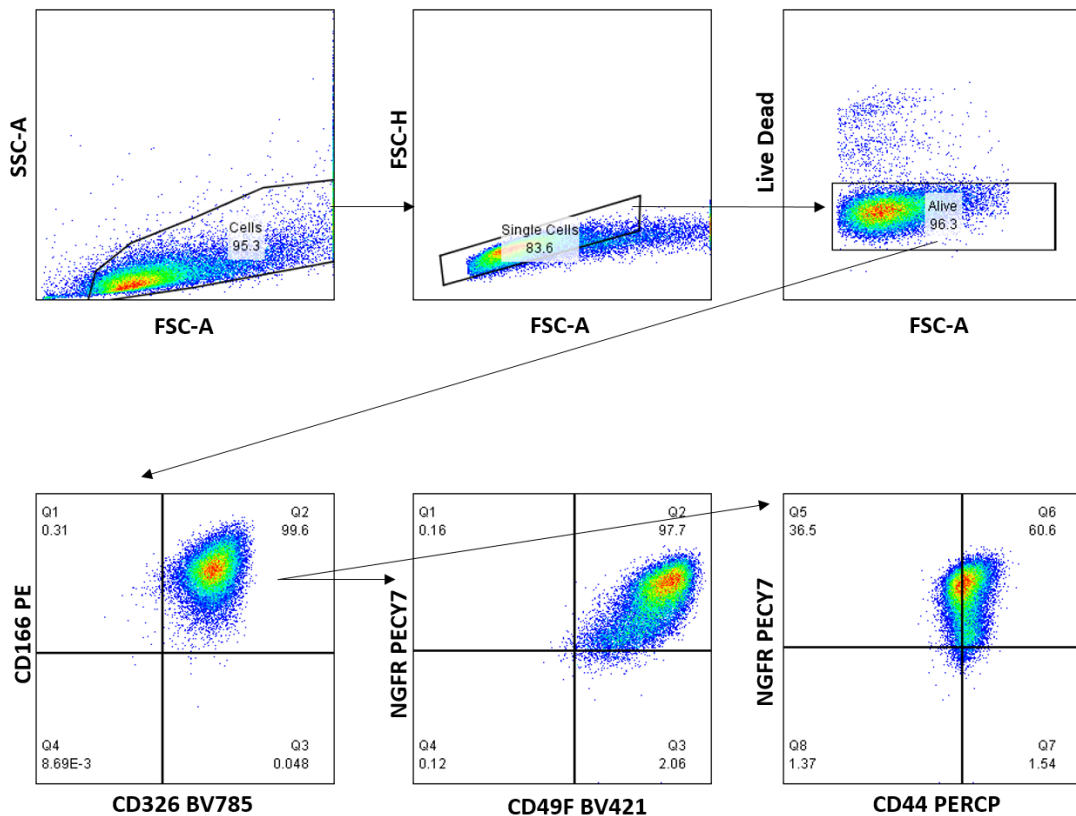


Figure 2.13 Submerged Human Bronchial Epithelial Cell Gating on Epithelial and Basal Cell Markers

2.16 Flow Cytometry

2.16.1 Preparing Single Cell Suspensions from Biopsies

Biopsies were homogenised into a single cell suspension using GentleMACS C tubes (Miltenyi Biotec, cat no 130-093-237), a Tumour Dissociation kit (Miltenyi Biotec, cat no 130-095-929) and GentleMACS Dissociator (program 37C_h_TDK_2), The single cell suspension was then filtered using a 70µm cell strainer and washed once with PBS. Samples were then stained according to a previously reported flow cytometry method and acquired on the Attune.

2.16.2 Basal Cell Phenotyping

Bronchial brush and biopsy cell suspensions were stained with Fixable Viability Dye eFluor 780 (Fisher Scientific) for 15 minutes at room temperature. Cells were then FC blocked with Human TruStain FcX (Biolegend, cat no 422302) for 15

minutes at room temperature, and then surface stained for 15 minutes on ice in 100µl cell suspension. Cells were then fixed for 30 minutes on ice and permeabilised with eBioscience intracellular fix and permeabilisation buffers according to manufacturer’s recommendations (Fisher Scientific, cat no 88-8824-00). Cells were then intracellularly stained for 30 minutes at room temperature in 100µl cell suspension before washing twice with permeabilisation buffer and acquiring on the Attune NxT flow cytometer. For analysis, gates were set using FMO controls. The antibody panel is shown in **Table 2.8**.

The data was compensated using Invitrogen eBioscience UltraComp eBeads (Fisher Scientific, cat no 15536296) for all antibodies of mouse, rat or hamster origin. The viability compensation tube, as it is a dye rather than an antibody, was a 50:50 live:dead mix of viability dyed cells.

Table 2.8 Basal Cell Phenotyping Antibody Panel

	1	2	3	4	5	6	7	Antibody volume (µl)
VL1 BV421	CD49F	FMO	CD49F	CD49F	CD49F	CD49F	CD49F	5
VL4 BV785	CD326	CD326	FMO	CD326	CD326	CD326	CD326	7.5
BL3 PerCP	CD44	CD44	CD44	FMO	CD44	CD44	CD44	0.5
RL1 AF647	NGFR	NGFR	NGFR	NGFR	FMO	NGFR	NGFR	5
RL3	Live/dead & CD45						FMO	L/D: 1 (of 1 in 20 dilution) CD45=5
YL1 PE	CD166	CD166	CD166	CD166	CD166	FMO	CD166	5

2.16.3 EMT Marker Expression With and Without Stimulation

For EMT experiments, cell cultures were stimulated for 48 hours with 1µg/ml rhWNT5A, 10ng/ml rhTGF-β1, or appropriate vehicle control, and harvested using trypsin-EDTA (Fisher Scientific, cat no 11677104). The staining, data acquisition and analysis was performed as mentioned previously in the basal cell phenotyping method. The antibody panel is shown in **Table 2.9**.

Table 2.9 EMT Phenotyping Antibody Panel

	8	9	10	11	12	13	14	15	Antibody volume (μl)
VL1 BV421	CD49F	FMO	CD49F	CD49F	CD49F	CD49F	CD49F	CD49F	5
VL4 BV785	CD326	CD326	FMO	CD326	CD326	CD326	CD326	CD326	7.5
BL1 AF488	Vim	Vim	Vim	FMO	Vim	Vim	Vim	Vim	7.5
BL3 PerCP	CD44	CD44	CD44	CD44	FMO	CD44	CD44	CD44	0.5
RL1 AF647	NGFR	NGFR	NGFR	NGFR	NGFR	FMO	NGFR	NGFR	5
RL3	Live/dead & CD45						FMO	Live/dead & CD45	L/D: 1 (of 1 in 20 dilution) CD45=5
YL1 PE	Ecad	Ecad	Ecad	Ecad	Ecad	Ecad	Ecad	FMO	5

2.16.4 WNT Receptor Phenotyping

For cultured cells, the cell cultures were stimulated for 48 hours with 10ng/ml rhTGF- β 1 or appropriate vehicle control and harvested using trypsin-EDTA (Fisher Scientific, cat no 11677104). Again, the staining, data acquisition and analysis was performed as mentioned previously in the basal cell phenotyping method. FMO controls were only used for ROR2 and FZD4 to set appropriate gating for those channels. The antibody panel is shown in **Table 2.10**.

For receptor staining of neat brushings, cells were viability stained and then single stained for ROR2 or FZD4. A viability stained control served as an FMO for setting the gates for each channel.

Table 2.10 WNT Receptor Phenotyping Antibody Panel

	16	17	18	Antibody volume (μ l)
VL1 BV421	CD49F	CD49F	CD49F	5
VL4 BV785	CD326	CD326	CD326	7.5
RL1 APC	FZD4	FMO	FZD4	10
RL3	L/D & CD45			L/D: 1 (of 1 in 20 dilution) CD45=5
YL1 PE	ROR2	ROR2	FMO	5

2.16.5 pSMAD2/3 Expression

After 1 week of recovery from scratch wounding, ALI cultures were washed twice with PBS, and whilst still attached per well, stained with 250 μ l fixable viability dye (diluted 1:2000 with PBS) (Fisher Scientific, cat no 13539140) for 15 minutes at 37°C. The dead dye was washed off with PBS, and then 700 μ l Takinib and BOX-5 (or vehicle controls) was added at 7.5nM and 250 μ M respectively for 30 minutes at 37°C. The cells were then stimulated with either 1 μ g/ml rhWNT5A and/or 10ng/ml rhTGF- β 1 for 30 minutes at 37°C by adding 100 μ l of stimulant into the existing 700 μ l inhibitor/vehicle control cocktail. The cells were then detached rapidly with 250 μ l trypsin-EDTA solution (Fisher Scientific, cat no 11677104) and fixed immediately with pre-warmed Cytifix for 10 minutes at 37°C

to preserve phosphorylated SMAD2/3 expression. The cells were then transferred to FACs tubes, FC blocked at room temperature for 15 minutes, stained for surface markers (in 100µl cell suspension) for 15 minutes on ice in the dark, and permeabilised with 100µl ice cold Phosflow Perm Buffer III (BD Biosciences, cat no 558050) for 30 minutes on ice. The cells were washed twice before intracellular staining for 1 hour on ice in the dark. Cells were then washed a further two times and resuspended in PBS before data acquisition on the Attune. The pSMAD2/3 gating was set using FMO controls.

2.17 WNT5A Antibody Validation

2.17.1 Assessing the Literature for WNT5A Antibody Validation

Pubmed was investigated for string term ((WNT5A) AND (IMMUNOHISTOCHEMISTRY) AND (LUNG)). Twenty-four papers were listed, of which eight papers were excluded as they lacked WNT5A immunohistochemistry data. Of the 16 remaining papers, only six had any form of validation to support antibody specificity. Immunohistochemistry information provided in the literature has been summarised in **Table 2.11**. Antibody clone identifying information was often omitted, with only the supplier being consistently given in the methods sections of each paper.

The three antibodies chosen for validation were clones 6F2, 3A4 and A-5. Clone 6F2 was assessed because it was used by the previous PhD student working on this project (Daud 2017). Clone 3A4 was assessed as it was noted as the best WNT5A antibody for immunohistochemistry use by Prgomet, Andersson and Lindberg (2017) in their WNT5A antibody validation paper, and A-5 was selected as it was the replacement product for clone C-16, one of the most utilised WNT5A antibody clones in the literature investigated.

Table 2.11 Publications Containing WNT5A IHC Staining of Lung Tissue. Where information was not available in the literature, N/A is given. Discrepancy in information in literature to vendor website for the catalogue number given is shown in bold. The host is goat not rat on the Santa Cruz website.

Author	Publication Year	Clone Name/Cat #	Supplier	IHC Dilution	Clonality	Host	Retrieval method	IHC staining time/temp	Validation evident
Tenghao <i>et al.</i>	2020	N/A	Abcam	1:100	N/A	Rabbit	Citrate buffer	Overnight 4°C	Western blot of matched tissue
Wang <i>et al.</i>	2017	N/A	N/A	1:50	N/A	N/A	N/A	Overnight 4°C	None
Vesel <i>et al.</i>	2017	442625	R&D Systems	1:50	Monoclonal	Rat	N/A	1hour RT	Relative gene expression of tissue
Gu <i>et al.</i>	2016	N/A	Abcam	1:80	N/A	Rabbit	N/A	N/A	Relative gene expression of tissue
Rapp <i>et al.</i>	2016	442625	R&D Systems	1:100	Monoclonal	Rat	N/A	N/A	Relative gene expression of tissue
Dietz <i>et al.</i>	2017	N/A	Lifespan Bioscience	N/A	N/A	N/A	N/A	N/A	None
Xu <i>et al.</i>	2015	N/A	Santa Cruz Biotech	1:100	N/A	N/A	N/A	Overnight 4°C	None

Lu <i>et al.</i>	2015	N/A	Abcam	1:200	N/A	Mouse	N/A	Overnight 4°C	Relative gene expression of tissue
Villar <i>et al.</i>	2014	N/A	Abcam	N/A	Polyclonal	Rabbit	Citrate buffer	1hour RT	None
Yao <i>et al.</i>	2014	N/A	Abcam	N/A	N/A	N/A	N/A	Overnight 4°C	None
Villar <i>et al.</i>	2011: A	N/A	Abcam	1:150	Polyclonal	Rabbit	Citrate buffer	1hour	None
Nakashima <i>et al.</i>	2010	C-16	Santa Cruz Biotech	1:100	Polyclonal	Goat	Citrate buffer	Overnight	None
Doi and Puri	2009	C-16	Santa Cruz Biotech	1:100	N/A	Rat	N/A	Overnight 4°C	None
Christman <i>et al.</i>	2008	N/A	R&D Systems	N/A	N/A	Goat	N/A	N/A	None
Huang <i>et al.</i>	2005	C-16	Santa Crus Biotech	1:100	Polyclonal	Goat	Citrate buffer	Overnight	None
Li <i>et al.</i>	2002	N/A	R&D Systems	N/A	N/A	N/A	Citrate buffer	Overnight 4°C	WNT5A knockout tissue used

On investigating the literature for WNT5A immunohistochemistry in the lung, full methodology was not provided and antibody identifying information was often omitted. Antibody validation in four publications involved the comparison between transcriptional data and immunohistochemical staining (Vesel *et al.* 2017) (Gu *et al.* 2016) (Rapp *et al.* 2016) (Lu *et al.* 2015). This orthogonal approach to antibody validation is insufficient to determine antibody specificity, as expression was not investigated for multiple samples of variable expression, thereby limiting confidence in the antibody performance (Uhlen *et al.* 2016). The central dogma does suggest a direct relationship between mRNA and protein expression, of which quantitative comparison between mRNA and protein expression abundance can be useful in validating antibody staining; however, protein levels are influenced by post-translational modifications, and therefore, mRNA may not always correlate with protein expression (O’Hurley *et al.* 2014). Ergo, additional methods were required in these papers to fully validate the antibody specificity.

Tenghao *et al.* (2020) utilised western blot as a validation technique, however, as many proteins have a similar molecular weight, a band at the correct size is not informative enough to determine antibody specificity (O’Hurley *et al.* 2014). Furthermore, suitability in one application does not validate the antibody in another, as antibody-antigen binding may differ between techniques (O’Hurley *et al.* 2014). Li *et al.* (2002) was the only paper which utilised genetic manipulation to demonstrate specificity of the WNT5A antibody used.

2.17.2 Using Cloning to Produce a Positive Control

WNT5A is a potential target for metastatic cancer, with Foxy5 being in stage II clinical trials, but cellular and histological detection of WNT5A protein is problematic as antibody validation is lacking. The aim of this work was to validate a WNT5A antibody for numerous applications. First of all, the literature was assessed for WNT5A antibody validation. A genetic strategy producing negative and positive controls was then utilised to robustly evaluate antibody specificity. As WNT5A and WNT5B share similar homology, both WNT5A and WNT5B were

cloned into expression plasmids that were used for inducing gene expression. To achieve this, WNT5A and WNT5B were cloned into a plasmid with an RFP fluorescent reporter (pCDH-EF1-MCS-T2A-Puro) so that transfection efficiency would be visible. This backbone was also chosen based on its eukaryotic promoter EF1, as differentiation of HBECs silence the cytomegalovirus (CMV) promoter (Schmid *et al.* 2006), which was the promoter in the initial cloning vector used. The cloning vector would therefore not have been suitable for transduction of differentiated HBECs, which was another potential method of which the impact of WNT5A could have been assessed on wound healing, rather than through recombinant protein stimulation.

Untransfected cells and cells transfected with the red fluorescence protein empty vector (RFP EV) were used as experimental controls. The RFP EV did not contain the WNT5A/B insert but possessed the red fluorescence reporter. This control was created to ensure that observable differences in WNT5A expression was due to the independent variable (the WNT5A/B insertion). It would also distinguish whether the effects of transfection, such as cellular cytotoxicity, are associated with gene expression or the transfection process. The untransfected cells acted as the negative control, allowing the RFP gating to be set and the effect of transfection to be assessed.

2.17.2.1 Streaking and Isolating Bacteria from Bacterial Stabs

Active WNT5A-V5 (shown in **Figure 2.14**) and Active WNT5B-V5 (shown in **Figure 2.15**) were a gift from Xi He (Addgene plasmid # 43813 and 43814; http://n2t.net/addgene:43813;RRID:Addgene_43813; http://n2t.net/addgene:43814;RRID:Addgene_43814). On receiving bacterial stabs of plasmids 43813 and 43814, the bacteria were streaked onto ampicillin LB Agar plates and incubated overnight for 12-18 hours at 37°C. Ampicillin agar plates were prepared by

autoclaving 500ml distilled water, 5g tryptone, 2.5g yeast extract, 5g sodium chloride and 7.5g agar.

Created with SnapGene®

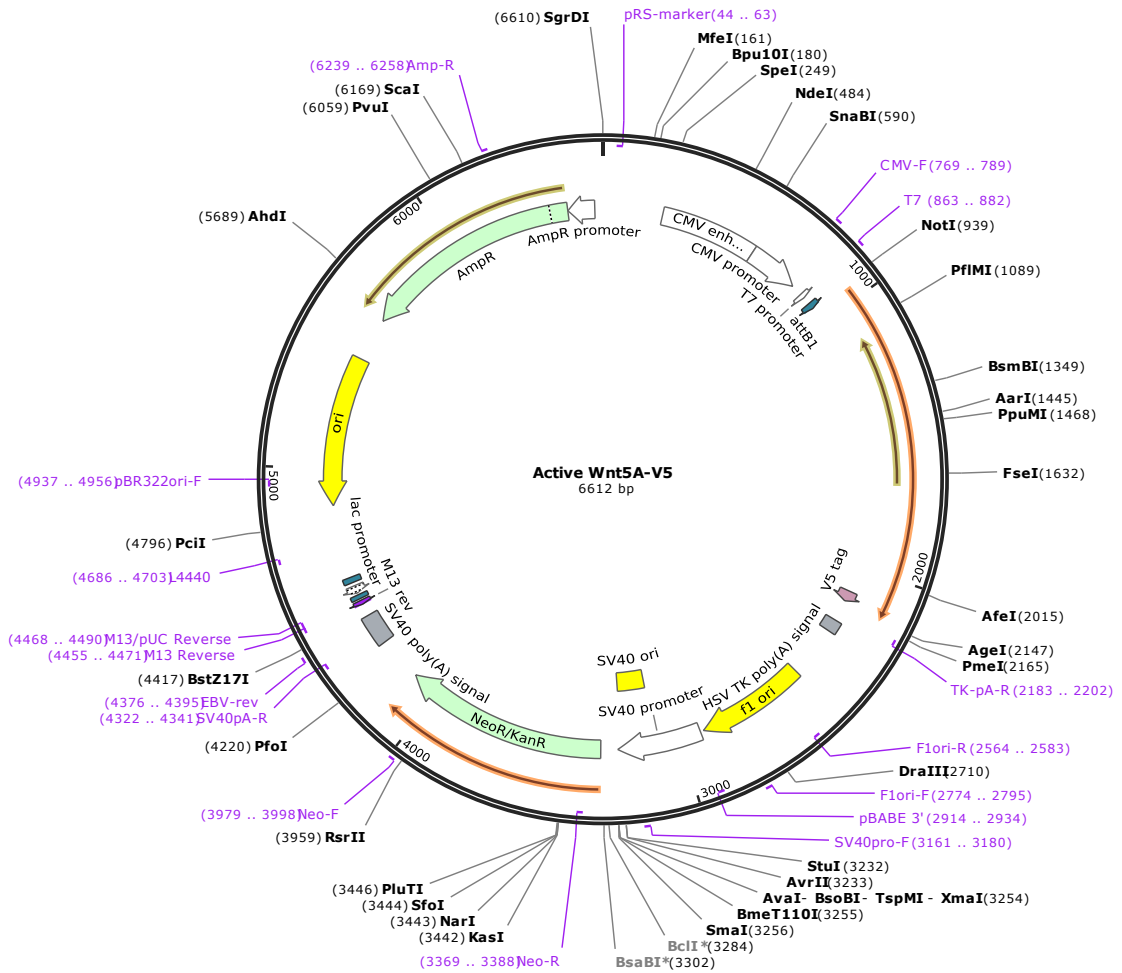


Figure 2.14 Plasmid Map of Active WNT5A-V5 (Addgene Plasmid Number 43813)

2.17.2.3 Linearising and Amplifying the Plasmid Sequence

Dried primers were re-suspended in sterile water to 100µM stock concentrations, and then diluted a further 1 in 16 to give a concentration of 6.25µM for the PCR reaction. The primers sequences used are given in **Table 2.12**. The PCR plasmid master mix was prepared according to **Table 2.13**, with 100ng of plasmid DNA and 12.5µl CloneAmp HiFi PCR premix from the In-Fusion HD Cloning Plus kit (Takara Bio, 638916) being added per reaction. The thermal profile used on the ProFlex PCR System was a 3-step 35 cycle reaction: 98°C for 10 seconds, 55°C for 15 seconds and 72°C for 90 seconds.

Table 2.12 Primer Sequences Used For Amplifying the Plasmid Sequence

RFP Backbone Plasmid	Oligo 1 GAGGGCAGAGGAAGTCTTC
	Oligo 2 CGCGGATCCGATTTAAATTCG
WNT5A Plasmid 43813	Oligo 3 WNT5A TAAATCGGATCCGCGCCCTTCACCATGAAGAAGTCCATTG
	Oligo 4 WNT5A ACTTCCTCTGCCCTCACCGGTACGCGTAGAATCGAG
WNT5A Plasmid 43814	Oligo 3 WNT5B TAAATCGGATCCGCGCCCTTCACCATGCCCAGC
	Oligo 4 WNT5B ACTTCCTCTGCCCTCACCGGTACGCGTAGAATCG

Table 2.13 Plasmid PCR Mastermix Constituents

Rx	Plasmid Name	Plasmid DNA Concentration	To get 100ng into mM	Primer 1 (μl) – 100μM diluted 1 in 16	Primer 2 (μl) - 100μM diluted 1 in 16	Ultrapure H ₂ O (μl)	CloneAmp Hifi PCR premix (μl)	Total vol (μl)	No of rx's required
1	RFP backbone plasmid	50ng/μl	Add 2μl	1μl Oligo1	1μl Oligo2	8.5	12.5	25	2
2	Plasmid 43813	2739.1ng/μl	Do 1 in 27.39 dilution, add 1μl	1μl Oligo 3 WNT5A	1μl Oligo 4 WNT5A	9.5	12.5	25	1
3	Plasmid 43814	71.17ng/μl	Add 1.4μl	1μl Oligo 3 WNT5B	1μl Oligo 4 WNT5B	9.1	12.5	25	1

To remove template circular plasmid DNA, the PCR plasmid fragments were also subjected to restriction digest with *dpnI* (New England Biolabs, R0176S) for 2 hours at 37°C. 1µl of *dpnI* was added per PCR reaction. *DpnI* was used as it only cleaves when its recognition site is methylated, and therefore would only cleave the circular plasmid DNA not PCR products.

The linearised plasmid DNA was then verified on a 1% agarose gel. 5.2µl 6x purple loading dye was added to each 26µl sample reaction. 30µl of 1kb Plus DNA ladder (Thermofisher, 10787018) was prepared (5µl of the ladder, 5µl 6x purple loading dye and 20µl ultrapure water) to assess plasmid fragment size. The gel was run at 90V using a VWR 300V power supply and visualised using a GenoSmart 2. Visualisation of the gel is shown in **Figure 2.16**. The expected band size for WNT5A was 1236bp, for WNT5B it was 1173bp, and for the whole pCDH-EF1-MCS-T2A-Puro plasmid back bone it was 9171bp.

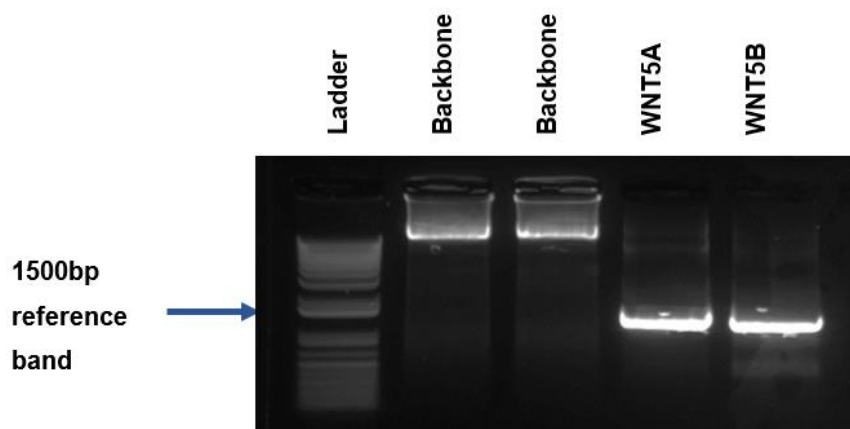


Figure 2.16 Verification of the Linearised Expression Plasmid Backbone and WNT5 Insert on a 1% Agarose Gel

2.17.2.4 Min Elute Gel Extraction of PCR Fragments

The DNA fragments were excised from the gel using a sterile scalpel, gel slices weighed, and DNA fragments extracted and purified from the gel using a MinElute Gel Extraction Kit (Qiagen, cat no 28606) according to manufacturer's instructions. Plasmid DNA was measured using a nanodrop 2000.

2.17.2.5 Infusion Cloning Procedure

As the WNT5A or WNT5B insert was shorter than 10kb in length (1.2kb), 50-100ng of insert was recommended per infusion cloning reaction. The linearised vector without the insert is <10kb (9kb), as shown in **Figure 2.17**, so again 50-100ng was recommended. The recommended 2:1 insert:linearised vector molar ratio was used (50ng insert:200ng linearised vector), but the recommended concentration range of the linear insert could not be satisfied. A negative and positive control reaction provided in the In-Fusion HD Cloning Plus kit (Takara Bio, 638916) was therefore included. The infusion cloning reaction was set-up and incubated at 50°C for 15 minutes in accordance with the manufacturer's instructions. **Figure 2.18** and **Figure 2.19** show the WNT5A and WNT5B respective insertions into the empty vector following the infusion cloning reaction.

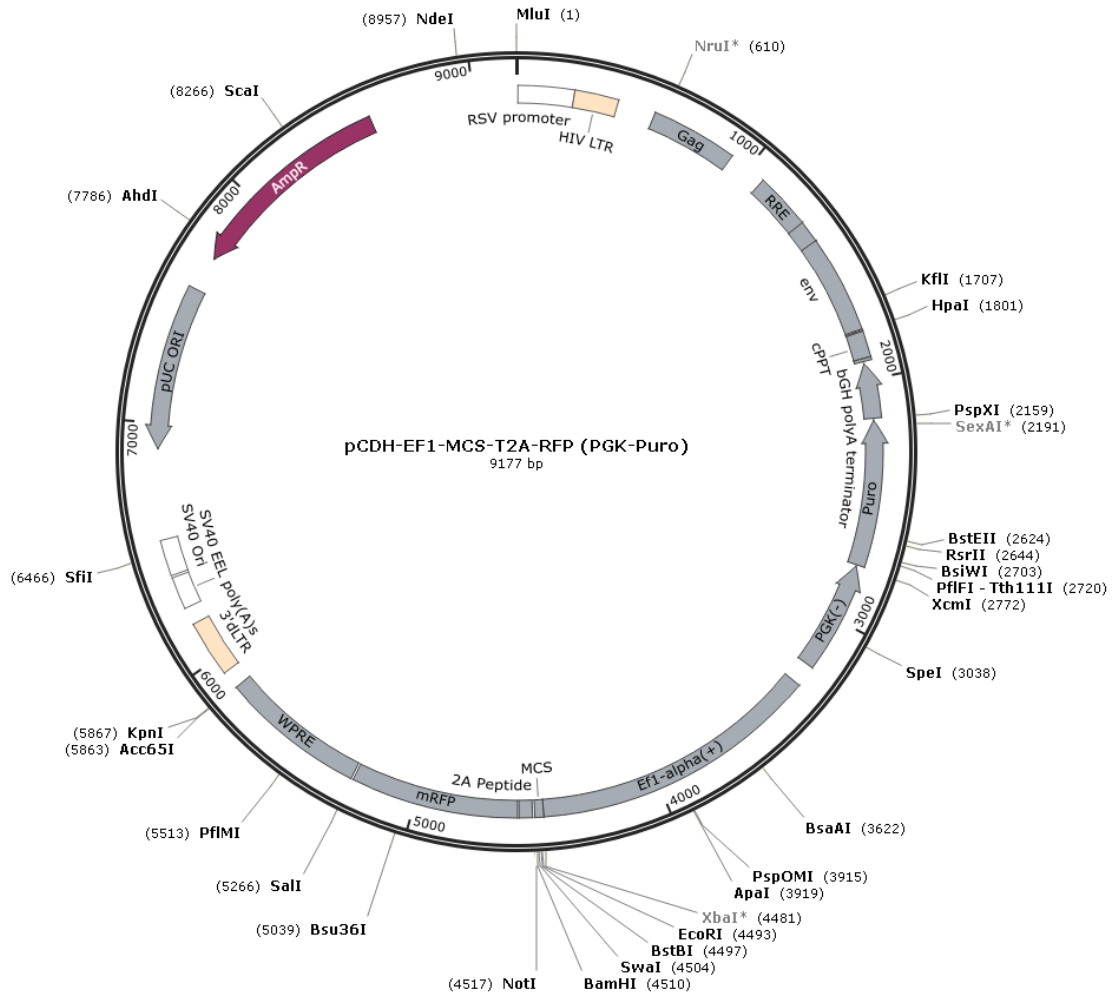


Figure 2.17 Plasmid Map of the Empty Vector (the plasmid without the WNT5A/B insert) After The Infusion Reaction

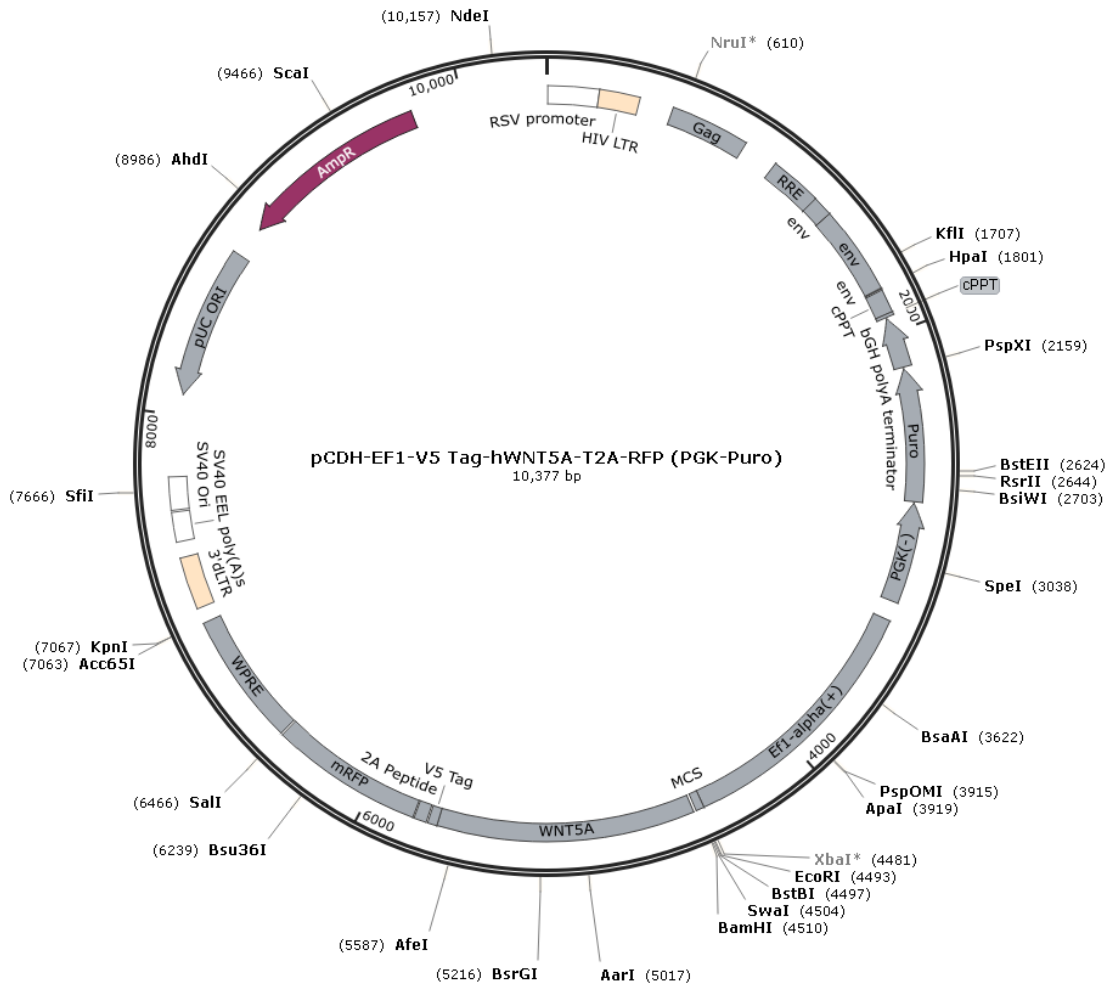


Figure 2.18 Plasmid Map of the WNT5A Plasmid After The Infusion Reaction

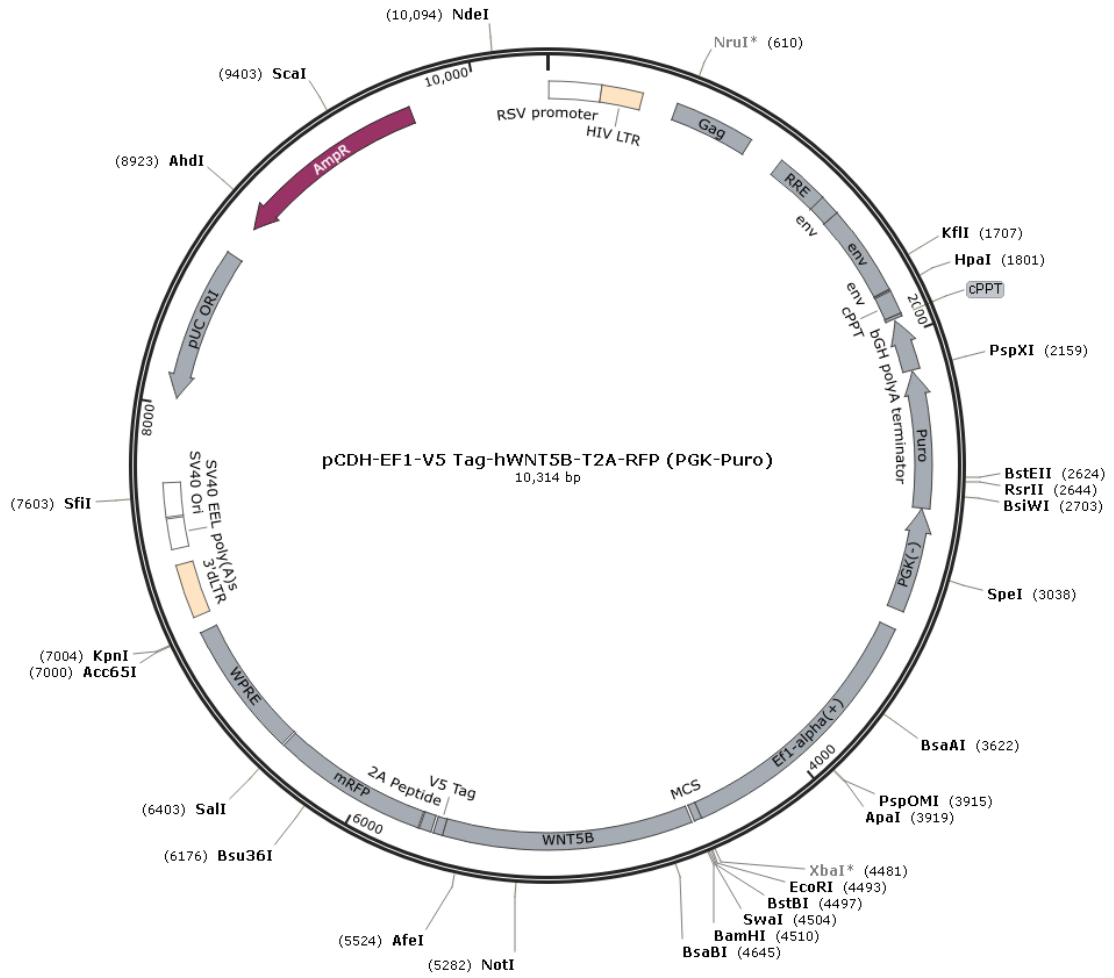


Figure 2.19 Plasmid Map of the WNT5B Plasmid After The Infusion Reaction

2.17.2.6 Transformation of Stellar Competent Cells

Stellar cells were transformed according to manufacturer's instructions. For each plasmid, two ampicillin plates were inoculated with 20 μ l and 50 μ l of transformation reaction for culture overnight. The plates were incubated for 12-18 hours at 37°C, and stored in the fridge until ready for mini-prep.

2.17.2.7 Mini-prep

Fifteen stellar competent cell colonies (for each plasmid) were inoculated into 20ml universals containing 5ml LB broth with ampicillin. These cultures were cultured overnight in an IKA KS 3000i Control shaker set to 37°C and 255rpm. The plasmid DNA was extracted using a BioBasic Mini-prep kit (Biobasic, cat no 9K-006-0009S) in accordance with manufacturer's instructions and concentration assessed using a nanodrop.

2.17.2.8 Screening Mini-prep for WNT5A/B Inserts

The PCR mastermix was made as shown in **Table 2.14**. The sequencing primers used are shown in **Table 2.15**. Each PCR reaction contained 9 μ l of mastermix and 1 μ l of plasmid DNA. The 3-step thermal profile used on the ProFlex PCR System was: 1 cycle at 95°C for 3 minutes, followed by 35 cycles of 95°C for 45 seconds, 60°C for 30 seconds and 72°C for 3 minutes, then a final 72°C cycle for 10 minutes.

Table 2.14 WNT5A Screening PCR Mastermix Constituents

	Volume to pipette (μ l)	
	Per rx	For 30 rx
Buffer (10x)	1	30
MgCl ₂ (50mM)	0.3	9
dNTPs (10mM)	0.2	6
Primer 1 (12.5 μ M)	0.2	6
Primer 2 (12.5 μ M)	0.2	6
Taq polymerase	0.1	3
PCR grade water	7	210

Table 2.15 WNT5 Sequencing Primers

Sequencing Primers for both WNT5A and WNT5B bands	Seq EF1alpha FW CTCAAGCCTCAGACAGTGGTTC
	Seq mRFP rev CGCTTCCCTCCATCTTGACC

The PCR products were then analysed on a 1% agarose gel. The original WNT5A and WNT5B plasmid DNA (# 43813 and 43814) used for cloning were loaded into the gel to act as a reference band for the samples (to help identify which colony DNA contained the WNT5A and WNT5B insert). Of the miniprep DNA which obtained bands at the correct weight, two for each plasmid were sent for sequencing to Source Bioscience Ltd. Miniprep DNA with correct sequencing was used for future transfections.

The plasmid DNA was isolated from 15 colonies for each vector (WNT5A: colonies A1-15, WNT5B: colonies B1-15). Nucleic acid concentration was determined using a Nanodrop, as shown in **Table 2.16**, and the DNA was analysed for the presence of inserts by PCR screening as shown in **Figure 2.20**. All samples had a 260/280 ratio over 1.8 and a 260/230 over 2.0 suggesting high quality DNA.

Table 2.16 WNT5A and WNT5B Plasmid DNA Nucleic Acid Concentrations

	Nucleic Acid Conc (ng/μl)	260/280	260/230		Nucleic Acid Conc (ng/μl)	260/280	260/230
A1	259.4	1.87	2.18	B1	57.2	1.88	2.12
A2	234.3	1.88	2.22	B2	435.8	1.88	2.21
A3	274.3	1.86	2.06	B3	459.7	1.87	2.16
A4	260.2	1.88	2.20	B4	332.8	1.87	2.17
A5	242.2	1.87	2.24	B5	429.9	1.88	2.19
A6	256.6	1.88	2.17	B6	265.2	1.87	2.12
A7	235.0	1.88	2.23	B7	372.6	1.87	2.20
A8	223.3	1.88	2.19	B8	322.8	1.88	2.21
A9	343.0	1.88	2.23	B9	449.8	1.87	2.19
A10	289.3	1.87	2.19	B10	370.1	1.88	2.17
A11	275.3	1.88	2.24	B11	249.9	1.88	2.13

A12	357.6	1.87	2.19	B12	390.5	1.87	2.19
A13	194.3	1.88	2.17	B13	403.4	1.88	2.19
A14	228.1	1.87	2.18	B14	466.7	1.87	2.20
A15	214.8	1.89	2.15	B15	426.1	1.88	2.20

Positive controls for WNT5A and WNT5B were loaded onto the gel (the original plasmid DNA of the cloning vector plasmids 43813 and 43814). These controls acted as a reference band for the samples to help identify which colony DNA contained the WNT5A and WNT5B insert. From the gel, it was identified colonies A5, A8, A12, A13, A14 and A15 were positive for WNT5A, and colonies B3, B5, B6, B7, B12, B13, B14 and B15 were positive for WNT5B, as highlighted within the white boxed regions.

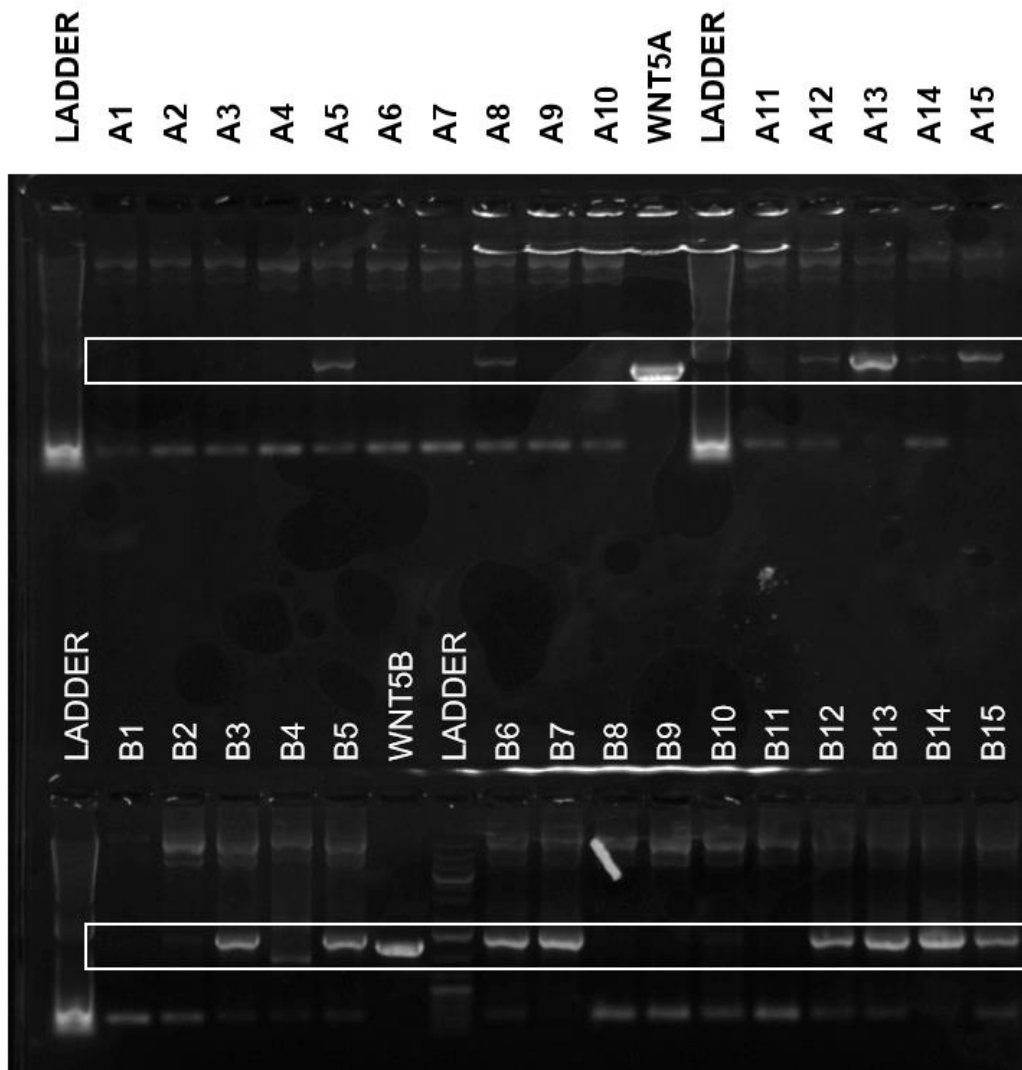


Figure 2.20 Colony Screening for WNT5A (top row) and WNT5B Inserts (bottom row)

Following verification on the 1% agarose gel, DNA of two colonies for each vector were sent for DNA sequencing (colonies A13, A15, B7 and B14) to ensure the plasmid sequences were inserted correctly without mutation. DNA sequencing determines the sequence of nucleotides of a DNA sample. It is a PCR reaction that involves incorporating fluorescently labelled dideoxynucleotides into the synthesised PCR products, of which each dideoxynucleotide has a different colour or fluorochrome. Dideoxynucleotides terminate extension at the 3' prime end, giving rise to multiple PCR product fragments of which the last base (the dideoxynucleotide) can be identified by its fluorochrome. By capillary electrophoresis the PCR products are separated by size to the resolution of one base via electrical field. Negatively charged DNA moves toward the positive electrode, with speed of movement correlating with molecular weight. At the end of the capillary, the dye is excited, and the characteristic wavelength emitted, which is specific to each dye. This is detected by a sensor that translates the signal into a base call. The resulting data file, an electropherogram, can be interpreted using FinchTV (Geospiza, version 1.4.0), and sequences aligned using MultAlin software (Corpet 1988).

Colonies A13 and B14 had correct sequencing and were therefore used for HEK293T transfection experiments. Sequencing results for A13 with forward and reverse sequencing primers aligned to the WNT5 insert region are shown in **Figure 2.21** and **Figure 2.22** respectively. The forward sequencing reaction has an extra base pair (bp) inserted at 1217. The reverse reaction was included to ensure any miss-called bases could be confirmed. The extra bp at position 1217 did not look like two distinguished peaks. This was most likely just one peak but due to a loss of resolution of the gel, the accuracy of the base call was reduced. The sequence was confirmed correct with the reverse sequencing reaction, as you cannot see the insertion between base position 173-174 in **Figure 2.22**. Forward and reverse sequencing results for B13, again aligned to the insertion site, are shown in **Figures 2.25 and 2.24**. The reverse primer showed an extra base pair at the end of the WNT5B region (position 1265), but the forward sequencing primer confirmed this was a miss-call and this was the correct

sequence as the insertion isn't shown between base position 62 and 63 of the forward sequencing result in **Figure 2.23**.

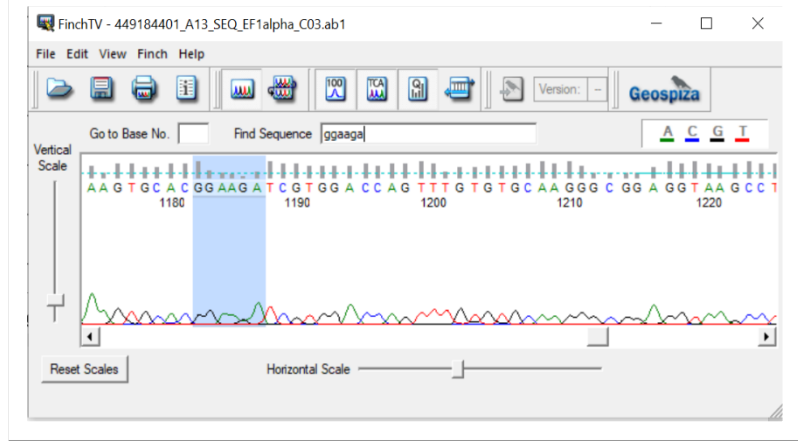
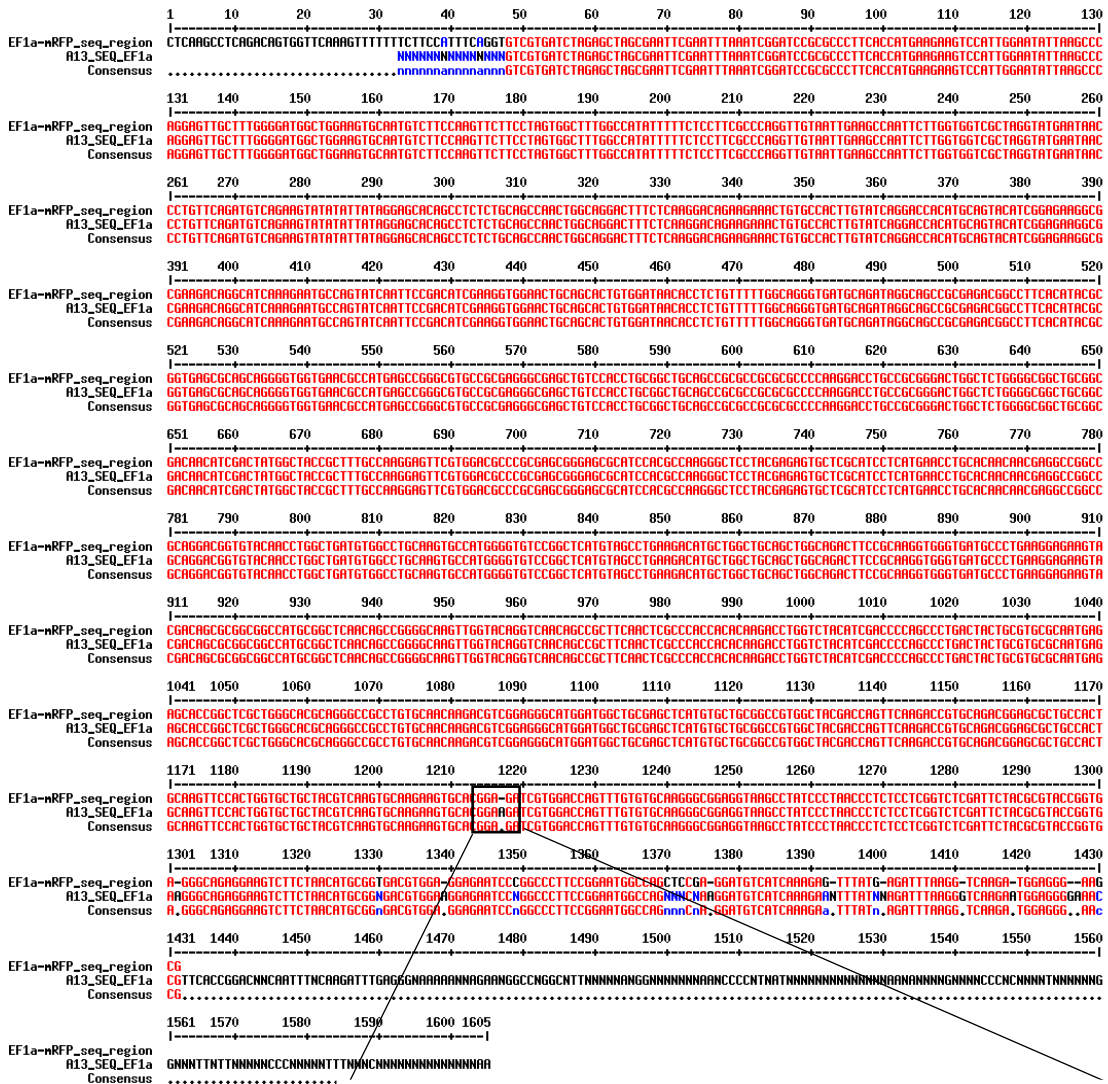


Figure 2.21 Colony A13 Forward Sequencing Results Aligned With the Expected WNT5A Insertion Site. The WNT5A sequence lies within base region 93-1299. The miss-call of a base insertion is highlighted in the boxed region of the WNT5A sequence alignments. FinchTV view of the electropherogram of this region is shown to confirm the miss-call.



Figure 2.22 Colony A13 Reverse Sequencing Results Aligned With the Expected WNT5A Insertion Site. The WNT5A sequence lies within base region 125-1338.



Figure 2.24 Colony B14 Reverse Sequencing Results Aligned With the Expected WNT5B Insertion Site. The WNT5B sequence lies within base region 124-1267. The miss-call of a base insertion is highlighted in the boxed region of the WNT5B sequence alignments. FinchTV view of the electropherogram of this region is shown to confirm the miss-call.

2.17.2.9 Confirmation of Transfection of HEK293T Cells

Successful transfection was confirmed by RT-qPCR. HEK293T cells were chosen for transfection as HEK293 cells (which HEK293T cells were derived from) do not endogenously express WNT5A (Jia *et al.* 2008). To confirm that HEK293T cells do not express WNT5A, RNA was extracted from untransfected, RFP EV, WNT5A and WNT5B transfected cells for RT-qPCR. RFP reporter expression following transfection is shown in **Figure 2.25A**. The RNA was extracted from those cells and quality checked using a non-denatured agarose gel (**Figure 2.25B**). The 28s band is twice as intense as the 18S band suggesting high quality intact RNA. Relative expression of WNT5A mRNA following RT-qPCR is shown in **Figure 2.25C**. The cells transfected with WNT5A had a 1223-fold increase from untransfected cells and 1440-fold increase in WNT5A mRNA from the RFP EV. The primers used were specific for WNT5A, as the WNT5B transfected cell lysate had a similar fold change in mRNA expression as the controls.

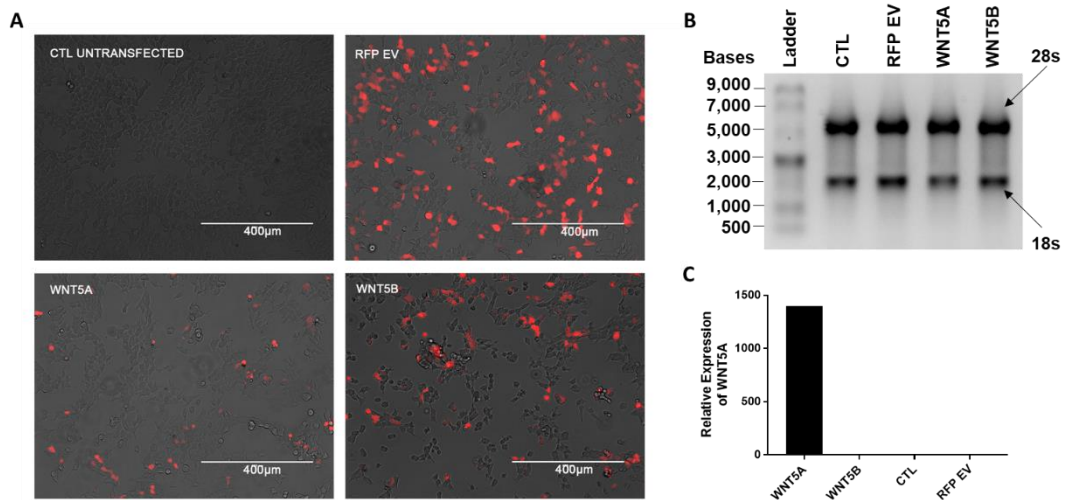


Figure 2.25 Validation of Negative and Positive Control Cells. (A) RFP reporter expression of the RFP EV, WNT5A and WNT5B transfected cells used in the RT-qPCR experiment. (B) Image of the non-denatured agarose gel with the extracted HEK293T RNA from the cells shown in (A). (C) Relative expression of WNT5A mRNA between the untransfected, and RFP EV, WNT5A and WNT5B transfected HEK293T cells shown in (A), $n=1$.

2.17.3 WNT5A Antibody Validation: Antibody Testing for Western Blot

2.17.3.1 Whole Cell Lysate Preparation

To validate WNT5A antibodies for specificity to WNT5A, protein lysates were prepared from untransfected cells, cells transfected with an empty vector (without a WNT5 insert) and cells transfected with either WNT5A or WNT5B. The untransfected and empty vector served as negative controls, and WNT5A as the positive control.

Protein lysates were prepared using ice cold RIPA buffer, containing 1% protease inhibitor, 1% sodium deoxycholate and 1% Phenylmethanesulphonylfluoride (PMSF). Samples were placed on ice for 30 minutes and periodically vortexed, followed by centrifugation at 12,000G for 10 minutes at 4°C. The supernatant was then transferred and aliquoted for storage at -20°C.

2.17.3.2 Western Blot

Samples were prepared with 2-Mercaptoethanol (Sigma, cat no M6250) and Laemmli Buffer (Bio-Rad, cat no 1610747), and denatured for 3 minutes at 95°C. The protein extracts were separated by gel electrophoresis on 10 or 12% Mini Protean TGX Polyacrylamide Pre-cast gels (Bio-Rad, cat no 4561034/4561044) in a Mini Protean Tetra Vertical electrophoresis chamber. 7µl of Novex MagicMark (Fisher Scientific, cat no 10610856) and 3.5µl of Prime-step pre-stained broad range ladder (Biolegend, cat no 773302) were used as western blot visual standards. Following 30-45 minutes of electrophoresis, protein transfer onto a 0.2µm PVDF membrane (Bio-Rad cat 1704156) was performed at 25V for 7 minutes. The membrane blot was then blocked with 5% Milk TBS Tween solution (Marvel, Dried skimmed milk powder) at room temperature for 1 hour on a roller mixer. The blots were probed with WNT5A primary antibodies clone 6F2 (Insight Biotech Inc, cat no GTX83127), 3A4 (Sigma Aldrich, cat no SAB1402393) and A-5 (Santa Cruz, cat no sc-365370) overnight at 4°C. Dilutions used for each antibody are shown in **Table 2.17**. For blots with β-catenin, the membranes were washed three times with TBS Tween wash buffer before probing further with β-actin (Santa Cruz, cat no sc-47778) for 1 hour at room

temperature protected from light. The membranes were washed a final three times with TBS Tween wash buffer, before adding Pierce ECL substrate reagent (ThermoFisher, cat no 32106) for chemiluminescence detection of the membrane bound WNT5A protein band. Images of the membrane blots were obtained using an ImageQuant LAS 4000.

Table 2.17 Antibodies Used for Western Blot

Target Protein	Primary Antibody	Dilution Factor	Secondary Antibody	Dilution Factor
WNT5A	WNT5A Clone 6F2 (Insight Biotech Inc, cat no GTX83127)	1:125	Polyclonal goat anti mouse IgG HRP (Agilent, cat no P0447)	1:1000
	WNT5A Clone 3A4 (Sigma Aldrich, cat no SAB1402393)	1:200		
	WNT5A Clone A-5 (Santa Cruz, cat no sc-365370)	1:200		
β -Actin	Santa Cruz, cat no sc47778			1:5000

The performance of the three antibodies are shown in **Figure 2.26**. Clone A-5 did not produce a single band although it is recommended for human WNT5A detection by western blot. Clone 6F2 produced numerous bands, of which none presented within the expected molecular weight of 42.3kDa. Out of the bands produced, none appeared only or of stronger intensity for the WNT5A (or WNT5B due to its close homology with WNT5A) cell lysate. This suggests that although this antibody detects multiple antigens by western blot, it does not detect WNT5A.

Clone 3A4 produced a single band at approximately 55kDa for the WNT5A overexpressed cell lysate, however, western blot is not a recommended application for this clone. As the band was present only in the WNT5A overexpressed cell line and not in the empty vector control, this indicated that the band was likely to be WNT5A as the molecular weight of WNT5A can differ from 42.3kDa due to varying levels of glycosylation. To confirm this result, and ensure reproducibility, the western blot was repeated a further two times, but the band was not seen in the further experiments. The band observed on the first western

blot, however, was weak for an overexpressed cell line. To confirm protein loading, the membrane was also probed for β -actin without stripping the WNT5A primary and secondary antibody. The band for β -actin was more pronounced than that of the expected WNT5A. This may be because the transfection efficiency for this experiment was low (approximately 10% transfection for WNT5A), and therefore β -actin may well have been more abundant as all eukaryotic cells express it.

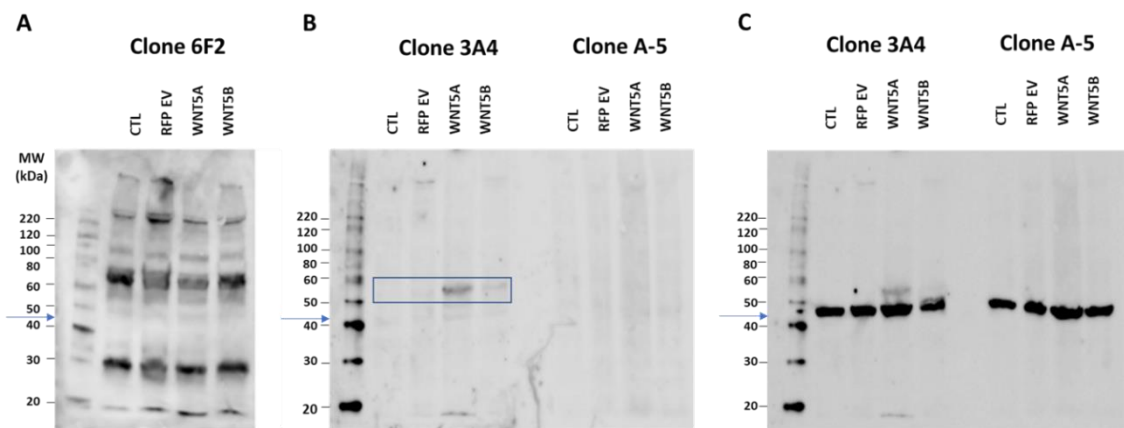


Figure 2.26 WNT5A Protein Expression in Overexpressed HEK293T Cells. Bands were detectable for WNT5A antibody clone 6F2 (A) and 3A4 (B- left hand side). No band was detected for clone A-5 (B-right hand side). To confirm protein loading for 3A4 and A-5, the membrane in B was stained with house-keeping gene β -actin to confirm protein loading (C).

2.17.4 WNT5A Antibody Validation: Antibody Testing for ICC

2.17.4.1 Embedding the Transfected HEK293T Cell Pellet in Paraffin

After trypsinisation, 10 million cells were fixed for 30 minutes at room temperature with 10% neutral buffered formalin and centrifuged at 600G for 5 minutes. The pellet was then washed with PBS and centrifuged again at 600G. The PBS was then aspirated, and the cell pellet resuspended slowly in 500 μ l of HistoGel (Thermofisher, cat no HG-4000-012) to avoid bubbles. The HistoGel cell suspension was pipetted into a 24-well plate and left to set for 5-10 minutes. The solidified pellet was then removed by scalpel, placed into a biopsy cassette (with foam insert on top to prevent HistoGel curling) and left in 70% industrial methylated spirit (IMS) until ready for processing on a Shandon tissue processor.

2.17.4.2 ICC of the Overexpressed Cell Pellet

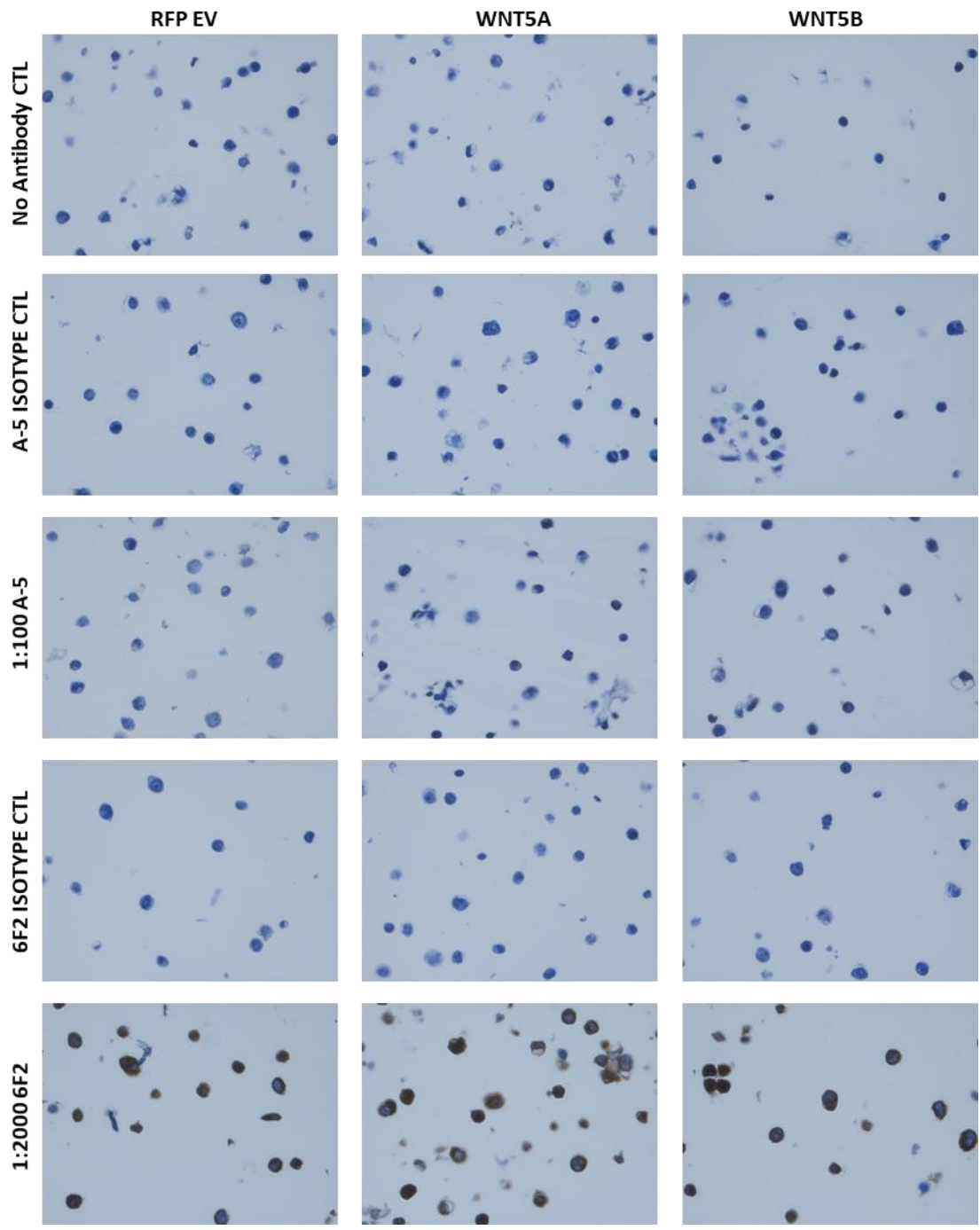
Overexpressed and control cell pellet blocks were cut and stained for WNT5A to assess antibody specificity for immunohistochemistry staining. Three WNT5A clones were assessed: 6F2 (Insight Biotech, cat no GTX83127), 3A4 (Sigma, cat no SAB1402393) and A-5 (Santa Cruz, cat no sc-365370). Immunohistochemistry staining was performed using a DAKO EnVision kit (DAKO, product code K8012).

Slides were deparaffinised and rehydrated, and subjected to pH low (AR6 Buffer 10x, AR600250ML) heat-induced (microwaving for 3 minutes at 700W) antigen retrieval. Pelleted sections were drawn around using a hydrophobic pen (Immedge, Vector labs), and non-specific background staining blocked with peroxidase block (provided in the kit) for 10 minutes at room temperature according to the manufacturer's instructions. Antibodies were diluted with DAKO antibody diluent and applied for 1 hour at room temperature. The antibodies used are listed in **Table 2.18**. The EnVision Flex linker was then applied for 20 minutes at room temperature, and the EnVision FLEX/HRP for 30 minutes at room temperature to all slides. DAB was applied for 5 minutes to visualise the immunoreaction. The sections were then counterstained with haematoxylin for 2 minutes, and washed, dehydrated and mounted using DAKO mounting media (DAKO, product code CS703). Wash steps were performed using 20x EnVision Flex Wash Buffer (DAKO, product code K8007) diluted to 1x with distilled water.

Table 2.18 Antibodies Used for Immunohistochemistry. The greyed out 6F2 antibody concentration was used solely as a stock dilution and was not used for staining.

Antibody	Antibody Stock Concentration	Dilution	Antibody Volume (μ l)	Diluent Volume (μ l)	Concentration (μ g/ml)
WNT5A 6F2	N/A	1 in 500	1	499	
		1 in 1000	300 μ l of 1 in 500	300	N/A ascites
		1 in 2000	200 μ l of 1 in 1000	200	N/A ascites
WNT5A 6F2 ISO IgG1	100 μ g/ml	1 in 10	30	270	10
WNT5A 3A4	1mg/ml	1 in 75	4	296	13.33
		1 in 200	1.5	298.5	5
		1 in 400	1	399	2.5
WNT5A 3A4 ISO IgG2a	100 μ g/ml	1 in 7.5	40	260	13.33
WNT5A A-5	200 μ g/ml	1 in 100	3	297	2
		1 in 200	1.5	298.5	1
		1 in 400	1	399	0.5
WNT5A A-5 ISO IgG2b	100 μ g/ml	1 in 50	6	294	2

Vector control and WNT5A/B transiently transfected cell pellets were fixed and embedded in paraffin to test WNT5A antibodies for immunocytochemistry. Representative images for each WNT5A antibody clone are shown in **Figure 2.27**. A low pH (citrate) antigen retrieval method was used, similarly to others investigating WNT5A in paraffin embedded tissue (as shown in **Table 2.11**). The transfection efficiency for this experiment was roughly 20-30% so not all cells would be expected to stain for WNT5A. Clone 6F2 stained the empty vector control and WNT5A/B overexpressed cells equally. This reinforces that this antibody binds non-specifically as seen in the western blot results. The dilution used was 1 in 2000 as this concentration was optimised for paraffin embedded tissue staining before antibody validation started. Despite using the same antigen retrieval method, clone A-5 did not stain the cells. Clone 3A4 showed equal staining between the RFP EV and WNT5A/B overexpressed cells, suggesting non-specific binding.



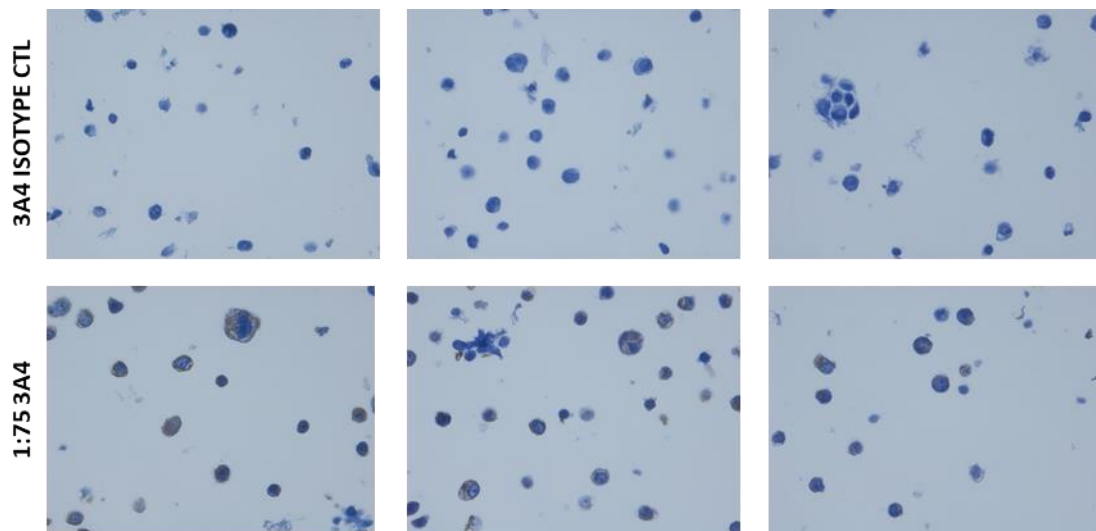


Figure 2.27 Immunocytochemistry Staining for WNT5A Protein Expression in Overexpressed HEK293T Cells. Paraffin embedded cell pellets of transiently transfected HEK293T cells (RFP empty vector, WNT5A and WNT5B) were stained with WNT5A antibody clones A-5, 6F2 or 3A4. Relevant isotype controls matched for clonality and antibody concentration (where possible) for each clone are also shown.

2.17.5 WNT5A Antibody Validation: Antibody Testing for Flow Cytometry

Overexpressed HEK293T cells were harvested and fixed with methanol (20 minutes on ice), neutral buffered formalin (10 minutes at room temperature), eBioscience fixation buffer (30 minutes at room temperature) and acetone (20 minutes at -20°C) or left unfixed. Cells were stained with Fixable Viability Dye eFluor 780 (Fisher Scientific) for 15 minutes at room temperature, and permeabilised with eBioscience permeabilisation buffer in accordance with manufacturer's recommendations. In the unconjugated experiments, WNT5A was stained for 40 minutes at room temperature, followed by secondary antibody staining for 20 minutes at room temperature with IgG1 (for clone 6F2) and IgG2a (for clone 3A4) AF647 antibodies. V5 tag staining was stained separately for 20 minutes at room temperature to prevent cross reactivity with the secondary antibodies. In the WNT5A conjugated experiment, the protocol remained the same but the V5 tag and the WNT5A staining was not performed in a single tube, as the WNT5A conjugation kit was on the same channel as the V5 tag antibody. Unfixed and matched IC fixation buffer controls were run on the Attune to assess the impact of fixation on the RFP reporter. As there was only partial degradation

by fixation, this was used as a marker for the conjugation experiments where the V5 tag antibody was omitted.

A-5 did not show any reactivity for western blot or immunocytochemistry and was therefore not included for flow cytometry validation. Fixed and unfixed cells were stained with clones 6F2 and 3A4 and analysed by flow cytometry (**Figure 2.28 and 2.29** respectively). Cells were fixed by multiple methods – neutral buffered formalin, Ebioscience intracellular fixation buffer (which is also neutral buffered formalin based), methanol and acetone. Because fixation and permeabilisation decreased RFP reporter fluorescence, the V5 tag was utilised as the marker for transfected cells by flow cytometry. Once dead cells were gated out using a viability dye, the correlation between the V5 tag and WNT5A antibody staining was assessed for the untransfected and RFP EV, WNT5A and WNT5B transiently transfected cells. As the V5 tag was tagged to the WNT5 sequences, the RFP EV did not express the V5 tag.

Out of all the fixation methods tested, only the neutral buffered formalin (NBF) based fixatives showed signs of positive indirect WNT5A staining which correlated with the V5-tag expression. Data is therefore only shown for NBF fixed experiments. Clone 6F2 did not show any affinity for WNT5A. Altering the antibody concentration just shifted both the negative and positive population. The 3A4 antibody did show binding in both WNT5A and WNT5B overexpressed cells. Although this staining wasn't as high as expected, the binding did correlate with V5 tag expression. This positivity however was not retracted with an omit primary antibody control as one would expect, suggesting non-specific binding of the secondary antibody to the WNT5 region within the expression plasmid. To omit the secondary antibody, and ensure the positive staining was non-specific, the primary antibody was conjugated using a Lightning-link antibody conjugation kit and the experiment repeated. This retracted all positive staining, supporting that the secondary antibody was non-specifically binding within the WNT5 region of the plasmid (data not shown). This experiment used RFP expression as a marker

of transfection as the V5 tag antibody was on the same fluorochrome as the WNT5A antibody. The V5 tag was therefore was not stained simultaneously.

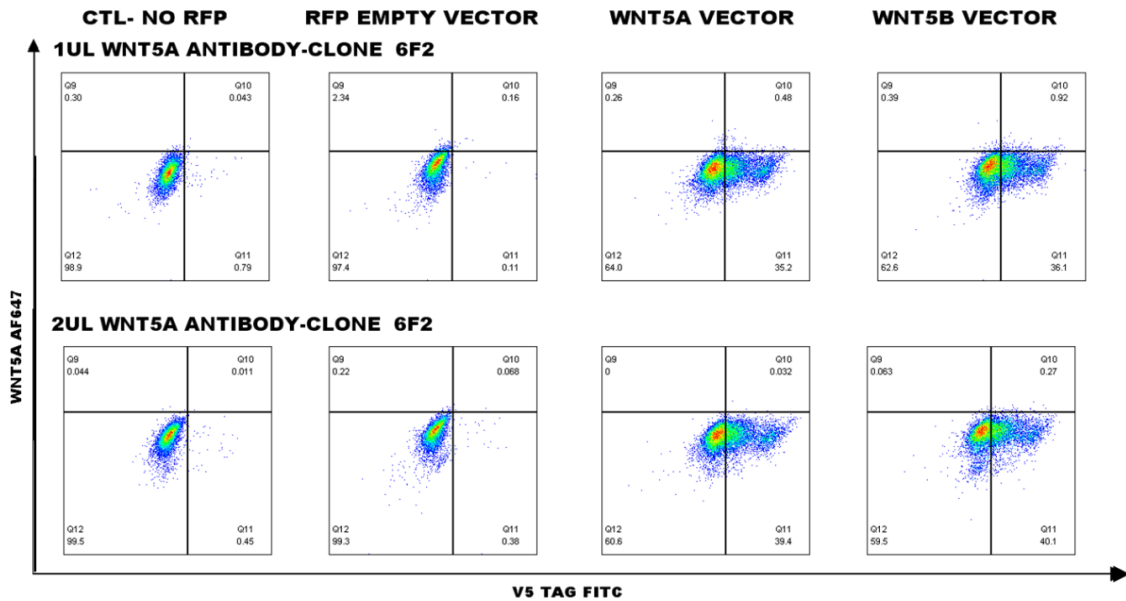


Figure 2.28 Assessment of the WNT5A mAb Clone 6F2 for Flow Cytometry Application. HEK293T without plasmid transfection and HEK293T cells transiently transfected with an RFP empty vector, WNT5A or WNT5B were stained with WNT5A antibody clone 6F2 to assess suitability for the application of flow cytometry.

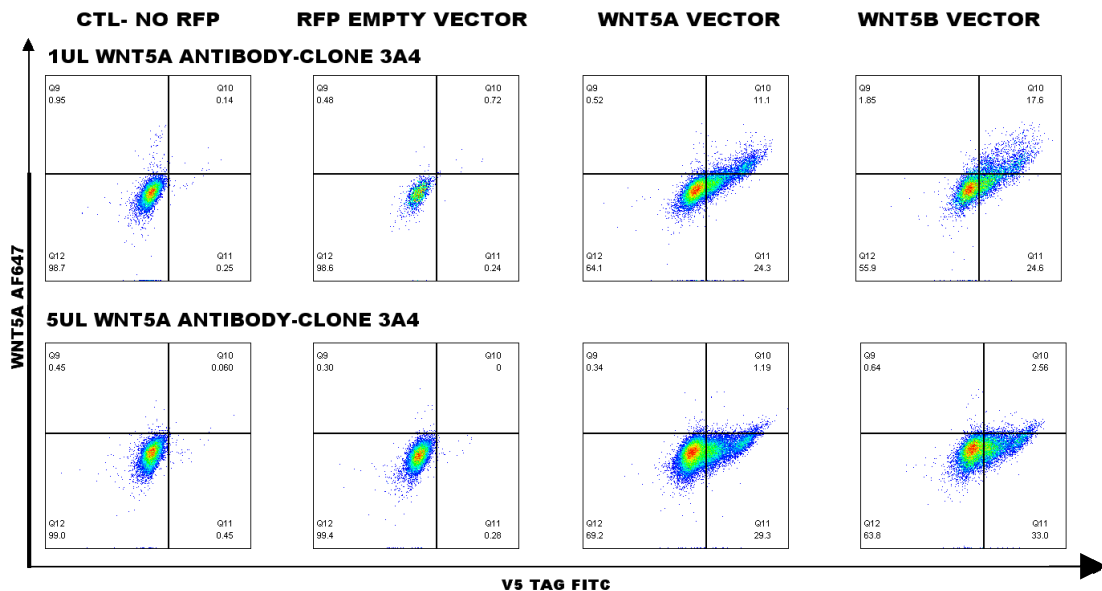


Figure 2.29 Assessment of the WNT5A mAb Clone 3A4 for Flow Cytometry Application. HEK293T without plasmid transfection and HEK293T cells transiently transfected with an RFP empty vector, WNT5A or WNT5B were stained with WNT5A antibody clone 3A4 to assess suitability for the application of flow cytometry.

2.17.6 Antibody Validation Summary of Outcomes and Method Limitations

None of the antibodies tested appear to be specific for the applications tested, irrespective of whether they were approved applications by the supplier or not. Clone 3A4 may be specific for western blot, but further testing would be necessary. On the contrary to Prgomet, Andersson and Lindberg (2017), we did not find 3A4 suitable for immunohistochemistry, with cytoplasmic staining found in the RFP EV control cell pellet. The WNT5A stained cell pellet did not present with obvious additional staining suggesting this clone is also non-specific. Clone A-5 did not show successful binding in either western blot or immunocytochemistry. Clone 6F2 on the contrary, appeared to bind non-specifically with numerous bands presenting at western blot, none of which were at the expected molecular weight or correlated with WNT5A overexpression. This was also shown by flow cytometry and immunocytochemistry where the antibody bound to most cells regardless of having a low transfection efficiency. Our 6F2 findings were agreeable with Prgomet, Andersson and Lindberg (2017) on that 6F2 presents numerous bands at western blot, of which none were specific for WNT5A as investigated by overexpression, and that immunohistochemical staining also stains negative control tissue through the vector controls.

To confirm that WNT5A was in fact being produced at the protein level as well as the RNA level following transfection for all methods, it would have been beneficial to use a negative and positive control tissue or cells to confirm the findings in the transfected HEK293T cells. HEK293T cells were chosen for transfection as HEK293 cells (which HEK293T cells are derived from) do not express WNT5A endogenously (Jia *et al.* 2008) and so staining should be absent in the untransfected and empty vector controls. For additional reassurance, however, normal liver tissue could have been used as a negative control tissue, as utilised by Prgomet, Andersson and Lindberg (2017) in their WNT5A antibody validation paper, and squamous cell carcinoma tissue as a positive control tissue, as WNT5A upregulation is characteristic of this tumour subtype (Rapp *et al.* 2016). WNT5A expressing L-cells could also have been utilised for all techniques as an alternative positive control to confirm the results observed.

2.18 Analysis

Statistical analysis was performed using Prism (GraphPad version 8.0). The two-way and three-way repeated measures Aligned ranks transformation ANOVA was performed using R (3.6.0) by Dr Matt Richardson. Data set normality was assessed prior to statistical testing to identify if data values were derived from a Gaussian distribution. All error bars presented are mean \pm standard deviation, and p value considered significant if less than .05.

Parametric data with 2 groups was analysed using a paired or unpaired t-test. Where multiple t-tests were conducted in the same data set, p values were adjusted for multiplicity using the Holm-Sidak method ($\alpha=0.05$). For more than two groups, a one-way ANOVA with Dunnett's *post hoc* test, two-way repeated measures ANOVA and three-way repeated measures mixed-effect model was conducted. For 2 grouped nonparametric data analysis, the Wilcoxon Matched Pairs Signed Rank test was used, and for 3 groups or more, either a two-way or three-way repeated measures Aligned ranks transformation ANOVA. For correlation analysis, Pearson correlation was used.

In the scratch wound healing TEER data there was one missing data point for one donor. As repeated measures ANOVA cannot handle missing values, the data was analysed by fitting a mixed model in GraphPad Prism v8.0, which statistically analyses the data the same way as a repeated measures ANOVA when all data values are present and can be interpreted like a repeated measures ANOVA. For statistical clarification, the mixed model used uses a compound symmetry covariance matrix, which is fit using Restricted Maximum Likelihood (REML). Where all values were present, ANOVA was used instead. Due to the complexity of the experiment design, scratch wound analysis readouts for healing and TEER were only assessed at 24 hours. As ANOVA requires a normal distribution, normality tests were conducted for each statistical test. The TEER data had a normal distribution, whereas the scratch wound data did not. Nonparametric test equivalents were therefore used for the 24-hour scratch wound analysis – a Wilcoxon matched-pairs signed rank test instead of a paired t-test and an Aligned ranks repeated measures ANOVA instead of fitting a mixed model or repeated-measures ANOVA.

3 ASSOCIATIONS BETWEEN WNT AND TGF- β TRANSCRIPTIONAL REPAIR MODULES, AIRFLOW OBSTRUCTION AND INFLAMMATORY PROFILES

3.1 Introduction

Persistent inflammation can lead to aberrant tissue repair and consequently airway remodelling (Hough *et al.* 2020). Airway remodelling is a classic pathological feature of asthma that is characterised by changes in the airway tissue architecture which are associated with narrowing of the airways and consequently loss of lung function (Bergeron, Tulic and Hamid 2010). Predictably, asthmatics are reported to have a greater decline in lung function over time compared to non-asthmatic controls (Lange *et al.* 1998), and that airflow obstruction increases with asthma severity (Moore *et al.* 2010), with fixed or incompletely reversible airflow obstruction being a key feature of severe disease (Lee *et al.* 2007).

Airflow obstruction is reported to be a clinical surrogate marker of airway remodelling (Benayoun *et al.* 2003) (Cohen *et al.* 2007). Therefore, airflow obstruction assessed via lung function tests may be useful in identifying asthmatic patients that have concurrent airway remodelling. By identifying associations between lung function and genetic changes in epithelial repair pathways, we may therefore provide insight into the pathophysiology of asthma and how therapeutically we could target repair to prevent airway remodelling. Key epithelial repair cell signalling pathway modules were therefore assessed for an association with lung function to identify if they are likely to be responsible for asthmatic airway remodelling if gone awry.

3.2 Methods

The methods are described in depth in Chapter 2.12 but a brief description is provided to aid readability of the chapter. As transcriptomic data sets have high dimensionality, a pathway gene set analysis method was applied to continuously link epithelial repair pathway transcriptomic genes, identified through KEGG pathway gene lists, into six single transcriptional modules. This list of module genes could be condensed into a single gene expression pattern profile representative of module expression. This linear single gene expression pattern profile explains the modular expression variance and is termed the module's eigengene. In this study, the association between the module eigengene expression and pre-bronchodilator FEV₁/FVC and TH status was investigated for two severe asthma transcriptional cohorts (SARP and U-BIOPRED).

3.3 Results

3.3.1 The SARP and U-BIOPRED Cohorts

The SARP discovery cohort consisted of 69 asthmatics with severe asthma. The U-BIOPRED cohort consisted of 49 severe asthmatics. Severe asthma is defined as asthmatics with GINA 4-5 treatment intensity (high dose ICS with additional controller or add on therapies such as OCS or biologic). Their clinical characteristics are shown in **Table 3.1**. There was a significant difference between the age, FEV₁ percent predicted, Pre-bronchodilator FEV₁/FVC Ratio, inflammatory blood cell counts and GINA treatment intensity between the two cohorts. The significant difference between lung function and GINA treatment step between the two cohorts highlighted that asthma severity significantly differed between the cohorts. The sex, fractional exhaled nitric oxide (FeNO), smoking history and asthma duration however did not differ between the two cohorts.

Table 3.1 Clinical Characteristics Table of the Transcriptional Cohorts.

All characteristics are presented mean with standard deviation unless otherwise stated. With partial clinical information available for some characteristics, the number of patients contributing to the characteristic statistical analysis is presented as ⁽ⁿ⁾. Lung function test results reported are pre-bronchodilator (Pre-BD). All tests were a Wilcoxon rank sum test, except for GINA treatment intensity and sex (a Chi-square test).

	SARP Cohort	U-BIOPRED Cohort	p Value
n	69	49	
Age (y), mean ± SD	42.55 ± 12.05	48.65 ± 14.36	0.0099
Sex (M/F), n	23/46	24/25	0.0871
GINA treatment step (4/5), n	19/50	30/18	0.0002
Asthma duration, (y), mean ± SD	26.53 ± 13.78 ⁽⁶⁷⁾	27.6 ± 16.65 ⁽⁴⁷⁾	0.9600
Smoking history (pack-year)	8.21 ± 8.60 ⁽¹⁹⁾	2.53 ± 1.67 ⁽⁹⁾	0.1238
FeNO (ppb), mean ± SD	48.16 ± 39.25 ⁽⁶⁰⁾	41.77 ± 29.49 ⁽⁴⁵⁾	0.4650
Blood eosinophil count (x10 ⁹ /L), mean ± SD	0.39 ± 0.32 ⁽⁶⁷⁾	0.29 ± 0.24	0.0407
Blood neutrophil count (x10 ⁹ /L), mean ± SD	5.93 ± 1.44 ⁽⁶⁷⁾	4.82 ± 2.00	0.0002
Pre-BD FEV ₁ (%) predicted, mean ± SD	58.72 ± 17.53	74.68 ± 22.21	0.0002
Pre-BD FEV ₁ /FVC Ratio (%), mean ± SD	63.68 ± 11.46	66.50 ± 12.22	<0.0001

3.3.2 Correlation between FEV₁/FVC and TH Status and the Transcriptional Module Scores for the SARP and U-BIOPRED Cohorts

The pre-bronchodilator (pre-BD) FEV₁/FVC ratio was used as a marker of airflow obstruction caused by airway remodelling, and type of airway inflammation by TH2 and TH17 transcriptional signatures derived from bronchial epithelial brushings. The observed pre-BD FEV₁ measurement, which is recorded after withholding bronchodilators for a period longer than their duration of action (Reddel *et al.* 2009), is then divided by the FVC value and converted to a percentage to form the FEV₁/FVC ratio.

Both pre- and post-bronchodilator FEV₁/FVC have a significant correlation with asthma severity (Chae *et al.* 2011). The pre-BD FEV₁/FVC was selected as it will account for airflow obstruction due to both ASM effects and airway remodelling,

unlike the post-BD FEV₁/FVC which accounts for remodelling independent of ASM tone. With pre-BD FEV₁/FVC, airflow obstruction is identified as being less than 0.7 (or 70% when expressed as a percentage) (Panigrahi and Padhi 2019) or the lower limit of normal, which is defined by prediction equations (Christopher *et al.* 2020). As the inflammatory phenotype will drive the cytokine milieu availability to the epithelial cells in times of repair, the correlation between the transcriptional modules and the TH subsets were also assessed. The correlation between the modular scores, the pre-BD FEV₁/FVC ratio and the TH status is shown in **Table 3.2**.

All modules had a weak correlation with pre-BD FEV₁/FVC, of which none of the modules had a statistically significant association across both cohorts. All modules bar the Noncanonical TGF- β signalling module failed to correlate with TH2 expression. The Noncanonical TGF- β signalling module (SARP: $p=0.0140$; U-BIOPRED: $p=0.0112$) displayed a significant negative correlation with TH2 expression in both cohorts. For TH17 expression, only the Noncanonical WNT signalling module had a significant association, of which a significant positive correlation between the module and TH17 was found (SARP: $p=0.0487$; U-BIOPRED: $p=0.0204$).

Table 3.2 Correlation of Transcriptomic Modular Scores With Pre-Bronchodilator FEV₁/FVC and TH Status. Pearson correlation, *r*, was assessed between pre-bronchodilator FEV₁/FVC ratio (%), TH2 and TH17 status and the modular scores of the six transcriptomic modules.

	SARP Cohort			U-BIOPRED Cohort		
	FEV ₁ /FVC Ratio (%) Correlation, <i>r</i>	<i>p</i> Value	95% CI	FEV ₁ /FVC Ratio (%) Correlation, <i>r</i>	<i>p</i> Value	95% CI
Canonical WNT Signalling Module	0.11	0.3659	(0.13, 0.34)	0.00	0.9932	(-0.28, 0.29)
Noncanonical WNT Signalling Module	-0.07	0.5520	(-0.30, 0.17)	-0.08	0.5886	(-0.36, 0.21)
Canonical TGF-β Signalling Module	-0.14	0.2354	(-0.37, 0.10)	0.08	0.6083	(-0.22, 0.35)
Noncanonical TGF-β Signalling Module	-0.14	0.2678	(-0.36, 0.10)	0.18	0.2293	(-0.11, 0.44)
WNT TGF-β Overlap Module	-0.26	0.0303	(-0.47, -0.03)	0.09	0.5500	(-0.20, 0.36)
WNT Notch TGF-β Module	-0.01	0.9231	(-0.25, 0.23)	0.03	0.8578	(-0.26, 0.31)
	TH2 Correlation, <i>r</i>	<i>p</i> Value	95% CI	TH2 Correlation, <i>r</i>	<i>p</i> Value	95% CI
Canonical WNT Signalling Module	-0.03	0.7133	(-0.20, 0.14)	0.25	0.0863	(-0.04, 0.50)
Noncanonical WNT Signalling Module	-0.03	0.6962	(-0.20, 0.13)	-0.22	0.1420	(-0.47, 0.07)
Canonical TGF-β Signalling Module	-0.08	0.3641	(-0.24, 0.09)	-0.05	0.7270	(-0.33, 0.24)
Noncanonical TGF-β Signalling Module	-0.21	0.0140	(-0.36, -0.04)	-0.36	0.0112	(-0.59, -0.08)
WNT TGF-β Overlap Module	-0.04	0.6736	(-0.20, 0.13)	-0.18	0.2179	(-0.44, 0.11)
WNT Notch TGF-β Module	0.06	0.4633	(-0.11, 0.23)	0.20	0.1793	(-0.09, 0.46)
	TH17 Correlation, <i>r</i>	<i>p</i> Value	95% CI	TH17 Correlation, <i>r</i>	<i>p</i> Value	95% CI
Canonical WNT Signalling Module	0.12	0.1596	(-0.05, 0.28)	0.03	0.8446	(-0.26, 0.31)
Noncanonical WNT Signalling Module	0.17	0.0487	(0.001, 0.33)	0.33	0.0204	(0.05, 0.56)
Canonical TGF-β Signalling Module	-0.08	0.3292	(-0.25, 0.08)	-0.03	0.8260	(-0.31, 0.25)
Noncanonical TGF-β Signalling Module	-0.14	0.1090	(-0.30, 0.03)	-0.17	0.2523	(-0.43, 0.12)
WNT TGF-β Overlap Module	-0.01	0.9187	(-0.18, 0.16)	-0.08	0.5828	(-0.36, 0.21)
WNT Notch TGF-β Module	0.00	0.9788	(-0.17, 0.17)	-0.03	0.8332	(-0.31, 0.26)

3.4 Discussion

3.4.1 Transcriptional Module Association with Pre-BD FEV₁/FVC and TH Status

Fixed or incompletely reversible airflow obstruction is a feature of severe asthma (Lee *et al.* 2007) (Moore *et al.* 2010). As airflow obstruction, measured via lung function tests, is reported to be a clinical surrogate marker of airway remodelling (Benayoun *et al.* 2003) (Cohen *et al.* 2007), airflow obstruction may be useful in identifying asthmatics with airway remodelling. By identifying gene expression modules in the airway epithelium and their association with lung function and inflammatory TH cell signatures, which drive the cytokine milieu surrounding epithelial cells during airway repair, we may be able to provide insight into the pathophysiology of asthma and how therapeutically we could target repair to prevent airway remodelling.

The SARP and U-BIOPRED cohorts did have a pre-BD FEV₁/FVC less than 70%, indicative of airflow obstruction and airway remodelling. However, none of the transcriptional modules had a consistent significant association with airflow limitation across the two cohorts. A significant, positive association between TH17 status and the noncanonical WNT signalling transcriptional module however was found, which was consistent across both cohorts. TH17 cells are reported to directly and indirectly promote airway neutrophilia (Pelletier *et al.* 2010). Supporting the link between TH17 status and WNT5A, WNT5A can also induce neutrophilic infiltration as it has a chemotactic effect on neutrophils, and induces neutrophilic production of chemokines CXCL8 and CCL2, which promote further neutrophil and leukocyte recruitment (Jung *et al.* 2013). More direct associations are also seen in the literature; WNT5A expression has been reported to induce IL-17 expression, and that dual expression of IL-17 and WNT5A exists in inflamed dental pulp and psoriatic lesions (Liu *et al.* 2019: B) (Tian, Mauro and Li 2019). Daud (2016) also reported an increase in WNT5A protein expression in the airway epithelium of asthmatics with a TH17 gene signature. This is on the contrary, however, to what is reported by Choy *et al.* (2011), who suggest a strong positive correlation exists between WNT5A and the

TH2 signature in bronchial biopsies. The differences observed between the study by Choy *et al.* (2011) and this study may be due to airway sampling differences (as biopsies will contain lower proportions of epithelial cells compared to brushings), and the patient subsets from which the samples were obtained (as the biopsies were taken from mild-moderate asthmatics, whereas, the brushings were taken from severe asthmatics).

A significant negative correlation between TH2 and noncanonical TGF- β signalling was also found. This is also reported in the literature with TAK1 knockdown inducing TH2 cytokine production (Vink *et al.* 2013), and TAK1 inhibition eliciting a TH1 to TH2 cytokine shift in T lymphocytes (Cao *et al.* 2015). This is also supported by Courties *et al.* (2010) who report that TAK1 silencing decreases TH1 and TH17 cell frequencies, which may skew inflammation towards a TH2 driven response. Relating this to WNT5A-TGF- β 1 crosstalk, WNT5A and TAK1 signalling may have parallel roles in promoting a TH17 inflammatory response, which although out of the scope of this thesis, warrants further investigation particularly as TH17 mediated disease is linked to steroid resistance, airway remodelling and more severe disease in asthmatics. This theory is supported by research published by Peters *et al.* (2016: A) who found co-stimulation of mouse fibroblasts with WNT5A and IL-17A enhanced TGF- β 1 fibroblast secretion.

3.4.2 Limitations

Although the application of transcriptomics to study the quantitative profiling of mRNA across the asthmatic genome has defined multiple asthma endotypes as summarised by Tyler and Bunyavanich (2019), mRNA expression does not always equate to protein expression and activity, and therefore it may provide limited insight into the associations being investigated (Evans 2015). To further enhance understanding of the association between TH status and the transcriptional modules, this study may have benefitted from further evaluation into how the correlation between the transcriptional modules vary with disease

severity, particularly whether a greater magnitude in correlation is found with increasing asthma severity.

The transcriptomics analysis may also be would also have benefited from use of another replication cohort to confirm the associations seen between the modules and lung function and the inflammatory TH cell signatures, as the SARP and U-BIOPRED cohort were significantly different for multiple clinical patient characteristics including age, GINA treatment intensity, blood cell counts and more importantly lung function. The SARP cohort consisted of a majority of GINA step 5 patients, whereas, the U-BIOPRED cohort consisted of mainly GINA step 4 severe asthmatics. The SARP cohort are therefore more likely to be receiving OCS which may target the WNT and TGF signalling pathways as highlighted in section 1.14.3. This may therefore have interfered with the ability of the analysis to identify the correlations between the modules.

Additionally, due to a lack of consistently available spirometry measurements across the cohorts, the pre-BD FEV₁/FVC was selected as the measure of lung function. Ideally this transcriptomics study would not have been assessed on a single lung function measure, but rather incorporated a reversibility test to consider lung function variation resulting from bronchodilator use.

4 EVALUATING WNT5A & TGF- β 1 WOUND HEALING IN DIFFERENTIATED HUMAN BRONCHIAL EPITHELIAL CELL CULTURES

4.1 Chapter Overview

The respiratory epithelium is the first line of defence against environmental agents within the air. Restoration of epithelium integrity following wounding is therefore paramount in protecting against microbial, allergen or pollutant permeability and the pursuant inflammatory response. The cell signalling mechanisms behind bronchial epithelial repair, however, are poorly understood. To address this, a scratch wound assay was utilised to assess single-stimulation and dual-stimulation effects of WNT5A and TGF- β 1 on repair, two signalling molecules that are vital in development.

Asthmatic differentiated HBEC cultures were pre-stimulated with either vehicle control or rhTGF- β 1 for 48 hours. The TGF- β 1 or vehicle control primed cultures were then wounded and stimulated with rhWNT5A to assess the effect of WNT5A signalling on wound healing with and without the presence of TGF- β 1. The cultures were pre-stimulated with TGF- β 1 for 48 hours to recapitulate the asthmatic airway mucosal environment, which expresses higher TGF- β 1 expression compared to healthy controls and would therefore be conducive of a migratory environment through increased EMT induction. TGF- β 1 and WNT5A are reported to exhibit crosstalk in repair, with WNT5A being reported downstream of TGF- β 1 in numerous cellular systems in the literature. TGF- β 1 has been reported to induce WNT5A transcription directly via the SMAD complex, and indirectly via TAK1 and NF κ B, to potentiate its own actions. The WNT5A Ca²⁺ signalling pathway also signals through TAK1, which may be fundamental in the crosstalk signal. A second WNT5A stimulation was therefore applied to TGF- β 1 pre-stimulated cultures to address the impact of this potential crosstalk signal in wound healing, which has not yet been investigated in primary, differentiated HBECs.

Using two inhibitors, one to inhibit WNT5A signalling at its receptor (BOX-5) and one to inhibit the potential crosstalk intermediary TAK1 (Takinib), the mechanism behind potential functional crosstalk between the two signalling pathways in wound healing was investigated. Repair was then assessed through measuring wound closure over a 24-hour period and via taking TEER readings before and after wounding, and 24 hours post-wounding to assess epithelial barrier integrity restoration. In hopes of assessing crosstalk further, the ability to transfect ALI cultures was determined using multiple transfection reagents.

CBF and pattern was assessed in asthma and in health and then correlated with lung function, to identify if a difference exists in mucociliary clearance in asthma and health, and whether this worsens with lung function. The impact of WNT5A stimulation on CBF was also determined, to address whether WNT5A can enhance mucociliary clearance.

4.2 Evaluating the Effects of WNT5A Inhibitor BOX-5 and Non-Canonical TGF- β Inhibitor Takinib on the Viability of Immortalised Human Bronchial Epithelial Cells

In order to manipulate the WNT5A and TGF- β 1 signalling axis, multiple inhibitors needed to be tested for cellular toxicity on epithelial cells, so appropriate concentrations could be selected for crosstalk studies. To do this, an MTS assay was performed. Summary results for the MTS assay are shown in **Figure 4.1**. For Takinib, concentrations 10nM and above significantly increased cell viability, indicative of enhanced cellular proliferation. 7.5nM was therefore chosen as the concentration to use for the crosstalk studies to remain as physiologically relevant as possible. For BOX-5, none of the tested concentrations had a significant effect on cell viability, although, at 500 μ M the cell viability trended towards significance ($p=0.0713$). 250 μ M BOX-5 was therefore used in future experimentation to inhibit WNT5A as effectively as possible without reducing cell viability.

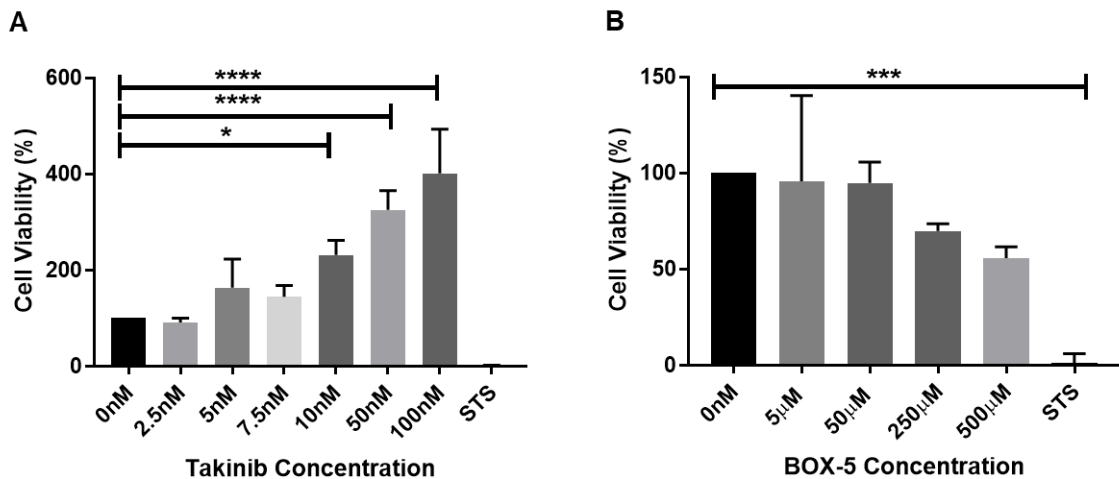


Figure 4.1 Effects of Takinib (A) and BOX-5 (B) Comparative to Basal Conditions on Metabolic Activity In Immortalised Human Bronchial Epithelial Cells. Stimulants were applied for 48 hours. Data is $n=3$ and presented as mean with standard deviation. $*p < 0.05$ by One-way ANOVA with Dunnett's post hoc test for intergroup comparisons. **** is p -value of <0.0001 .

4.3 Assessing ALI Culture Wound Healing With and Without TGF- β 1 Stimulation

The purpose of this experiment was to identify the optimal length of TGF- β 1 stimulation for EMT induction and investigate the effect of TGF- β 1 stimulation alone on wound healing. This was to recapitulate the impact of increased TGF- β 1 expression in the airway mucosa of asthmatic airways, which is reported to be upregulated in both animal and human studies (Bossé and Rola-Pleszczynski 2007).

Both inflammatory and structural cells produce TGF- β 1, with the major source of TGF- β in the airway mucosa being the eosinophils through their direct production of TGF- β 1, and indirect induction of ASM TGF- β 1 (Halwani *et al.* 2011) (Januskevicius *et al.* 2016). As the cultures required feeding every three days, a maximum stimulation of three days could be applied without having to re-dose the cells with recombinant protein. A 72-hour stimulation was performed once but it was determined that this stimulation time made wounding the cultures more difficult; the healthy cultures wounded with consistent widths without cell banking,

but the TGF- β 1 stimulated, although applying a similar pressure to wound, did not produce a consistent wound bed.

As 72-hour TGF- β 1 stimulation prevented uniform wounding, both 24 and 48-hour stimulations were assessed to identify maximum length of stimulation, and how length of pre-stimulation prior to wounding affects the wound healing response. The clinical characteristics detailed for the patients in **Figure 4.2 and 4.3** are shown in **Table 4.1**. The three healthy patient donors were the same for both the 24- and 48-hour stimulation, and epithelial cultures were derived from pooled epithelial cells retrieved from brushes obtained during bronchoscopy.

Table 4.1 Clinical Details of the Healthy Subjects Used in the TGF- β 1 Stimulation Experiments.

Date of Bronchoscopy	Age (y)	Sex (M/F)	FEV ₁ (L)	FEV ₁ (% predicted)	FEV ₁ /FVC Ratio (%)
03/12/2018	77	M	2.70	75	74
05/12/2018	57	M	3.73	79	77
09/01/2019	38	F	2.95	85	85

TEER was taken for each culture insert, before and after the TGF- β 1 pre-stimulation, to assess the effect of TGF- β 1 stimulation on epithelial layer integrity on unwounded cultures. The summary results of TGF- β 1 stimulation compared to basal are shown for both the 24- and 48-hour pre-stimulation in **Figure 4.2**. Non-stimulated cultures or cultures stimulated for only 24 hours with rhTGF- β 1 did not significantly change TEER over the 24-48 hours. Cultures which were stimulated for 48 hours with rhTGF- β 1, however, had significantly increased TEER ($p=0.0418$) compared to before stimulation.

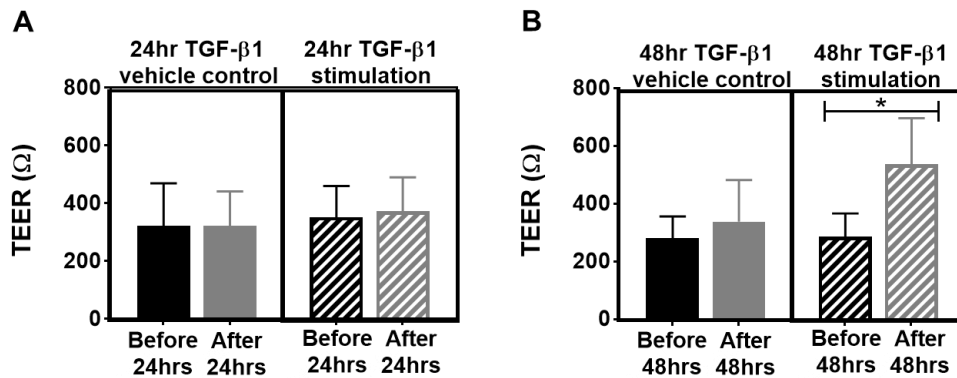


Figure 4.2 The Effect of TGF-β1 Pre-Stimulation on TEER Prior to Wounding. (A-B) Summary figure of the effect of a 24-hour (A) and 48-hour pre-stimulation (B) on TEER prior to wounding. Data is n of 3 and presented mean with standard deviation. * $p < 0.05$ by paired t-test.

Both the 24- and 48-hour stimulation had a non-significant effect on wound healing compared to non-stimulated controls. Representative images of the 48-hour pre-stimulation scratch wound assay are shown in **Figure 4.3A**, with summary figures of the 24- and 48-hour wounding healing assays shown in **Figure 4.3B-C** respectively. Out of the three healthy donors for each stimulation time, two donors had enhanced wound healing following TGF-β1 stimulation, whereas, the remaining one did not. The maximal time point of 48 hours was chosen for experiments, as this would initiate early stages of EMT in HBECs.

Both the 24- and 48-hour TGF-β1 stimulation displayed a numerical trend to increase TEER following wounding, but as TEER was only collected for two donors, statistical analysis was not performed (**Figure 4.3D-E**). TEER was originally collected for all three donors, but one donor was removed from the TEER analysis due to membrane damage induced by wounding. This did not appear to affect healing as the basal compartment volumes were not much higher than the transwell so leakage of media into the transwell was minimal. The membrane, however, could not sustain the volume apically for TEER analysis.

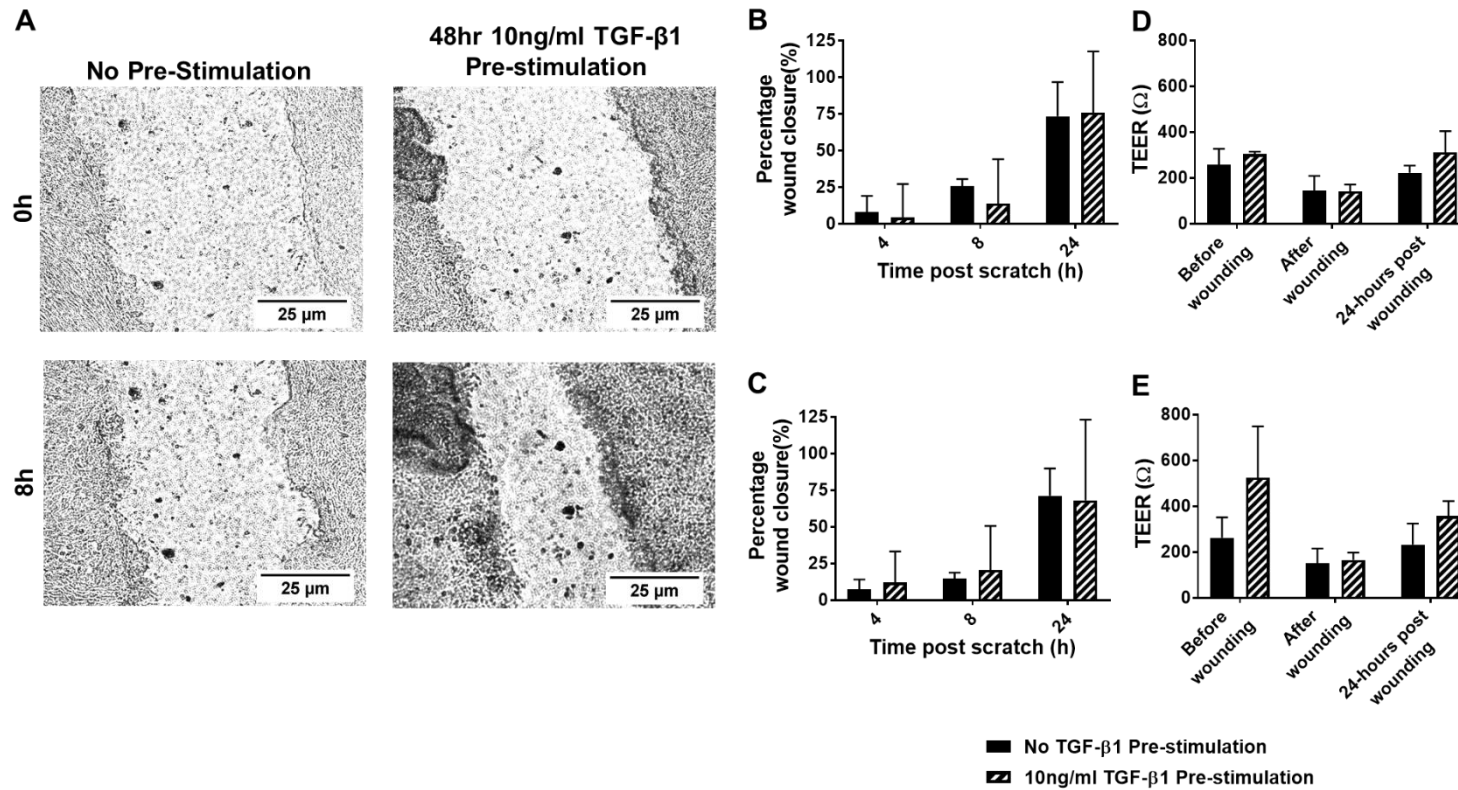


Figure 4.3 The Effect of TGF- β 1 Pre-Stimulation Duration on ALI Culture Wound Healing. (A) Representative images of the ALI culture scratch wound healing assay immediately after wound induction and after 8 hours of healing, with and without a 48-hour 10ng/ml rhTGF- β 1 stimulation. This donor had enhanced wound healing in response to TGF- β 1 stimulation. (B-C) Summary figure of the 24-hour (B) and 48-hour (C) 10ng/ml rhTGF- β 1 stimulation wound healing assay. Four time points were investigated – 0h, 4h, 8h and 24h. Data is n of 3, and presented mean with standard deviation. * $p < 0.05$ by two-way repeated measures (of both factors) ANOVA. (D-E) Summary figure of the 24-hour (D) and 48-hour (E) pre-stimulation. TEER results during the scratch wound healing assay. 3 time points were investigated – immediately before wounding, immediately after wounding and 24 hours post-wounding. Data is n of 2, and presented mean with standard deviation.

4.4 Assessing ALI Culture Wound Healing of TGF- β 1 Pre-Stimulated Cultures With and Without the Presence of Takinib

The rhTGF- β 1 concentration used in this scratch wound assay differs from the previous scratch wound experiments comparing the 24- and 48-hour stimulation to basal. A calculation error made during protocol design meant that double the concentration of rhTGF- β 1 (20ng/ml rather than 10ng/ml), and a slightly elevated concentration of Takinib was applied to the cultures (8.4nM rather than 7.5nM). The Takinib concentration was only slightly higher (rather than double the concentration) because the Takinib was added 30 minutes prior to TGF- β 1 stimulation and topped up when the TGF- β 1 was added. Both concentrations were doubled in that supplement containing the TGF- β 1. Following the 48-hour TGF- β 1 stimulation and wounding of the cultures, 500 μ M BOX-5 was added 30 minutes prior to rhWNT5A stimulation (at 1 μ g/ml). Referring to the MTS assay results in **Figure 4.1**, this would most likely subject the cells to a cell death fate.

The relationship between a 48-hour TGF- β 1 stimulation and TEER was assessed further in this experiment. The clinical characteristics detailed for the patients are shown in **Table 4.2**. All donors were asthmatic, of which six out of the nine were on GINA treatment step 4-5, unlike the earlier TGF- β 1 optimisation experiments where all three patients were healthy. A 48-hour 20ng/ml TGF- β 1 stimulation did not significantly increase TEER in the absence of Takinib ($p=0.1290$) (see **Figure 4.4A**). The 48-hour 20ng/ml TGF- β 1 stimulation and Takinib combined, however, significantly increased TEER ($p=0.0488$) compared to before their addition (**Figure 4.4B**).

Table 4.2 Clinical Details of the Asthmatic Subjects Used in the TGF- β 1 and WNT5A Wounding Experiments. Data not available is indicated as N/A.

Date of Bronchoscopy	Age (y)	Sex (M/F)	Serum IgE (kU/L)	FEV₁ (L)	FEV₁ (% predicted)	FEV₁/FVC Ratio (%)	GINA Treatment Intensity
08/05/2019	61	F	338	2.06	100	81.3	4
09/05/2019	52	M	103	3.62	95	95.4	2
14/05/2019	55	M	N/A	2.99	72	84	3
26/06/2019	68	M	497	3.68	117	116	5
10/07/2019	62	M	450	2.5	78	75	4
13/08/2019	56	F	N/A	N/A	N/A	N/A	3
23/10/2019	51	M	23.5	1.93	57	59	5
04/11/2019	46	M	125	3.17	79	88	5
11/11/2019	60	M	1340	3.15	93	90	5

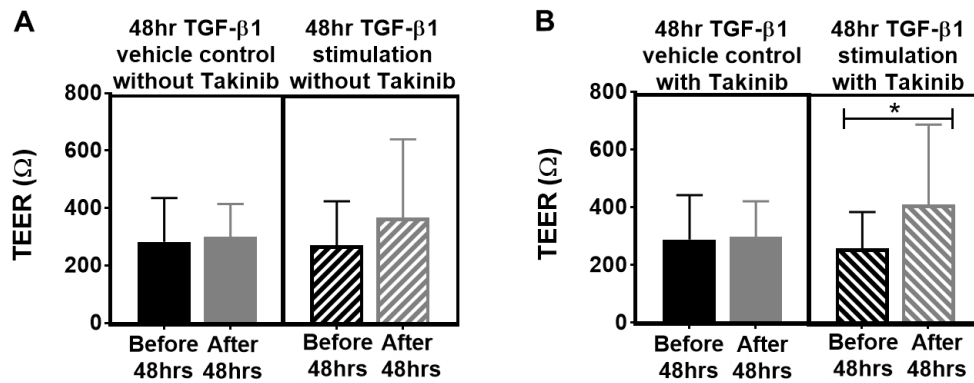


Figure 4.4 The Effect of TGF-β1 Pre-Stimulation With and Without TAK1 Inhibition on TEER Prior to Wounding. (A-B) Summary figures of the effect of 48-hour 20ng/ml TGF-β1 pre-stimulation without TAK1 inhibition (A), and with TAK1 inhibition (B) using Takinib on TEER prior to wounding. Data is n of 9 and presented mean with standard deviation. * $p < 0.05$ by paired t-test.

Moving onto the scratch wound analysis, TGF-β1 stimulation did not significantly enhance wound healing or TEER (**Figure 4.5A-B**) compared to basal in the absence of Takinib, WNT5A stimulation or WNT5A inhibitor BOX-5 ($p=0.4375$ and $p=0.1486$ respectively). To assess the impact of TAK1 inhibition on TGF-β1 stimulation, TGF-β1 stimulation with and without Takinib (or rhWNT5A or BOX-5) were compared 24 hours post-wounding (**Figure 4.5C-D**). Takinib did not significantly alter the wound healing response ($p=0.6250$), or TEER ($p=0.3342$) at 24 hours post-wounding.

To assess whether oral corticosteroids can modify the TGF-β1-mediated wound healing response (which could contribute to asthmatic airway remodelling), GINA2-4 and GINA5 patients were analysed separately. TGF-β1 stimulation did not significantly enhance wound healing or TEER compared to basal in the absence of Takinib, WNT5A stimulation or WNT5A inhibitor BOX-5 for GINA2-4 (**Appendix 8: A-B**, $p=0.2500$ and $p=0.5315$ respectively) or GINA5 (**Appendix 9: A-B**, $p=0.5000$ and $p=0.1075$ respectively) patient cultures. To assess the impact of TAK1 inhibition on TGF-β1 stimulation, TGF-β1 stimulation with and without Takinib (or WNT5A or inhibitor BOX-5) was compared 24 hours post-wounding in both GINA2-4 (**Appendix 8: C-D**) and GINA5 patient cultures (**Appendix 9: C-D**). Takinib did not significantly alter the wound healing response

or TEER at 24 hours post-wounding for GINA2-4 ($p > 0.9999$ and $p = 0.6725$), or GINA 5 patients ($p = 0.5000$ and $p = 0.0653$) respectively.

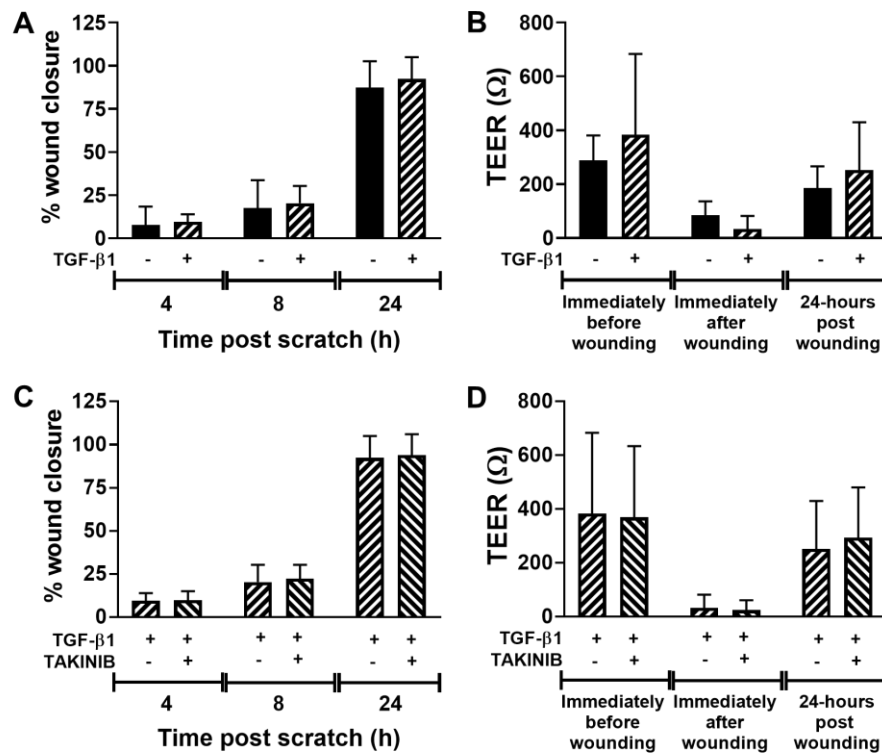


Figure 4.5 The Effect of TGF-β1 Pre-Stimulation With and Without Inhibition With Takinib on Wound Healing and TEER. (A-B) Summary figure of the effect of a 48-hour 20ng/ml TGF-β1 pre-stimulation on wound healing (A) and TEER (B). Data is n of 8 (as unpaired data excluded) and presented mean with standard deviation. * $p < 0.05$ by Wilcoxon matched-pairs signed rank test for wound healing and a paired t-test for TEER at 24 hours. (C-D) Summary figure of Takinib inhibition of TGF-β1 on wound healing (C) and TEER (D). Takinib (8.4nM) was added 30 minutes prior to TGF-β1 stimulation. Data is n of 9 and presented mean with standard deviation. * $p < 0.05$ by Wilcoxon matched-pairs signed rank test for wound healing and a paired t-test for TEER at 24 hours

4.5 Assessing the Effect of WNT5A on ALI Culture Wound Healing With and Without TGF- β 1 Pre-Stimulation

Before assessing the effect of WNT5A crosstalk, the impact of WNT5A stimulation on wound healing alone was assessed compared to basal (**Figure 4.6A**). A paired t-test (for TEER) and Wilcoxon matched-pairs signed rank test (for assessing healing) on cultures without TGF- β 1 stimulation or Takinib were used for analysis. The analysis indicated WNT5A induced a non-significant increase in wound healing compared to basal ($p=0.1250$) at 24 hours post-wounding. WNT5A did not have a significant effect on TEER at 24 hours post-wounding ($p=0.6109$) (**Figure 4.6B**). To assess whether WNT5A inhibitor BOX-5 could reverse this non-significant effect, WNT5A in the presence of BOX-5 was compared against WNT5A alone irrespective of TGF- β 1 stimulation or Takinib at 24 hours post-wounding. As WNT5A did not induce a significant effect on wound healing, the effect of BOX-5 was expected to be negligible. A Wilcoxon matched-pairs signed rank test or a multiple t-test indicated that BOX-5 inhibition of WNT5A did not significantly alter wound healing (**Figure 4.6C**) or TEER (**Figure 4.6D**). All adjusted p values were >0.93 for the 4 groupings (no stimulation with Takinib, no stimulation without Takinib, TGF- β 1 pre-stimulation with Takinib or TGF- β 1 pre-stimulation without Takinib).

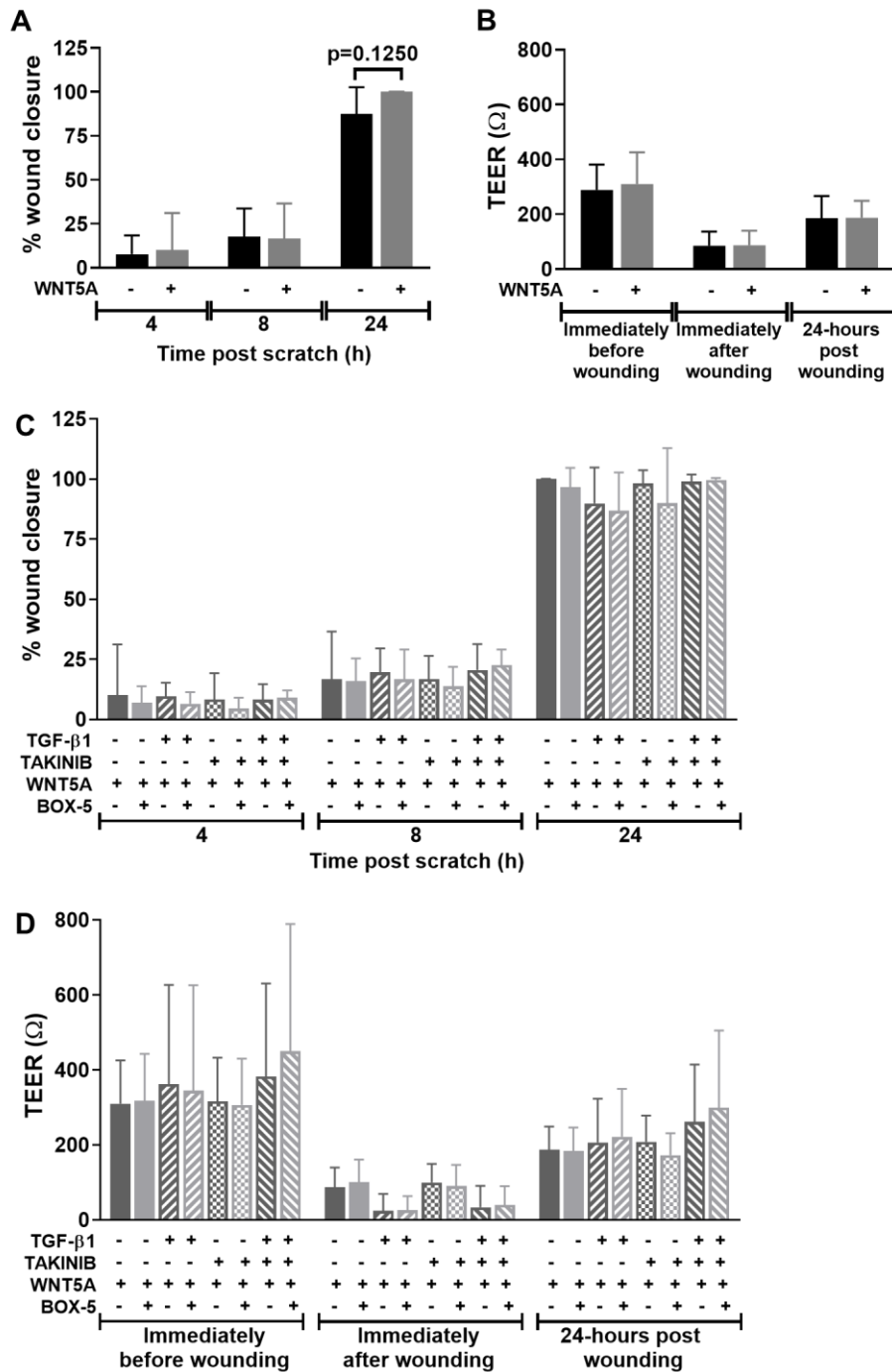


Figure 4.6 The Effect of WNT5A Stimulation With and Without Signalling Inhibitor BOX-5 on Wound Healing and TEER. (A-B) Summary figures comparing the impact of WNT5A stimulation (1 μ g/ml) against basal on wound healing (A) and TEER (B). WNT5A was added after wounding following a 30-minute incubation with BOX-5 or vehicle control, and the effect on wound healing observed at 4-, 8- and 24-hours post-wounding. Data is n of 8 (as unpaired data was excluded). (C-D) Summary figures comparing BOX-5 inhibition of WNT5A on wound healing. BOX-5 (500 μ M) was added 30 minutes prior to WNT5A stimulation. Data is n of 9. All data is presented mean with standard deviation. 24-hour time points were used for statistical analysis. * $p < 0.05$ by Wilcoxon matched-pairs signed rank test for wound healing and a paired t-test for TEER. All p-values were adjusted to account for multiple comparisons.

To assess crosstalk between WNT5A and TGF- β 1, the effect of dual stimulation was assessed (**Figure 4.7A-B**). WNT5A does not significantly increase wound healing ($p=0.5625$), or TEER ($p=0.3534$) at 24 hours post-wounding in the presence of TGF- β 1 stimulation. To see if Takinib reversed the negative impact of TGF- β 1 pre-stimulation on WNT5A wound healing, cultures dual stimulated with TGF- β 1 and WNT5A with and without TAK1 inhibition was assessed. Takinib was able to non-significantly reverse the effect ($p=0.0625$) on wound healing (**Figure 4.7C**), but TEER did not significantly differ ($p=0.1784$) (**Figure 4.7D**).

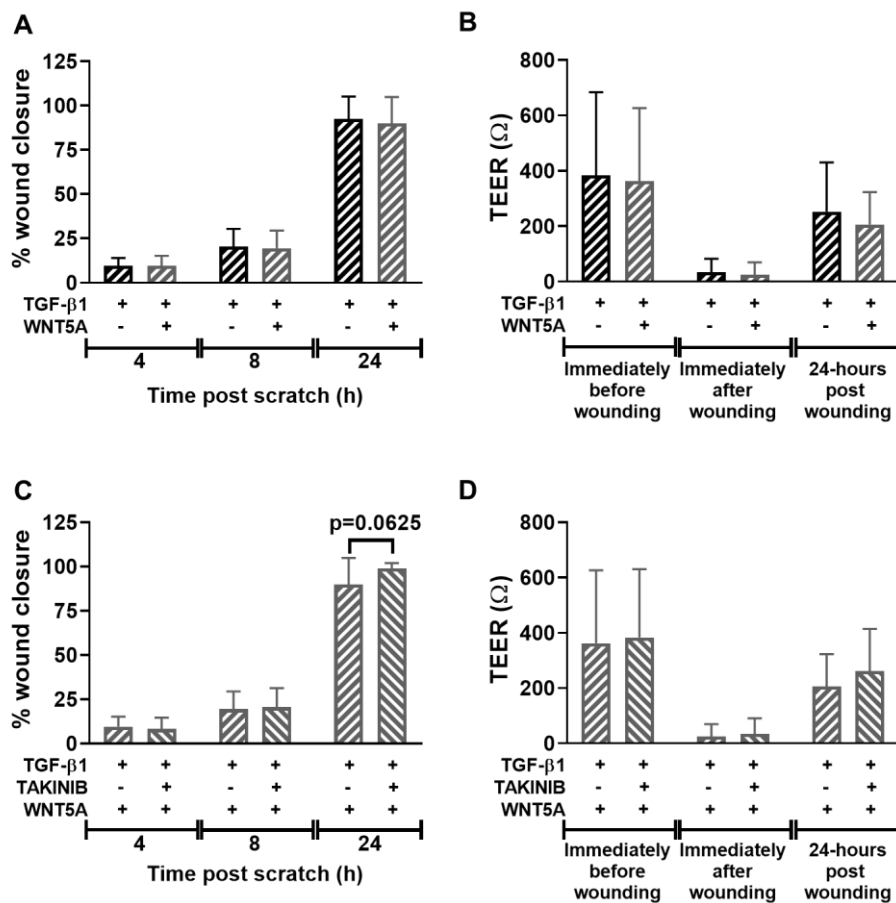


Figure 4.7 The Effect of a 48-Hour TGF- β 1 Pre-Stimulation on WNT5A-Mediated Wound Healing and TEER. (A-B) Summary figures comparing the impact of WNT5A stimulation ($1\mu\text{g/ml}$) against basal conditions on wound healing (A) and TEER (B) following a 20ng/ml 48-hour TGF- β 1 pre-stimulation. (C-D) Summary figures assessing the impact of TAK1 inhibition (8.4nM Takinib) on 48-hour TGF- β 1 pre-stimulation on wound healing (C) and TEER (D) of WNT5A stimulated cultures. Data is n of 9 and presented mean with standard deviation. * $p < 0.05$ by Wilcoxon matched-pairs signed rank test for wound healing and paired t -test for TEER.

4.6 Overall Effect of Takinib and TGF- β 1 on WNT5A-Mediated Wound Healing at 24 Hours

A two-way repeated measures Aligned ranks transformation ANOVA indicated a significant effect of both Takinib ($p=0.0055$) and 48-hour TGF- β 1 pre-stimulation ($p=0.0174$) on percentage wound closure of WNT5A stimulated cultures. A significant interaction between both Takinib and TGF- β 1 stimulation was also found, $p=0.0027$ (**Figure 4.8A**).

The relationships observed during wound healing was not recapitulated in TEER analysis, with fixed effect analysis of Takinib, 48-hour TGF- β 1 pre-stimulation and the interaction between the two yielding the following results: ($F(1,8)=2.903$, $p=0.1268$) ($F(1,8)=1.429$, $p=0.2662$) and ($F(1,8)=0.8549$, $p=0.3822$) respectively (**Figure 4.8B**).

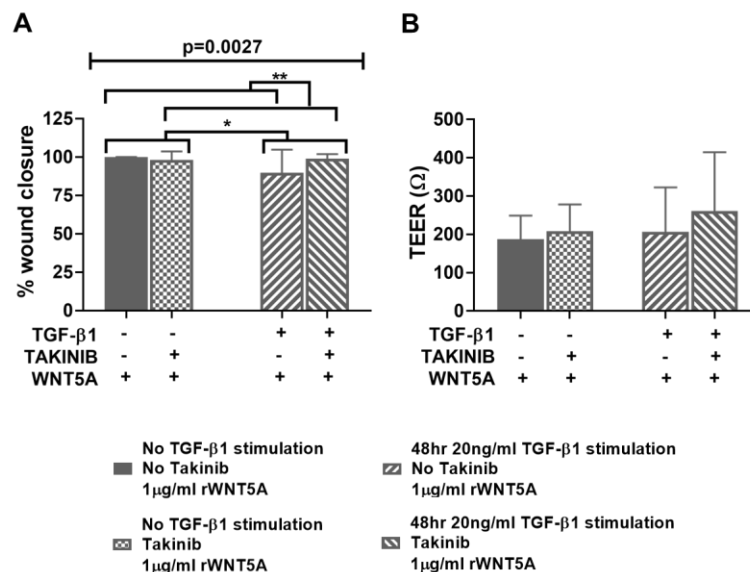


Figure 4.8 The Effect of Takinib and TGF- β 1 Pre-Stimulation on WNT5A-Mediated Wound Healing and TEER. Summary figure comparing the impact of Takinib and TGF- β 1 stimulation on WNT5A stimulated cultures 24 hours post-wounding on wound closure (A) and TEER (B). Data is n of 9 and presented mean with standard deviation for B and C. $*p < 0.05$ by two-way repeated measures (by both factors) Aligned ranks transformation ANOVA for wound healing and two-way repeated measures (by both factors) ANOVA for TEER.

4.7 Overall Effect of All Stimulation Conditions on Wound Healing at 24 Hours

To assess the 3-way relationship between WNT5A, TGF- β 1 and Takinib, a three-way repeated measures (by all three factors) Aligned Ranks ANOVA for wound healing and a three-way repeated measures (by all three factors) mixed-effect model for TEER was applied to the 24-hour data as shown in **Figure 4.9**. The 3-way interaction demonstrated no effect on wound healing ($p=0.2584$), or TEER ($p=0.4524$). WNT5A and Takinib did not have a significant effect on wound healing ($p=0.7090$ and $p=0.2409$ respectively). TGF- β 1 stimulation alone, however, had a significant effect on the wound healing response ($p=0.0336$). Neither WNT5A, TGF- β 1 or Takinib alone had a significant effect on TEER ($p=0.4680$, $p=0.1108$ and $p=0.1058$ respectively).

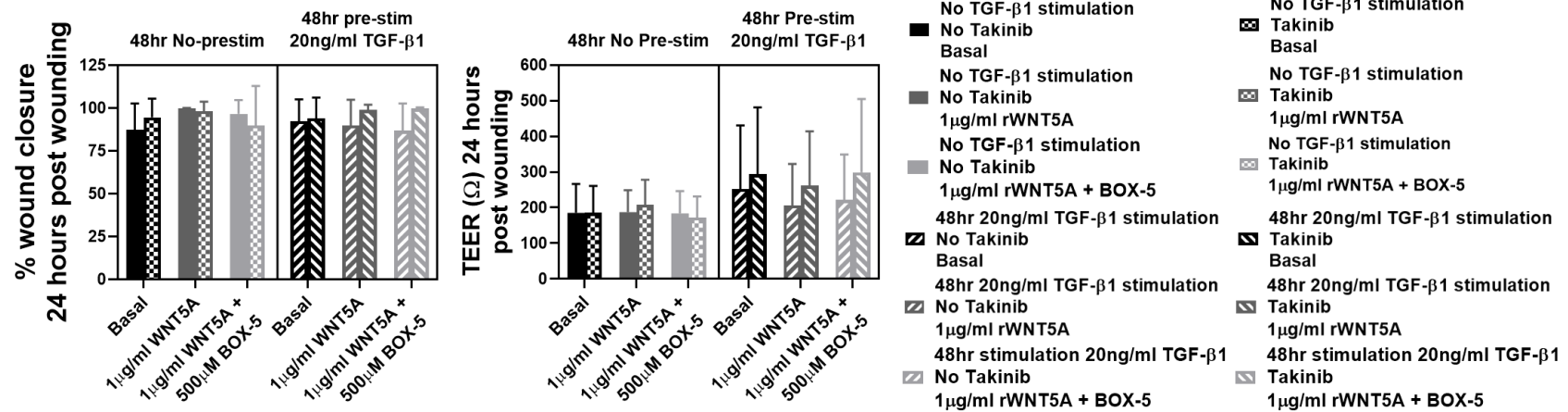


Figure 4.9 The Effect of Takinib, TGF-β1 and WNT5A Stimulation on Wound Healing and TEER. Summary figure comparing the impact of Takinib and rhTGF-β1 and rhWNT5A stimulation on all conditions 24 hours post-wounding on percentage culture wound closure and TEER. Data is n of 9 and presented mean with standard deviation. *p < 0.05 by three-way repeated measures (by all three factors) Aligned Ranks ANOVA for wound healing and a three-way repeated measures (by all three factors) mixed-effect model for TEER.

4.8 Exploring Transfection Efficiency of ALI Cultures

To identify whether crosstalk intermediaries could be silenced with siRNA prior to scratch wounding, ALI cultures were transfected with fluorescently labelled non-targeting siRNA to compare transfection efficiency of numerous transfection reagents: Lipofectamine 2000, Viromer Blue, Viromer Green and Interferin. ALI cultures proved difficult to transfect with less than 1% of cells expressing FAM labelling (**Figure 4.10: top panel**). To ensure the reagents were working, HEK293T cells, which are prototypically used for transfection studies, were also transfected (**Figure 4.10: bottom panel**). Again, lower than expected transfection efficiency was achieved in HEK293T cells, but Lipofectamine 2000 and Interferin did show obvious transfection – 25.4% and 62.7% respectively, suggesting the ALI cultures would not be easy to transfect. With little time left of active research to optimise these experiments, the experiments were abandoned.

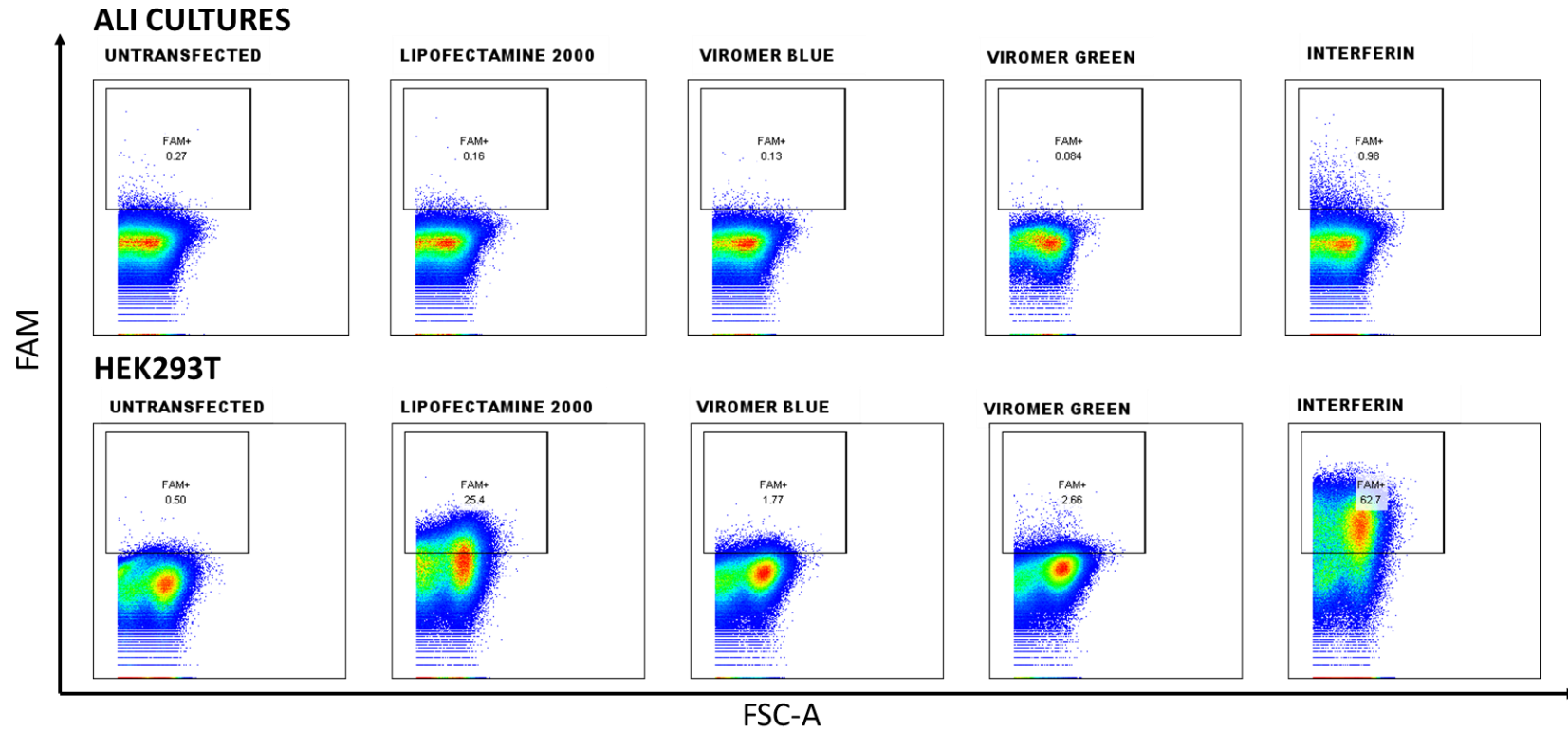


Figure 4.10 Exploring Transfection Efficiency of ALI Cultures in Comparison to HEK293T Cells Using Numerous Transfection Reagents. The efficiency of Lipofectamine 2000, Viromer Blue, Viromer Green and Interferin was tested on ALI cultures (top row) and HEK293T cells (bottom row). Experiment is n=1.

4.9 Summary

- A 48-hour 10ng/ml rhTGF- β 1 stimulation significantly increased TEER of healthy cultures compared to vehicle control. This was not observed in the asthmatic cultures stimulated with 20ng/ml rhTGF- β 1.
- WNT5A stimulation alone did not have a significant effect on wound healing or TEER 24 hours post-wounding.
- TGF- β 1 pre-stimulation alone did not have a significant effect on wound healing or TEER 24 hours post-wounding compared to basal conditions. Across all 12 conditions, however, TGF- β 1 did have a significant effect on wound healing.
- The two-way analysis comparing the effect of rhTGF- β 1 pre-stimulation and Takinib on rhWNT5A-mediated culture wound healing indicated that crosstalk between WNT5A and TGF- β 1 signalling exists in wound repair, although neither significantly enhanced the wound healing response independently. This crosstalk relationship was not observed on TEER 24 hours post-wounding.
- ALI cultures are difficult to transfect with less than 1% efficiency achieved using numerous transfection reagents (including Lipofectamine 2000 and Interferin). HEK293T cells tested alongside as a positive control, however, showed positive transfection.

4.10 Discussion

4.10.1 The Wound Healing Response to WNT5A and TGF- β 1

The lung epithelium is not constantly renewed as seen with other epithelial tissues (the gut, skin etc), but it rapidly proliferates following damage. Approximately 1% of epithelial cells enter S-phase during a 24-hour period. This proliferation rate can increase 10-fold after injury by naphthalene exposure, as demonstrated by *in vivo* 3H-thymidine mouse studies (Reynolds *et al.* 2000). Primarily wound closure up to 24 hours post-injury consists of cell spreading and migration to cover the wound bed. This is followed by proliferation (15-24 hours post-wounding) and differentiation to fully restore epithelium functionality in animal trachea wound repair studies (Crosby and Waters 2010). The cell migration and spreading of the differentiated HBEC cultures following mechanical scratch wounding in this study was rapid, with most ALI cultures healing within 24 hours. As wound healing was assessed over 24 hours only, the effect of proliferation would be minimal, which is what was reported by Neurohr, Nishimura and Sheppard (2006) in monolayers of normal HBECs.

The length of reepithelialisation in these ALI culture scratch wound assays is similar to what is reported by Stewart *et al.* (2012: A) following wounding of ALI cultures with a P200 pipette tip. There are only two other ALI scratch wound assay studies to my knowledge, both of which report a longer healing process, with approximately 50-80% wound closure at 24 hours post-wounding for differentiated primary HBEC cultures, of which time taken differed considerably between donors (Milara *et al.* 2010) (Carlsson 2013). The difference in migration speed may be partially due to the use of different apparatus to wound (therefore inflicting different wound widths), the passage number of the cells, the growth factors supplemented into the cell media (such as hepatocyte growth factor) and the use of different matrices for seeding the cells onto (Mereness *et al.* 2018) (Huguet *et al.* 1995).

Primary human nasal epithelial cells cultured to ALI also take longer to heal, with cultures displaying 45-80% wound closure 24 hours post-wounding, with full re-

epithelisation taking 68 hours (Ramezanzpour *et al.* 2019). Undifferentiated primary HBEC cultures also typically show slower healing, with cultures taking longer than 2 days to only partially cover the wound bed with varying apparatus choice (approximately 25% wound closure at 48-hours with a P200 tip and 45% at 72 hours post-wounding with a P1000 tip) (Nguyen *et al.* 2020) (Kaur *et al.* 2020). Due to limited access to primary bronchial biopsies, most HBEC wounding assays in the literature are conducted in immortalised bronchial epithelial cell lines such as BEAS-2B and 16HBE. 16HBE have a similar healing rate as normal HBECs cultured to ALI, taking approximately 24 hours for full closure (Desai *et al.* 2004) (Zhu *et al.* 2007) (Ren and MacKichan 2014). BEAS-2Bs, however, take considerably longer to heal from personal experience, which is also supported by the literature (Daud 2017) (Passantino, Muñoz, and Costa 2013).

WNT5A expression is upregulated in response to pulmonary damage. Mechanical ventilation-induced and sepsis-induced acute lung injury upregulates WNT5A protein expression *in vivo* (Villar *et al.* 2011: B) (Villar *et al.* 2014). When mimicking sepsis *in vitro* with LPS, WNT5A expression is also increased in BEAS-2Bs and MRC-5 cells (Villar *et al.* 2014). There is a considerable amount of evidence in the literature for a role of WNT5A in the context of repair, however we still have little understanding of whether WNT5A enhances or diminishes healing, and whether this is cell context dependent. The wound assays conducted in this thesis indicate WNT5A did not have a significant impact on HBEC wound healing although a non-significant increase was observed. Potentially, this may be because of a plateau effect at 24 hours post-wounding, which would diminish the observed effect of the stimulation on the wound healing response. The true wound healing kinetics would therefore be reduced as full wound closure was achieved. Due to the length of the stimulation and wounding aspect of the assay, only a 24-hour post-wounding time point was feasible. This appeared suitable on the initial healthy donor setup of the assay without full wound closure being reached. As healthy undifferentiated and differentiated human airway epithelial cells (HAECs) are reported to heal faster than asthmatic HAEC cultures (Inoue *et al.* 2019) (Stevens *et al.* 2008), theoretically this time point should have been suitable. In hindsight, however, a 0, 4, 8 and 20-hour time

point may have been more suitable. The healthy donors used for assay setup also had a lower lung function than that of the asthmatic donors, which may also explain the difference in healing kinetics.

Similar to the observed WNT5A finding in these scratch wound assays, Baarsma *et al.* (2017) showed that WNT5A stimulation alone non-significantly increased wound healing in murine lung epithelial cells (MLE12 cells). Investigating the role of WNT5A in repair for other cell types, NIH3T3 (a mouse embryonic fibroblast cell line) stimulated with purified WNT5A significantly promoted wound closure by inducing cell polarisation and migration. Proliferation, assessed by brdU, however did not differ (Nomachi *et al.* 2008). Mouse mesenchymal stem cells (mMSCs) also have enhanced wound healing at 12 hours post-wounding following WNT5A stimulation, with WNT5A inhibition via PKC inhibitor GF109203X or JNK blocker SP600125 partially or fully blocking the reparative effects. The healing response seen may have been due to enhanced migration of the mMSCs, as WNT5A signalling through PKC and JNK increased mMSC migration towards conditioned media from healthy and ARDS mice-derived lung tissue (Liu *et al.* 2014). Other WNT5A signalling components, RhoA, Rac1 and PKA, are also reported to contribute to bronchial epithelial wound repair (Desai *et al.* 2004) (Spurzem *et al.* 2002). The literature appears to support a significant role for WNT5A in enhancing wound healing in mesenchymal cells, however this is not reported for airway epithelial cells, thereby raising the question whether WNT5A does play an important role in airway epithelial repair, or whether it is just a marker of damage.

Active TGF- β 1 levels are also increased by epithelial wounding, to exert a variety of biological functions contributing to epithelial wound repair. HBEC culture wounding activates latent TGF- β 1 via integrins α β 6 and α β 8. Neurohr, Nishimura and Sheppard (2006) demonstrated that the integrin α β 8 significantly enhanced wound healing of HBECs, whereas, α β 6 did not have a significant effect. This was because α β 6 exerts competing effects on wound healing, one dependent on TGF- β activation and the other independent (Neurohr, Nishimura

and Sheppard 2006). Expression of these two integrins at an individual donor level may therefore govern the TGF- β effect on wound healing, potentially explaining the heterogeneity observed between donors. During epithelial reparation, TGF- β 1 can induce ECM synthesis (providing the cells with a substrate to migrate over), MMP synthesis (to degrade ECM components to permit cellular migration), and EMT (transitioning cells from an epithelial to a migratory, mesenchymal phenotype) (Lechapt-Zalcman *et al.* 2006).

The overall effect of TGF- β on wound closure however is controversial, with enhanced and diminished wound healing being reported in similar cellular contexts. A dose dependent increase in wound healing was seen in hyperoxic rat alveolar type 2 monolayer cell cultures (50pg/ml and 5ng/ml) (Buckley *et al.* 2008) and monolayer normal human bronchial epithelial (NHBE) and 1HAEo⁻ cells (0.1-100ng/ml) (Ito *et al.* 2011). A 10ng/ml TGF- β stimulation significantly enhanced wound healing of scratch wounded undifferentiated, primary HBEC cultures (Kaur *et al.* 2020). Moreover, TGF- β 1 silencing resulted in reduced healing of primary monolayer AEC cultures of children with asthma (Ling *et al.* 2016). Lechapt-Zalcman *et al.* (2006) also report that TGF- β 1 stimulation promotes healing of differentiated HNEC cultures via MMP-2 upregulation.

On the other hand, Neurohr, Nishimura and Sheppard (2006) report that TGF- β stimulation inhibits wound closure of HBECs, and that blocking TGF- β enhances wound healing. Bovine bronchial epithelial cells also show diminished repair following TGF- β treatment due to enhanced cellular adhesion via the integrins (Spurzem *et al.* 1993). Pirfenidone, an idiopathic pulmonary fibrosis (IPF) medication thought to target TGF- β signalling, however, does not impair wound healing post lung transplantation (if administered without a washout period prior to surgery), suggesting minimal impact of TGF- β on wound healing (Mortensen, Cherrier and Walia 2018). In the wound repair studies conducted, TGF- β 1 stimulation did not have a significant effect on wound healing compared to basal (in the absence of WNT5A, Takinib or BOX-5). However, TGF- β 1 had a

significant effect on WNT5A-mediated wound healing in the 2-way analysis, and on repair overall in the 3-way analysis conducted.

Having considered the individual effects of WNT5A and TGF- β 1 on wound healing, the effect of all three independent variables (WNT5A, TGF- β 1 and Takinib) were assessed on wound healing in **Figure 4.9**. The three-way analysis did not show a significant interaction of all three individual conditions with wound healing, but the effect of TGF- β 1 alone did. However, as the three-way repeated measures Aligned ranks transformation ANOVA contained all 12 conditions, the interaction effects were likely to be diminished as groupings include control and TGF- β or WNT pathway inhibitor conditions, which are not expected to have an interactive effect. For example, as a TGF- β 1 noncanonical pathway inhibitor of TAK1, Takinib would influence wound healing of TGF- β 1 stimulated conditions but not necessarily TGF- β 1 unstimulated vehicle controls unless there is active TGF- β present at basal. BOX-5, a WNT5A inhibitor, again should only inhibit the WNT5A-mediated response, so theoretically the two-way analysis investigating the effect of TGF- β 1 and Takinib purely on the WNT5A-mediated wound healing response should therefore be more useful for assessing TGF- β 1 crosstalk with WNT5A during wound healing. The two-way analysis (**Figure 4.8**) did in fact indicate that both TGF- β 1 and Takinib had a significant interaction with WNT5A during wound healing in the two-way analysis, suggesting that TGF- β signalling does influence the effects of WNT5A during repair. TAK1 inhibition reversed the TGF- β 1 mediated effects suggesting crosstalk exists between the noncanonical WNT and TGF- β pathways. This crosstalk is supported in the literature throughout development and repair. However, as WNT5A and TGF- β 1 do not significantly impact the wound healing response independently, the significance of this finding is limited in terms of epithelial repair.

WNT5A and TGF- β 1 crosstalk is evident throughout organogenesis and has been reported in multiple cell types. In mammary gland development, TGF inhibits mammary branching in the presence of WNT5A signalling; this branching

inhibitory effect was reliant on WNT5A, as WNT5A knockout disables the TGF suppression of mammary branching (Roarty and Serra 2007). Also, when WNT5A and TGF- β were suppressed, the activity of the β -catenin dependent pathway increased, suggesting a dual role of WNT5A and TGF- β in inhibiting the β -catenin canonical WNT pathway (Roarty and Serra 2007). Kumawat *et al.* (2014) report that TGF- β 1 signalling induces WNT5A transcription via the non-canonical TGF- β -TAK1 pathway in an immortalised ASM cell line; by which TAK1 regulated β -catenin levels, which bound to the WNT5A transcription factor sp1 to promote TGF- β induced WNT5A transcription. In ASM, SMAD3 inhibition significantly increased WNT5A mRNA 2-fold, suggesting that the canonical TGF- β pathway may negatively regulate WNT5A transcription in this cell type (Kumawat *et al.* 2014). TGF- β stimulation is also reported to induce WNT5A expression in a dose dependent manner in LX-2 cells; TAK1 inhibition (using LL-Z1640-2), however, did not reduce WNT5A induction, suggesting another mechanism may exist by which TGF- β can regulate WNT5A expression (Beljaars *et al.* 2017).

On the contrary to TGF- β 1-induced WNT5A expression, WNT5A can also potentiate TGF- β signalling. WNT5A is reported to promote TGF- β 1 signalling via ROR2 SMAD transactivation in colonic crypt repair, to locally inhibit canonical WNT driven proliferation of stem cells within the wound channel, thereby ensuring crypt regeneration in the wound bed (Miyoshi *et al.* 2012). TGF- β receptor signalling was required for these WNT5A effects, as a TGF- β 1 receptor inhibitor (SB431542) suppressed all WNT5A effects on proliferation (Miyoshi *et al.* 2012). Perhaps TGF- β R1 complexes with ROR2 to induce SMAD signalling in colonic repair, as RYK is reported to form a complex with TGF- β R1 to induce SMAD2 phosphorylation upon WNT5A ligand binding in basal tumour-initiating cells (Borcherding *et al.* 2015). WNT5A can also promote TGF- β signalling through induction of TGF- β RNA and protein expression in intestinal intraepithelial lymphocytes to (Zhao *et al.* 2015).

TGF- β is not always reported to induce WNT5A expression, and instead can suppress it, although there are more reports of TGF- β 1-WNT5A induction in the literature. Mesenchymal suppression of TGF- β signalling with inhibitor SB431542 and by deletion of TGF- β R2 has been shown to significantly elevate WNT5A expression, indicating TGF- β downregulates WNT5A (Yang *et al.* 2014). High glucose levels, which are reported to induce TGF- β 1, decrease WNT5A expression in rat mesangial cells, highlighting that TGF- β 1 may negatively or positively regulate WNT5A expression in a cell dependent fashion (Ho *et al.* 2016). In diabetic mesangial cells, on exposure to nitric oxide, TGF- β 1 is downregulated, whereas, WNT5A expression is increased, again reinforcing the potential of a reciprocal relationship in mesangial cells (Hsu *et al.* 2015). The results of the scratch wound assay indicate that both WNT5A and TGF- β 1 independently cannot significantly enhance HBEC repair. However, TGF- β 1 and Takinib have a significant effect on WNT5A-mediated repair, suggesting crosstalk exists between these signalling pathways in HBECs.

4.10.2 The TEER Response to WNT5A and TGF- β 1

ALI cultures are reported to have a TEER ranging from 500-1000 Ω cm², which is affected by passage number before differentiation at ALI (Rayner *et al.* 2019). The average TEER of the nine donors used in the scratch wound assay was lower than this TEER range at approximately 300-400 Ω cm², but all cultures were used after approximately three weeks of culturing at ALI, and maximum TEER is reported to be established at approximately five weeks post culturing at ALI (Schagen, Sly and Fantino 2018). Cilia was however present on all cultures prior to their use. TEER dropped substantially following wounding but did not drop to zero. TEER recorded pre- and post-wounding of epidermal models suggest TEER does not drop to zero (Kiesewetter *et al.* 2019), and that the remaining attached cells still provide some resistance.

WNT5A did not have a significant effect on epithelial integrity following wounding. Prior to wounding, however, a 48-hour 10ng/ml rhTGF- β 1 pre-stimulation on healthy cultures significantly increased TEER. This effect, although, was not seen

following a 24-hour 10ng/ml or 48-hour 20ng/ml rhTGF- β 1 stimulation. This is contrary to what Haghi *et al.* (2015) report in that they found a 24-hour 10ng/ml TGF- β 1 stimulation significantly increased TEER in HBEC ALI cultures. TGF- β 1 stimulation has also been reported to prevent cigarette smoke-mediated TEER decrease and tight junction protein (zonular occludin 1/2) downregulation in 16HBE cells. However, TGF- β 1 stimulation alone did not induce a change in TEER (Schamberger *et al.* 2014). On the contrary to the previous studies suggesting a beneficial effect, TGF- β 1 has also been reported to decrease barrier integrity in small airway and alveolar cultures. Pittet *et al.* (2001) report that rhTGF- β 1 significantly decreased TEER in a dose- and time-dependent manner in primary cultures of rat alveolar type 2 cell monolayers via intracellular glutathione depletion. This is supported by Bluhmki *et al.* (2020) who also report TGF- β 1 induced a concentration dependent breakdown in TEER in primary human small airway epithelial cells. TGF- β 1 stimulation may therefore have differing effects across numerous cellular systems.

Stimulating differentiated HBECs with rhTGF- β 1 made wounding the cultures more difficult, with a uniform wound bed harder to achieve. The significant increase in TEER following 48-hours TGF- β 1 stimulation may be the result of excessive mucus production, as ALI cultures had noticeably higher secretions. Although two warm washes were performed prior to recording TEER, it may not have sufficiently removed particularly abundant or viscous mucus. Kim *et al.* (2019) reported that 10ng/ml TGF- β 1 stimulation increased mucus hypersecretion, and decreased CBF and ASL volume of fully differentiated cystic fibrosis ALI cultures homozygous for F508del. Chu *et al.* (2004), however, report that TGF- β 1 cannot induce mucin expression of HBECs whereas TGF- β 2 on the other hand can, as it significantly correlates with mucin expression in bronchial tissue. TGF- β 2 stimulation could also significantly induce MUC5AC mRNA and protein expression in both healthy and asthmatic cultured epithelial cells and was reported as differentially expressed between asthma and health, whereas TGF- β 1 expression remained unchanged (Chu *et al.* 2004). This specific TGF- β isoform activity on mucus production is supported further by Harrop *et al.* (2013). Neurohr, Nishimura and Sheppard (2006) also report TGF- β 2 expression is 20-

fold higher in HBECs, but that only TGF- β 1 not TGF- β 2 is activated on wound healing. There is conflicting evidence in the literature on the impact of TGF- β 1 on TEER of which none propose a mechanism in which TGF- β 1 mediates its effects.

4.10.3 Limitations

The scratch wound assay does not mimic all types of damage present in the asthmatic airways. Airway epithelial damage results from infection, inflammation or exposure to inhaled chemicals (such as cigarette smoke), and mechanical forces such as cough and compressive stress that occur during bronchoconstriction, which results in buckling of the airway (Crosby and Waters 2010) (Veerati *et al.* 2020). Generally, only mechanical forces are utilised by the scratch wound assay, however, it also simplistically incorporates epithelial-derived growth factor release following damage, and to some extent mimics cell migration *in vivo*. The epithelial repair process, however, is likely to be governed by other surrounding cells not contained within the ALI model such as ASM, fibroblasts and tissue-residing inflammatory cells. This is supported by Swartz *et al.* (2001) who report mechanical stress is communicated between epithelial and lung fibroblasts to elicit ECM remodelling.

The scratch wound assay also only considers a 2D wound healing process, whereas, *in vivo* airway wound healing would be 3D. Ng-Blichfeldt *et al.* (2019) demonstrated that a 48-hour TGF- β 1 pre-stimulation induces myofibroblast differentiation in MRC-5 and primary human lung fibroblasts, which impairs epithelial lung organoid synthesis and alters organoid diameter size. Additionally, a 24-hour TGF- β 1 stimulation significantly induced WNT5A expression but downregulated TCF/LEF transcriptional activators of β -catenin signalling, suggesting that TGF- β 1-WNT5A crosstalk downregulates canonical WNT signalling. WNT5A stimulation also had a similar effect on TGF- β 1 in inhibiting organoid synthesis, but it did not influence a change in organoid size (Ng-Blichfeldt *et al.* 2019). Borchering *et al.* (2015), however, report WNT5A significantly reduced basal tumour-initiating cell derived organoids, but that WNT5A and TGF- β 1 dual-stimulation significantly enhanced organoid size. In 3D

human mammary organoid cultures, WNT5A expression is reported to be downregulated compared to 2D cultures, and that the downregulation occurred prior to the branching process, suggesting WNT5A inhibits expansion of cells to restrict spatio-temporal restoration of tissue and restore tissue architecture (Huguet *et al.* 1995). This is also supported by Miyoshi *et al.* (2012) who showed that WNT5A soaked beads induced clefts in 3D colonic organoids. Taking this into account, this raises the question whether in the *in vivo* environment an effect of WNT5A on 2D wound healing seen at ALI would still be observed on 3D wound healing in HBEC and fibroblast co-culture models.

For the scratch wound assay, a calculation error meant that double the concentration of rhTGF- β 1 (20ng/ml rather than 10ng/ml), a slightly higher concentration of Takinib (8.4nM rather than 7.5nM) and double the concentration of BOX-5 (500nM rather than 250nM) was used. Treatment of rabbit tracheal epithelial cells with 0.1-100ng/ml TGF- β 1 inhibits cellular proliferation in a dose-dependent manner, but concentrations above 10ng/ml of TGF- β 1 did not have an additive effect on cellular proliferation (Jetten, Shirley and Stoner 1986). Whereas in normal HBECs, concentrations above 10ng/ml continued to decrease cellular proliferation, but at 20ng/ml this effect would be minimal (Jetten, Shirley and Stoner 1986). This suggests that a 48-hour pre-stimulation with 20ng/ml rather than 10ng/ml would not have had a significant impact on proliferation during wound healing of the ALI cultures in this study. This is supported by Ito *et al.* (2011) who report a TGF- β 1 dose-dependent (between 0.1ng/ml and 100ng/ml) increase in wound healing of monolayer NHBE and 1HAEo⁻ cells, but again a minimal additional response was observed between 10ng/ml and 100ng/ml. Dose-response curves investigating the effect of TGF- β 1 stimulation on EMT induction in BEAS-2Bs also support a limiting effect at higher TGF- β 1 concentrations, with 5ng/ml and 10ng/ml inducing similar EMT marker gene fold change (Doerner and Zuraw 2009).

Referring to the MTS assay results to determine how this error would have affected wound healing in the assay, 500nM of BOX-5 would non-significantly

reduce viability, whereas, the higher concentration of Takinib would non-significantly enhance cell survival of the cultures. As the dose for BOX-5 was double, whereas the concentration for Takinib was less than 1nM out, the cells are most likely subjected to a cell death fate, meaning wound healing may be underestimated in these scratch wound assays.

5 INVESTIGATING SMAD2/3 AND TAK1 AS CROSSTALK INTERMEDIARIES BETWEEN TGF- β 1 AND WNT5A IN EPITHELIAL WOUND HEALING AND EMT

5.1 Chapter Overview

The scratch wound data provided evidence of a potential crosstalk mechanism between TGF- β 1 and WNT5A signalling. This chapter investigates this relationship further. Both TGF- β 1 pre-stimulation and Takinib had a significant effect on rhWNT5A stimulated ALI culture wound healing, indicating that crosstalk between WNT5A and TGF- β 1 signalling may exist in wound healing, although neither significantly enhanced the wound healing response independently. To identify if the crosstalk was at the transcriptional level, the effect of rhTGF- β 1 stimulation on WNT5A mRNA was assessed in both BEAS-2Bs and iHBECs. To identify if the impact on the healing response was related to reduced WNT5A receptor expression, two potential receptors which WNT5A could be signalling through was investigated following a 48-hour rhTGF- β 1 stimulation.

As rhWNT5A stimulation non-significantly enhanced wound healing, markers of EMT were assessed following stimulation to identify if the healing effect was due to increased cellular motility. As pSMAD2/3 has been reported to directly affect WNT5A transcription, and act as a feedback mechanism for TGF- β -WNT5A crosstalk in ASM, the phosphorylation of SMAD2/3 following both WNT5A and TGF- β 1 stimulation was investigated as a crosstalk intermediary.

5.2 Effect of TGF- β 1 Stimulation on WNT5A and TGF- β Associated Gene Expression in BEAS-2Bs and iHBECs

Prior to running the BEAS-2B Qiagen RT² custom profiling arrays, the quality of RNA was assessed using an Agilent RNA 6000 Pico kit and Agilent 2100 Bioanalyser. The results are shown in **Figure 5.1A**. As you can see, bands are

present for both 18s and 28s, and two clean peaks are present at the 18s and 28s fragments. All samples had RIN numbers between 9.10 and 9.80, indicating high integrity of the RNA. For the iHBEC RNA, the RNA was checked using a non-denatured agarose gel (**Figure 5.1B**). The 28s band is twice (to 2.7 times) as intense as the 18S band suggesting high quality intact RNA.

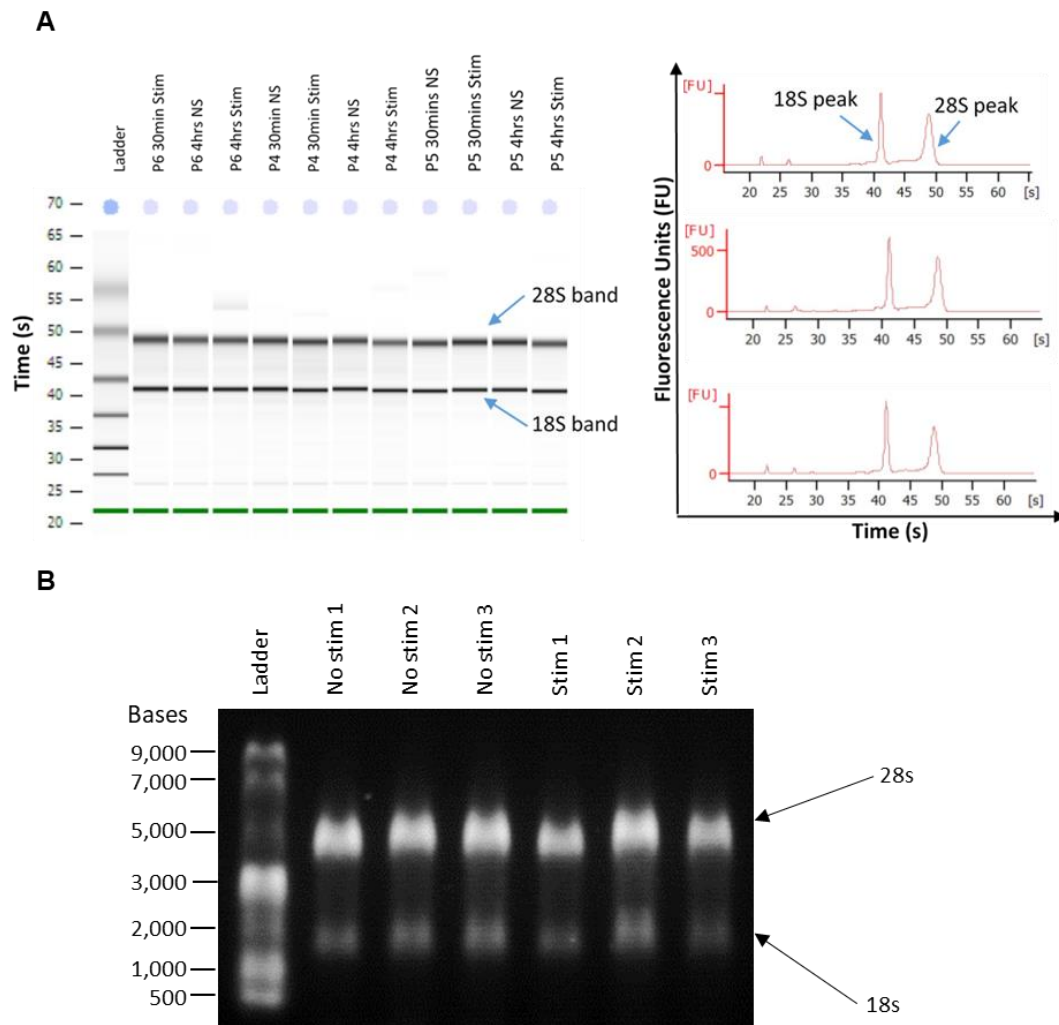


Figure 5.1 Assessing RNA Quality Prior to RT-qPCR. (A) Bioanalyser profiles of the BEAS-2B samples. Eleven out of twelve samples were tested on this chip. (B) Non-denatured Agarose gel results of the iHBEC RNA. The 28S band and peak widths for all samples are 2-2.7 times larger than those of 18S indicating intact RNA.

BEAS-2Bs were stimulated for 30 minutes and 4 hours with 10ng/ml rhTGF- β 1, and the gene expression of *WNT5A*, *TGFB1* and 14 associated genes assessed by RT-qPCR (**Figure 5.2**). 18S and β -actin in combination or 18S alone was used as the housekeeping gene. None of the genes were differentially expressed at

30 minutes (**Figure 5.2A**). After 4 hours 10ng/ml TGF- β 1 stimulation, only Filamin A was differentially expressed, however, this did not pass false discovery (**Figure 5.2B**). These time points were selected because the TGF- β 1 pathway is reported to take 30-60 minutes to induce transcriptional changes (Bauge *et al.* 2011), and 3 hours for canonical WNT signalling to (Gujral and MacBeath 2010). A paper indicating the time to induce transcriptional activity for the noncanonical pathways could not be sourced. Stimulation of 4 hours would therefore give approximately enough time for both signalling pathways to have a transcriptional effect if the length of time given for canonical signalling is comparable to noncanonical WNT signalling.

Comparing the log₂FC between the 30-minute and 4-hour gene expression for each gene did not highlight a significant change in gene expression between these two time points (**Figure 5.2C**). TGF- β 1 stimulation induced a non-statistically numerical trend in reducing WNT5A mRNA in both BEAS-2Bs ($p=0.0983$ after 4-hours stimulation compared to basal) and iHBECs ($p=0.0871$ after 48-hour stimulation compared to basal), as shown in **Figure 5.2B** and **Figure 5.2D**.

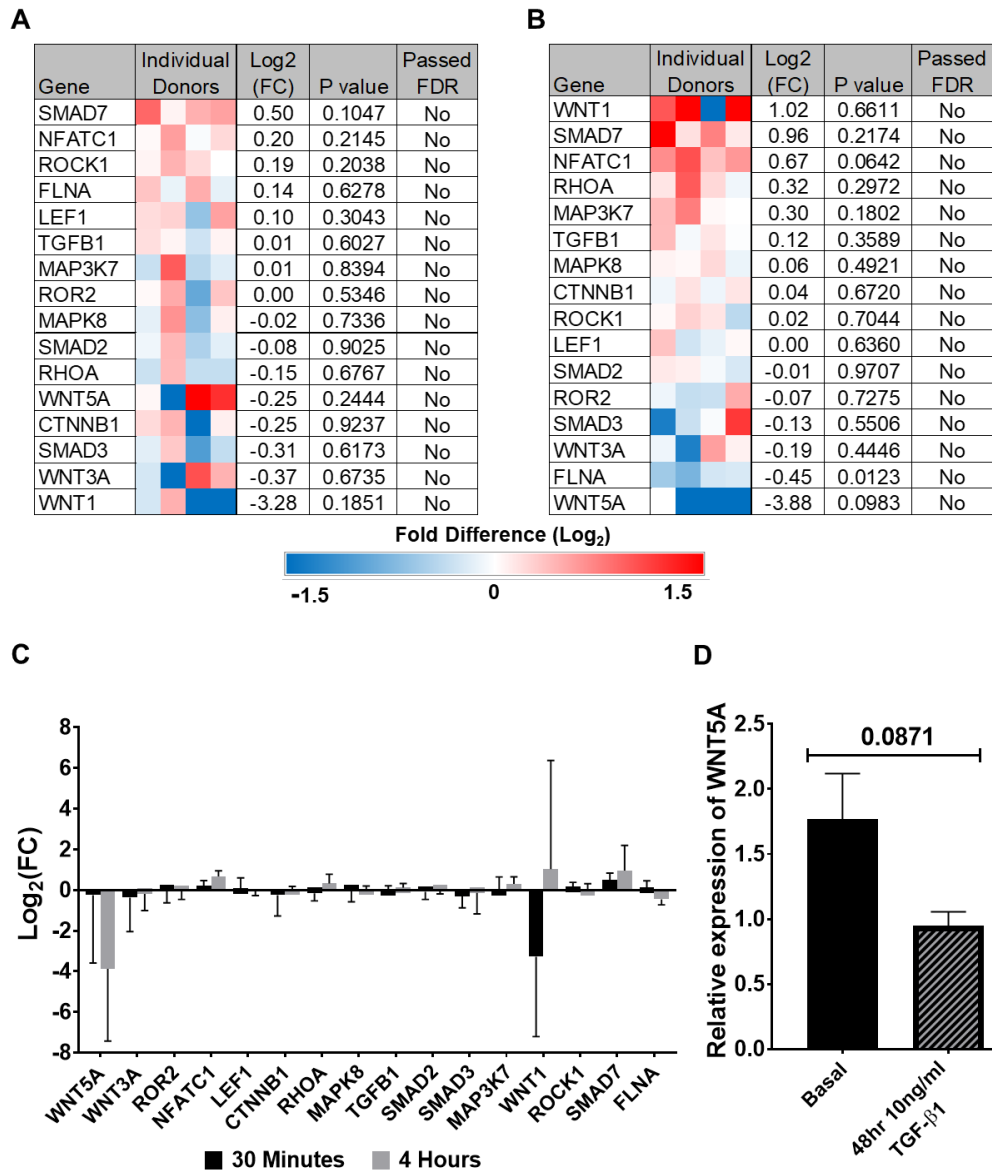


Figure 5.2 RT-qPCR Analysis of WNT5A and TGF- β 1 Pathway Signalling Effectors in BEAS-2Bs and iHBECs. (A-B) The log₂ fold change of 16 WNT5A and TGF- β 1 related genes in individual BEAS-2B passages are depicted in these heatmaps following a 30-minute (A) and 4-hour (B) 10ng/ml rhTGF- β 1 stimulation. The mean log₂(FC) and statistical significance are indicated ($n=4$). Statistical significance was calculated using a paired *t*-test on the $\Delta\Delta$ CT of each gene. (C) Graph comparing the 30-minute and 4-hour log₂FC. Statistical comparisons were made between the 30-minute and 4-hour stimulations using a paired *t*-test for each gene. Data is presented mean with standard deviation. (D) Relative expression of WNT5A mRNA between non-stimulated iHBEC cells (which received vehicle control) and cells stimulated with 48-hours 10ng/ml TGF- β 1. Data is $n=3$ and presented mean with standard deviation. * $p < 0.05$ by paired *t*-test.

5.3 TGF- β 1 Stimulation Effect on WNT5A Receptor Expression in BEAS-2Bs and HBECs

A 48-hour TGF- β 1 stimulation did not induce a significant change in ROR2 or FZD4 expression in either EpCAM- or EpCAM+ BEAS-2B cell populations, as shown in **Figure 5.3A-D** (ROR2: EpCAM- $p=0.75$, EpCAM+ $p=0.5$; FZD4: EpCAM- $p=0.75$, EpCAM+ $p=0.25$). As BEAS-2Bs differ substantially from HBECs phenotypically, ROR2 and FZD4 protein expression was also assessed via flow cytometry in uncultured HBECs retrieved by bronchoscopy. For this experiment, immunostaining and data acquisition were completed on the same day as bronchoscopy. On average, uncultured HBECs expressed higher ROR2 (25.61%) expression than FZD4 (3.48%), as shown in **Figure 5.4A**. This expression level did not significantly differ to unstimulated HBECs cultured to ALI for either ROR2 ($p=0.40$) or FZD4 ($p=0.20$) as assessed by a Mann-Whitney statistical test. A 48-hour TGF- β 1 stimulation did not affect ROR2 ($p>0.9999$) or FZD4 expression in ALI cultures ($p=0.75$) (**Figure 5.4B**).

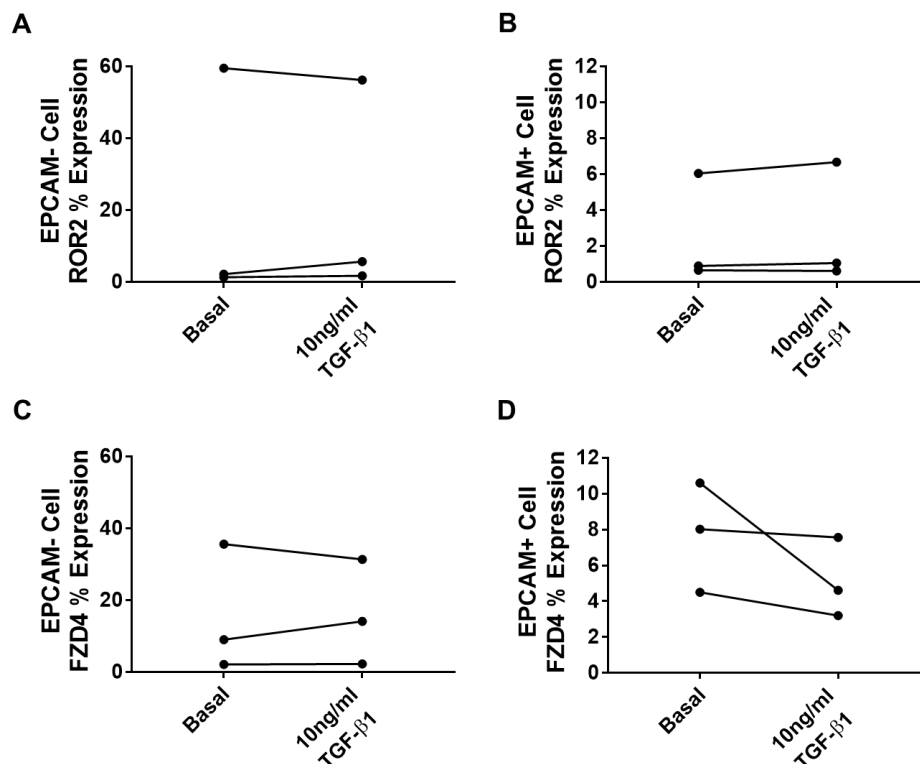


Figure 5.3 BEAS-2B ROR2 and FZD4 Expression Before and After TGF- β 1 Stimulation. Flow cytometry summary figures of percentage expression of ROR2 in EpCAM- (A) and EpCAM+ (B) and FZD4 in EpCAM- (C) and EpCAM+ (D) BEAS-2B populations before and after a 48-hour stimulation with 10ng/ml rhTGF- β 1, $n=3$. * $p < 0.05$ by Wilcoxon matched-pairs signed rank test.

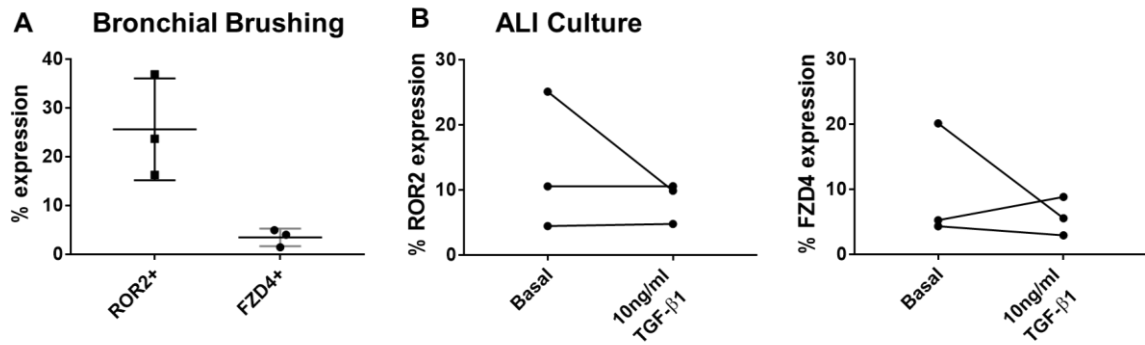


Figure 5.4 HBEC ROR2 and FZD4 Expression Before and After TGF- β 1 Stimulation. (A) Summary figure of ROR2 and FZD4 percentage expression on HBECs retrieved from bronchial brushings. Data is presented mean with standard deviation. (B) Summary figures of ROR2 and FZD4 percentage expression on ALI cultures before and after a 48-hour stimulation with 10ng/ml rhTGF- β 1, n=3. *p < 0.05 by Wilcoxon matched-pairs signed rank test.

5.4 Effect of TGF- β 1 and WNT5A Stimulation on EMT Induction in BEAS-2B Cells

Initially, immunofluorescence staining of EMT markers were used to examine upregulation of early EMT markers in response to TGF- β 1 and WNT5A stimulation in BEAS-2Bs. Representative images are shown for the expression of CK5, COL1A1 and Vimentin with and without rhTGF- β 1 stimulation (**Figure 5.5**) and rhWNT5A stimulation (**Figure 5.6**). Summary figures of the change in protein expression for both stimulations are shown in **Figure 5.7**. Cytokeration-5 and COL1A1 expression did not show a clear change in expression ($p=0.9177$ and $p=0.2127$ respectively) following a 48-hour 10ng/ml TGF- β 1 stimulation (**Figure 5.7A-B**). However, there was a significant increase in expression of vimentin ($p=0.0088$) (**Figure 5.7C**). In comparison, a 48-hour WNT5A stimulation did not significantly alter CK5 (**Figure 5.7D**, $p=0.2209$), COL1A1 (**Figure 5.7E**, $p=0.2009$) or vimentin (**Figure 5.7F**, $p=0.8554$) expression. Although protein expression was relatively unchanged, cellular elongation was assessed to identify if a change in protein expression correlated with morphological change typical of mesenchymal cells. TGF- β 1 stimulation significantly increased mean length to width ratio (**Figure 5.8A**, $p=0.0229$), whereas, WNT5A stimulation did not (**Figure 5.8B**, $p=0.9240$). This supports the protein expression data,

providing further resolution that TGF- β 1 induces EMT, whereas WNT5A does not.

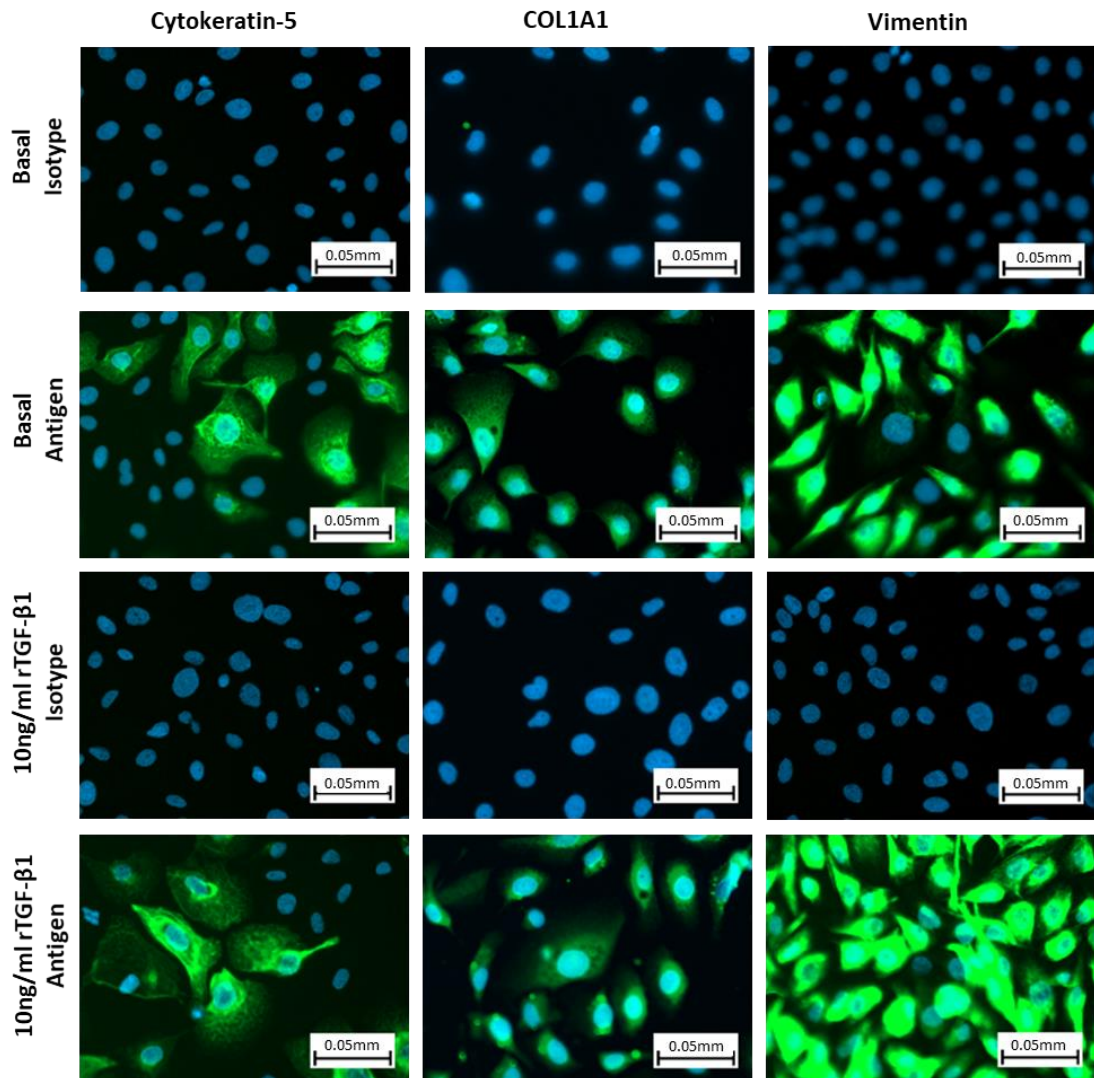


Figure 5.5 BEAS-2B Cytokeratin-5, COL1A1 and Vimentin Expression Before and After 48-Hour 10ng/ml rhTGF- β 1 Stimulation. Images are representative of four independent passages. All images taken at x200 magnification.

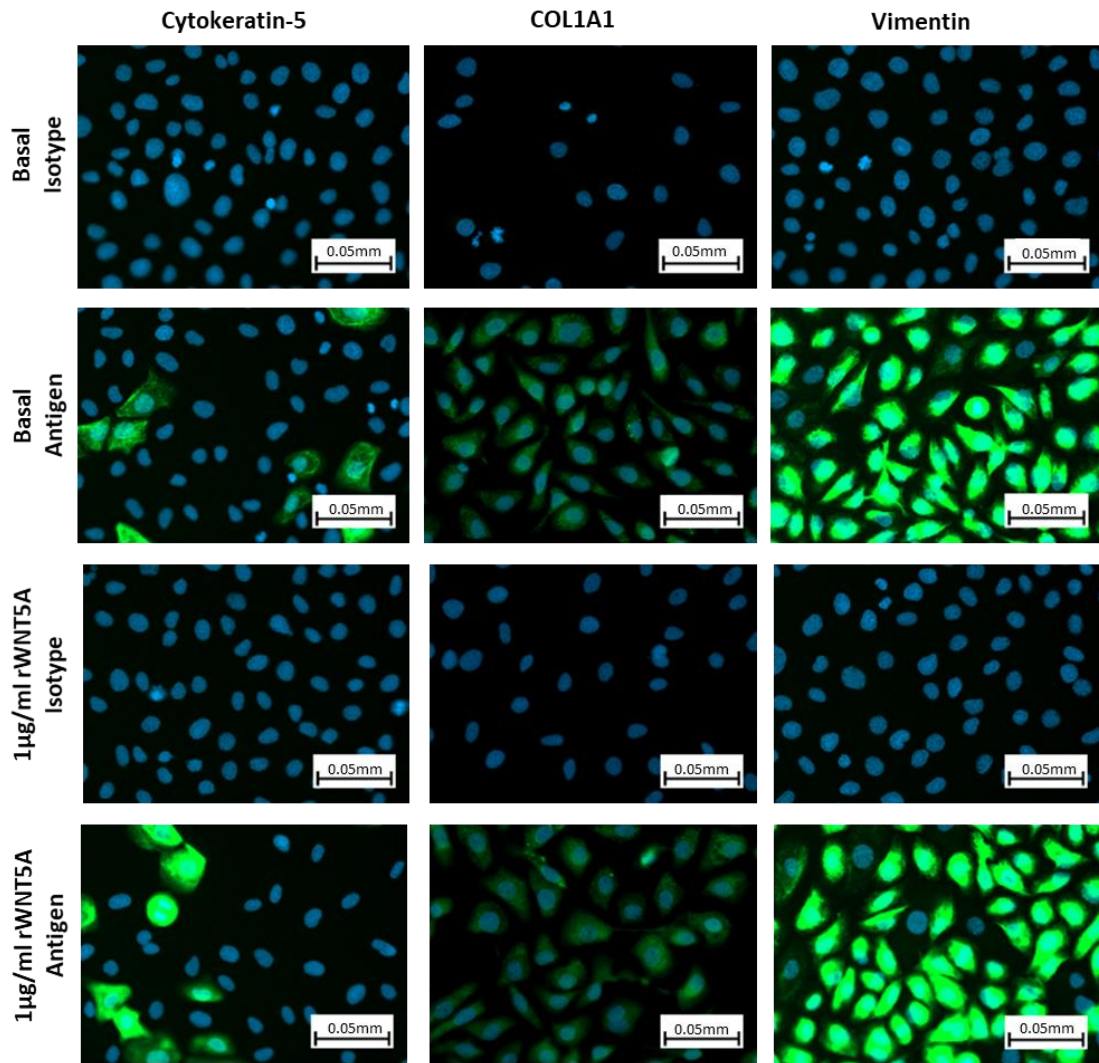


Figure 5.6 BEAS-2B Cytokeratin-5, COL1A1 and Vimentin Expression Before and After 48-Hour 1µg/ml rhWNT5A Stimulation. Images are representative of three independent passages. All images taken at x200 magnification.

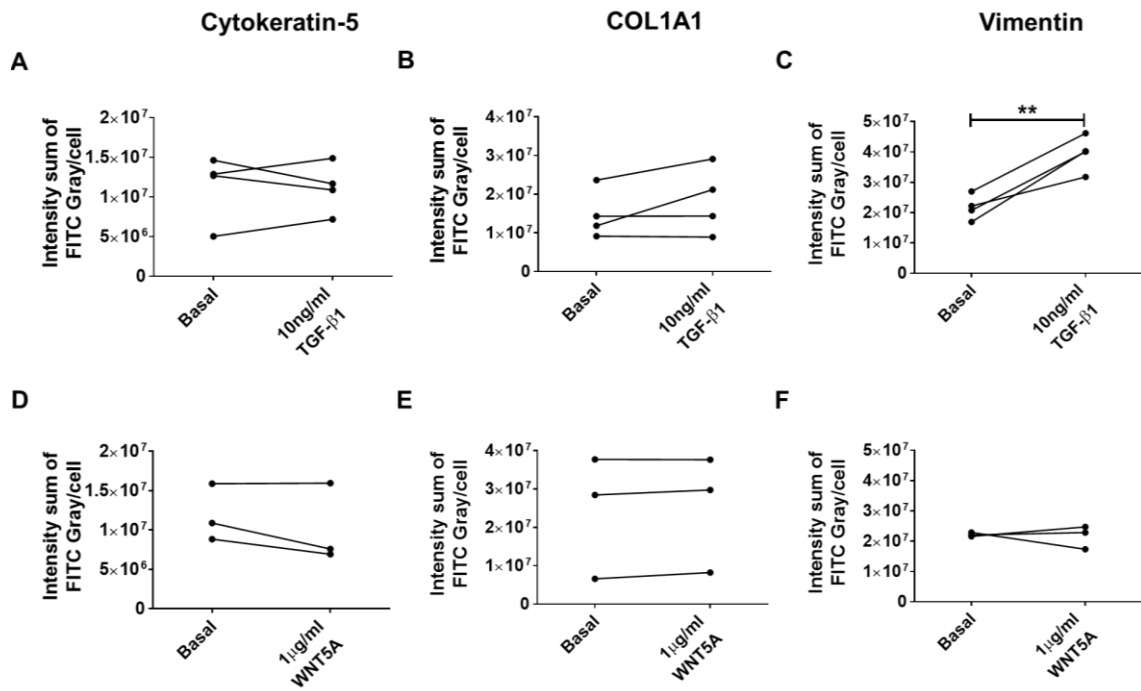


Figure 5.7 BEAS-2B Cytokeratin-5, COL1A1 and Vimentin Expression Before and After rhTGF-β1 and rhWNT5A Stimulation. Summary figures of CK5 (A, D), COL1A1 (B, E) and Vimentin (C, F) immunofluorescence staining following a 48-hour 10ng/ml rhTGF-β1 (top row A-C), $n=4$, and 1μg/ml rhWNT5A (bottom row D-F) stimulation compared to vehicle control (basal). $n=3$, * $p < 0.05$ by paired t-test.

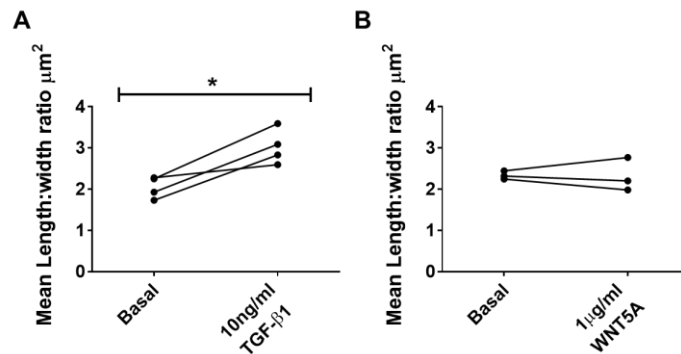


Figure 5.8 BEAS-2B Cellular Elongation Before and After rhTGF-β1 and rhWNT5A Stimulation. Summary figures of cellular elongation assessed by measuring vimentin stained cells with and without a 48-hour 10ng/ml rhTGF-β1 (A), $n=4$, or 1μg/ml rhWNT5A (B) stimulation, $n=3$, compared to vehicle control (basal). * $p < 0.05$ by paired t-test.

To confirm what was seen by immunofluorescence staining, BEAS-2Bs were also phenotyped for basal cell markers and assessed for early EMT marker expression by flow cytometry, with and without TGF- β 1 stimulation. For this experiment, vimentin, E-cadherin and multiple basal cell markers were assessed. A specific COL1A1 or CK5 antibody was not available for flow cytometry. As multiple protein expressions were measured per sample, to retain independent sampling, statistical tests were performed for each marker. BEAS-2Bs consist of two main populations – an EpCAM positive (EpCAM+), a phenotypically basal-like population which accounts for approximately 10% of cells, and an EpCAM negative (EpCAM-) population, which accounts for the remaining cells. The EpCAM+ population expressed higher levels of NGFR, CD49F and E-cadherin in comparison to the EpCAM- population, which expressed higher levels of Vimentin and CD44 but lower E-cadherin expression, which is more consistent with a mesenchymal phenotype.

The EpCAM+ population was more responsive than the EpCAM- population in response to rhTGF- β 1 stimulation, as three basal cell or EMT markers had a significant change in geometric mean fluorescence intensity (GMFI) in comparison to just one marker seen for the EpCAM- population. Change in marker expression for the EpCAM- population is shown in **Figure 5.9A** and the EpCAM+ population in **Figure 5.9B**. In response to rhTGF- β 1 stimulation, the EpCAM- population significantly downregulated integrin α 6 ($p=0.0406$). The remaining markers showed a similar trend in response to rhTGF- β 1 stimulation as the EpCAM+ population, but these did not reach statistical significance; the EpCAM+ population significantly downregulated basal cell marker NGFR ($p=0.0282$) and EpCAM ($p=0.0282$) expression, and significantly upregulated CD44 ($p=0.0036$). A numerical trend was also seen for Vimentin expression which was upregulated ($p=0.0773$), but E-cadherin and CD49F did not differ.

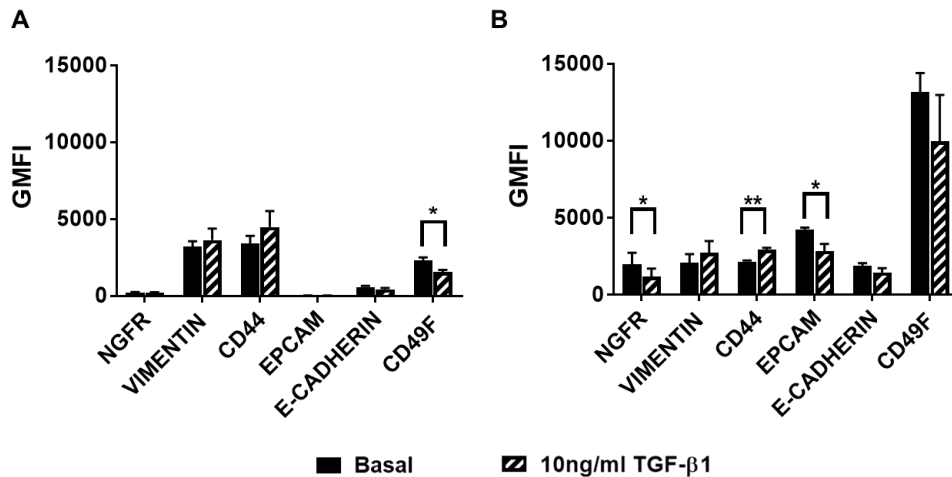


Figure 5.9 Geometric Mean Fluorescence Intensity of Basal Cell and EMT Marker Expression Before and After rhTGF-β1 Stimulation in BEAS-2B Cells. Summary figures of geometric mean fluorescence intensity (GMFI) of basal cell and EMT markers with and without a 48-hour 10ng/ml rhTGF-β1 stimulation compared to vehicle control (basal) for BEAS-2B EpCAM- (A) and EpCAM+ (B) populations, n=5. *p < 0.05 by paired t-test. A single t-test was conducted for each protein per population, and p values adjusted using the Holm-Sidak method (α=0.05).

5.5 Effect of TGF-β1 and WNT5A Stimulation on EMT Induction in HBEC ALI Cultures

Repeating the experiment in ALI cultures, three populations were evident. The gating strategy for these populations are shown in **Figure 5.10**. The EpCAM- population significantly increased NGFR expression following rhTGF-β1 stimulation (p=0.0461), but rhWNT5A stimulation did not (p=0.9940) (**Figure 5.10A**). Whereas, the EpCAM+ population and basal cell population sub-phenotype significantly decreased EpCAM expression following rhTGF-β1 stimulation (EpCAM+: p value=0.0093 **Figure 5.10B**; Basal Cell: p value=0.0424 **Figure 5.10C**); WNT5A stimulation, however, did not have a significant effect on EpCAM expression intensity for either population (EpCAM+: p value=0.7811; Basal Cell: p value=0.9757). All remaining epitopes did not show a significant observable change in GMFI following either a rhTGF-β1 or rhWNT5A stimulation from basal. Statistical readouts for all markers are shown in **Table 5.1**. WNT5A stimulation did not induce a significant phenotypic change in expression of any of the epitopes.

Table 5.1 ANOVA Summary Table for Basal Cell and EMT Marker Expression Before and After rhWNT5A and rhTGF- β 1 Stimulation in ALI Cultures. Data summarised is $n=4$ (3 asthmatic, 1 healthy) for rhTGF- β 1 and $n=3$ for rhWNT5A (2 asthmatic, 1 healthy).

Cell population	Across all groups		Between group analysis	
	Unadjusted p value	Adjusted p value	Basal: 1 μ g/ml WNT5A	Basal: 10ng/ml TGF- β 1
EpCAM-				
NGFR	0.047	0.5371	0.9940	0.0461
VIMENTIN	0.588	0.9996	0.6574	0.5314
CD44	0.3793	0.9915	0.6419	0.2931
EpCAM	0.7396	0.9996	0.7417	0.7224
E-CADHERIN	0.2318	0.9619	0.6466	0.1652
CD49F	0.0937	0.7714	0.9973	0.0906
EpCAM+				
NGFR	0.6608	0.9996	0.6631	0.6458
VIMENTIN	0.7529	0.9996	0.8576	0.6818
CD44	0.1355	0.8698	0.8238	0.1012
EpCAM	0.0091	0.1517	0.7811	0.0093
E-CADHERIN	0.7817	0.9996	0.7894	0.7598
CD49F	0.2223	0.9619	0.9618	0.1882
BASAL CELL				
NGFR	0.6791	0.9996	0.6782	0.6663
VIMENTIN	0.5866	0.9996	0.6261	0.5470
CD44	0.2712	0.9692	0.6310	0.1971
EpCAM	0.035	0.4543	0.9757	0.0424
E-CADHERIN	0.6052	0.9996	0.9759	0.6422
CD49F	0.9286	0.9996	0.9975	0.9322

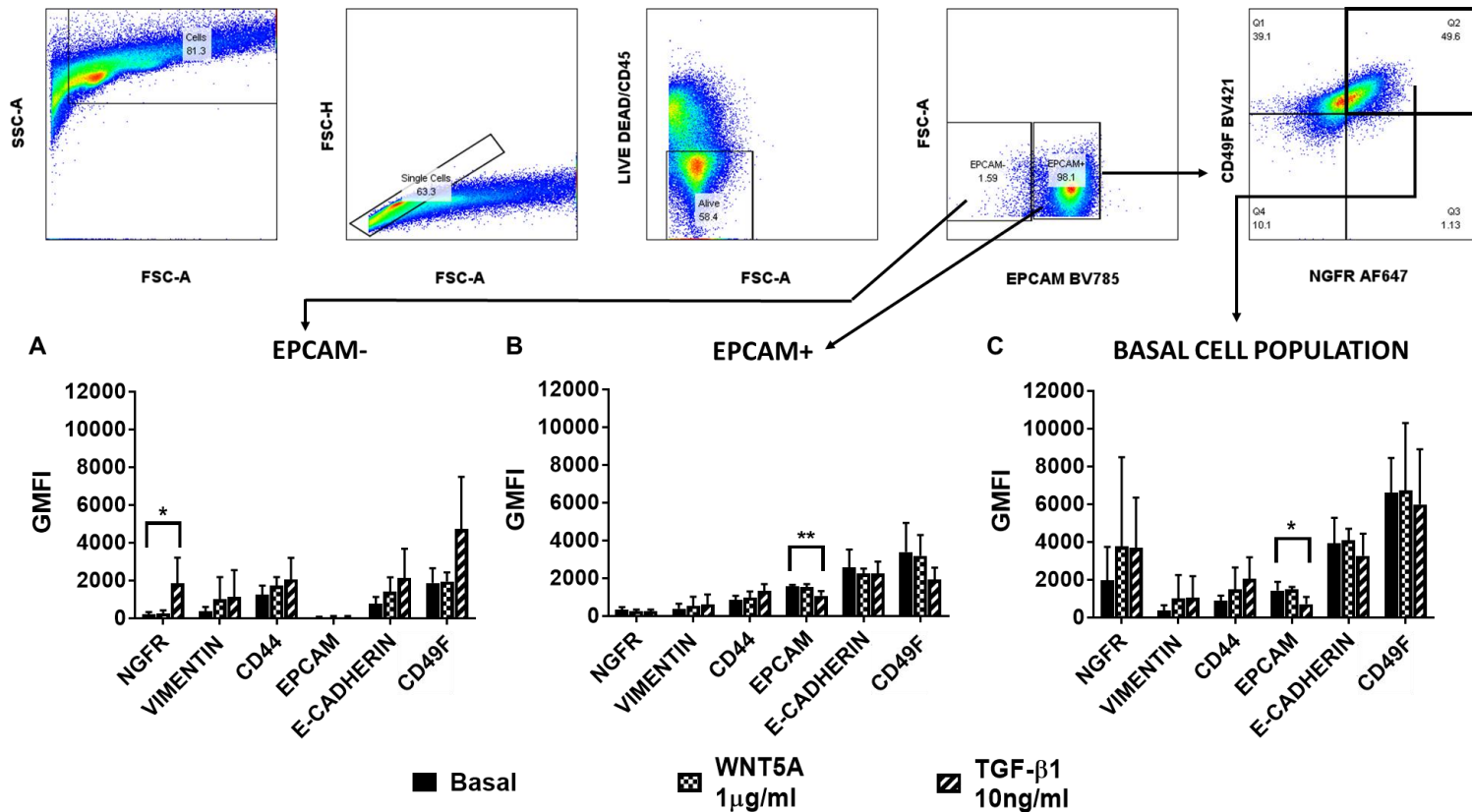


Figure 5.10 Geometric Mean Fluorescence Intensity of Basal Cell and EMT Marker Expression Before and After rhWNT5A and rhTGF-β1 Stimulation in ALI Cultures. Gating strategy used to select each population is shown. A-C represent geometric mean fluorescence intensity (GMFI) summary figures of basal cell and EMT marker expression after a 48-hour 10ng/ml rhTGF-β1 or 1µg/ml rhWNT5A stimulation compared to vehicle control (basal) for EpCAM- (A), EpCAM+ (B) and basal cell populations (C). Data is n=4 (3 asthmatic, 1 healthy) for rhTGF-β1 and n=3 for rhWNT5A (2 asthmatic, 1 healthy). *p < 0.05 by one-way repeated measures ANOVA with Dunnett's multiple comparison post hoc test. Significance testing shown is between each stimulation compared to vehicle control rather than across all groups. A single one-way ANOVA was conducted for each protein per population, and ANOVA summary p values adjusted using the Holm-Sidak method ($\alpha=0.05$). Post hoc analysis p values were adjusted for multiplicity within each ANOVA.

5.6 Effect of TGF- β 1 and WNT5A Stimulation on SMAD2/3 Phosphorylation in HBECs

Phosphorylated SMAD2/3 (pSMAD2/3) was highlighted as a potential intermediary between TGF- β 1 and WNT5A by Daud (2016). A 2-hour rhWNT5A stimulation was reported to significantly increase pSMAD2/3 expression in BEAS-2B cells by immunofluorescence. To identify if this was the case in HBECs, a similar experiment was conducted by flow cytometry with the same experimental design as the scratch wound assay. As TGF- β 1 is known to induce phosphorylation of SMAD2/3 via its canonical signalling pathway, rhTGF- β 1 stimulation served as a positive control to show this assay was working correctly. As phosphorylated protein staining requires a harsh permeabilisation method (which breaks down fluorochromes as previously mentioned in the methods section of this thesis), the basal cell panel had to be restricted to EpCAM and NGFR. These experiments were performed in ALI cultures only, due to high experimental cost. Epithelial cell populations were gated by first removing cellular debris, doublets and dead cells before separation by EpCAM and NGFR expression. Three populations (termed EpCAM^{HI} NGFR^{HI}, EpCAM^{HI} NGFR^{LO} and EpCAM^{LO} NGFR^{LO}) were evident as shown in **Figure 5.11A**. As the populations were within the same sample, independent sampling would have been violated if statistical testing were to be made across all three populations. Statistical testing was therefore performed for each population and p-values adjusted for multiplicity.

A 30-minute rhTGF- β 1 stimulation non-significantly increased pSMAD2/3 expression in the EpCAM^{HI} NGFR^{HI} ($p=0.3301$), EpCAM^{HI} NGFR^{LO} ($p=0.3301$) and EpCAM^{LO} NGFR^{LO} ($p=0.3301$) as shown in **Figure 5.11B**. To assess whether inhibiting the noncanonical TGF- β pathway through TAK1 would redirect further TGF- β signalling down the canonical SMAD2/3 pathway, rhTGF- β 1 stimulation with and without Takinib was compared (**Figure 5.11C**). Takinib did not have a significant impact on pSMAD2/3 expression for either population (EpCAM^{HI} NGFR^{HI}, $p=0.8594$; EpCAM^{HI} NGFR^{LO}, $p=0.8594$; and EpCAM^{LO} NGFR^{LO}, $p=0.5781$).

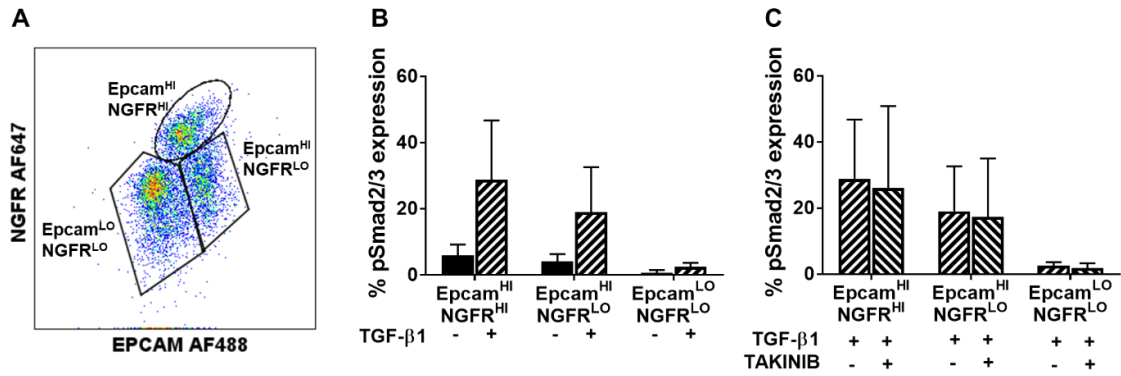


Figure 5.11 The Effect of rhTGF-β1 Stimulation With and Without TAK1 Inhibition on SMAD2/3 Phosphorylation of ALI Cultures. (A) EpCAM and NGFR population gating applied to ALI cultures following cellular debris, dead cell and doublet exclusion. (B) Summary figure of the effect of a 30-minute 10ng/ml rhTGF-β1 stimulation compared to basal on phosphorylated SMAD2/3 expression. (C) Summary figure of the effect of Takinib on ALI cultures stimulated with 10ng/ml rhTGF-β1 for 30 minutes. Data is presented mean with standard deviation, n=4. *p < 0.05 by Wilcoxon matched-pairs signed rank test. All p-values were adjusted to account for multiple comparisons.

The effect of WNT5A on SMAD2/3 compared to basal was then assessed (**Figure 5.12A**). WNT5A did not have a significant effect on pSMAD2/3 expression for either of the three subpopulations (EpCAM^{HI} NGFR^{HI}, p=0.6250; EpCAM^{HI} NGFR^{LO}, p=0.3301; and EpCAM^{LO} NGFR^{LO}, p=0.4375). Although we did not see a signal in WNT5A SMAD2/3 induction, we also investigated the effect of BOX-5 on pSMAD2/3 expression. WNT5A stimulated cultures with and without BOX-5 were compared irrespective of TGF-β1 stimulation (**Figure 5.12B**). As expected, because WNT5A did not induce a significant effect on SMAD2/3 phosphorylation, inhibition of WNT5A signalling with BOX-5 also had no effect. All adjusted p values were >0.7986 for the 4 groupings (no stimulation with Takinib, no stimulation without Takinib, TGF-β1 pre-stimulation with Takinib or TGF-β1 pre-stimulation without Takinib) across all three populations.

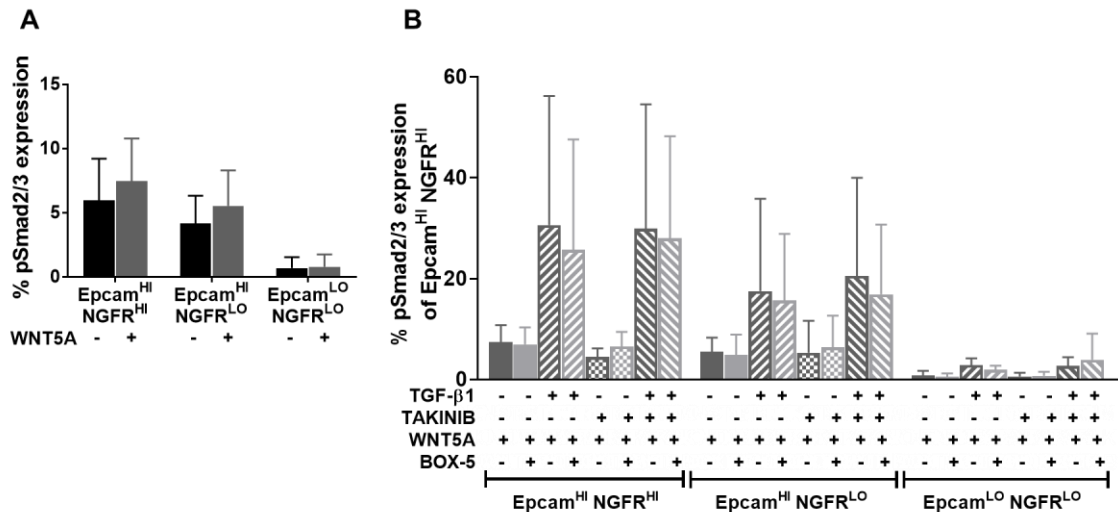


Figure 5.12 The Effect of WNT5A Stimulation With and Without Receptor Inhibition on SMAD2/3 Phosphorylation of ALI Cultures.

(A) Summary figure comparing the impact of a 30-minute 1 μ g/ml WNT5A stimulation (1 μ g/ml) against basal. (B) Summary figure comparing BOX-5 inhibition of WNT5A on phosphorylated SMAD2/3 expression. BOX-5 was added 30 minutes prior to WNT5A stimulation. Data is presented mean with standard deviation, n=4. *p < 0.05 by Wilcoxon matched-pairs signed rank test. All p-values were adjusted to account for multiple comparisons.

To assess crosstalk with TGF- β 1, the effect of TGF- β 1 and WNT5A dual stimulation was compared to TGF- β 1 stimulation alone to identify if WNT5A has an additional effect on SMAD2/3 phosphorylation (**Figure 5.13A**). WNT5A did not have a significant effect on pSMAD2/3 expression across the three populations (p=0.998 for each subpopulation) in the presence of TGF- β 1 stimulation. To see if TAK1 noncanonical TGF- β 1 signalling inhibition influenced canonical SMAD2/3 TGF- β 1 signalling in the presence of WNT5A, cultures dual stimulated with rhTGF- β 1 and rhWNT5A with and without Takinib were compared. In line with its lack of effect on TGF- β 1 induced SMAD2/3 phosphorylation, Takinib did not have an effect on SMAD phosphorylation of WNT5A stimulated cultures (p=0.9844 for both the EpCAM^{HI} NGFR^{HI} and EpCAM^{LO} NGFR^{LO} subpopulation, and p=0.5781 for the EpCAM^{HI} NGFR^{LO}) (**Figure 5.13B**).

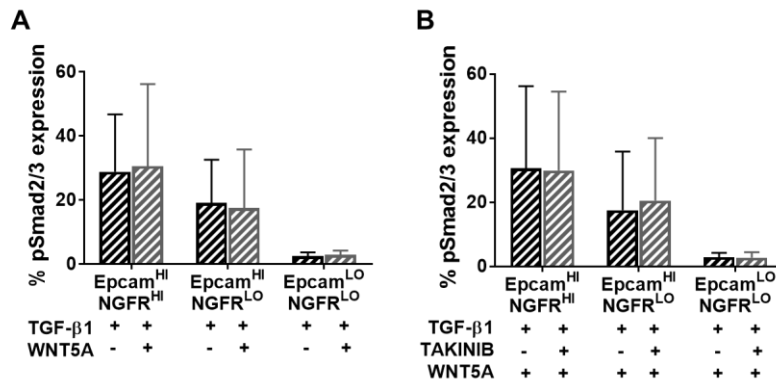


Figure 5.13 The Effect of WNT5A and TGF-β1 Dual Stimulation With and Without Receptor Inhibition on SMAD2/3 Phosphorylation of ALI Cultures. (A) Summary figure comparing the impact of a 30-minute 1μg/ml rhWNT5A and 10ng/ml rhTGF-β1 dual stimulation against rhTGF-β1 alone. (B) Summary figure comparing TAK1 inhibition on WNT5A phosphorylated SMAD2/3 expression. Takinib was added 30 minutes prior to dual stimulation. Data is presented mean with standard deviation, n=4. *p < 0.05 by Wilcoxon matched-pairs signed rank test. All p-values were adjusted to account for multiple comparisons.

5.7 Overall Effect of Takinib and TGF-β1 on WNT5A-Mediated SMAD2/3 Phosphorylation

A two-way repeated measures Aligned ranks transformation ANOVA indicated a significant effect of rhTGF-β1 stimulation (p=2.673e-05) on rhWNT5A-mediated SMAD2/3 phosphorylation of the EpCAM^{HI} NGFR^{HI} population, whereas Takinib did not (p=0.8958); the interaction between both Takinib and TGF-β1 stimulation on WNT5A-mediated SMAD2/3 phosphorylation in this population was not significant, p=0.4260 (**Figure 5.14A**). Again, a significant effect of rhTGF-β1 stimulation was found for the EpCAM^{HI} NGFR^{LO} (**Figure 5.14B**) and EpCAM^{LO} NGFR^{LO} (**Figure 5.14C**) populations, p=0.0106 and p=0.0005 respectively, but Takinib did not (p=0.8980 and p=0.7106). The interaction for both Takinib and rhTGF-β1 stimulation on both of these populations in mediating pSMAD2/3 expression was also none significant (EpCAM^{HI} NGFR^{LO}: p= 0.3829 and EpCAM^{LO} NGFR^{LO}: p= 0.8042).

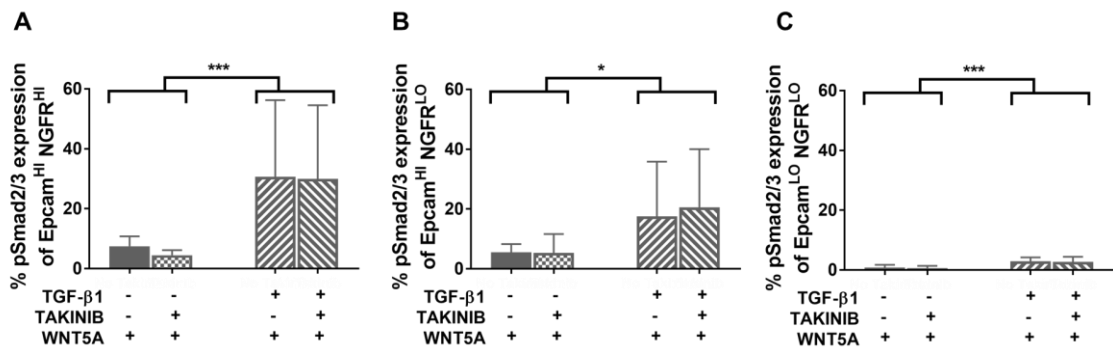


Figure 5.14 The Effect of WNT5A Stimulation With and Without Takinib Inhibition on SMAD2/3 Phosphorylation. Summary figures of phosphorylated SMAD2/3 expression following a 30-minute 1µg/ml rhWNT5A stimulation without (A) and with Takinib inhibition (B) for the three populations present within ALI cultures, which are categorised by their EpCAM and NGFR dual expression. Data is presented mean with standard deviation, n=4. *p < 0.05 by two-way repeated measures Aligned ranks transformation ANOVA.

5.8 Overall Effect of TGF-β1, WNT5A and Takinib on SMAD2/3 Phosphorylation

To assess the 3-way relationship between WNT5A, TGF-β1 and Takinib, a three-way repeated measures (by all three factors) Aligned Ranks ANOVA for SMAD2/3 phosphorylation was applied as shown in **Figure 5.15**. The 3-way interaction did not have a significant effect on SMAD2/3 phosphorylation (p=0.3558), neither did the single effect of rhWNT5A or Takinib (p=0.4236 and p=0.6527 respectively); however, rhTGF-β1 stimulation, as expected as the positive control, had a significant effect on SMAD2/3 phosphorylation (p=4.0569e-13).

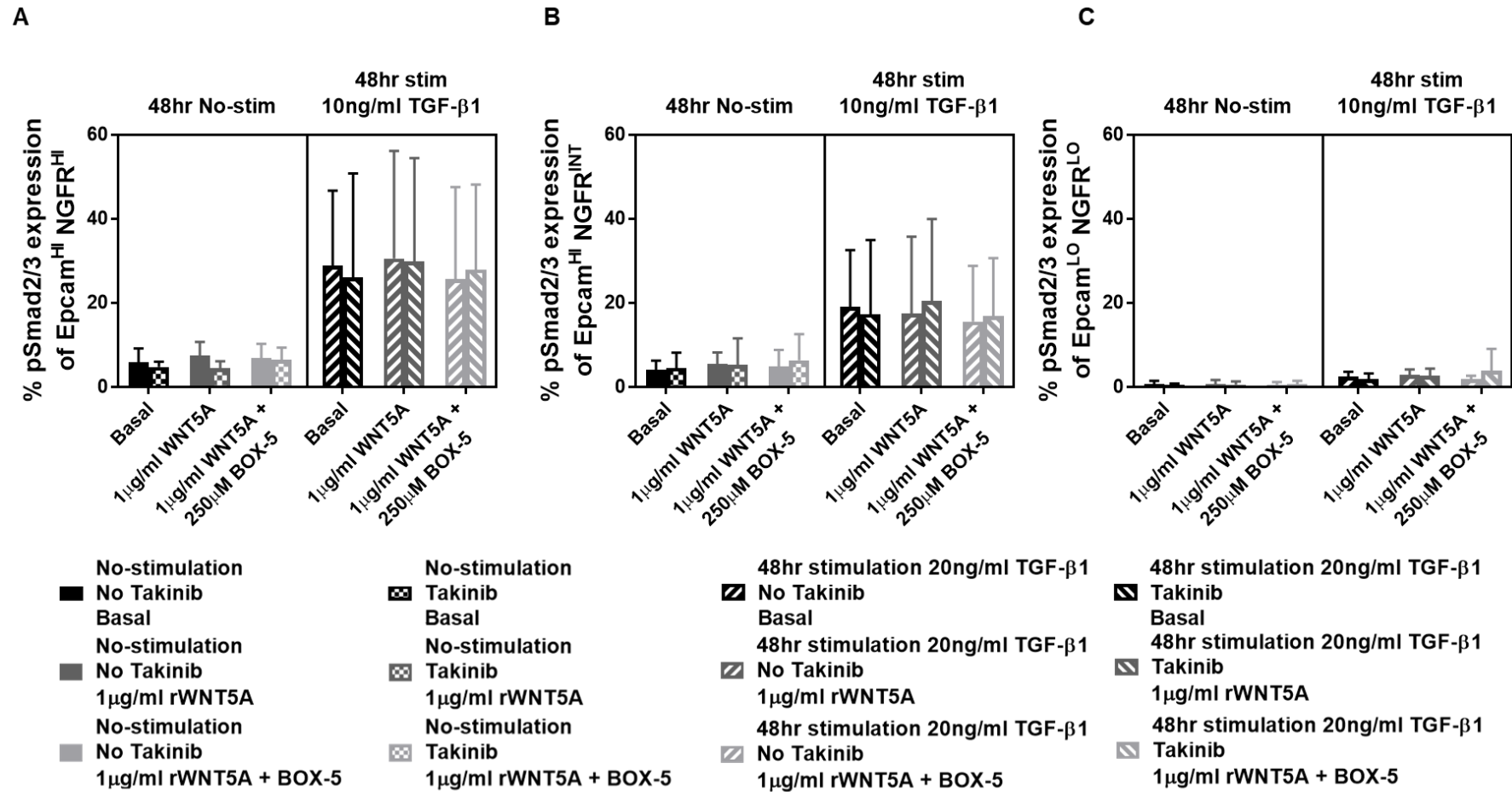


Figure 5.15 The Effect of Takinib, TGF-β1 and WNT5A Stimulation on SMAD2/3 Phosphorylation. Summary figures of phosphorylated SMAD2/3 expression comparing the impact of Takinib and rhTGF-β1 and rhWNT5A stimulation on all conditions for the three populations present within ALI cultures, as categorised by their EpCAM and NGFR dual expression. Data is presented mean with standard deviation, n=4. *p < 0.05 by three-way repeated measures (by all three factors) Aligned Ranks ANOVA.

5.9 Summary

- A 10ng/ml rhTGF- β 1 stimulation non-significantly downregulated WNT5A mRNA in BEAS-2Bs ($p=0.0983$ after 4-hours stimulation) and iHBECs ($p=0.0871$ after 48-hour stimulation) compared to basal.
- A 48-hour 10ng/ml rhTGF- β 1 stimulation did not affect WNT5A ROR2 or FZD4 receptor expression in BEAS-2Bs or HBECs.
- A 10ng/ml rhTGF- β 1 stimulation induced phenotypic and morphological changes associated with early stage EMT in BEAS-2Bs and HBECs, but a 1 μ g/ml rhWNT5A stimulation did not.
- A 30-minute 1 μ g/ml rhWNT5A stimulation did not induce pSMAD2/3 expression in HBECs, unlike 10ng/ml rhTGF- β 1.

5.10 Discussion

5.10.1 TGF- β 1 Effect on WNT5A mRNA

TGF- β has been shown to upregulate WNT5A expression directly through the SMAD2/3 transcriptional complex with SMAD4, and indirectly through SMAD-induced CUX1 and TAK1-mediated NF-KB (Katoh and Katoh 2009). TGF- β 1 can induce WNT5A in numerous cell types: SMAD3 transduced primary aortic smooth muscle cells (Shi *et al.* 2014) (DiRenzo *et al.* 2016), basal tumour-initiating cells (Borcherding *et al.* 2015), LX-2 cells (Beljaars *et al.* 2017), mammary epithelial cells and fibroblasts (Roarty and Serra 2007), normal human lung fibroblasts (Newman *et al.* 2016) (Baarsma *et al.* 2017), IPF lung fibroblasts (Contreras *et al.* 2020), cardiac fibroblasts (Contreras *et al.* 2020), the human marrow stromal cell line KM101 (Zhou, Eid and Glowacki 2004) and ASM cells (Kumawat *et al.* 2014). Surprisingly, rhTGF- β 1 stimulation non-significantly downregulated WNT5A expression in both BEAS-2Bs following a 4-hour stimulation and in iHBECs following a 48-hour stimulation. The iHBECs were exposed to a 48-hour stimulation to assess whether WNT5A would be upregulated or downregulated at the time of wounding and rhWNT5A stimulation (in the scratch wound assay). Obviously due to the calculation error, 20ng/ml rhTGF- β 1 was exposed to the cells, indicating WNT5A would most likely be significantly downregulated at the time of wounding due to the higher

concentration. This outcome therefore offers a potential explanation as to why the 48-hour TGF- β 1 pre-stimulation had a significant effect on WNT5A-mediated wound closure.

On the contrary to what we found in BEAS-2Bs, Daud (2017) saw an increase in WNT5A protein expression following a 48-hour rhTGF- β 1 stimulation in BEAS-2B cells. This may be due to non-specific binding of the WNT5A 6F2 antibody discussed earlier on in this thesis. Although not as frequently reported, a suppressive effect of rhTGF- β 1 on WNT5A expression has been reported in the literature. High glucose levels induced TGF- β 1 expression but decreased WNT5A and β -catenin expressions in rat mesangial cells (Ho *et al.* 2016). Whereas, nitric oxide induced WNT5A expression but decreased TGF- β 1 in diabetic mesangial cells (Hsu *et al.* 2015), reinforcing that in mesangial cells a reciprocal relationship may exist. A direct link, however, was not reported in either of these two studies. Furthermore, in mesenchymal cells, TGF- β is also reported to downregulate WNT5A expression, where TGF- β R2 deletion and TGF- β signalling inhibition with SB431542 caused a significant elevation in WNT5A expression (Yang *et al.* 2014). This suggests TGF- β effects on WNT5A expression is cell context dependent.

5.10.2 TGF- β 1 Effect on WNT Receptor Expression

FZD4 and ROR2 were investigated as WNT5A can signal through the non-canonical axis via ROR2 and through the β -catenin dependent canonical WNT pathway via FZD4 (Mikels and Nusse 2006). ROR2 was also of key interest because ROR2 knock-out mice display similar abnormalities in lung development as WNT5A knock-out mice (Oishi *et al.* 2003), indicating an important role in WNT5A ROR2 signalling in lung development that may be recruited again in repair. Unfortunately, no other Frizzled receptor or RYK antibody was available for the application of flow cytometry. Neither ROR2 or FZD4 were differentially expressed in BEAS-2B or ALI cultures following a 48-hour 10ng/ml rhTGF- β 1 stimulation. To identify if receptor expression is altered by ALI culture, expression was compared against HBECs within hours of retrieval by bronchoscopy - there

was no significant change in expression between pre- and post-culture. Although TGF- β 1 did not induce a significant change in ROR2 and FZD4 expression in iHBECs and BEAS-2Bs, there are numerous reports reporting an upregulation of WNT receptors alongside WNT ligands. A 24-hour 2ng/ml TGF- β 1 stimulation was reported to induce FZD8 expression in MCR-5 and primary human lung fibroblasts but had little effect on the other nine Frizzled receptors (Spanjer *et al.* 2016). On the contrary, Guan and Zhou (2017) report that FZD7 rather than FZD8 is upregulated in MRC-5 cells by a 24-hour stimulation with 3ng/ml TGF- β 1 in a SMAD-dependent manner. Additionally, in response to TGF- β 1 stimulation, hTERT-airway smooth muscle cells significantly decreased FZD1-5 and non-significantly decreased ROR2 and RYK, whereas, FZD6 and FZD8-10 were significantly increased; FZD7, however, remained unchanged (Kumawat *et al.* 2013). In human hepatic LX-2 cells, TGF- β has also been reported to induce FZD2 and FZD8 expression (Beljaars *et al.* 2017). These reports were what prompted us to investigate change in receptor expression alongside the functional assays performed.

5.10.3 TGF- β 1 and WNT5A Effect on EMT in BEAS-2Bs and Differentiated HBECs

TGF- β has been reported to induce EMT through both SMAD-dependent and SMAD-independent signalling in pulmonary epithelial cells (Câmara and Jarai 2010) (Kolossova, Nethery and Kern 2011). In this study, we found that a 10ng/ml 48-hour rhTGF- β 1 stimulation significantly induced vimentin and cellular elongation in BEAS-2Bs detected via immunofluorescence. Daud (2017), however, reported that a 48-hour 10ng/ml rhTGF- β 1 stimulation in BEAS-2Bs, also observed by immunofluorescence microscopy, significantly induced cellular elongation but only downregulated E-cadherin and CK-5 protein expression, vimentin expression was unchanged. The enhanced vimentin expression and cellular elongation reported in this study coincided as expected, as vimentin is essential for cellular extensions (Ding *et al.* 2020). The discrepancy here between the observations in BEAS-2Bs could be due to differences in methodology in image acquisition as the staining protocol, fluorescence bulb intensity and exposure times were identical. Images in this study were focused

and acquired on DAPI without FITC staining to alleviate observer bias, and FITC staining was reported per cell to standardise the results, as confluency affected the intensity sum of FITC staining reported per image. Multiple images were acquired for each condition per experiment, and the average taken for statistical analysis. Daud (2017), however, reported the intensity sum of FITC per image, potentially overestimating the staining intensity.

Doerner and Zuraw (2009) also investigated the effect of rTGF- β 1 on EMT in BEAS-2Bs. They reported that a 5ng/ml stimulation induced a significant downregulation in E-cadherin and a significant upregulation in collagen 1 mRNA expression 24-hours post-stimulation; the 5ng/ml TGF- β 1 stimulation, however, failed to increase vimentin mRNA expression. This is on the contrary to what was found in this study, as vimentin protein expression was significantly induced 48-hours post-stimulation with 10ng/ml rhTGF- β 1 detected by Immunofluorescence, but collagen 1 was not. Doerner and Zuraw (2009) also investigated EMT in NHBEs but with a lower dose of rTGF- β 1 (2ng/ml). A 3-day 2ng/ml stimulation decreased E-cadherin mRNA, whilst both collagen 1 and vimentin mRNA were notably increased at 24 hours (Doerner and Zuraw 2009).

On the contrary to EMT protein expression assessed by IF, flow cytometry did not detect a significant change in vimentin protein expression 48-hours post 10ng/ml rhTGF- β 1 stimulation compared to basal, although a non-significant trend was observed in the BEAS-2B EpCAM+ population ($p=0.0773$). Epithelial cell markers, EpCAM and NGFR, were however significantly downregulated, and CD44 upregulated. Flow cytometry is generally considered complementary to immunofluorescence microscopy (Godfrey *et al.* 2005), and in this application its multiparametric capabilities allows multiple EMT proteins to be investigated at once to give a more holistic view of the EMT process in a single sample. The significant change in EpCAM expression is as expected for a 72-hour 5ng/ml rhTGF- β 1 and 10ng/ml TNF α stimulation induced vimentin expression and downregulated EpCAM in MCF-10A, A549 and HaCaT cells (Sankpal *et al.* 2017). EpCAM downregulation may enhance migratory ability as shown in the

oesophageal Kyse-30 cell line (Driemel *et al.* 2014). However, regulation of EpCAM during EMT does seem to be context dependent as numerous studies also report a promoting role for EpCAM in EMT (Keller, Werner and Pantel 2019). For example, EpCAM was induced by TGF- β 1 treatment in MCF-7 breast cancer cells to promote EMT and migration (Gao *et al.* 2015).

NGFR was also significantly downregulated in the BEAS-2B EpCAM positive population, but significantly upregulated in the HBEC ALI culture EpCAM negative population. NGFR was significantly upregulated by a 5ng/ml TGF- β 1 stimulation in an NGFR low-expressing melanoma cell line (M010817). Its expression controlled the switch between proliferation and invasive ability, with high expression defining reduced proliferation but increased invasion, and lower basal expression defining high proliferation but reduced invasion (Restivo *et al.* 2017). Similarly, induced NGFR expression also resulted in a more metastatic and invasive phenotype of the MOC2 murine oral cancer cell line (Chung *et al.* 2018). Applying this to the BEAS-2B findings, the EpCAM+ NGFR+ population may potentially be decreasing NGFR expression to increase proliferation of the population, whereas, in the EpCAM negative population of the ALI cultures, a more migratory phenotype may be being acquired.

CD44 was also significantly upregulated in the BEAS-2B EpCAM+ population. CD44 is the Hyaluronan (HA) receptor. Its involvement in HA remodelling and degradation implements it as playing a key role in cellular migration (Cho *et al.* 2012). CD44 is important for cytoskeletal remodelling, and for facilitating an organised directional migratory response following injury (Acharya *et al.* 2008). It is therefore an important mediator in EMT and is often associated with metastatic spread in cancer (Mima *et al.* 2012). CD44 is reported to regulate the mesenchymal transition, with abrogation of CD44 reducing EMT associated protein changes and cellular migration (Acharya *et al.* 2008) (Mima *et al.* 2012). TGF- β 1 stimulation is reported to induce CD44 expression (Park *et al.* 2016) (Katsuno *et al.* 2019). CD44 can also potentiate TGF- β 1 signalling through

mediating its proteolytic activation via MMP9 cell surface localisation (Yu and Stamenkovic 2000) (Acharya *et al.* 2008).

A 24-hour 10ng/ml TGF- β 1 stimulation is also reported to significantly upregulate gene expression of vimentin, collagen 1 α 1, CD44, and numerous other mesenchymal markers, and significantly downregulate E-cadherin mRNA in primary airway epithelial cells (Hackett *et al.* 2009). This was not observed in this study at the protein level by flow cytometry for vimentin, E-cadherin or CD44 following a 48-hour 10ng/ml rhTGF- β 1 stimulation in the HBEC ALI cultures. This is most likely the result of patient heterogeneity, combined with being statistically underpowered (n=4), as early EMT expression changes were evident.

WNT5A promotes EMT through the noncanonical WNT-Ca²⁺ pathway (Abedini *et al.* 2020), of which vimentin and CD44 are WNT5A target genes (Dissanayake *et al.* 2007) (Abedini *et al.* 2020). However, we found that WNT5A did not induce EMT in either BEAS-2Bs or differentiated HBEC ALI cultures. This is surprising as WNT5A is reported to induce EMT in numerous cellular systems (Abedini *et al.* 2020) (Bo *et al.* 2013) (Dissanayake *et al.* 2007), including A549 cells (Wang *et al.* 2017), and was reported to induce EMT in BEAS-2Bs (Daud 2017). WNT5A (1 μ g/ml) was reported to significantly induce cellular elongation, and significantly reduce CK5 and E-cadherin expression in BEAS-2B cells (Daud 2017). This may differ to what we what we found in BEAS-2Bs, due to as mentioned later in this discussion, the rhWNT5A protein was potentially contaminated with TGF- β , of which the level of contamination differed between lots. If the rhWNT5A lot used by Daud (2017) had higher contamination with TGF- β , then this would explain the EMT induction observed.

5.10.4 WNT5A Effect on SMAD2/3

TGF- β significantly increased SMAD2/3 phosphorylation in the three-way repeated measures Aligned Ranks ANOVA, as expected as the experimental positive control. Takinib did not have a significant effect on SMAD2/3 phosphorylation, suggesting inhibition of TAK1 does not attenuate SMAD2

phosphorylation as reported by van Caam *et al.* (2017) with TAK1 inhibitor 5ZO, or re-direct signalling down the canonical pathway. We found WNT5A can neither induce SMAD2/3 phosphorylation or EMT marker induction at 48 hours, suggesting that a direct mechanism does not exist for WNT5A EMT induction in primary HBECs. A 72-hour stimulation with WNT5A has been reported to have a direct effect via the TGF- β R on SMAD2 phosphorylation in basal mammary epithelial cells (Borcherding *et al.* 2015). Miyoshi *et al.* (2012) also report SMAD3 phosphorylation following a 2-hour 400ng/ml WNT5A stimulation in colonic epithelial cells. Coster *et al.* (2017), however, suggests that WNT5A-induced SMAD signalling is down to TGF- β 1 contamination of the WNT5A recombinant protein. This is plausible as the TGF- β R is required for signalling to take place, and all the recombinant proteins used in the papers are purchased from RnD. On the contrary, Kumawat *et al.* (2014) inhibited SMAD3 in hTERT ASM cells, which resulted in a significant (2-fold) increase in WNT5A mRNA, suggesting that the SMAD pathway may negatively regulate WNT5A transcription in this cell type (Kumawat *et al.* 2014). This supports the potential for WNT5A to induce SMAD2/3 phosphorylation without the possibility of TGF- β contamination.

Coster *et al.* (2017) suggested WNT5A recombinant protein 645-WN was contaminated with TGF- β . As the purity claims are <80% for this product, rather than <98% for other recombinant proteins, there was cause for concern, and further investigation was initiated. On contacting R&D Systems of Bio-technie, the supplier of 645-WN, the contamination with TGF- β was confirmed using a TGF- β Quantikine ELISA kit (DB100B). Between two different lots tested in circulation (master lots MCR47 and MCR49), 19.2pg and 30 pg TGF- β , either in its inactive form latency-associated peptide (LAP) or active form, was detected per μ g of rhWNT5A. The 19.2 pg/ μ g vial contained purely LAP, whereas the 30 pg/ μ g vial contained 10 pg/ μ g active TGF- β and 20pg/ μ g LAP. As WNT5A was used at a concentration of 1 μ g/ml, it can be deduced on average that the cultures were potentially exposed to 30pg/ml TGF- β . As cultures were stimulated with 10ng/ml rhTGF- β 1 for TGF- β stimulation, this is unlikely to be sufficient enough to induce a significant change in SMAD2/3 phosphorylation. As the vials were tested in November 2018, the lot used by Daud (2017) may, and most likely, would be

different and therefore may have had higher contamination. The results seen in BEAS-2Bs, reported by Daud (2017), may therefore be an artefact due to trace contamination, potentially explaining the difference between the two observations. When Coster *et al.* (2017) compared rWNT3A 5036-WN (75% purity) to purer version 5036-WNP (90% purity), the higher purity did not induce SMAD2/3 phosphorylation, supporting the potential for this theory further.

6 OVERALL DISCUSSION

The airway epithelium provides a physical, chemical and immunological barrier against inhaled pathogens. The combined effectiveness of each of these barrier functions protects the lungs against environmental challenges. GWAS studies have identified numerous epithelial susceptibility genes in asthmatics, which may contribute to dysregulated repair. If the EMTU model is correct in saying that a defective epithelium consequently leads to repetitive environmental challenge, which results in a persistent inflammatory response and airway injury that drives pathological remodelling (Shifren *et al.* 2012), then it is paramount to identify the cell signalling pathways involved in airway restitution and delineate mechanisms which could be manipulated to enhance repair. This is especially true considering evidence suggests recommended asthma therapies such as β -agonists (Schnackenberg *et al.* 2006) (Wadsworth, Nijmeh and Hall 2006) and ICSs attenuate epithelial repair (Yu, Jiang and Sun 2020) (Li *et al.* 2020) (Liu *et al.* 2013) (Wadsworth *et al.* 2006). It is important to note, however, that Wadsworth *et al.* (2006), also reported that although Dexamethasone diminishes the healing response, Dexamethasone beneficially extended ALI culture longevity when subjected to repetitive damage. Nonetheless, this indicates the necessity of a therapeutic targeting epithelial repair in order to negate the negative impact of these asthma therapies on early airway epithelial repair, to restore barrier function and impede airway remodelling.

WNT5A and TGF- β 1 signalling are two of the signalling pathways that may mediate epithelial repair, and also express a strong association with development of asthma (Singhania *et al.* 2017) (Barreto-Luis *et al.* 2017). TGF- β 1 expression is also linked with airway remodelling (Murdoch and Lloyd 2010) (Hough *et al.* 2020). For this reason, these two signalling pathways and their potential crosstalk were selected for further investigation. As mentioned previously, the effect of TGF- β on wound closure is controversial, with conflicting outcomes being reported in similar cellular contexts. The scratch wound assays conducted support a diminishing effect on repair in the presence of WNT5A, which was effectively reversed by TAK1 inhibition. This does not support my hypothesis that

TGF- β 1 promotes WNT5A signalling to potentiate TGF- β 1-mediated cellular migration in HBEC wound repair, and in fact suggests the opposite. Additionally, TGF- β 1 stimulation did not influence WNT5A receptor expression (ROR2 and FZD4), but it did appear to down-regulate WNT5A transcription, again refuting my hypothesis. This was not significant, but a downregulation in WNT5A mRNA was observed in both BEAS-2Bs and HBECs suggesting that an association exists, but that sample size was not enough to reach statistical significance. Referring to section 1.15 and what is considered signalling crosstalk, the data provided in this thesis does not fully establish evidence of crosstalk, as an endpoint of which the two signalling pathways converge has not been identified, as defined in **Figure 6.1**. WNT5A did not induce SMAD2/3 phosphorylation or EMT, which are crosstalk mechanisms in other cell types (Beljaars *et al.* 2017) (Miyoshi *et al.* 2012) (Borcherding *et al.* 2015). However, this does not definitively mean crosstalk does not exist between WNT5A and TGF- β 1, as other endpoints may exist which have not been investigated. Conversely, TGF- β 1 may inhibit WNT5A transcription in order to promote canonical WNT signalling, of which there are also numerous studies identifying crosstalk between these two pathways within epithelium (Nlandu-Khodo *et al.* 2017) (Sun *et al.* 2015) (Kwak *et al.* 2015).

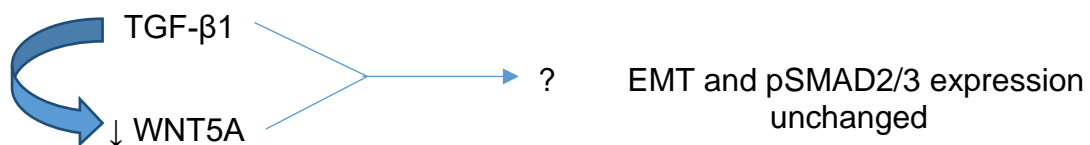


Figure 6.1 Summary of WNT5A and TGF- β 1 Crosstalk Results

The benefit of targeting epithelial repair is that its clinical applications would be applicable for all endotypes, offering the long overdue therapeutic advancement required particularly for type2-low asthmatics. With poor adherence to ICS, offering another type of treatment may be beneficial to steer away from over reliance on short- and long-acting beta agonists, which are associated with uncontrolled asthma and death (Gauvreau *et al.* 1997) (Spitzer *et al.* 1992) (Royal College of Physicians 2014). As the epithelium can repair rapidly within 24 hours, the symptomatic effects could be seen quite quickly, but it would most

likely induce greater benefits after at least two weeks of administration given the time epithelial cells need to differentiate. Also, as ALI cultures possess increased proliferation and cell cycle genes compared to uncultured cells (Dvorak *et al.* 2011), the wound healing response may take longer *in vivo*. Through increasing barrier effectiveness, allergens and infective agents infiltrating the epithelium will be decreased, reducing the pursuant inflammatory response. Corticosteroid use, and biologics, can then further dampen the inflammatory response.

The results of the wound healing assay highlight TAK1 may be a potential therapeutic target to enhance airway epithelial wound repair. TGF- β 1 expression, although controversial in whether it correlates with asthma severity, if increased in the airway epithelium may reduce airway epithelial repair. In order to therapeutically target TAK1 to enhance wound healing, the impact on other airway structural or trafficked cells would need to be considered. Favourably, TAK1 inhibition is reported to reduce TH1 and TH17 cell frequencies (Courties *et al.* 2010); as TH17 is associated with more severe disease and steroid-resistance, TAK1 inhibition may therefore provide dual-therapeutic effects on both inflammation and epithelial repair. Through reversing steroid-resistance, if Dexamethasone does in fact inhibit initial wound healing but prolong regenerative capacity during airway repair as reported by Wadsworth *et al.* (2006), then TAK1 inhibition can enhance the immediate wound response, and Dexamethasone can support long-term repair following repetitive injury and promote ciliogenesis as reported by Khan *et al.* (2016). Caution however would need to be exercised, as WNT-mediated effects by corticosteroids can induce osteoporosis (Li *et al.* 2013), and dysregulated WNT signalling is associated with cancer and bone related toxicity risks (Moore *et al.* 2019). By using inhalers as the application, targeting epithelial repair could at least be localised to the bronchial airway, reducing systemic effects.

6.1 Further Work

TGF- β 1 pre-stimulation, and the inhibition of noncanonical TGF- β signalling via Takinib, had a significant effect on WNT5A stimulated culture wound healing,

suggestive of crosstalk between noncanonical WNT and noncanonical TGF- β signalling in HBEC repair. WNT5A stimulation, however, did not have a significant effect on wound healing alone. This may be due to a relatively low sample size, and so it may be beneficial to conduct a power calculation using the preliminary data conducted in this thesis to identify the n number required for sufficient statistical power, and perform the additional experiments if cost effective to do so. If WNT5A was found to significantly enhance repair, investigating the effect of corticosteroids in tandem with WNT5A, TGF- β 1 and Takinib in a repeat wounding assay may identify if TAK1 inhibition, along with corticosteroids, would increase immediate wound healing whilst also prolonging proliferative ability of basal cells to promote repair over long-term damage-repair cycles.

Additionally, the scratch wound assay does not consider the complex interactions between the epithelial and mesenchymal compartments within the EMTU. As such, further airway wound healing investigations would incorporate fibroblast co-culture to more appropriately model the lung environment. As TGF- β 1 can induce WNT5A expression in fibroblasts and smooth muscle (Newman *et al.* 2016) (Baarsma *et al.* 2017) (Contreras *et al.* 2020) (Kumawat *et al.* 2014) (Newman *et al.* 2016), this cell-cell communication may promote epithelial wound healing through increasing WNT5A protein expression available to epithelial cells.

TGF- β 1 stimulation also induced a non-significant trend in downregulating WNT5A at the transcriptional level in both BEAS-2Bs and iHBECs. It would be useful to repeat this with primary, differentiated HBECs to see if the same observation is made. As mentioned within this overall discussion, it would also be useful to assess transcriptional activity of the canonical WNT β -catenin pathway alongside WNT5A mRNA expression to identify if TGF- β 1 downregulates noncanonical WNT signalling to promote the canonical axis. It would also be useful to assess WNT5A at the protein level. Therefore, further transfection studies would be conducted to assess the WNT5A/B antibody

#2530, as Newman *et al.* (2016) reported specific antibody binding to WNT5A overexpressed cell lysate by western blot.

6.2 Conclusion

To summarise, the findings for each chapter will briefly be recapped. The bronchial epithelial brush transcriptomics analysis identified a significant, positive correlation between noncanonical WNT and TH17 status, and a significant, negative correlation between noncanonical TGF- β signalling and TH2 status. Although outside the scope of this thesis, this may be of importance and warrants further investigation.

ALI culture wound healing was rapid, with full closure evident 24 hours post-wounding in most donors. Prior to wounding, a 48-hour rhTGF- β 1 stimulation significantly increased TEER of healthy cultures compared to vehicle control. The mechanism behind this is unknown, but mucus secretion did appear to be enhanced following the stimulation. Neither rhWNT5A nor rhTGF- β 1 stimulation had a significant effect on wound healing or TEER compared to basal conditions, but this may be partly due to low sample size and being statistically underpowered. In support of this, rhTGF- β 1 did have a significant effect on wound healing across all conditions combined, and both TGF- β 1 signalling and its inhibition with Takinib had a significant effect on WNT5A-mediated wound healing suggestive of crosstalk in HBEC repair. Although WNT5A-TGF- β 1 crosstalk has been investigated in ASM and fibroblasts, this is the first study to my knowledge investigating WNT5A-TGF- β 1 crosstalk in primary HBEC cultures.

As CBF is important in mucociliary clearance, CBF was assessed in healthy and asthma patients and correlated with FEV₁/FVC to identify if mucociliary clearance worsens with lung function. In agreement with some studies in the literature, CBF and pattern did not significantly differ between asthma and health. A 30-60 and 60-90-minute WNT5A stimulation also conferred no effect on CBF. However, surprisingly, a non-significant, but negative trend in correlation was found

between CBF and FEV₁/FVC, and CBF and percentage of normal cilia, and a significant positive correlation was found between percentage of static cilia and FEV₁/FVC. This controversial finding may potentially be due to the ciliogenic effects of corticosteroids.

On investigating the relationship further between WNT5A and TGF- β 1 signalling, TGF- β 1 stimulation was found to induce a non-significant but trending downregulation in WNT5A mRNA in both BEAS-2Bs and iHBECs compared to basal conditions, corroborating the potential for WNT5A and TGF- β 1 crosstalk. Protein expression of FZD4 and ROR2 receptor expression however was unchanged. The change in WNT5A expression could not be investigated at the protein level because the three WNT5A antibodies tested by transient transfection (clones A-5, 3A4 and 6F2) lacked affinity for epitope binding or binding was not specific in the applications tested. Numerous novel flow cytometry panels were set up to investigate potential mechanisms of crosstalk. However, WNT5A did not induce early EMT or pSMAD2/3 expression, which are reported crosstalk mechanisms in other cell types.

To conclude, the data provided in this thesis does not fully establish evidence of WNT5A and TGF- β 1 crosstalk, as an endpoint of which one pathway potentiates or negates the other was not elucidated. As TGF- β 1 inhibits WNT5A transcription and WNT5A-mediated effects on wound healing, this suggests negative crosstalk may exist between these two pathways. Crosstalk mechanisms evident in other cell types (EMT induction and SMAD phosphorylation) were not evident in differentiated ALI cultures, and so further investigation is required to identify whether crosstalk truly exists.

7 APPENDIX

7.1 APPENDIX 1

Table 7.1 List of Reagents Used for Cell Culture

Reagent	Supplier	Cat No
Dulbecco's Phosphate Buffered Saline	Sigma Aldrich	D8537
PureCol Solution	Advanced BioMatrix	5005
Bronchial Epithelial Growth Medium	Lonza	CC-3170
Gibco LHC-9 Medium	Fisher Scientific	11508866
Gibco DMEM, high glucose, no glutamine	Fisher Scientific	11500416
PneumaCult™-ALI media	StemCell Technologies	05001
PneumaCult™-Ex Plus media	StemCell Technologies	05040
Hydrocortisone Stock Solution	StemCell Technologies	07925
Heparin Solution	StemCell Technologies	07980
Gibco Antibiotic/Antimycotic 100x	Fisher Scientific	11570486
Gibco Fungizone	Fisher Scientific	11520496
Penicillin-streptomycin	Sigma Aldrich	P4333
Gibco™ Fetal Bovine Serum, One Shot™ format	Fisher Scientific	15595309
Gibco Trypsin/EDTA Solution	Fisher Scientific	11677104
Trypsin/EDTA	Sigma Aldrich	T3924
Corning Transwell 12mm 0.4µm pore polyester transwell	Fisher Scientific	10565482

7.2 APPENDIX 2

4. [E18D65](#) Mass: 43763 Score: 498 Queries matched: 28 emPAI: 3.94
 Protein Wnt OS=Bos taurus GN=WNT5A PE=3 SV=1

Query	Observed	Mr(expt)	Mr(calc)	ppm	Miss	Score	Expect	Rank	Peptide
49	365.7249	729.4353	729.4385	-4.32	1	38	0.0039	1	R.KVGDALK.E
54	368.6818	735.3491	735.3551	-8.24	0	30	0.013	1	K.EFVDAR.E
60	379.1765	756.3385	756.3443	-7.57	0	27	0.0074	1	R.GYDQFK.T
91	403.7112	805.4079	805.4116	-4.59	0	37	0.0056	1	R.VIQIGSR.E
100	408.2388	814.4630	814.4661	-3.81	0	40	0.0034	1	K.LVQVNSR.F
126	430.2454	858.4762	858.4811	-5.70	1	60	3.4e-005	1	K.VGDALKEK.Y
134	442.6965	883.3785	883.3858	-8.22	0	48	7.1e-005	1	K.YDSAAAMR.L
275	329.8641	986.5704	986.5760	-5.71	2	39	0.0033	1	R.KVGDALKEK.Y
285	500.7963	999.5781	999.5825	-4.41	1	36	0.0071	1	R.GKLVQVNSR.F
467	571.2640	1140.5135	1140.5233	-8.58	1	48	0.00017	1	K.EKYDSAAAMR.L
829	655.3195	1308.6244	1308.6285	-3.15	0	39	0.002	1	K.TCWLQLADFR.K
926	461.2356	1380.6849	1380.6932	-6.03	0	(28)	0.036	1	R.ILMNLHNEAGR.R
936	699.3475	1396.6804	1396.6881	-5.52	0	73	8.4e-007	1	R.ILMNLHNEAGR.R 937
939	699.8208	1397.6270	1397.6319	-3.50	0	17	0.14	1	K.CTEIVDQFVCK.-
1021	477.2309	1428.6710	1428.6820	-7.71	1	38	0.0018	1	K.TGIKECQYQFR.H
1028	479.9138	1436.7195	1436.7235	-2.78	1	31	0.015	1	K.TCWLQLADFRK.V
1311	385.2036	1536.7853	1536.7943	-5.82	1	(11)	1.9	1	R.ILMNLHNEAGR.R.T
1331	518.5992	1552.7759	1552.7892	-8.57	1	28	0.034	1	R.ILMNLHNEAGR.R.T 1332 1333
1897	897.8094	1793.6042	1793.6147	-5.86	0	53	4.9e-006	1	K.TSEGIDGCELMCCGR.G
2162	973.9077	1945.8009	1945.8054	-2.31	0	59	2e-006	1	R.DNLWGGCGDNIDYGYR.F 2161
2358	548.5142	2190.0275	2190.0350	-3.41	1	4	7	1	K.KLCHLYQDHMOYIGEGAK.T
2458	1214.5389	2427.0633	2427.0702	-2.85	1	50	5.6e-005	1	K.DLPRDNLWGGCGDNIDYGYR.F 2459
2488	1244.0760	2486.1375	2486.1424	-1.96	0	61	1.1e-005	1	R.FNSPTTQDLVYIDPSDYCVR.N

Proteins matching the same set of peptides:
[P41221](#) Mass: 43680 Score: 498 Queries matched: 28
 Protein Wnt-5a OS=Homo sapiens GN=WNT5A PE=1 SV=2

5. [Q9H177](#) Mass: 41665 Score: 200 Queries matched: 9 emPAI: 0.79
 Protein Wnt-5b OS=Homo sapiens GN=WNT5B PE=2 SV=2

Query	Observed	Mr(expt)	Mr(calc)	ppm	Miss	Score	Expect	Rank	Peptide
54	368.6818	735.3491	735.3551	-8.24	0	30	0.013	1	K.EFVDAR.E
91	403.7112	805.4079	805.4116	-4.59	0	37	0.0056	1	R.VIQIGSR.E
134	442.6965	883.3785	883.3858	-8.22	0	48	7.1e-005	1	K.YDSAAAMR.V
467	571.2640	1140.5135	1140.5233	-8.58	1	48	0.00017	1	K.EKYDSAAAMR.V
1897	897.8094	1793.6042	1793.6147	-5.86	0	53	4.9e-006	1	K.TSEGIDGCELMCCGR.G
2162	973.9077	1945.8009	1945.8054	-2.31	0	47	3.4e-005	2	R.DNLWGGCGDNVEYGYR.F 2161
2458	1214.5389	2427.0633	2427.0702	-2.85	1	39	0.0008	2	K.DLPRDNLWGGCGDNVEYGYR.F 2459

Figure 7.1 rhWNT5A Proteomic Results. The first 3 protein hits were for Serum albumin (*Bos Taurus*), ALB protein (*Bos Taurus*) and Serum albumin (*homo-sapiens*). Hits for both *homo-sapien* WNT5A and WNT5B were then observed.

7.3 APPENDIX 3

Table 7.2 Transfection Methods for All Transfection Reagents Tested on ALI Cultures and HEK293T Cell Cultures

	INTERFERin (Polyplus-transfection, cat no 409-01)	Viomer Blue or Green (Cambridge bioscience, cat no VB-01LB-TS, VG-01LB-00)	Lipofectamine 2000 (Thermofisher, cat no 11668030)
Tube 1 (siRNA final concentration will be 20nM)	Pipette 2µl siRNA into 198µl of media without serum. Mix well.	Pipette 2µl siRNA & 8ul Viomer Green/Blue buffer into an Eppendorf	Add 98µl media and 2µl of siRNA (<i>must have 1:1 ratio mix with tube 2</i>)
Tube 2	-	Place 1µl droplet of Viomer onto wall of fresh Eppendorf. Immediately add 90µl of buffer & vortex for 3-5s	Pipette 100µl media and 6µl Lipofectamine into an Eppendorf. Leave for 5 minutes
Complexation	Vortex INTERFERin reagent for 5s & spin down, then add 6µl into tube 1. Immediately vortex for 10s.	Add 90µl of Viomer Sol (Tube 2) into Tube 1. Mix.	Add tube 1 and tube 2 together. Mix.
Incubation time at room temperature	10 minutes	15 minutes	20 minutes
Addition to ALI cells (800ul basally, 200ul apically)	Add 800µl media. Mix. Pipette 800µl basally and 200µl apically	Add 900µl media. Mix. Pipette 800µl basally and 200µl apically	Add 800µl media. Mix. Pipette 800µl basally and 200µl apically
Incubation time at 37°C	5 hours (as the siRNA FAP reporter disappears quickly)		

7.4 APPENDIX 4

Table 7.3 Genes Included in the Canonical WNT Transcriptional Module, With Rationale of Inclusion in the Module

Gene Full Name	Gene I.D.	Rationale
Cadherin 1, type 1 (E-cadherin)	CDH1	Associates with β -catenin to form adherens junctions.
Calpain-1	CAPN1	Cleaves E-cadherin and β -catenin at adherens junction.
Wingless Type MMTV integration site family, member 1/2/2B/3/3A/5A/8A/8B/9A/9B/10A/10B/11/16	WNT1, WNT2 WNT2B, WNT3 WNT3A, WNT5A, WNT8A, WNT8B, WNT9A, WNT9B, WNT10A, WNT10B, WNT11, WNT16	Canonical WNT ligands
Norrin	NDP	Norrin can bind to FZD4 and LRP5/6 to activate the WNT/ β -catenin pathway.
Frizzled class receptor 1/ 2/ 3/ 4/ 5/ 6/ 7/ 8/ 9/ 10	FZD1, FZD2, FZD3, FZD4, FZD5, FZD6, FZD7, FZD8, FZD9, FZD10	WNT Receptors
Low density lipoprotein receptor-related protein 5/6	LRP5 LRP6	WNT signalling Co-receptors
R-spondin1/2/3/4	RSPO1, RSPO2 RSPO3, RSPO4	RSPO are ligands for the LGR receptors. On LGR/RSPO binding, ZNFR3 and RNF43 (which ubiquitinate frizzleds) are inhibited therefore augmenting WNT signalling (increasing response to WNT ligand).
Leucine-rich repeat containing G protein-coupled receptor 4/5/6	LGR4, LGR5, LGR6	
Porcupine	PORCN	Key regulator of the WNT signalling pathway. Mediates the attachment of palmitoleate to WNT proteins,

		which is required for efficient binding to frizzled receptors.
Notum	NOTUM	Key negative regulator of the WNT signalling pathway by specifically mediating palmitoylation of WNT proteins.
Glypican 4 (Knypek on KEGG pathway)	GPC4	GPC4 expression enhances WNT/ β -catenin signalling. Its knockdown suppresses the activation of the WNT/ β -catenin pathway.
Inversin	INVS	Inhibits the canonical WNT pathway by targeting cytoplasmic dishevelled (DVL1) for degradation by the ubiquitin-proteasome.
WNT Inhibitory Factor 1	WIF1	Binds to WNT ligands preventing cell signalling.
Dickkopf 1/2/4	DKK1, DKK2, DKK4	Antagonizes canonical WNT signalling by inhibiting LRP5/6 interaction with WNT and by forming a ternary complex with the transmembrane protein KREMEN that promotes internalization of LRP5/6.
Kringle Containing Transmembrane Protein 1/2	KREMEN1, KREMEN2	Cooperates with Dickkopf to block WNT/ β -catenin signalling.
Serpin Family F Member 1 (PEDF on KEGG pathway)	SERPINF1	Inhibits WNT/ β -catenin signalling by binding to co-receptor LRP6.
Sclerostin	SOST	A ligand for LRP5/6, and thus antagonises WNT signalling by disrupting the FZD-LRP complex formation.
Sclerostin domain containing 1 (WISE)	SOSTDC1	Either increases or decreases canonical WNT signalling, depending on cellular context.
BMP and activin membrane-bound inhibitor	BAMBI	Promotes canonical WNT signalling. BAMBI knockdown reduced WNT β -catenin signalling.
Secreted Frizzled-Related Protein 1/2/4/5	SFRP1, SFRP2, SFRP4, SFRP5	Soluble modulators of WNT signalling. By binding to WNT ligands they prevent WNT-FZD binding.
Casein kinase 1, epsilon	CSNK1E	Dishevelled (Dvl) becomes phosphorylated by CK1 ϵ upon pathway activation by WNTs

Dishevelled segment polarity protein ½/3	DVL1, DVL2, DVL3	Dishevelled proteins are cytoplasmic phosphoproteins that act directly downstream of Frizzled receptors.
Naked cuticle homolog ½	NKD1, NKD2	Nkd is a Dishevelled-binding protein that functions as a negative regulator of the WNT β-catenin pathway.
Frequently rearranged in advanced T-cell lymphomas ½	FRAT1, FRAT2	Inhibits GSK-3-mediated phosphorylation of β-catenin and positively regulates the WNT signalling pathway.
Casein kinase 2 alpha 1 polypeptide Casein kinase 2, alpha prime polypeptide Casein kinase 2, beta polypeptide Casein kinase 2, alpha 3 polypeptide	CSNK2A1, CSNK2A2, CSNK2B, CSNK2A3	Is activated via dishevelled 2 (DVL2) in WNT-β-catenin signalling. Inhibiting CK2, represses TCF/LEF dependent transcription.
Glycogen Synthase Kinase 3 β (GSK3β)	GSK3B	Part of the β-catenin APC/Axin destruction complex.
Axin 1/ 2	AXIN, AXIN2	Part of the β-catenin APC/Axin destruction complex.
Adenomatous polyposis coli Adenomatous polyposis coli 2	APC, APC2	A tumour suppressor protein that acts as an antagonist of the β-catenin WNT signalling pathway in APC/Axin destruction complex.
Casein kinase 1 α1 Casein kinase 1 α1 like	CSNK1A1 CSNK1AL	Part of the β-catenin APC/Axin destruction complex.
β Catenin	CTNNB1	Critical for canonical WNT signalling
β Catenin Interacting Protein 1	CTNNBIP1	Negative regulator of WNT signalling – binds CTNNB1 to prevent TCF interaction.
Chromodomain helicase DNA binding protein 8 (Duplin on KEGG pathway)	CHD8	It binds β-catenin and negatively regulates the WNT signalling pathway.
Presenilin 1	PSEN1	PSEN1 is a negative regulator of β-catenin signalling. PSEN1 deficiency enhances β-catenin signalling.
Protein kinase, Camp-dependent, catalytic, alpha PKA Protein kinase, Camp-dependent, catalytic, beta PKA	PRKACA, PRKACB, PRKACG	PKA activators increased the cytoplasmic and nuclear β-catenin protein level. They phosphorylate β-catenin preventing its ubiquitination. There is also evidence to suggest PKA activators

Protein kinase, Camp-dependent, catalytic, gamma PKA		can inhibit the β -catenin pathway so perhaps it's cell context dependent.
Creb Binding Protein	CREBBP	CREBBP can influence β -catenin signalling by acting as a co-transcriptional factor.
Mitogen-activated protein kinase kinase kinase 7 (TAK1)	MAP3K7	TAK1 inhibits CTNNB1 transcriptional activity via NLK.
Nemo-like Kinase	NLK	NLK inhibits CTNNB1 transcriptional activity.
Transducin-like enhancer of split 1	TLE1	TLE1 inhibits FOXA2, NF κ B, β -catenin and TGF- β signalling
Transcription factor 7 (T-cell specific, HMG-box) Transcription factor 7-like 1 (T-cell specific, HMG-box) Transcription factor 7-like 2 (T-cell specific, HMG-box)	TCF7 TCF7L1 TCF7L2	Transcription factors that plays a key role in the canonical WNT signalling pathway
Lymphoid enhancer-binding factor 1	LEF1	
V-myc avian myelocytomatosis viral oncogene homolog	MYC	Target genes of canonical WNT signalling
Jun proto-oncogene	JUN	

Table 7.4 Genes Included in the Non-Canonical WNT Transcriptional Module, With Rationale of Inclusion in the Module

Gene Full Name	Gene I.D.	Rationale
Nuclear Factor kappa beta (P50)	NFKB1	WNT5A signals through MAP3K7-NFkB. There is also a NFkB binding site within the WNT5A promoter.
Transducin-like enhancer of split 1	TLE1	TLE1 inhibits FOXA2, NFkB, β -catenin and TGF- β signalling.
Cut-like homeobox 1	CUX1	Transcription factors found within promoters for WNT5A.
Forkhead Box A2	FOXA2	
Sp1 transcription factor	SP1	
cMyb	MYB	
Paired box 2	PAX2	
Wingless Type MMTV integration site family, member 2B/4/5A/5B/6/7A/7B/9A/9B/11/16	WNT2B, WNT4, WNT5A, WNT5B, WNT6, WNT7A, WNT7B, WNT9A, WNT9B, WNT11, WNT16	
Norrin	NDP	Norrin can bind to FZD4. FZD4 is also a WNT5A receptor, so may act as a competitive antagonist through FZD4 binding.
Frizzled class receptor 1/ 2/ 3/ 4/ 5/ 6/ 7/ 8/ 9/ 10	FZD1, FZD2, FZD3, FZD4, FZD5, FZD6, FZD7, FZD8, FZD9, FZD10	WNT Receptors
Receptor Tyrosine Kinase-like Orphan Receptor 1/2	ROR1, ROR2	ROR1 is a WNT5B receptor. ROR2 is a WNT5A noncanonical receptor.
Receptor-like Tyrosine Kinase	RYK	A WNT5A Receptor
Melanoma Cell Adhesion Molecule/MUC18/CD146	MCAM	WNT5A uses CD146 as a receptor to regulate cell motility and convergent extension, and is upregulated by IL-13 in asthma.
R-spondin1/2/3/4	RSPO1, RSPO2, RSPO3, RSPO4	RSPO are ligands for the LGR receptors. On LGR/RSPO binding,

Leucine-rich repeat containing G protein-coupled receptor 4/5/6	LGR4, LGR5, LGR6	ZNFR3 and RNF43 (which ubiquitinate frizzleds) are inhibited therefore augmenting WNT signalling (increasing response to WNT ligand)
Porcupine	PORCN	Key regulator of the WNT signalling pathway. Mediates the attachment of palmitoleate to WNT proteins, which is required for efficient binding to frizzled receptors.
Notum	NOTUM	Key negative regulator of the WNT signalling pathway by specifically mediating palmitoylation of WNT proteins.
Glypican 4 (Knypek on KEGG pathway)	GPC4	GPC4 expression enhances noncanonical WNT signalling. WNT5A has a higher affinity for binding to GPC4 than WNT3A. GPC4 knockdown decreases WNT5A signalling.
Inversin	INVS	Inhibits the canonical WNT pathway by targeting cytoplasmic dishevelled (DVL1) for degradation by the ubiquitin-proteasome, and acts as a molecular switch between canonical and noncanonical WNT signalling cascades.
WNT Inhibitory Factor 1	WIF1	Binds to WNT ligands preventing cell signalling.
Dishevelled segment polarity protein 1/2/3	DVL1, DVL2, DVL3	Dishevelled proteins are cytoplasmic phosphoproteins that act directly downstream of Frizzled receptors.
Naked cuticle homolog 1/2	NKD1, NKD2	Nkds can antagonise both the canonical and noncanonical PCP WNT pathway.
Secreted Frizzled-Related Protein 1/2/4/5	SFRP1, SFRP2, SFRP4, SFRP5	Soluble modulators of WNT signalling.
VANGL Planar Cell Polarity Protein 1/2	VANGL1, VANGL2	Core PCP scaffolding proteins necessary for the assembly of PCP signalling complexes.
Phospholipase C β 1/ β 2/ β 3/ β 4	PLCB1, PLCB2, PLCB3, PLCB4	Involved in WNT-Ca ²⁺ pathway.
Protein Kinase C α / β / γ	PRKCA, PRKCB, PRKCG	Involved in WNT-Ca ²⁺ pathway.

Cell division cycle 42	CDC42	PKCa (WNT-Ca ²⁺ pathway) may activate CDC42. Important for cytoskeletal organisation and cell motility.
Mitogen-activated protein kinase kinase 7	MAP2K7	Involved in WNT-ROR2 pathway.
Calcium/calmodulin-dependent protein kinase II $\alpha/\beta/\delta/\gamma$	CAMK2A, CAMK2B, CAMK2D, CAMK2G	CAMKII is involved in the WNT Ca ²⁺ pathway.
Mitogen-activated protein kinase kinase kinase 7 (TAK1)	MAP3K7	Common to both TGF- β and WNT5A pathway. TAK1 is downstream of WNT Ca ²⁺ pathway. It inhibits CTNNB1 transcriptional activity via NLK.
Dishevelled associated activator of morphogenesis 1	DAAM1	Part of PCP pathway. Thought to function as a scaffolding protein for the WNT-induced assembly of a dishevelled (Dvl)-Rho complex. DVL2 & DAAM1 activate profilin1 - actin cytoskeleton changes.
Dishevelled associated activator of morphogenesis 2	DAAM2	Daam2 plays a functional role in non-canonical WNT signalling but Daam2 in contrast to Daam1 regulates vertebrate neural tube closure.
Ras homolog family member A	RHOA	Common to both TGF- β and WNT5A pathway for cytoskeletal organization and cell motility.
Rho associated coiled-coil containing protein kinase 2	ROCK2	Involved in WNT PCP pathway.
Ras-related C3 botulinum toxin substrate 1 (rho family, Rac1/2/3)	RAC1, RAC2, RAC3	DVL-Rac activates JNK. Important for cytoskeletal organisation and cell motility.
Filamin A	FLNA	Involved in WNT5A-ROR2 signalling.
Calpain-1	CAPN1	Mediates cleavage of Filamin A in WNT5A signalling.
Mitogen-activated protein kinase 8/9/10 (JNK)	MAPK8, MAPK9, MAPK10	JNK proteins are activated in the PCP pathway.
Mitogen-activated protein kinase 11/12/13/14	MAPK11, MAPK12,	P38 MAPK pathway proteins (labelled p38 on MAPK KEGG

	MAPK13, MAPK14	pathway) – part of noncanonical WNT Ca ²⁺ pathway.
Protein Phosphatase, Mg ²⁺ /Mn ²⁺ dependent, 1A	PPM1A	Shown to inhibit the activation of p38 and JNK kinase cascades induced by environmental stresses.
Protein phosphatase 3, catalytic subunit, α/β/γ isozyme Protein phosphatase 3, regulatory subunit B, α/β	PPP3CA, PPP3CB, PPP3CC, PPP3R2, PPP3R1,	Calcineurin A - Part of WNT Ca ²⁺ pathway. Activates NFAT.
Nemo-like Kinase	NLK	TAK1 (downstream of WNT-Ca ²⁺ pathway can inhibit β-catenin transcriptional activity through NLK.
Nuclear factor of activated T-cells 1/2/3/4	NFATC1, NFATC2, NFATC3, NFATC4	Transcription factor family regulated by calcium signalling.
Runt-related Transcription Factor 2	RUNX2	WNT signalling induces RUNX2. TGFBR1 is a RUNX2 -sensitive gene.
Creb Binding Protein	CREBBP	Noncanonical WNT has been reported to signal through the JNK-CREB pathway in the developing heart to mediate transcriptional activity of TGF-β2.
E1A binding protein p300	EP300	EP300 can bind to TCF4 to repress TCF4 WNT induced signalling.

Table 7.5 Genes Included in the Canonical TGF- β Transcriptional Module, With Rationale of Inclusion in the Module

Gene Full Name	Gene I.D.	Rationale
Transducin-like enhancer of split 1	TLE1	TLE1 inhibits FOXA2, NF κ B, β -catenin and TGF- β signalling
Integrin α 6	ITGA6	Integrin expressed highly in HBECs
Thrombospondin-1	THBS1	Activates latent TGF- β
Decorin	DCN	Decorin has been shown to either enhance or inhibit the activity of TGF- β 1.
Runt-related Transcription Factor 2	RUNX2	WNT signalling induces RUNX2. TGFBR1 is a RUNX2 -sensitive gene.
Transcription Factor 4	TCF4	RUNX2 and TCF4 functionally associate to induce TGFBR1
Transforming Growth Factor - β 1	TGFB1	
Transforming Growth Factor β Receptor 1 (ALK5) Transforming Growth Factor β Receptor 2	TGFBR1, TGFBR2	TGFB1 type 1 and 2 receptor.
Transforming Growth Factor β Receptor 3	TGFBR3	Glucocorticoids may act as a switch between TGF- β R1/SMAD2/3 signalling to ACVRL1/SMAD1 signalling following glucocorticoids exposure.
BMP and activin membrane-bound inhibitor	BAMBI	Pseudoreceptor for TGF- β R1.
SMAD specific E3 ubiquitin protein ligase 1/2	SMURF1, SMURF2	Regulates SMAD1, SMAD2, SMAD3, SMAD6 and SMAD7. It enhances the inhibitory action of SMAD7 while reducing the transcriptional activities of SMAD2.
SMAD family member 2/3/4	SMAD2, SMAD3, SMAD4	TGF- β R-SMAD
SMAD family member 6/7	SMAD6, SMAD7	Inhibitory SMADs
SMAD family member 9	SMAD9	BMP R-SMAD
Zinc finger, FYVE domain containing 9	ZFYVE9	Interacts directly with SMAD2 and SMAD3, and recruits SMAD2 to the TGF- β R.

Zinc finger, FYVE domain containing 16 (Endofin)	ZFYVE16	Endofin interacts with SMAD4 to mediate SMAD complex formation facilitating TGF- β signalling.
TGFB-induced factor homeobox 1	TGIF1	TGIF1 represses canonical TGF- β signalling by binding directly to DNA or by interacting with SMAD complexes.
TGFB-induced factor homeobox 2	TGIF2	Represses TGF- β transcription by recruiting histone deacetylases to TGF- β -responsive genes and by interacting with TGF- β activated SMADs to repress TGF- β induced transcription.
Transmembrane prostate androgen-induced protein (TMEPAI)	PMEPAI	Interferes with TGF- β R1 SMAD phosphorylation.
Ski Like Proto-Oncogene (SnoN)	SKIL	Co-repressors of the SMAD signalling complex in TGF- β signalling. Are destabilised in early phase of TGF- β signalling.
SKI Proto-Oncogene	SKI	
Creb Binding Protein	CREBBP	WNT-PKA pathway and TGF- β SMAD3/4-PKA pathway induces CREB. Could potentially be crosstalk through this transcription factor.
E1A binding protein p300	EP300	It mediates cAMP-gene regulation by binding specifically to phosphorylated CREB protein.
Sp1 transcription factor	SP1	Transcription factor Sp1 is required for TGF- β -induced EMT.
V-myc avian myelocytomatosis viral oncogene homolog	MYC	TGF- β has been shown to inhibit growth by reducing c-myc expression and p15 INK.
Cyclin Dependent Kinase Inhibitor 2B (p15/Ink4b)	CDKN2B	The SMAD complex cooperates with Sp1 to induce p15 transcription.

Table 7.6 Genes Included in the Non-Canonical TGF- β Transcriptional Module, With Rationale of Inclusion in the Module

Gene Full Name	Gene I.D.	Rationale
Integrin α 6	ITGA6	Integrin expressed highly in HBECs
Thrombospondin-1	THBS1	Activates latent TGF- β .
Decorin	DCN	Decorin has been shown to either enhance or inhibit the activity of TGF- β 1.
Runt-related Transcription Factor 2	RUNX2	WNT signalling induces RUNX2. TGFBR1 is a RUNX2-sensitive gene.
Transcription Factor 4	TCF4	RUNX2 and TCF4 functionally associate to induce TGF- β R1.
Transforming Growth Factor - β 1	TGFB1	
Transforming Growth Factor β Receptor 1 (ALK5) Transforming Growth Factor β Receptor 2	TGFBR1, TGFBR2	TGFB1 type 1 and 2 receptor.
Transforming Growth Factor β Receptor 3	TGFBR3	Glucocorticoids may act as a switch between TGFBR1/SMAD2/3 signalling to ACVRL1/SMAD1 signalling following glucocorticoids exposure.
BMP and activin membrane-bound inhibitor	BAMBI	Pseudoreceptor for TGF- β R1.
Mitogen-activated protein kinase kinase kinase 7 (TAK1)	MAP3K7	TAK1 in noncanonical TGF- β 1 pathway.
Nemo-like Kinase	NLK	Noncanonical TGF- β signalling includes a TAK1-NLK cascade.
Mitogen-activated protein kinase kinase kinase 14	MAP3K14	NIK (NF- κ B-inducing kinase) on MAPK signalling pathway. Downstream of TAK1, it forms a complex with IKK to activate NF κ B signalling.
IKK- α	CHUK	Subunits of IKK. 2 subunits which make up the catalytic subunit of the I κ B kinase complex which inhibits the NF κ B complex (NF κ B proteins + I κ B α) until phosphorylation. Once the I κ B α protein is phosphorylated, NF κ B is activated and can translocate into the nucleus.
IKK- β	IKBKB, IKBKG	
Nuclear Factor kappa beta (P50)	NFKB1, NFKB2,	These proteins are the most abundant form of NF κ B. TGF- β can

V-rel avian reticuloendotheliosis viral oncogene homolog A/B	RELA, RELB	signal through TAK1 to mediate TGF- β induced NF- κ B activation.
Nuclear factor of kappa light polypeptide gene enhancer in B-cells inhibitor, alpha	NFKB1A	Interacts with REL dimers to inhibit NF- κ B/REL complexes.
Transducin-like enhancer of split 1	TLE1	TLE1 inhibits FOXA2, NF κ B, β -catenin and TGF- β signalling.
Mitogen-activated protein kinase kinase 4/7	MAP2K4, MAP2K7	MKK4 and MKK7 on MAPK KEGG pathway which signals through JNK. TGF- β KEGG pathway highlights a TGF-JNK-MAPK signalling pathway.
Mitogen-activated protein kinase 8/9/10 (JNK)	MAPK8, MAPK9, MAPK10	JNK proteins involved in TGF-JNK signalling pathway.
Nuclear factor of activated T-cells 1/3	NFATC1, NFATC3	Transcription factor family regulated by calcium signalling. JNK signalling inhibits them.
Death-domain associated protein	DAXX	Daxx is involved in TGF- β -JNK activation.
Mitogen-activated protein kinase kinase kinase 5	MAP3K5	ASK1 on MAPK pathway. Activates MAP2K3/MAP2K6.
Mitogen-activated protein kinase kinase 3/6	MAP2K3, MAP2K6	MKK3 on MAPK pathway. MKK6 on MAPK pathway. Activates p38.
TNF receptor-associated factor 2 TNF receptor-associated factor 6, E3 ubiquitin protein ligase	TRAF2, TRAF6	TRAF6 binds to the TGF- β R to activate TAK1 downstream signalling. TRAF2 inhibition suppresses TGF- β induced EMT in lung cancer through the down-regulation of TGF- β R1 mRNA levels suggesting a supportive role in TGF- β signalling.
Mitogen-activated protein kinase 11/12/13/14	MAPK11, MAPK12, MAPK13, MAPK14	P38 MAPK pathway proteins (labelled p38 on MAPK KEGG pathway).
Ras homolog family member A	RHOA	TGF- β -induces cytoskeletal reorganisation and cell motility

		through RhoA/ROCK1 (as shown on the TGF- β KEGG pathway)
Rho associated coiled-coil containing protein kinase 1	ROCK1	TGF- β -induces cytoskeletal reorganisation and cell motility through RhoA/ROCK1 (as shown on the TGF- β KEGG pathway).
Ras-related C3 botulinum toxin substrate 1 (rho family, Rac1/2/3)	RAC1, RAC2, RAC3	TGF- β R1 activates RAC1 to increase collagen synthesis and motility. In MAPK Kegg pathway, listed alongside CDC42.
Cell division cycle 42	CDC42	TGF- β activates CDC42 to induce cytoskeletal organisation alongside RhoA. In MAPK KEGG pathway, it is listed alongside RAC.
Protein Kinase C α , β , γ	PRKCA, PRKCB, PRKCG	PKC phosphorylates and activates Ras and Raf1 then ERK signalling in the MAPK KEGG pathway.
Protein kinase, cAMP-dependent, catalytic, alpha PKA Protein kinase, cAMP-dependent, catalytic, beta PKA Protein kinase, cAMP-dependent, catalytic, gamma PKA	PRKACA, PRKACB, PRKACG	cAMP-PKA has been reported to negatively regulate TGF- β 1 induced ERK signalling.
Raf-1 proto-oncogene, serine/threonine kinase	RAF1	TGF- β induces Erk activation in mesenchymal cells by phosphorylating Raf-1 to activate phosphatidylinositol 3-kinase (PI3K).
Mitogen-activated protein kinase kinase 1	MAP2K1, MAP2K2	Forms a scaffold complex with ERK leading to its activation. Called MEK1 and MEK2 on MAPK signalling pathway.
Mitogen-activated protein kinase 1/3	MAPK1, MAPK3	ERK proteins 1 and 2.
V-myc avian myelocytomatosis viral oncogene homolog	MYC	TAK1 and c-Myc antagonise each other via acetylation of histone H4 to trigger cellular senescence.
Activating transcription factor 4	ATF4	CREB on MAPK pathway. It is phosphorylated downstream of ERK and p38.

Table 7.7 Genes Included in the WNT TGF- β Overlap Transcriptional Module, With Rationale of Inclusion in the Module

Gene Full Name	Gene I.D.	Rationale
Cut-like homeobox 1	CUX1	Transcription factors found within promoters for WNT5A. There is an association between TGF- β signalling and each of these transcription factors.
Forkhead Box A2	FOXA2	
Sp1 transcription factor	SP1	
cMyb	MYB	
Paired box 2	PAX2	
Porcupine	PORCN	Key regulator of the WNT signalling pathway. Mediates the attachment of palmitoleate to WNT proteins, which is required for efficient binding to frizzled receptors.
Notum	NOTUM	Key negative regulator of the WNT signalling pathway by specifically mediating palmitoylation of WNT proteins.
Glypican 4 (Knypek on KEGG pathway)	GPC4	GPC4 expression enhances noncanonical WNT signalling. GPC4 knockdown decreases WNT5A signalling.
Inversin	INVS	Inhibits the canonical WNT pathway by targeting cytoplasmic dishevelled (DVL1) for degradation by the ubiquitin-proteasome, and acts as a molecular switch between canonical and noncanonical WNT signalling cascades.
WNT Inhibitory Factor 1	WIF1	Binds to WNT ligands preventing cell signalling.
Wingless Type MMTV integration site family, member 5A	WNT5A	
Integrin α 6	ITGA6	Integrin expressed highly in HBECs
Latent-transforming growth factor beta-binding protein 1	LTBP1	Key regulator of TGF- β 1 bioavailability
Thrombospondin-1	THBS1	Activates latent TGF- β .
Decorin	DCN	Decorin is a natural inhibitor of TGF- β 1.
Receptor Tyrosine Kinase-like Orphan Receptor 1/2	ROR2	ROR2 is a WNT5A noncanonical receptor. WNT5A potentiates TGF- β 1 in colonic organoids through ROR2.

Receptor-like Tyrosine Kinase	RYK	WNT5A Receptor
Melanoma Cell Adhesion Molecule/MUC18/CD146	MCAM	WNT5A uses CD146 as a receptor to regulate cell motility and convergent extension, and is upregulated by IL-13 in asthma. CD146 can also be induced by TGF- β .
Frizzled class receptor 2/ 3/ 4/ 5/ 6/ 7/ 8	FZD2, FZD3, FZD4, FZD5, FZD6, FZD7, FZD8	WNT Receptors. TGF- β 1 stimulation has been reported to induce FZD6 and FZD8 in human lung fibroblasts. TGF- β 1 induced FZD8 expression was shown to be SMAD dependent.
Low-density lipoprotein receptor-related protein 5	LRP5	A WNT signalling co-receptor. LRP5 expression induces lung fibrosis through altering TGF- β protein levels. A LRP5 mice knockout study highlighted LRP5 knockdown significantly decreased latent and active TGF- β level.
R-spondin1/2/3/4	RSPO1, RSPO2, RSPO3, RSPO4	RSPO are ligands for the LGR receptors. On LGR/RSPO binding, ZNFR3 and RNF43 (which ubiquitinate frizzleds) are inhibited therefore augmenting WNT sig (increasing response to WNT ligand)
Leucine-rich repeat containing G protein-coupled receptor 4/5/6	LGR4, LGR5, LGR6	RSPO1 and LGR5 are also reported to directly bind and activate TGF- β signalling in colon cancer linking these proteins to both TGF- β and WNT signalling.
Runt-related Transcription Factor 2	RUNX2	Both WNT and TGF- β signalling induce RUNX2. TGFBR1 is a RUNX2 - sensitive gene.
Transcription Factor 4	TCF4	RUNX2 and TCF4 functionally associate to induce TGF- β R1.
Transforming Growth Factor - β 1	TGFB1	
Transforming Growth Factor β Receptor 1 (ALK5) Transforming Growth Factor β Receptor 2	TGFBR1, TGFBR2	TGFB1 type 1 and 2 receptor.
Transforming Growth Factor β Receptor 3	TGFBR3	Glucocorticoids may act as a switch between TGF- β R1/SMAD2/3 signalling to ACVRL1/SMAD1

		signalling following glucocorticoids exposure.
BMP and activin membrane-bound inhibitor	BAMBI	Pseudoreceptor for TGF- β 1. BAMBI can also cooperate with SMAD7 to inhibit TGF- β signalling. BAMBI expression is induced by both TGF- β and canonical WNT signalling. BAMBI can also positively modulate canonical WNT signalling through interacting with FZD-5, LRP6 and DSH enhancing FZD5-DSH signalling.
SMAD specific E3 ubiquitin protein ligase 1/2	SMURF1, SMURF2	Regulates SMAD1, SMAD2, SMAD3, SMAD6 and SMAD7. It enhances the inhibitory action of SMAD7 while reducing the transcriptional activities of SMAD2. Smurf1 has also been reported to negatively regulate canonical WNT signalling through modulating Axin activity.
SMAD family member 2/3/4	SMAD2, SMAD3, SMAD4	SMAD2/3/4 are TGF- β R-SMADs. SMAD3 inhibitor SIS3 increased WNT5A expression in airway smooth muscle cells suggesting SMADs may provide a negative feedback loop between WNT5A and TGF- β . In lens epithelial cells, SIS3 blocked β -catenin delocalisation from the adherens junctions. SMAD3 and 4 have also been reported to form a complex with β -catenin in chondrocytes mediating canonical WNT signalling.
SMAD family member 6/7	SMAD6, SMAD7	Inhibitory SMADs. Literature indicates SMAD7 and β -catenin form a complex to control transcriptional response in myogenic cells. TGF- β NF κ B signalling also promotes SMAD7 expression to suppress canonical WNT signalling and NF κ B signalling. SMAD6 reported to promote neuronal differentiation through inhibiting canonical WNT signalling.

Zinc finger, FYVE domain containing 9	ZFYVE9	Interacts directly with SMAD2 and SMAD3, and recruits SMAD2 to the TGF- β receptor.
Zinc finger, FYVE domain containing 16	ZFYVE16	Endofin interacts with SMAD4 to mediate SMAD complex formation facilitating TGF- β signalling.
TGFB-induced factor homeobox 1	TGIF1	TGIF1 represses canonical TGF- β signalling by binding directly to DNA or by interacting with SMAD complexes. TGIF1 interacts with Axin 1 and 2 to promote canonical WNT signalling.
TGFB-induced factor homeobox 2	TGIF2	Represses TGF- β transcription by recruiting histone deacetylases to TGF- β -responsive genes and by interacting with TGF- β activated SMADs to repress TGF- β induced transcription.
Transmembrane prostate androgen-induced protein (TMEPAI)	PMEPA1	Interferes with TGF- β R1 SMAD phosphorylation. TMEPAI has also been shown to suppress canonical WNT signalling through effecting β -catenin stability. The knockdown of TMEPAI in breast cancer cell lines promoted canonical WNT signalling and increased mRNA of Axin2 and c-MYC.
Ski Like Proto-Oncogene (SnoN)	SKIL	Co-repressors of the SMAD signalling complex in TGF- β signalling. Are destabilised in early phase of TGF- β signalling.
SKI Proto-Oncogene	SKI	
Mitogen-activated protein kinase kinase 4/7	MAP2K4 MAP2K7	MKK4 and MKK7 on MAPK KEGG pathway which signals through JNK. TGF- β KEGG pathway highlights a TGF-JNK-MAPK signalling pathway.
Mitogen-activated protein kinase 8/9/10 (JNK)	MAPK8, MAPK9, MAPK10	JNK proteins. JNK is activated by TGF- β 1 and noncanonical WNT planar cell polarity signalling.
Nuclear factor of activated T-cells 1/3	NFATC1, NFATC3	Transcription factor family regulated by WNT/calcium signalling. NFATC1 and NFATC3 are also shown as transcriptional targets in the TGF- β JNK and p38 MAPK KEGG pathway.

		JNK signalling has been shown to regulate NFATC1-3, but not NFATC4 in cardiomyocytes. Out of these three factors, NFATC2 was excluded due to absence on the p38 MAPK KEGG pathway.
Death-domain associated protein	DAXX	Part of TGF- β JNK and p38 MAPK KEGG pathway. Daxx is also reported to bind to TCF4 to potentiate canonical WNT signalling.
TNF receptor-associated factor 6, E3 ubiquitin protein ligase	TRAF6	TRAF6 binds to the TGF- β R to activate TAK1 downstream signalling. Canonical WNT signalling through WNT3A has been reported to promote binding of LRP5/6 and TRAF6 to activate β -catenin signalling in PC3U (prostate cancer) cells.
Mitogen-activated protein kinase kinase kinase 7 (TAK1)	MAP3K7	TAK1 inhibits CTNNB1 transcriptional activity via NLK. TGF- β has also been reported to induce WNT5A expression through TAK1 signalling in airway smooth muscle cells, suggesting a possible link between TGF- β 1 and the WNT noncanonical and canonical signalling switch.
Protein kinase, cAMP-dependent, catalytic, alpha PKA Protein kinase, cAMP-dependent, catalytic, beta PKA Protein kinase, cAMP-dependent, catalytic, gamma PKA	PRKACA, PRKACB, PRKACG	PKA activators increased the cytoplasmic and nuclear β -catenin protein level. They phosphorylate β -catenin preventing its ubiquitination. There is also evidence to suggest PKA activators can inhibit the β -catenin pathway so perhaps it's cell context dependent. cAMP-PKA has been reported to negatively regulate TGF- β 1 induced ERK signalling. There may be a feedback mechanism here.
Creb Binding Protein	CREBBP	The WNT-PKA pathway and the TGF- β SMAD3/4-PKA pathway induces CREBBP. Both WNT5A and TGF- β 1 also signal through p38 to phosphorylate CREBBP. CREBBP also acts as a co-transcriptional factor for

		WNT- β -catenin signalling. There could potentially be crosstalk through this transcription factor.
Mitogen-activated protein kinase 11/12/13/14	MAPK11, MAPK12, MAPK13, MAPK14	P38 MAPK pathway proteins (labelled p38 on MAPK KEGG pathway). The WNT-PCP pathway and noncanonical TGF- β 1 pathway both activate MAPK signalling.
Nemo-like Kinase	NLK	TAK1 signalling activates NLK. NLK inhibits CTNNB1 transcriptional activity. Both WNT5A and TGF- β 1 are known to activate TAK1-NLK signalling. This may function as a dual feedback mechanism to inhibit canonical WNT signalling.
Ras homolog family member A	RHOA	Common to both the TGF- β and WNT5A PCP KEGG pathway. Induces ROCK1/2 (TGF- β : ROCK1, WNT PCP:ROCK2) for cytoskeletal change.
Ras-related C3 botulinum toxin substrate 1 (rho family, Rac1/2/3)	RAC1, RAC2, RAC3	Activated by both WNT and TGF- β signalling. Plays a role in cytoskeletal organisation and cell motility. DVL-Rac activates JNK in WNT PCP signalling whereas TGF- β R1 activates RAC1 to increase collagen synthesis and motility. In MAPK KEGG pathway, it is listed alongside CDC42.
Protein Kinase C $\alpha/\beta/\gamma$	PRKCA, PRKCB, PRKCG	Involved in WNT-Ca ²⁺ pathway. PKC phosphorylates and activates Ras and Raf1 then ERK signalling in the MAPK KEGG pathway which is activated by both noncanonical WNT and noncanonical TGF- β 1 signalling. WNT5A reported to inhibit canonical WNT signalling partly through PKC in murine alveolar epithelial cells.
Cell division cycle 42	CDC42	PKC α (Noncanonical WNT-Ca ²⁺ pathway) activates CDC42. TGF- β activates CDC42 to induce cytoskeletal organisation alongside RhoA. In the MAPK KEGG pathway, it is listed alongside RAC. It plays an

		important role in cytoskeletal organisation and cell motility.
Mitogen-activated protein kinase kinase kinase 5	MAP3K5	ASK1 on MAPK pathway. Activates MAP2K3/MAP2K6.
Mitogen-activated protein kinase kinase 3/6	MAP2K3, MAP2K6	MKK3 on MAPK pathway MKK6 on MAPK pathway Activates p38.
Mitogen-activated protein kinase kinase kinase 14	MAP3K14	NIK (NF- κ B-inducing kinase) on MAPK signalling pathway. Downstream of TAK1, it forms a complex with IKK to activate NF κ B signalling. Both noncanonical WNT and TGF- β signal through TAK1 to induce NF κ B.
IKK- α	CHUK	Subunits of IKK. 2 subunits which make up the catalytic subunit of the I κ B kinase complex which inhibits the NF κ B complex (NF κ B proteins + I κ B α) until phosphorylation. Once the I κ B α protein is phosphorylated, NF κ B is activated and can translocate into the nucleus. Both noncanonical WNT and TGF- β signal through TAK1 to induce NF κ B.
IKK- β	IKKBK, IKBKG	
Nuclear factor of kappa light polypeptide gene enhancer in B-cells inhibitor, alpha	NFKB1A	Interacts with REL dimers to inhibit NF- κ B/REL complexes. Both noncanonical WNT and TGF- β signal through TAK1 to induce NF κ B.
Nuclear Factor kappa beta (P50)	NFKB1, NFKB2	These proteins are the most abundant form of NF κ B. TGF- β can signal through TAK1 to mediate TGF- β induced NF- κ B activation. Both noncanonical WNT and TGF- β signal through TAK1 to induce NF κ B.
V-rel avian reticuloendotheliosis viral oncogene homolog A/B	RELA, RELB	
Transducin-like enhancer of split 1	TLE1	TLE1 inhibits FOXA2, NF κ B, β -catenin and TGF- β signalling. Appears as a negative feedback mechanism for both the canonical and noncanonical WNT and TGF- β pathway.
Raf-1 proto-oncogene, serine/threonine kinase	RAF1	TGF- β induces Erk activation in mesenchymal cells by phosphorylating Raf-1 to activate phosphatidylinositol 3-kinase (PI3K).
Mitogen-activated protein kinase kinase 1	MAP2K1, MAP2K2	Forms a scaffold complex with ERK leading to its activation. Called MEK1

		and MEK2 on MAPK signalling pathway.
Mitogen-activated protein kinase 1/3	MAPK1, MAPK3	ERK proteins 1 and 2.
V-myc avian myelocytomatosis viral oncogene homolog	MYC	TAK1 and c-Myc antagonise each other via acetylation of histone H4 to trigger cellular senescence. c-Myc is also a target gene of canonical WNT signalling. Perhaps a negative feedback loop for WNT5A and TGF-induced-TAK signalling.
Activating transcription factor 4	ATF4	CREB on MAPK pathway. MAPK signalling common to both noncanonical WNT and TGF- β signalling. It is phosphorylated downstream of ERK and p38.

Table 7.8 Genes Included in the WNT Notch TGF- β Overlap Transcriptional Module, with Rationale of Inclusion in the Module

Gene Full Name	Gene I.D.	Rationale
NOTCH1	NOTCH1	A Notch receptor. Notch signalling affects basal cell differentiation into the luminal cell types.
Delta-like 1/3/4	DLL1, DLL3, DLL4	<p>Notch ligand. In HepG2 cells, the DLL1-IC domain has been reported to bind to R-SMADs to enhance SMAD-induced transcriptional activity.</p> <p>LEF1, a canonical WNT transcription factor that binds to β-catenin to regulate WNT target gene expression, can bind to multiple sites within the DLL1 promoter. Canonical WNT signalling therefore promotes Notch signalling (in NIH cells).</p>
Jagged 1/2	JAG1, JAG2	<p>Notch ligand. JAG1 can be induced by RBPJ – a potential way of amplifying Notch signalling through positive feedback.</p> <p>JAG1 is also reported to be a target gene of TGF-β and canonical WNT signalling, suggesting Notch acts downstream of both these signalling pathways.</p>
ADAM metallopeptidase domain 17	ADAM17	<p>TACE on Notch KEGG pathway. Initiates Notch signalling through S2 cleavage to break ligand-receptor bonds.</p> <p>Following MAPK signalling activation, ADAM17 cleaves TGF-βR1 reducing its expression. The inhibition of ADAM17 can therefore enhance TGF-βR1 expression.</p>
Lunatic Fringe	LFNG	Fringe proteins modulate the ability of Notch ligands to activate the Notch receptor signalling.
Manic Fringe	MFNG	
Radical Fringe	RFNG	

Disheveled segment polarity protein 1/2/3	DVL1, DVL2, DVL3	Dishevelled proteins are cytoplasmic phosphoproteins that act directly downstream of Frizzled receptors. DVL2 inhibits Notch signalling through binding to RBPJk reducing its activity.
Numb	NUMB, NUMBL	Inhibits Notch receptor transportation to the plasma membrane where it can undergo ligand binding. In mouse models of renal fibrosis, Numb knockout decreased TGF- β 1 expression in kidney sections of knockout mice compared to wildtype. Numb has recently also been reported to regulate EMT through WNT signalling.
Presenilin 1/2	PSEN1, PSEN2	Inhibits CTNNB1 signalling and activates Notch signalling by cleaving notch at S3 to release its NICD. PSEN1 can also cleave the TGF- β R1 following recruitment by TRAF6 to reduce TGF- β signalling.
Nuclear Receptor Co-repressor 2 (or SMRT)	NCOR2	Corepressor of Notch signalling. Downstream WNT5A signalling protein CAMKII reduces SMRT stability enhancing Notch signalling.
HIF-1 α (Hypoxia inducible factor 1 alpha)	HIF1A	Oxygen availability is a known activator of Notch. Hypoxia, which induces HIF-1 α nuclear translocation and transcriptional activity, is reported to inhibit canonical WNT signalling. Hypoxia reported to potentiate TGF- β 1/SMAD3 signalling to increase dermal fibroblast transition into myofibroblasts.
Mastermind-like 1/2/3	MAML1, MAML2, MAML3	MAML proteins are Notch coactivators. MAML1 functions as a coactivator for both Notch and canonical β -catenin signalling.

Recombination signal binding protein for immunoglobulin kappa J region (CSL)	RBPJ, RBPJL	CSL on KEGG Notch signalling pathway. SMAD3/4 interacts with CSL and NICD. DVL2 inhibits Notch signalling through binding to RBPJ κ reducing its activity, as increased RBPJ κ expression increases Notch signalling.
Glycogen Synthase Kinase 3 β (GSK3 β)	GSK3B	Part of the β -catenin APC/Axin destruction complex. Also reported to phosphorylate NICD, and prevent its degradation. However, some studies report the exact opposite that the phosphorylation reduced Notch1 and its transcriptional activity, suggesting this may be cell context dependent. TGF- β reported to initiate SNAIL through AKT signalling. AKT signalling inactivated GSK-3 β , which negatively regulates SNAIL expression.
Transforming Growth Factor - β 1	TGFB1	TGF- β induced HEY1 and JAGGED1. HEY1 expression was induced first through SMAD signalling (independent of Notch activation) which was followed by a delayed Notch activation through Jagged1. This Notch signalling via Hey1 was required for EMT onset in HaCaT keratinocytes. In myoblasts (C2C12 cells), Hes-1 gene transcription was reported as a target of TGF- β . Notch signalling was necessary for this induction however.
SMAD family member 3/4	SMAD3, SMAD4	TGF- β R-SMADs. SMAD3/4 can be recruited by NICD to the CSL DNA-binding sites to upregulate Notch target genes, such as Hes-1 transcription. This transcriptional activity required SMAD3 and NICD direct interaction.

		SMAD3 and 4 have also been reported to form a complex with β -catenin in chondrocytes mediating canonical WNT signalling.
β Catenin	CTNNB1	Critical for canonical WNT signalling. β -catenin interacts with the NICD promoting NICD transcriptional activity on CSL and HES1. The presence of LEF1 reduces this effect.
Transducin-like enhancer of split 1	TLE1	TLE1 inhibits FOXA2, NF κ B, β -catenin and TGF- β signalling. TLE1 is also a co-repressor of Notch signalling (Groucho in Notch KEGG Pathway – named TLE in mammals). TLE proteins also interact with Hes1 to repress Notch signalling transcription.
Lymphoid enhancer-binding factor 1	LEF1	Transcription factors that plays a key role in the canonical WNT signalling pathway. With active canonical WNT signalling, TCF/LEF forms a transcriptional complex with β -catenin. Whereas, in the absence of β -catenin canonical signalling, TCF/LEF binds to co-repressor TLE. TLE represses canonical WNT, Notch and TGF- β signalling. LEF1 can bind to multiple sites within the DLL1 promoter. Canonical WNT signalling therefore promotes Notch signalling. SMAD3 has also been reported to bind to LEF1 activating its target genes irrespective of β -catenin signalling.
Transcription factor 7 (T-cell specific, HMG-box)	TCF7	
Transcription factor 7-like 1/2 (T-cell specific, HMG-box)	TCF7L1, TCF7L2	
Hes Related Family BHLH Transcription Factor With YRPW Motif 1	HEY1	Downstream effector of Notch signalling - transcriptional repressor. TGF- β stimulation has reported to upregulate HEY1 expression in osteoblast precursor MC3T3-E1 cells and ovarian cancer cells lines IGROV1 and SKOV3.
Hes Family BHLH Transcription Factor 1	HES1	Downstream effector of Notch signalling - transcriptional repressor. TGF- β stimulation has reported to

		upregulate HES1 expression in osteoblast precursor MC3T3-E1 cells and ovarian cancer cells lines IGROV1 and SKOV3.
--	--	--

7.5 APPENDIX 5

Table 7.9 RT² Profiler PCR Array Gene List

Gene	Full Gene Name	Gene I.D.
WNT5A	Wingless-type MMTV Integration Site Family, Member 5a	7474
WNT3A	Wingless-type MMTV Integration Site Family, Member 3a	89780
ROR2	Receptor Tyrosine Kinase-like Orphan Receptor 2	4920
NFATC1	Nuclear factor of activated T-cells 1	4772
LEF1	Lymphoid enhancer-binding factor 1	51176
CTNNB1	β -catenin	1499
RHOA	Ras homolog family member A	387
MAPK8	Mitogen-activated protein kinase 8	5599
TGFB1	Transforming Growth Factor - β 1	7040
SMAD2	SMAD family member 2	4087
SMAD3	SMAD family member 3	4088
MAP3K7	Mitogen-activated protein kinase kinase kinase 7 (TAK1)	6885
WNT1	Wingless-type MMTV Integration Site Family, Member 1	7471
ROCK1	Rho associated coiled-coil containing protein kinase 1	6093
SMAD7	SMAD family member 7	4092
FLNA	Filamin A	2316
ACTB	β -actin	60
GAPDH	Glyceraldehyde 3-phosphate dehydrogenase	2597
18SrRNA	18S ribosomal RNA	

7.6 APPENDIX 6

Table 7.10 Constituents of the PCR Mastermix

Mastermix components for entire plate	Volume to add (µl)
2x RT ² SYBR Green Mastermix (Qiagen, cat no 330523)	1350
RNase-free water	1248
TOTAL VOLUME OF DILUTED SYBR GREEN MASTERMIX	2598
Mastermix components for each stimulation condition	
Volume of diluted SYBR green mastermix	649.5
Volume of cDNA synthesis reaction	25.5

7.7 APPENDIX 7

Fluorochrome	%Max	<input type="checkbox"/> Ex	<input checked="" type="checkbox"/> Em	Filters	Alexa...	PerCP	PE-Cy7	PE-CF...	PE	Alexa...	Alexa...	APC-C...	BV786	BV421
1 Alexa Fluor® 488	0.1	<input type="checkbox"/>	<input checked="" type="checkbox"/>	530/30	48.5%	x	1.8%	0.1%	0.4%	x	x	x	0.3%	1.1%
2 PerCP	2.3	<input type="checkbox"/>	<input checked="" type="checkbox"/>	695/40	x	63.0%	1.4%	5.7%	2.0%	37.4%	34.0%	2.3%	0.1%	x
3 PE-Cy7	12.2	<input type="checkbox"/>	<input checked="" type="checkbox"/>	780/60	x	2.7%	60.5%	0.1%	x	1.6%	15.8%	77.6%	61.3%	x
4 PE-CF594	0.0	<input type="checkbox"/>	<input checked="" type="checkbox"/>	610/20	1.9%	x	3.3%	40.8%	12.6%	x	x	x	x	x
5 PE	0.2	<input type="checkbox"/>	<input checked="" type="checkbox"/>	585/16	4.0%	x	7.1%	5.9%	31.6%	x	x	x	0.1%	x
6 Alexa Fluor® 647	92.4	<input type="checkbox"/>	<input checked="" type="checkbox"/>	670/14	0.2%	35.9%	0.8%	4.5%	1.3%	33.5%	1.2%	2.3%	x	x
7 Alexa Fluor® 700	50.8	<input type="checkbox"/>	<input checked="" type="checkbox"/>	720/30	x	8.0%	1.7%	1.2%	0.5%	8.6%	52.0%	2.3%	0.7%	x
8 APC-Cy7	71.2	<input type="checkbox"/>	<input checked="" type="checkbox"/>	780/60	x	2.7%	60.5%	0.1%	x	1.6%	15.8%	77.6%	61.3%	x
9 BV786	3.0	<input type="checkbox"/>	<input checked="" type="checkbox"/>	780/60	x	2.7%	60.5%	0.1%	x	1.6%	15.8%	77.6%	61.3%	x
10 BV421	0.0	<input type="checkbox"/>	<input checked="" type="checkbox"/>	440/50	x	x	x	x	x	x	x	x	9.5%	79.5%

Show All
 BL1-A :: BL1-A
 BL3-A :: BL3-A
 YL4-A :: YL4-A
 YL2-A :: YL2-A
 YL1-A :: YL1-A
 RL1-A :: RL1-A
 RL2-A :: RL2-A
 RL3-A :: RL3-A
 VL4-A :: VL4-A
 VL3-A :: VL3-A
 VL1-A :: VL1-A

BL1-A :: BL1-A	BL3-A :: BL3-A	YL4-A :: YL4-A	YL2-A :: YL2-A	YL1-A :: YL1-A	RL1-A :: RL1-A	RL2-A :: RL2-A	RL3-A :: RL3-A	VL4-A :: VL4-A	VL3-A :: VL3-A	VL1-A :: VL1-A
100	1.9508	0.0066	0	0	0.0066	0.0308	0	0	0.011	0.0309
0	100	2.2121	0.3711	0	5.991	10.8258	0.1774	1.2799	0	0.1294
0.1667	0.8506	100	2.2541	1.3701	0.0196	0.6921	0.7958	2.5323	0.0195	0.027
0.0591	27.304	1.4106	100	2.3792	0.0414	0.0947	0.0089	0.0591	0.0828	0.0504
0.5868	26.3733	1.1083	142.4003	100	0.0078	0.0521	0.013	0.0391	0.4089	0.0287
0.2814	2.6685	2.2265	0.469	0.2818	100	229.9481	1.6913	0	0.2501	0.1881
0.0664	0.895	1.2037	0.0602	0.0249	0.1781	100	0.5969	0.2369	0.0062	0.0229
2.5	3.5767	127.1417	3.8985	0.7021	2.6493	60.2884	100	56.4448	-0.1468	1.73
0.1207	0.329	3.5775	0.2373	0.058	0.2911	5.6099	3.2389	100	0.0965	34.4752
0.0913	208.627	52.243	2022.5016	159.48	2.9496	9.3997	0.0304	53.7468	100	130.2728
0.0035	0.0078	0.002	0.0067	0.0024	0.0023	0.0224	0	0.0031	0.0335	100

Figure 7.2. Selecting Antibody Panel Fluorochromes. (Top panel) shows the BD Biosciences spectra viewer prediction of spectral spillovers between potential fluorochromes. (Bottom panel) shows the compensation matrix of potential fluorochromes using compensation beads run on the Attune.

7.8 APPENDIX 8

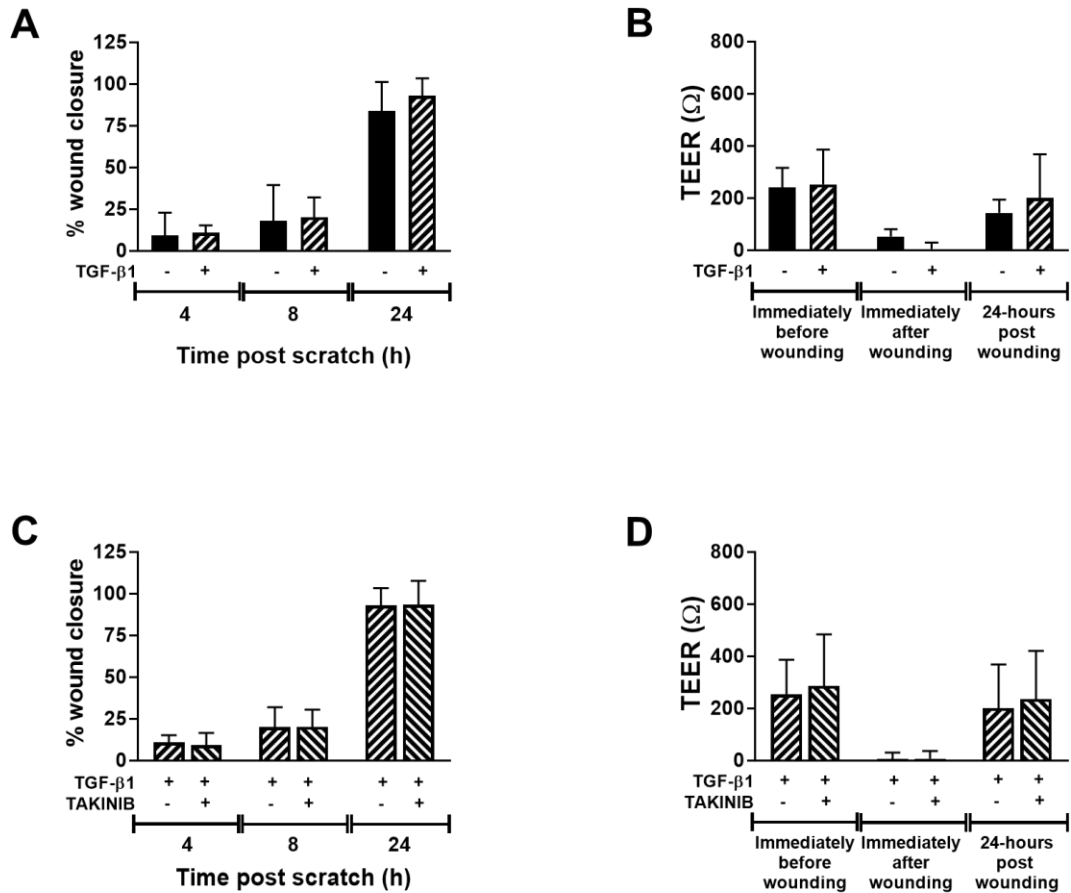


Figure 7.3 The Effect of TGF-β1 Pre-Stimulation With and Without Inhibition With Takinib on Wound Healing and TEER in GINA2-4 Patients. (A-B) Summary figure of the effect of a 48-hour 20ng/ml rhTGF-β1 pre-stimulation on wound healing (A) and TEER (B). Data is n of 5 and presented mean with standard deviation. *p < 0.05 by Wilcoxon matched-pairs signed rank test for wound healing and a paired t-test for TEER at 24 hours. (C-D) Summary figure of Takinib inhibition of TGF-β1 on wound healing (C) and TEER (D). Takinib (8.4nM) was added 30 minutes prior to TGF-β1 stimulation. Data is n of 5 and presented mean with standard deviation. *p < 0.05 by Wilcoxon matched-pairs signed rank test for wound healing and a paired t-test for TEER at 24 hours.

7.9 APPENDIX 9

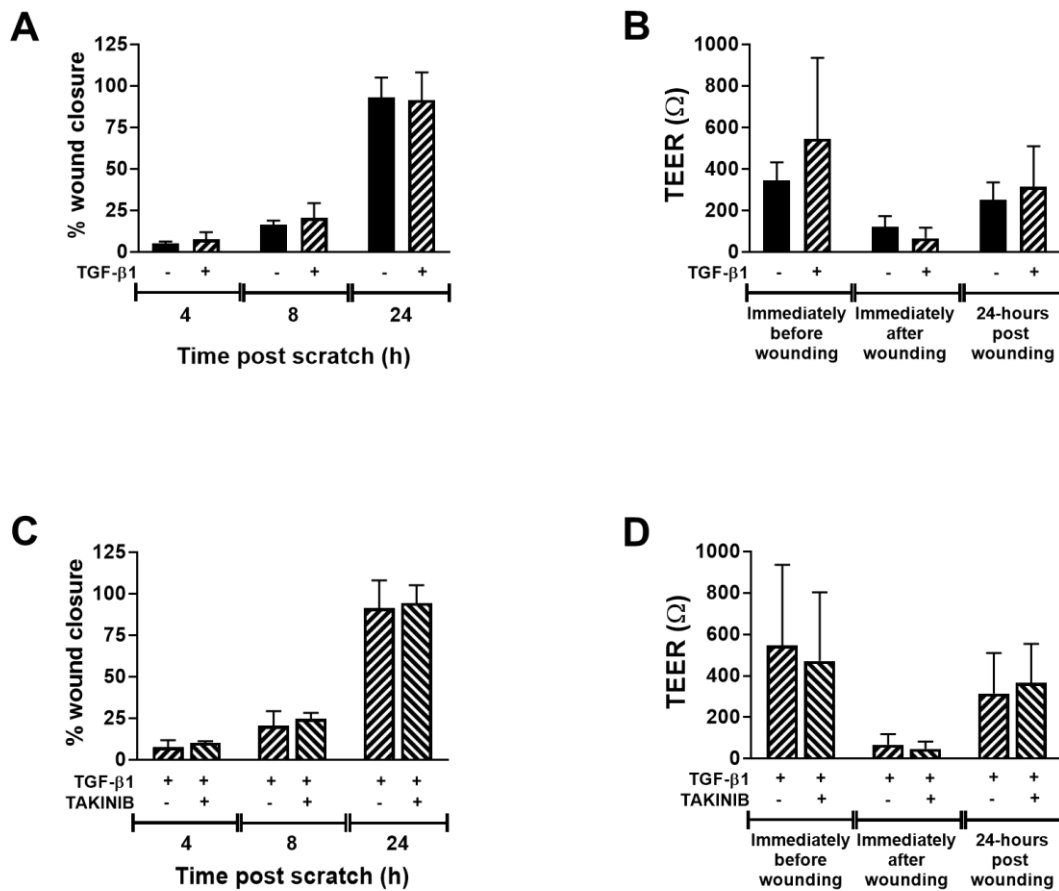


Figure 7.4 The Effect of TGF-β1 Pre-Stimulation With and Without Inhibition With Takinib on Wound Healing and TEER in GINA5 Patients. (A-B) Summary figure of the effect of 48-hour 20ng/ml TGF-β1 pre-stimulation on wound healing (A) and TEER (B). Data is n of 3 (as unpaired data excluded) and presented mean with standard deviation. * $p < 0.05$ by Wilcoxon matched-pairs signed rank test for wound healing and a paired t-test for TEER at 24 hours. (C-D) Summary figure of Takinib inhibition of TGF-β1 on wound healing (C) and TEER (D). Takinib (8.4nM) was added 30 minutes prior to TGF-β1 stimulation. Data is n of 4 and presented mean with standard deviation. * $p < 0.05$ by Wilcoxon matched-pairs signed rank test for wound healing and a paired t-test for TEER at 24 hours.

8 REFERENCES

- Abedini, A., Sayed, C., Carter, L.E., Boerboom, D. and Vanderhyden, B.C. (2020) 'Non-canonical WNT5a regulates Epithelial-to-Mesenchymal Transition in the mouse ovarian surface epithelium', *Scientific Reports*, 10(1), pp. 9695.
- Acharya, P.S., Majumdar, S., Jacob, M., Hayden, J., Mrass, P., Weninger, W., Assoian, R.K. and Puré, E. (2008) 'Fibroblast migration is mediated by CD44-dependent TGF β activation', *Journal of cell science*, 121(9), pp. 1393.
- Acosta, H., López, S.L., Revinski, D.R. and Carrasco, A.E. (2011) 'Notch destabilises maternal β -catenin and restricts dorsal-anterior development in *Xenopus*', *Development*, 138(12), pp. 2567-2579.
- Allam, M.H., Said, A.F., Omran, A.A.E.S., El-Reheim, D.M.A. and Kasem, A.H. (2009) 'High sensitivity C-reactive protein: Its correlation with sputum cell counts in bronchial asthma', *Respiratory medicine*, 103(12), pp. 1878.
- Al-Muhsen, S., Johnson, J.R. and Hamid, Q. (2011) 'Remodeling in asthma', *Journal of Allergy and Clinical Immunology*, 128(3), pp. 451.
- Anderson, G.P. (2008) 'Endotyping asthma: new insights into key pathogenic mechanisms in a complex, heterogeneous disease', *Lancet (London, England)*, 372(9643), pp. 1107-1119.
- Andersson, S., Sundberg, M., Pristovsek, N., Ibrahim, A., Jonsson, P., Katona, B., Clausson, C.M., Zieba, A., Ramström, M., Söderberg, O., Williams, C. and Asplund, A. (2017) 'Insufficient antibody validation challenges oestrogen receptor beta research', *Nature communications*, 8, pp. 15840.
- Anzai, S., Kawamoto, A., Nagata, S., Takahashi, J., Kawai, M., Kuno, R., Kobayashi, S., Watanabe, S., Suzuki, K., Shimizu, H., Hiraguri, Y., Takeoka, S., Sugihara, H.Y., Yui, S., Oshima, S., Watanabe, M. and Okamoto, R. (2020) 'TGF- β promotes fetal gene expression and cell migration velocity in a wound repair model of untransformed intestinal epithelial cells', *Biochemical and biophysical research communications*, 524(3), pp. 533.
- Aros, C.J., Paul, M.K., Pantoja, C.J., Bisht, B., Meneses, L.K., Vijayaraj, P., Sandlin, J.M., France, B., Tse, J.A., Chen, M.W., Shia, D.W., Rickabaugh, T.M., Damoiseaux, R. and Gomperts, B.N. (2020) 'High-Throughput Drug Screening Identifies a Potent Wnt Inhibitor that Promotes Airway Basal Stem Cell Homeostasis', *Cell reports*, 30(7), pp. 2055-2064.e5.
- Aschner, Y. and Downey, G.P. (2016) 'Transforming Growth Factor- β : Master Regulator of the Respiratory System in Health and Disease', *American Journal of Respiratory Cell and Molecular Biology*, 54(5), pp. 647-655.
- Asker, S., Asker, M. and Ozbay, B. (2014) 'Evaluation of airway wall thickness via high-resolution computed tomography in mild intermittent asthma', *Respiratory care*, 59(4), pp. 550-556.
- Atherton, H.C., Jones, G. and Danahay, H. (2003) 'IL-13-induced changes in the goblet cell density of human bronchial epithelial cell cultures: MAP kinase and phosphatidylinositol 3-kinase regulation', *American Journal of Physiology-Lung Cellular and Molecular Physiology*, 285(3), pp. 730-739.

-
- Atkinson, J.J., Adair-Kirk, T.L., Kelley, D.G., Demello, D. and Senior, R.M. (2008) 'Clara cell adhesion and migration to extracellular matrix', *Respiratory research*, 9(1), pp. 1-9921-9-1.
- Atsuta, J., Sterbinsky, S.A., Plitt, J., Schwiebert, L.M., Bochner, B.S. and Schleimer, R.P. (1997) 'Phenotyping and cytokine regulation of the BEAS-2B human bronchial epithelial cell: demonstration of inducible expression of the adhesion molecules VCAM-1 and ICAM-1', *American journal of respiratory cell and molecular biology*, 17(5), pp. 571-582.
- Baarsma, H.A. and Königshoff, M. (2017) 'WNT-er is coming': WNT signalling in chronic lung diseases', *Thorax*, 72(8), pp. 746-759.
- Baarsma, H.A., Skronska-Wasek, W., Mutze, K., Ciolek, F., Wagner, D.E., John-Schuster, G., Heinzelmann, K., Gunther, A., Bracke, K.R., Dagouassat, M., Boczkowski, J., Brusselle, G.G., Smits, R., Eickelberg, O., Yildirim, A.O. and Königshoff, M. (2017) 'Noncanonical WNT-5A signaling impairs endogenous lung repair in COPD', *The Journal of experimental medicine*, 214(1), pp. 143-163.
- Baarsma, H.A., Spanjer, A.I., Haitsma, G., Engelbertink, L.H., Meurs, H., Jonker, M.R., Timens, W., Postma, D.S., Kerstjens, H.A. and Gosens, R. (2011) 'Activation of WNT/beta-catenin signaling in pulmonary fibroblasts by TGF-beta(1) is increased in chronic obstructive pulmonary disease', *PloS one*, 6(9), pp. e25450.
- Bailey, K.L., Bonasera, S.J., Wilderdyke, M., Hanisch, B.W., Pavlik, J.A., DeVasure, J., Robinson, J.E., Sisson, J.H. and Wyatt, T.A. (2014) 'Aging causes a slowing in ciliary beat frequency, mediated by PKC ϵ ', *American journal of physiology. Lung cellular and molecular physiology*, 306(6), pp. L584-9.
- Barkauskas, C.E., Chung, M.I., Fioret, B., Gao, X., Katsura, H. and Hogan, B.L. (2017) 'Lung organoids: current uses and future promise', *Development (Cambridge, England)*, 144(6), pp. 986-997.
- Barnes, P.J. (2010) 'Inhaled Corticosteroids', *Pharmaceuticals (Basel, Switzerland)*, 3(3), pp. 514-540.
- Barnes, P.J. (1996) 'Pathophysiology of asthma', *British journal of clinical pharmacology*, 42(1), pp. 3-10.
- Barnes, P.J., Adcock, I.M. and Ito, K. (2005) 'Histone acetylation and deacetylation: importance in inflammatory lung diseases', *European Respiratory Journal*, 25(3), pp. 552-563.
- Barré-Sinoussi, F. and Montagutelli, X. (2015) 'Animal models are essential to biological research: issues and perspectives', *Future Science OA*, 1(4), pp. nu.
- Barreto-Luis, A., Corrales, A., Acosta-Herrera, M., Gonzalez-Colino, C., Cumplido, J., Martinez-Tadeo, J., Carracedo, A., Villar, J., Carrillo, T., Pino-Yanes, M. and Flores, C. (2017) 'A pathway-based association study reveals variants from Wnt signalling genes contributing to asthma susceptibility', *Clinical and experimental allergy : journal of the British Society for Allergy and Clinical Immunology*, 47(5), pp. 618-626.
- Basu, K., Palmer, C.N., Lipworth, B.J., McLean, W.H., Terron-Kwiatkowski, A., Zhao, Y., Liao, H., Smith, F.J., Mitra, A. and Mukhopadhyay, S. (2008) 'Filaggrin null mutations are associated with increased asthma exacerbations in children and young adults', *Allergy*, 63(9), pp. 1211-1217.
- Batra, V., Musani, A.I., Hastie, A.T., Khurana, S., Carpenter, K.A., Zangrilli, J.G. and Peters, S.P. (2004) 'Bronchoalveolar lavage fluid concentrations of transforming growth factor (TGF)- β 1, TGF- β 2, interleukin (IL)-4 and IL-13 after segmental allergen challenge and

-
- their effects on α -smooth muscle actin and collagen III synthesis by primary human lung fibroblasts', *Clinical & Experimental Allergy*, 34(3), pp. 437-444.
- Bauché, D. and Marie, J.C. (2017) 'Transforming growth factor β : a master regulator of the gut microbiota and immune cell interactions', *Clinical & translational immunology*, 6(4), pp. e136.
- Bauge, C., Cauvard, O., Leclercq, S., Galera, P. and Boumediene, K. (2011) 'Modulation of transforming growth factor beta signalling pathway genes by transforming growth factor beta in human osteoarthritic chondrocytes: involvement of Sp1 in both early and late response cells to transforming growth factor beta', *Arthritis research & therapy*, 13(1), pp. R23.
- Bayram, H., Devalia, J.L., Khair, O.A., Abdelaziz, M.M., Sapsford, R.J., Sagai, M. and Davies, R.J. (1998) 'Comparison of ciliary activity and inflammatory mediator release from bronchial epithelial cells of nonatopic nonasthmatic subjects and atopic asthmatic patients and the effect of diesel exhaust particles in vitro', *Journal of Allergy and Clinical Immunology*, 102(5), pp. 771-782.
- Bel, E.H., Sousa, A., Fleming, L., Bush, A., Chung, K.F., Versnel, J., Wagener, A.H., Wagers, S.S., Sterk, P.J., Compton, C.H. and , (2011) 'Diagnosis and definition of severe refractory asthma: an international consensus statement from the Innovative Medicine Initiative (IMI)', *Thorax*, 66(10), pp. 910-917.
- Belgrave, D., Henderson, J., Simpson, A., Buchan, I., Bishop, C. and Custovic, A. (2017) 'Disaggregating asthma: Big investigation versus big data', *The Journal of allergy and clinical immunology*, 139(2), pp. 400-407.
- Beljaars, L., Daliri, S., Dijkhuizen, C., Poelstra, K. and Gosens, R. (2017) 'WNT-5A regulates TGF- β -related activities in liver fibrosis', *American Journal of Physiology-Gastrointestinal and Liver Physiology*, 312(3), pp. G219-G227.
- Benayoun, L., Druilhe, A., Dombret, M.C., Aubier, M. and Pretolani, M. (2003) 'Airway structural alterations selectively associated with severe asthma', *American journal of respiratory and critical care medicine*, 167(10), pp. 1360-1368.
- Bergeron, C., Al-Ramli, W. and Hamid, Q. (2009) 'Remodeling in asthma', *Proceedings of the American Thoracic Society*, 6(3), pp. 301-305.
- Bergeron, C., Tulic, M.K. and Hamid, Q. (2010) 'Airway remodelling in asthma: from benchside to clinical practice', *Canadian respiratory journal*, 17(4), pp. e85-93.
- Berglund, L., Björling, E., Oksvold, P., Fagerberg, L., Asplund, A., Szigartyo, C.A., Persson, A., Ottosson, J., Wernérus, H., Nilsson, P., Lundberg, E., Sivertsson, A., Navani, S., Wester, K., Kampf, C., Hober, S., Pontén, F. and Uhlén, M. (2008) 'A genecentric Human Protein Atlas for expression profiles based on antibodies', *Molecular & cellular proteomics : MCP*, 7(10), pp. 2019-2027.
- Bettelli, E., Carrier, Y., Gao, W., Korn, T., Strom, T.B., Oukka, M., Weiner, H.L. and Kuchroo, V.K. (2006) 'Reciprocal developmental pathways for the generation of pathogenic effector TH17 and regulatory T cells', *Nature*, 441(7090), pp. 235-238.
- Bhatia, S.N. and Ingber, D.E. (2014) 'Microfluidic organs-on-chips', *Nature biotechnology*, 32(8), pp. 760-772.
- Bhatt, L., Roinestad, K., Van, T. and Springman, E.B. (2017) 'Recent advances in clinical development of leukotriene B4 pathway drugs', *Seminars in immunology*, 33, pp. 65.

-
- Bhowmick, N.A., Ghiassi, M., Bakin, A., Aakre, M., Lundquist, C.A., Engel, M.E., Arteaga, C.L. and Moses, H.L. (2001) 'Transforming growth factor-beta1 mediates epithelial to mesenchymal transdifferentiation through a RhoA-dependent mechanism', *Molecular biology of the cell*, 12(1), pp. 27-36.
- Bigler, J., Boedigheimer, M., Schofield, J.P.R., Skipp, P.J., Corfield, J., Rowe, A., Sousa, A.R., Timour, M., Twehues, L., Hu, X., Roberts, G., Welcher, A.A., Yu, W., Lefaudeux, D., Meulder, B., Auffray, C., Chung, K.F., Adcock, I.M., Sterk, P.J., Djukanović, R. and U-BIOPRED Study Group II (2017) 'A Severe Asthma Disease Signature from Gene Expression Profiling of Peripheral Blood from U-BIOPRED Cohorts', *American journal of respiratory and critical care medicine*, 195(10), pp. 1311-1320.
- Billington, C.K., Penn, R.B. and Hall, I.P. (2017) ' $\beta(2)$ Agonists', *Handbook of Experimental Pharmacology*, 237, pp. 23-40.
- Bjornsdottir, U.S., Holgate, S.T., Reddy, P.S., Hill, A.A., McKee, C.M., Csimma, C.I., Weaver, A.A., Legault, H.M., Small, C.G., Ramsey, R.C., Ellis, D.K., Burke, C.M., Thompson, P.J., Howarth, P.H., Wardlaw, A.J., Bardin, P.G., Bernstein, D.I., Irving, L.B., Chupp, G.L., Bensch, G.W., Bensch, G.W., Stahlman, J.E., Karetzky, M., Baker, J.W., Miller, R.L., Goodman, B.H., Raible, D.G., Goldman, S.J., Miller, D.K., Ryan, J.L., Dorner, A.J., Immermann, F.W. and O'Toole, M. (2011) 'Pathways activated during human asthma exacerbation as revealed by gene expression patterns in blood', *PLoS one*, 6(7), pp. e21902.
- Blokzijl, A., Dahlqvist, C., Reissmann, E., Falk, A., Moliner, A., Lendahl, U. and Ibáñez, C.F. (2003) 'Cross-talk between the Notch and TGF-beta signaling pathways mediated by interaction of the Notch intracellular domain with Smad3', *The Journal of cell biology*, 163(4), pp. 723-728.
- Bluhmki, T., Bitzer, S., Gindele, J.A., Schruf, E., Kiechle, T., Webster, M., Schymeinsky, J., Ries, R., Gantner, F., Bischoff, D., Garnett, J. and Heilker, R. (2020) 'Development of a miniaturized 96-Transwell air-liquid interface human small airway epithelial model', *Scientific Reports*, 10(1), pp. 13022.
- Bo, H., Zhang, S., Gao, L., Chen, Y., Zhang, J., Chang, X. and Zhu, M. (2013) 'Upregulation of Wnt5a promotes epithelial-to-mesenchymal transition and metastasis of pancreatic cancer cells', *BMC Cancer*, 13(1), pp. 496.
- Boku, S., Nakagawa, S., Masuda, T., Nishikawa, H., Kato, A., Kitaichi, Y., Inoue, T. and Koyama, T. (2009) 'Glucocorticoids and Lithium Reciprocally Regulate the Proliferation of Adult Dentate Gyrus-Derived Neural Precursor Cells Through GSK-3 β and β -Catenin/TCF Pathway', *Neuropsychopharmacology*, 34(3), pp. 805-815.
- Borcherding, N., Kusner, D., Kolb, R., Xie, Q., Li, W., Yuan, F., Velez, G., Askeland, R., Weigel, R.J. and Zhang, W. (2015) 'Paracrine WNT5A Signaling Inhibits Expansion of Tumor-Initiating Cells', *Cancer research*, 75(10), pp. 1972-1982.
- Borggreffe, T., Lauth, M., Zwijsen, A., Huylebroeck, D., Oswald, F. and Giaimo, B.D. (2016) 'The Notch intracellular domain integrates signals from Wnt, Hedgehog, TGF β /BMP and hypoxia pathways', *Biochimica et Biophysica Acta (BBA) - Molecular Cell Research*, 1863(2), pp. 303.
- Borish, L., Aarons, A., Rumbyrt, J., Cvietusa, P., Negri, J. and Wenzel, S. (1996) 'Interleukin-10 regulation in normal subjects and patients with asthma', *The Journal of allergy and clinical immunology*, 97(6), pp. 1288-1296.
- Bossé, Y. and Rola-Pleszczynski, M. (2007) 'Controversy surrounding the increased expression of TGF beta 1 in asthma', *Respiratory research*, 8(1), pp. 66-9921-8-66.

-
- Bousquet, J., Jeffery, P.K., Busse, W.W., Johnson, M. and Vignola, A.M. (2000) 'Asthma. From bronchoconstriction to airways inflammation and remodeling', *American journal of respiratory and critical care medicine*, 161(5), pp. 1720-1745.
- Boxall, C., Holgate, S.T. and Davies, D.E. (2006) 'The contribution of transforming growth factor-beta and epidermal growth factor signalling to airway remodelling in chronic asthma', *The European respiratory journal*, 27(1), pp. 208-229.
- Brechbuhl, H.M., Ghosh, M., Smith, M.K., Smith, R.W., Li, B., Hicks, D.A., Cole, B.B., Reynolds, P.R. and Reynolds, S.D. (2011) 'Î2-Catenin Dosage is a Critical Determinant of Tracheal Basal Cell Fate Determination', *The American journal of pathology*, 179(1), pp. 367-379.
- Brembeck, F.H., Rosario, M. and Birchmeier, W. (2006) 'Balancing cell adhesion and Wnt signaling, the key role of beta-catenin', *Current opinion in genetics & development*, 16(1), pp. 51-59.
- Brewster, C.E.P., Howarth, P.H., Djukanovic, R., Wilson, J., Holgate, S.T. and Roche, W.R. (1990) 'Myofibroblasts and Subepithelial Fibrosis in Bronchial Asthma', *American Journal of Respiratory Cell and Molecular Biology*, 3(5), pp. 507-511.
- Brujeni, G.N (2010) 'Immunofluorescent protein detection in Western blotting', *International Journal of Veterinary Science*, 3(2), pp. 107-111
- Bucchieri, F., Pitruzzella, A., Fucarino, A., Gammazza, A.M., Bavisotto, C.C., Marcianò, V., Cajozzo, M., Iacono, G.L., Marchese, R., Zummo, G., Holgate, S.T. and Davies, D.E. (2017) 'Functional characterization of a novel 3D model of the epithelial-mesenchymal trophic unit', *Experimental lung research*, 43(2), pp. 82-92.
- Buckley, S., Shi, W., Barsky, L. and Warburton, D. (2008) 'TGF-β signaling promotes survival and repair in rat alveolar epithelial type 2 cells during recovery after hyperoxic injury', *American Journal of Physiology-Lung Cellular and Molecular Physiology*, 294(4), pp. 739-748.
- Bustamante-Marin, X.M. and Ostrowski, L.E. (2017) 'Cilia and Mucociliary Clearance', *Cold Spring Harbor perspectives in biology*, 9(4), pp. a028241. doi: 10.1101/cshperspect.a028241.
- Button, B., Boucher, R.C. and University of North Carolina Virtual Lung Group (2008) 'Role of mechanical stress in regulating airway surface hydration and mucus clearance rates', *Respiratory physiology & neurobiology*, 163(1-3), pp. 189-201.
- Calapai, G., Casciaro, M., Miroddi, M., Calapai, F., Navarra, M. and Gangemi, S. (2014) 'Montelukast-induced adverse drug reactions: a review of case reports in the literature', *Pharmacology*, 94(1-2), pp. 60-70.
- Câmara, J. and Jarai, G. (2010) 'Epithelial-mesenchymal transition in primary human bronchial epithelial cells is Smad-dependent and enhanced by fibronectin and TNF-alpha', *Fibrogenesis & tissue repair*, 3(1), pp. 2-1536-3-2.
- Cantero-Recasens, G., Fandos, C., Rubio-Moscardo, F., Valverde, M.A. and Vicente, R. (2010) 'The asthma-associated ORMDL3 gene product regulates endoplasmic reticulum-mediated calcium signaling and cellular stress', *Human molecular genetics*, 19(1), pp. 111-121.
- Cao, H., Lu, J., Du, J., Xia, F., Wei, S., Liu, X., Liu, T., Liu, Y. and Xiang, M. (2015) 'TAK1 inhibition prevents the development of autoimmune diabetes in NOD mice', *Scientific reports*, 5, pp. 14593.

-
- Carlsson, A. (2013) *Wound healing in an in vitro bronchial epithelial cell model*. Master's thesis. Chalmers University of Technology. (Accessed: 22 Jan 2020).
- Carraro, G. and Stripp, B.R. (2015) 'A new notch for lung stem cells', *Cell stem cell*, 16(2), pp. 107-109.
- Cayrol, C., Duval, A., Schmitt, P., Roga, S., Camus, M., Stella, A., Burlet-Schiltz, O., Gonzalez-de-Peredo, A. and Girard, J.P. (2018) 'Environmental allergens induce allergic inflammation through proteolytic maturation of IL-33', *Nature immunology*, 19(4), pp. 375-385.
- Chae, E.J., Kim, T., Cho, Y.S., Park, C., Seo, J.B., Kim, N. and Moon, H. (2011) 'Airway Measurement for Airway Remodeling Defined by Post-Bronchodilator FEV1/FVC in Asthma: Investigation Using Inspiration-Expiration Computed Tomography', *Allergy, asthma & immunology research*, 3(2), pp. 111–117.
- Chakir, J., Shannon, J., Molet, S., Fukakusa, M., Elias, J., Laviolette, M., Boulet, L.P. and Hamid, Q. (2003) 'Airway remodeling-associated mediators in moderate to severe asthma: effect of steroids on TGF-beta, IL-11, IL-17, and type I and type III collagen expression', *The Journal of allergy and clinical immunology*, 111(6), pp. 1293-1298.
- Chen, J., Zeng, F., Forrester, S.J., Eguchi, S., Zhang, M. and Harris, R.C. (2016) 'Expression and Function of the Epidermal Growth Factor Receptor in Physiology and Disease', *Physiological Reviews*, 96(3), pp. 1025-1069.
- Cheng, C., Yeh, J., Fan, T., Smith, S.K. and Charnock-Jones, D.S. (2008) 'Wnt5a-mediated non-canonical Wnt signalling regulates human endothelial cell proliferation and migration', *Biochemical and biophysical research communications*, 365(2), pp. 285.
- Chilvers, M.A., McKean, M., Rutman, A., Myint, B.S., Silverman, M. and O'Callaghan, C. (2001) 'The effects of coronavirus on human nasal ciliated respiratory epithelium', *The European respiratory journal*, 18(6), pp. 965-970.
- Chilvers, M.A. and O'Callaghan, C. (2000) 'Analysis of ciliary beat pattern and beat frequency using digital high speed imaging: comparison with the photomultiplier and photodiode methods', *Thorax*, 55(4), pp. 314-317.
- Chilvers, M.A., Rutman, A. and O'Callaghan, C. (2003) 'Functional analysis of cilia and ciliated epithelial ultrastructure in healthy children and young adults', *Thorax*, 58(4), pp. 333-338.
- Cho, S.H., Park, Y.S., Kim, H.J., Kim, C.H., Lim, S.W., Huh, J.W., Lee, J.H. and Kim, H.R. (2012) 'CD44 enhances the epithelial-mesenchymal transition in association with colon cancer invasion', *International journal of oncology*, 41(1), pp. 211-218.
- Choe, M.M., Sporn, P.H. and Swartz, M.A. (2003) 'An in vitro airway wall model of remodeling', *American journal of physiology. Lung cellular and molecular physiology*, 285(2), pp. L427-33.
- Choi, G., Park, Y.J., Cho, M., Moon, H., Kim, D., Kang, C.Y., Chung, Y. and Kim, B.S. (2021) 'A critical role for Th17 cell-derived TGF-β1 in regulating the stability and pathogenicity of autoimmune Th17 cells', *Experimental & molecular medicine*, 53(5), pp. 993-1004.
- Choy, D.F., Hart, K.M., Borthwick, L.A., Shikotra, A., Nagarkar, D.R., Siddiqui, S., Jia, G., Ohri, C.M., Doran, E., Vannella, K.M., Butler, C.A., Hargadon, B., Sciurba, J.C., Gieseck, R.L., Thompson, R.W., White, S., Abbas, A.R., Jackman, J., Wu, L.C., Egen, J.G., Heaney, L.G., Ramalingam, T.R., Arron, J.R., Wynn, T.A. and Bradding, P. (2015) 'TH2 and TH17 inflammatory pathways are reciprocally regulated in asthma', *Science translational medicine*, 7(301), pp. 301ra129.

-
- Choy, D.F., Modrek, B., Abbas, A.R., Kummerfeld, S., Clark, H.F., Wu, L.C., Fedorowicz, G., Modrusan, Z., Fahy, J.V., Woodruff, P.G. and Arron, J.R. (2011) 'Gene expression patterns of Th2 inflammation and intercellular communication in asthmatic airways', *Journal of immunology (Baltimore, Md.: 1950)*, 186(3), pp. 1861-1869.
- Christman, M.A., 2nd, Goetz, D.J., Dickerson, E., McCall, K.D., Lewis, C.J., Benencia, F., Silver, M.J., Kohn, L.D. and Malgor, R. (2008) 'Wnt5a is expressed in murine and human atherosclerotic lesions', *American journal of physiology. Heart and circulatory physiology*, 294(6), pp. H2864-70.
- Christopher, D.J., Oommen, A.M., George, K., Shankar, D., Agrawal, A. and Thangakunam, B. (2020) 'Prevalence of Airflow Obstruction as Measured by Spirometry, in Rural Southern Indian Adults', *Copd*, 17(2), pp. 128-135.
- Chu, H.W., Balzar, S., Seedorf, G.J., Westcott, J.Y., Trudeau, J.B., Silkoff, P. and Wenzel, S.E. (2004) 'Transforming growth factor-beta2 induces bronchial epithelial mucin expression in asthma', *The American journal of pathology*, 165(4), pp. 1097-1106.
- Chung, E., Ojiaku, C.A., Cao, G., Parikh, V., Deeney, B., Xu, S., Wang, S., Panettieri, R.A. and Koziol-White, C. (2020) 'Dexamethasone rescues TGF- β 1-mediated β 2-adrenergic receptor dysfunction and attenuates phosphodiesterase 4D expression in human airway smooth muscle cells', *Respiratory Research*, 21(1), pp. 256.
- Chung, F.T., Huang, H.Y., Lo, C.Y., Huang, Y.C., Lin, C.W., He, C.C., He, J.R., Sheng, T.F. and Wang, C.H. (2019) 'Increased Ratio of Matrix Metalloproteinase-9 (MMP-9)/Tissue Inhibitor Metalloproteinase-1 from Alveolar Macrophages in Chronic Asthma with a Fast Decline in FEV(1) at 5-Year Follow-up', *Journal of clinical medicine*, 8(9), pp. 1451. doi: 10.3390/jcm8091451.
- Chung, K.F., Wenzel, S.E., Brozek, J.L., Bush, A., Castro, M., Sterk, P.J., Adcock, I.M., Bateman, E.D., Bel, E.H., Bleecker, E.R., Boulet, L.P., Brightling, C., Chanez, P., Dahlen, S.E., Djukanovic, R., Frey, U., Gaga, M., Gibson, P., Hamid, Q., Jajour, N.N., Mauad, T., Sorkness, R.L. and Teague, W.G. (2014) 'International ERS/ATS guidelines on definition, evaluation and treatment of severe asthma', *The European respiratory journal*, 43(2), pp. 343-373.
- Chung, M.K., Jung, Y.H., Lee, J.K., Cho, S.Y., Murillo-Sauca, O., Uppaluri, R., Shin, J.H. and Sunwoo, J.B. (2018) 'CD271 Confers an Invasive and Metastatic Phenotype of Head and Neck Squamous Cell Carcinoma through the Upregulation of Slug', *Clinical cancer research : an official journal of the American Association for Cancer Research*, 24(3), pp. 674-683.
- Clary-Meinesz, C., Cosson, J., Huitorel, P. and Blaive, B. (1992) 'Temperature effect on the ciliary beat frequency of human nasal and tracheal ciliated cells', *Biology of the Cell*, 76, pp. 335.
- Cohen, L., E, X., Tarsi, J., Ramkumar, T., Horiuchi, T.K., Cochran, R., DeMartino, S., Schechtman, K.B., Hussain, I., Holtzman, M.J., Castro, M. and NHLBI Severe Asthma Research Program (SARP) (2007) 'Epithelial cell proliferation contributes to airway remodeling in severe asthma', *American journal of respiratory and critical care medicine*, 176(2), pp. 138-145.
- Collu, G.M., Hidalgo-Sastre, A., Acar, A., Bayston, L., Gildea, C., Leverentz, M.K., Mills, C.G., Owens, T.W., Meurette, O., Dorey, K. and Brennan, K. (2012) 'Dishevelled limits Notch signalling through inhibition of CSL', *Development (Cambridge, England)*, 139(23), pp. 4405-4415.
- Contreras, O., Soliman, H., Theret, M., Rossi, F.M.V. and Brandan, E. (2020) 'TGF- β -driven downregulation of the Wnt/ β -Catenin transcription factor TCF7L2/TCF4 in PDGFR α + fibroblasts', *bioRxiv*, .

-
- Coster, A.D., Thorne, C.A., Wu, L.F. and Altschuler, S.J. (2017) 'Examining Crosstalk among Transforming Growth Factor β , Bone Morphogenetic Protein, and Wnt Pathways', *The Journal of biological chemistry*, 292(1), pp. 244-250.
- Courties, G., Seiffart, V., Presumey, J., Escriou, V., Scherman, D., Zwerina, J., Ruiz, G., Zietara, N., Jablonska, J., Weiss, S., Hoffmann, A., Jorgensen, C., Apparailly, F. and Gross, G. (2010) 'In vivo RNAi-mediated silencing of TAK1 decreases inflammatory Th1 and Th17 cells through targeting of myeloid cells', *Blood*, 116(18), pp. 3505-3516.
- Crawford, S.E., Stellmach, V., Murphy-Ullrich, J.E., Ribeiro, S.M., Lawler, J., Hynes, R.O., Boivin, G.P. and Bouck, N. (1998) 'Thrombospondin-1 is a major activator of TGF-beta1 in vivo', *Cell*, 93(7), pp. 1159-1170.
- Crosby, L.M. and Waters, C.M. (2010) 'Epithelial repair mechanisms in the lung', *American journal of physiology. Lung cellular and molecular physiology*, 298(6), pp. L715-31.
- Crystal, R.G., Randell, S.H., Engelhardt, J.F., Voynow, J. and Sunday, M.E. (2008) 'Airway Epithelial Cells', *Proceedings of the American Thoracic Society*, 5(7), pp. 772-777.
- Cui, A.H., Zhao, J., Liu, S.X. and Hao, Y.S. (2017) 'Associations of IL-4, IL-6, and IL-12 levels in peripheral blood with lung function, cellular immune function, and quality of life in children with moderate-to-severe asthma', *Medicine*, 96(12), pp. e6265.
- Danopoulos, S., Shiosaki, J. and Al Alam, D. (2019) 'FGF Signaling in Lung Development and Disease: Human Versus Mouse', *Frontiers in genetics*, 10, pp. 170.
- Das, J., Ren, G., Zhang, L., Roberts, A.I., Zhao, X., Bothwell, A.L., Van Kaer, L., Shi, Y. and Das, G. (2009) 'Transforming growth factor beta is dispensable for the molecular orchestration of Th17 cell differentiation', *The Journal of experimental medicine*, 206(11), pp. 2407-2416.
- Daud, T. (2017) *The role of WNT5a in asthmatic airway epithelial repair*. PhD thesis. University of Leicester. (Accessed: 22 Jan 2018).
- Daud, T., Parmar, A., Sutcliffe, A., Choy, D., Arron, J., Amrani, Y., Bradding, P. and Siddiqui, S. (2016) 'The role of WNT5a in Th17 asthma', *European Respiratory Journal*, 48(suppl 60).
- Davies, D.E. (2014) 'Epithelial barrier function and immunity in asthma', *Annals of the American Thoracic Society*, 11 Suppl 5, pp. S244-51.
- Davis, S.L., Cardin, D.B., Shahda, S., Lenz, H., Dotan, E., O'Neil, B.H., Kapoun, A.M., Stagg, R.J., Berlin, J., Messersmith, W.A. and Cohen, S.J. (2020) 'A phase 1b dose escalation study of Wnt pathway inhibitor vanttictumab in combination with nab-paclitaxel and gemcitabine in patients with previously untreated metastatic pancreatic cancer', *Investigational new drugs*, 38(3), pp. 821-830.
- de Boer, W.I., Sharma, H.S., Baelemans, S.M., Hoogsteden, H.C., Lambrecht, B.N. and Braunstahl, G.J. (2008) 'Altered expression of epithelial junctional proteins in atopic asthma: possible role in inflammation', *Canadian journal of physiology and pharmacology*, 86(3), pp. 105-112.
- Deliu, M., Yavuz, T.S., Sperrin, M., Belgrave, D., Sahiner, U.M., Sackesen, C., Kalayci, O. and Custovic, A. (2018) 'Features of asthma which provide meaningful insights for understanding the disease heterogeneity', *Clinical and experimental allergy : journal of the British Society for Allergy and Clinical Immunology*, 48(1), pp. 39-47.

-
- Desai, L.P., Aryal, A.M., Ceacareanu, B., Hassid, A. and Waters, C.M. (2004) 'RhoA and Rac1 are both required for efficient wound closure of airway epithelial cells', *American journal of physiology.Lung cellular and molecular physiology*, 287(6), pp. L1134-44.
- DeVries, A., Wlasiuk, G., Miller, S.J., Bosco, A., Stern, D.A., Lohman, I.C., Rothers, J., Jones, A.C., Nicodemus-Johnson, J., Vasquez, M.M., Curtin, J.A., Simpson, A., Custovic, A., Jackson, D.J., Gern, J.E., Lemanske, R.F., Jr, Guerra, S., Wright, A.L., Ober, C., Halonen, M. and Vercelli, D. (2017) 'Epigenome-wide analysis links SMAD3 methylation at birth to asthma in children of asthmatic mothers', *The Journal of allergy and clinical immunology*, 140(2), pp. 534-542.
- Dietz, K., de Los Reyes Jiménez, M., Gollwitzer, E.S., Chaker, A.M., Zissler, U.M., Rådmark, O.P., Baarsma, H.A., Königshoff, M., Schmidt-Weber, C.B., Marsland, B.J. and Esser-von Bieren, J. (2017) 'Age dictates a steroid-resistant cascade of Wnt5a, transglutaminase 2, and leukotrienes in inflamed airways', *The Journal of allergy and clinical immunology*, 139(4), pp. 1343-1354.e6.
- Ding, I., Ostrowska-Podhorodecka, Z., Lee, W., Liu, R.S.C., Carneiro, K., Janmey, P.A. and McCulloch, C.A. (2020) 'Cooperative roles of PAK1 and filamin A in regulation of vimentin assembly and cell extension formation', *Biochimica et Biophysica Acta (BBA) - Molecular Cell Research*, 1867(9), pp. 118739.
- DiRenzo, D.M., Chaudhary, M.A., Shi, X., Franco, S.R., Zent, J., Wang, K., Guo, L.W. and Kent, K.C. (2016) 'A crosstalk between TGF- β /Smad3 and Wnt/ β -catenin pathways promotes vascular smooth muscle cell proliferation', *Cellular signalling*, 28(5), pp. 498-505.
- Dissanayake, S.K., Wade, M., Johnson, C.E., O'Connell, M.P., Leotlela, P.D., French, A.D., Shah, K.V., Hewitt, K.J., Rosenthal, D.T., Indig, F.E., Jiang, Y., Nickoloff, B.J., Taub, D.D., Trent, J.M., Moon, R.T., Bittner, M. and Weeraratna, A.T. (2007) 'The Wnt5A/protein kinase C pathway mediates motility in melanoma cells via the inhibition of metastasis suppressors and initiation of an epithelial to mesenchymal transition', *The Journal of biological chemistry*, 282(23), pp. 17259-17271.
- Dobrowolski, R., Vick, P., Ploper, D., Gumper, I., Snitkin, H., Sabatini, D.D. and De Robertis, E.M. (2012) 'Presenilin deficiency or lysosomal inhibition enhances Wnt signaling through relocalization of GSK3 to the late-endosomal compartment', *Cell reports*, 2(5), pp. 1316-1328.
- Doerner, A.M. and Zuraw, B.L. (2009) 'TGF-beta1 induced epithelial to mesenchymal transition (EMT) in human bronchial epithelial cells is enhanced by IL-1beta but not abrogated by corticosteroids', *Respiratory research*, 10(1), pp. 100-9921-10-100.
- Doi, T. and Puri, P. (2009) 'Up-regulation of Wnt5a gene expression in the nitrofen-induced hypoplastic lung', *Journal of pediatric surgery*, 44(12), pp. 2302-2306.
- Driemel, C., Kremling, H., Schumacher, S., Will, D., Wolters, J., Lindenlauf, N., Mack, B., Baldus, S.A., Hoya, V., Pietsch, J.M., Panagiotidou, P., Raba, K., Vay, C., Vallböhmer, D., Harréus, U., Knoefel, W.T., Stoecklein, N.H. and Gires, O. (2014) 'Context-dependent adaption of EpCAM expression in early systemic esophageal cancer', *Oncogene*, 33(41), pp. 4904-4915.
- Duncan, E.M., Watchorn, D.C. and Fahy, J.V. (2018) 'Autopsy and Imaging Studies of Mucus in Asthma. Lessons Learned about Disease Mechanisms and the Role of Mucus in Airflow Obstruction', *Annals of the American Thoracic Society*, 15(Suppl 3), pp. S184-S191.
- Duncan, E.M., Elicker, B.M., Gierada, D.S., Nagle, S.K., Schiebler, M.L., Newell, J.D., Raymond, W.W., Lachowicz-Scroggins, M., Di Maio, S., Hoffman, E.A., Castro, M., Fain, S.B., Jarjour, N.N., Israel, E., Levy, B.D., Erzurum, S.C., Wenzel, S.E., Meyers, D.A., Blecker, E.R., Phillips, B.R., Mauger, D.T., Gordon, E.D., Woodruff, P.G., Peters, M.C.,

-
- and Fahy, J.V. (2018) 'Mucus plugs in patients with asthma linked to eosinophilia and airflow obstruction', *The Journal of clinical investigation*, 128(3), pp. 997-1009.
- Dvorak, A., Tilley, A.E., Shaykhiev, R., Wang, R. and Crystal, R.G. (2011) 'Do airway epithelium air-liquid cultures represent the in vivo airway epithelium transcriptome?', *American journal of respiratory cell and molecular biology*, 44(4), pp. 465-473.
- Egelhofer, T.A., Minoda, A., Klugman, S., Lee, K., Kolasinska-Zwierz, P., Alekseyenko, A.A., Cheung, M.S., Day, D.S., Gadel, S., Gorchakov, A.A., Gu, T., Kharchenko, P.V., Kuan, S., Latorre, I., Linder-Basso, D., Luu, Y., Ngo, Q., Perry, M., Rechtsteiner, A., Riddle, N.C., Schwartz, Y.B., Shanower, G.A., Vielle, A., Ahringer, J., Elgin, S.C., Kuroda, M.I., Pirrotta, V., Ren, B., Strome, S., Park, P.J., Karpen, G.H., Hawkins, R.D. and Lieb, J.D. (2011) 'An assessment of histone-modification antibody quality', *Nature structural & molecular biology*, 18(1), pp. 91-93.
- Erle, D.J. and Sheppard, D. (2014) 'The cell biology of asthma', *The Journal of cell biology*, 205(5), pp. 621-631.
- Eskandari, M., Pfaller, M.R. and Kuhl, E. (2013) 'On the Role of Mechanics in Chronic Lung Disease', *Materials (Basel, Switzerland)*, 6(12), pp. 5639-5658.
- Evans, M.J., Van Winkle, L.S., Fanucchi, M.V. and Plopper, C.G. (1999) 'The Attenuated Fibroblast Sheath of the Respiratory Tract Epithelial-Mesenchymal Trophic Unit', *American Journal of Respiratory Cell and Molecular Biology*, 21(6), pp. 655-657.
- Evans, T.G. (2015) 'Considerations for the use of transcriptomics in identifying the 'genes that matter' for environmental adaptation', *The Journal of experimental biology*, 218(Pt 12), pp. 1925-1935.
- Fahy, J.V. (2015) 'Type 2 inflammation in asthma--present in most, absent in many', *Nature reviews.Immunology*, 15(1), pp. 57-65.
- Faura Tellez, G., Willemse, B.W., Brouwer, U., Nijboer-Brinksma, S., Vandepoele, K., Noordhoek, J.A., Heijink, I., de Vries, M., Smithers, N.P., Postma, D.S., Timens, W., Wiffen, L., van Roy, F., Holloway, J.W., Lackie, P.M., Nawijn, M.C. and Koppelman, G.H. (2016) 'Protocadherin-1 Localization and Cell-Adhesion Function in Airway Epithelial Cells in Asthma', *PLoS one*, 11(10), pp. e0163967.
- Faura Tellez, G., Vandepoele, K., Brouwer, U., Koning, H., Elderman, R.M., Hackett, T., Willemse, B.W.M., Holloway, J., Van Roy, F., Koppelman, G.H. and Nawijn, M.C. (2015) 'Protocadherin-1 binds to SMAD3 and suppresses TGF- β 1-induced gene transcription', *American Journal of Physiology-Lung Cellular and Molecular Physiology*, 309(7), pp. 725-735.
- Fedorov, I.A., Wilson, S.J., Davies, D.E. and Holgate, S.T. (2005) 'Epithelial stress and structural remodelling in childhood asthma', *Thorax*, 60(5), pp. 389-394.
- Fernandes-Silva, H., Correia-Pinto, J. and Moura, R.S. (2017) 'Canonical Sonic Hedgehog Signaling in Early Lung Development', *Journal of developmental biology*, 5(1), pp. 3. doi: 10.3390/jdb5010003.
- Foltz, D.R., Santiago, M.C., Berechid, B.E. and Nye, J.S. (2002) 'Glycogen synthase kinase-3 β modulates notch signaling and stability', *Current biology : CB*, 12(12), pp. 1006-1011.
- Forbes, B. (2000) 'Human airway epithelial cell lines for in vitro drug transport and metabolism studies', *Pharmaceutical science & technology today*, 3(1), pp. 18-27.

-
- Frey, A., Lunding, L.P., Ehlers, J.C., Weckmann, M., Zissler, U.M. and Wegmann, M. (2020) 'More Than Just a Barrier: The Immune Functions of the Airway Epithelium in Asthma Pathogenesis', *Frontiers in immunology*, 11, pp. 761.
- Gao, J., Yan, Q., Wang, J., Liu, S. and Yang, X. (2015) 'Epithelial-to-Mesenchymal Transition Induced by TGF- β 1 Is Mediated by AP1-Dependent EpCAM Expression in MCF-7 Cells', *Journal of cellular physiology*, 230(4), pp. 775-782.
- Gauvreau, G.M., Jordana, M., Watson, R.M., Cockcroft, D.W. and O'Byrne, P.M. (1997) 'Effect of regular inhaled albuterol on allergen-induced late responses and sputum eosinophils in asthmatic subjects', *American journal of respiratory and critical care medicine*, 156(6), pp. 1738-1745.
- Gauvreau, G.M., Parameswaran, K.N., Watson, R.M. and O'Byrne, P.M. (2001) 'Inhaled leukotriene E(4), but not leukotriene D(4), increased airway inflammatory cells in subjects with atopic asthma', *American journal of respiratory and critical care medicine*, 164(8 Pt 1), pp. 1495-1500.
- Georas, S.N. and Rezaee, F. (2014) 'Epithelial barrier function: at the front line of asthma immunology and allergic airway inflammation', *The Journal of allergy and clinical immunology*, 134(3), pp. 509-520.
- Gerovac, B.J., Valencia, M., Baumlin, N., Salathe, M., Conner, G.E. and Fregien, N.L. (2014) 'Submersion and hypoxia inhibit ciliated cell differentiation in a notch-dependent manner', *American journal of respiratory cell and molecular biology*, 51(4), pp. 516-525.
- Global Initiative for Asthma. (2020: A) Global Strategy for Asthma Management and Prevention. Available at: www.ginasthma.org
- Global Initiative for Asthma. (2020: B) Asthma Management and Prevention for adults and children older than 5 years: A pocket guide for health professionals. Available at: www.ginasthma.org
- Giuranno, L., Roig, E.M., Wansleben, C., van den Berg, A., Groot, A.J., Dubois, L. and Vooijs, M. (2020) 'NOTCH inhibition promotes bronchial stem cell renewal and epithelial barrier integrity after irradiation', *STEM CELLS Translational Medicine*, 9(7), pp. 799-812.
- Godfrey, W.L., Hill, D.M., Kilgore, J.A., Buller, G.M., Bradford, J.A., Gray, D.R., Clements, I., Oakleaf, K., Salisbury, J.J., Ignatius, M.J. and Janes, M.S. (2005) 'Complementarity of Flow Cytometry and Fluorescence Microscopy', *Microscopy and Microanalysis*, 11, pp. 246-247.
- Gohy, S., Hupin, C., Ladjemi, M.Z., Hox, V. and Pilette, C. (2020) 'Key role of the epithelium in chronic upper airways diseases', *Clinical & Experimental Allergy*, 50(2), pp. 135-146.
- Gosens, R., Zaagsma, J., Meurs, H. and Halayko, A.J. (2006) 'Muscarinic receptor signaling in the pathophysiology of asthma and COPD', *Respiratory research*, 7(1), pp. 73-9921-7-73.
- Grainge, C.L. and Davies, D.E. (2013) 'Epithelial injury and repair in airways diseases', *Chest*, 144(6), pp. 1906-1912.
- Green, J., Nusse, R. and van Amerongen, R. (2014) 'The role of Ryk and Ror receptor tyrosine kinases in Wnt signal transduction', *Cold Spring Harbor perspectives in biology*, 6(2), pp. a009175. doi: 10.1101/cshperspect.a009175.

-
- Green, R.H., Brightling, C.E., Woltmann, G., Parker, D., Wardlaw, A.J. and Pavord, I.D. (2002) 'Analysis of induced sputum in adults with asthma: identification of subgroup with isolated sputum neutrophilia and poor response to inhaled corticosteroids', *Thorax*, 57(10), pp. 875-879.
- Grumolato, L., Liu, G., Mong, P., Mudbhary, R., Biswas, R., Arroyave, R., Vijayakumar, S., Economides, A.N. and Aaronson, S.A. (2010) 'Canonical and noncanonical Wnts use a common mechanism to activate completely unrelated coreceptors', *Genes & development*, 24(22), pp. 2517-2530.
- Gu, L., Feng, J., Zheng, Z., Xu, H. and Yu, W. (2016) 'Polyphyllin I inhibits the growth of ovarian cancer cells in nude mice', *Oncology letters*, 12(6), pp. 4969-4974.
- Guan, S. and Zhou, J. (2017) 'Frizzled-7 mediates TGF- β -induced pulmonary fibrosis by transmitting non-canonical Wnt signaling', *Experimental cell research*, 359(1), pp. 226-234.
- Gudey, S.K., Sundar, R., Mu, Y., Wallenius, A., Zang, G., Bergh, A., Heldin, C.H. and Landström, M. (2014) 'TRAF6 stimulates the tumor-promoting effects of TGF β type I receptor through polyubiquitination and activation of presenilin 1', *Science signaling*, 7(307), pp. ra2.
- Guha, S., Cullen, J.P., Morrow, D., Colombo, A., Lally, C., Walls, D., Redmond, E.M. and Cahill, P.A. (2011) 'Glycogen synthase kinase 3 beta positively regulates Notch signaling in vascular smooth muscle cells: role in cell proliferation and survival', *Basic research in cardiology*, 106(5), pp. 773-785.
- Gujral, T.S. and MacBeath, G. (2010) 'A system-wide investigation of the dynamics of Wnt signaling reveals novel phases of transcriptional regulation', *PLoS one*, 5(4), pp. e10024.
- Gunawardhana, L.P., Gibson, P.G., Simpson, J.L., Benton, M.C., Lea, R.A. and Baines, K.J. (2014) 'Characteristic DNA methylation profiles in peripheral blood monocytes are associated with inflammatory phenotypes of asthma', *Epigenetics*, 9(9), pp. 1302-1316.
- Gupta, S., Hartley, R., Khan, U.T., Singapuri, A., Hargadon, B., Monteiro, W., Pavord, I.D., Sousa, A.R., Marshall, R.P., Subramanian, D., Parr, D., Entwisle, J.J., Siddiqui, S., Raj, V. and Brightling, C.E. (2014) 'Quantitative computed tomography-derived clusters: redefining airway remodeling in asthmatic patients', *The Journal of allergy and clinical immunology*, 133(3), pp. 729-38.e18.
- Gwak, J., Cho, M., Gong, S., Won, J., Kim, D., Kim, E., Lee, S.S., Kim, M., Kim, T.K., Shin, J. and Oh, S. (2006) 'Protein-kinase-C-mediated β -catenin phosphorylation negatively regulates the Wnt/ β -catenin pathway', *Journal of cell science*, 119(22), pp. 4702-4709.
- Györfi, A.H., Matei, A.E. and Distler, J.H.W. (2018) 'Targeting TGF- β signaling for the treatment of fibrosis', *Matrix biology : journal of the International Society for Matrix Biology*, 68-69, pp. 8-27.
- Habib, S.J., Chen, B.C., Tsai, F.C., Anastassiadis, K., Meyer, T., Betzig, E. and Nusse, R. (2013) 'A localized Wnt signal orients asymmetric stem cell division in vitro', *Science (New York, N.Y.)*, 339(6126), pp. 1445-1448.
- Hackett, N.R., Shaykhiev, R., Walters, M.S., Wang, R., Zwick, R.K., Ferris, B., Witover, B., Salit, J. and Crystal, R.G. (2011) 'The human airway epithelial basal cell transcriptome', *PLoS one*, 6(5), pp. e18378.
- Hackett, T.L., Ferrante, S.C., Hoptay, C.E., Engelhardt, J.F., Ingram, J.L., Zhang, Y., Alcalá, S.E., Shaheen, F., Matz, E., Pillai, D.K. and Freishtat, R.J. (2017) 'A Heterotopic Xenograft Model of Human Airways for Investigating Fibrosis in Asthma', *American journal of respiratory cell and molecular biology*, 56(3), pp. 291-299.

-
- Hackett, T.L., Warner, S.M., Stefanowicz, D., Shaheen, F., Pechkovsky, D.V., Murray, L.A., Argentieri, R., Kicic, A., Stick, S.M., Bai, T.R. and Knight, D.A. (2009) 'Induction of epithelial-mesenchymal transition in primary airway epithelial cells from patients with asthma by transforming growth factor-beta1', *American journal of respiratory and critical care medicine*, 180(2), pp. 122-133.
- Haghi, M., Hittinger, M., Zeng, Q., Oliver, B., Traini, D., Young, P.M., Huwer, H., Schneider-Daum, N. and Lehr, C.M. (2015) 'Mono- and Cocultures of Bronchial and Alveolar Epithelial Cells Respond Differently to Proinflammatory Stimuli and Their Modulation by Salbutamol and Budesonide', *Molecular pharmaceuticals*, 12(8), pp. 2625-2632.
- Haldar, P., Pavord, I.D., Shaw, D.E., Berry, M.A., Thomas, M., Brightling, C.E., Wardlaw, A.J. and Green, R.H. (2008) 'Cluster analysis and clinical asthma phenotypes', *American journal of respiratory and critical care medicine*, 178(3), pp. 218-224.
- Halwani, R., Al-Muhsen, S., Al-Jahdali, H. and Hamid, Q. (2011) 'Role of Transforming Growth Factor- β in Airway Remodeling in Asthma', *American Journal of Respiratory Cell and Molecular Biology*, 44(2), pp. 127-133.
- Han, X., Na, T., Wu, T. and Yuan, B.Z. (2020) 'Human lung epithelial BEAS-2B cells exhibit characteristics of mesenchymal stem cells', *PLoS one*, 15(1), pp. e0227174.
- Harrop, C.A., Gore, R.B., Evans, C.M., Thornton, D.J. and Herrick, S.E. (2013) 'TGF- β ₂ decreases baseline and IL-13-stimulated mucin production by primary human bronchial epithelial cells', *Experimental lung research*, 39(1), pp. 39-47.
- Hayward, P., Brennan, K., Sanders, P., Balayo, T., DasGupta, R., Perrimon, N. and Martinez Arias, A. (2005) 'Notch modulates Wnt signalling by associating with Armadillo/beta-catenin and regulating its transcriptional activity', *Development (Cambridge, England)*, 132(8), pp. 1819-1830.
- Heijink, I.H., Kuchibhotla, V.N.S., Roffel, M.P., Maes, T., Knight, D.A., Sayers, I. and Nawijn, M.C. (2020) 'Epithelial cell dysfunction, a major driver of asthma development', *Allergy*, 75(8), pp. 1898-1913.
- Heijink, I.H., de Bruin, H.G., van den Berge, M., Bennink, L.J.C., Brandenburg, S.M., Gosens, R., van Oosterhout, A.J. and Postma, D.S. (2013) 'Role of aberrant WNT signalling in the airway epithelial response to cigarette smoke in chronic obstructive pulmonary disease', *Thorax*, 68(8), pp. 709-716.
- Heijink, I., van Oosterhout, A., Kliphuis, N., Jonker, M., Hoffmann, R., Telenga, E., Klooster, K., Slebos, D., ten Hacken, N., Postma, D. and van den Berge, M. (2014) 'Oxidant-induced corticosteroid unresponsiveness in human bronchial epithelial cells', *Thorax*, 69(1), pp. 5-13.
- Hellings, P.W. and Steelant, B. (2020) 'Epithelial barriers in allergy and asthma', *The Journal of allergy and clinical immunology*, 145(6), pp. 1499-1509.
- Henderson, A.J. and Warner, J.O. (2012) 'Fetal origins of asthma', *Seminars in Fetal and Neonatal Medicine*, 17(2), pp. 82.
- Higashiyama, H., Yoshimoto, D., Okamoto, Y., Kikkawa, H., Asano, S. and Kinoshita, M. (2007) 'Receptor-activated Smad localisation in Bleomycin-induced pulmonary fibrosis', *Journal of clinical pathology*, 60(3), pp. 283-289.
- Hirai, H., Tanaka, K., Yoshie, O., Ogawa, K., Kenmotsu, K., Takamori, Y., Ichimasa, M., Sugamura, K., Nakamura, M., Takano, S. and Nagata, K. (2001) 'Prostaglandin D₂ selectively induces chemotaxis in T helper type 2 cells, eosinophils, and basophils via seven-transmembrane receptor CRTH2', *The Journal of experimental medicine*, 193(2), pp. 255-261.

-
- Ho, C., Hsu, Y.C., Lei, C.C., Mau, S.C., Shih, Y.H. and Lin, C.L. (2016) 'Curcumin Rescues Diabetic Renal Fibrosis by Targeting Superoxide-Mediated Wnt Signaling Pathways', *The American Journal of the Medical Sciences*, 351(3), pp. 286-295.
- Ho, J.C., Chan, K.N., Hu, W.H., Lam, W.K., Zheng, L., Tipoe, G.L., Sun, J., Leung, R. and Tsang, K.W. (2001) 'The effect of aging on nasal mucociliary clearance, beat frequency, and ultrastructure of respiratory cilia', *American journal of respiratory and critical care medicine*, 163(4), pp. 983-988.
- Holgate, S.T. (2000) 'Epithelial damage and response', *Clinical and experimental allergy : journal of the British Society for Allergy and Clinical Immunology*, 30 Suppl 1, pp. 37-41.
- Holgate, S.T., Holloway, J., Wilson, S., Bucchieri, F., Puddicombe, S. and Davies, D.E. (2004) 'Epithelial-Mesenchymal Communication in the Pathogenesis of Chronic Asthma', *Proceedings of the American Thoracic Society*, 1(2), pp. 93-98.
- Hollenhorst, M.I., Richter, K. and Fronius, M. (2011) 'Ion transport by pulmonary epithelia', *Journal of biomedicine & biotechnology*, 2011, pp. 174306.
- Hoshino, M., Nakamura, Y. and Sim, J.J. (1998) 'Expression of growth factors and remodelling of the airway wall in bronchial asthma', *Thorax*, 53(1), pp. 21-27.
- Hough, K.P., Curtiss, M.L., Blain, T.J., Liu, R., Trevor, J., Deshane, J.S. and Thannickal, V.J. (2020) 'Airway Remodeling in Asthma', *Frontiers in Medicine*, 7, pp. 191.
- Hsu, Y.C., Lee, P.H., Lei, C.C., Ho, C., Shih, Y.H. and Lin, C.L. (2015) 'Nitric oxide donors rescue diabetic nephropathy through oxidative-stress-and nitrosative-stress-mediated Wnt signaling pathways', *Journal of diabetes investigation*, 6(1), pp. 24-34.
- Hu, X., Gao, J.H., Liao, Y.J., Tang, S.J. and Lu, F. (2013) 'Dexamethasone alters epithelium proliferation and survival and suppresses Wnt/ β -catenin signaling in developing cleft palate', *Food and Chemical Toxicology*, 56, pp. 67.
- Huang, A.X., Lu, L.W., Liu, W.J. and Huang, M. (2016) 'Plasma Inflammatory Cytokine IL-4, IL-8, IL-10, and TNF- α Levels Correlate with Pulmonary Function in Patients with Asthma-Chronic Obstructive Pulmonary Disease (COPD) Overlap Syndrome', *Medical science monitor : international medical journal of experimental and clinical research*, 22, pp. 2800-2808.
- Huang, C.L., Liu, D., Nakano, J., Ishikawa, S., Kontani, K., Yokomise, H. and Ueno, M. (2005) 'Wnt5a expression is associated with the tumor proliferation and the stromal vascular endothelial growth factor--an expression in non-small-cell lung cancer', *Journal of clinical oncology : official journal of the American Society of Clinical Oncology*, 23(34), pp. 8765-8773.
- Huguet, E.L., Smith, K., Bicknell, R. and Harris, A.L. (1995) 'Regulation of Wnt5a mRNA expression in human mammary epithelial cells by cell shape, confluence, and hepatocyte growth factor', *The Journal of biological chemistry*, 270(21), pp. 12851-12856.
- Hussain, M., Xu, C., Lu, M., Wu, X., Tang, L. and Wu, X. (2017: A) 'Wnt/ β -catenin signaling links embryonic lung development and asthmatic airway remodeling', *Biochimica et biophysica acta. Molecular basis of disease*, 1863(12), pp. 3226-3242.
- Hussain, M., Xu, C., Ahmad, M., Yang, Y., Lu, M., Wu, X., Tang, L. and Wu, X. (2017: B) 'Notch Signaling: Linking Embryonic Lung Development and Asthmatic Airway Remodeling', *Molecular pharmacology*, 92(6), pp. 676-693.

-
- Inoue, H., Akimoto, K., Homma, T., Tanaka, A. and Sagara, H. (2020) 'Airway Epithelial Dysfunction in Asthma: Relevant to Epidermal Growth Factor Receptors and Airway Epithelial Cells', *Journal of Clinical Medicine*, 9(11), pp. 3698.
- Inoue, H., Hattori, T., Zhou, X., Etling, E.B., Modena, B.D., Trudeau, J.B., Holguin, F. and Wenzel, S.E. (2019) 'Dysfunctional ErbB2, an EGF receptor family member, hinders repair of airway epithelial cells from asthmatic patients', *The Journal of allergy and clinical immunology*, 143(6), pp. 2075-2085.e10.
- Iosifidis, T., Sutanto, E.N., Buckley, A.G., Coleman, L., Gill, E.E., Lee, A.H., Ling, K.M., Hillas, J., Looi, K., Garratt, L.W., Martinovich, K.M., Shaw, N.C., Montgomery, S.T., Kicic-Starcevic, E., Karpievitch, Y.V., Le Souëf, P., Laing, I.A., Vijayasekaran, S., Lannigan, F.J., Rigby, P.J., Hancock, R.E., Knight, D.A., Stick, S.M., Kicic, A., Western Australian Epithelial Research Program (WAERP) and Australian Respiratory Epithelium Consortium (AusREC) (2020) 'Aberrant cell migration contributes to defective airway epithelial repair in childhood wheeze', *JCI insight*, 5(7), pp. e133125. doi: 10.1172/jci.insight.133125.
- Irvine, A.D., McLean, W.H. and Leung, D.Y. (2011) 'Filaggrin mutations associated with skin and allergic diseases', *The New England journal of medicine*, 365(14), pp. 1315-1327.
- Ishitani, T., Hirao, T., Suzuki, M., Isoda, M., Ishitani, S., Harigaya, K., Kitagawa, M., Matsumoto, K. and Itoh, M. (2010) 'Nemo-like kinase suppresses Notch signalling by interfering with formation of the Notch active transcriptional complex', *Nature cell biology*, 12(3), pp. 278-285.
- Ishitani, T., Kishida, S., Hyodo-Miura, J., Ueno, N., Yasuda, J., Waterman, M., Shibuya, H., Moon, R.T., Ninomiya-Tsuji, J. and Matsumoto, K. (2003) 'The TAK1-NLK mitogen-activated protein kinase cascade functions in the Wnt-5a/Ca(2+) pathway to antagonize Wnt/beta-catenin signaling', *Molecular and cellular biology*, 23(1), pp. 131-139.
- Ishitani, T., Ninomiya-Tsuji, J., Nagai, S., Nishita, M., Meneghini, M., Barker, N., Waterman, M., Bowerman, B., Clevers, H., Shibuya, H. and Matsumoto, K. (1999) 'The TAK1-NLK-MAPK-related pathway antagonizes signalling between β -catenin and transcription factor TCF', *Nature*, 399(6738), pp. 798-802.
- Ito, J., Harada, N., Nagashima, O., Makino, F., Usui, Y., Yagita, H., Okumura, K., Dorscheid, D.R., Atsuta, R., Akiba, H. and Takahashi, K. (2011) 'Wound-induced TGF- β 1 and TGF- β 2 enhance airway epithelial repair via HB-EGF and TGF- α ', *Biochemical and biophysical research communications*, 412(1), pp. 109.
- Jain, R., Ray, J.M., Pan, J.H. and Brody, S.L. (2012) 'Sex hormone-dependent regulation of cilia beat frequency in airway epithelium', *American journal of respiratory cell and molecular biology*, 46(4), pp. 446-453.
- Jakiela, B., Brockman-Schneider, R., Amineva, S., Lee, W.M. and Gern, J.E. (2008) 'Basal cells of differentiated bronchial epithelium are more susceptible to rhinovirus infection', *American journal of respiratory cell and molecular biology*, 38(5), pp. 517-523.
- James, A.L., Maxwell, P.S., Pearce-Pinto, G., Elliot, J.G. and Carroll, N.G. (2002) 'The Relationship of Reticular Basement Membrane Thickness to Airway Wall Remodeling in Asthma', *American Journal of Respiratory and Critical Care Medicine*, 166(12), pp. 1590-1595.
- James, B., Milstien, S. and Spiegel, S. (2019) 'ORMDL3 and allergic asthma: From physiology to pathology', *The Journal of allergy and clinical immunology*, 144(3), pp. 634-640.
- Januskevicius, A., Vaitkiene, S., Gosens, R., Janulaityte, I., Hoppenot, D., Sakalauskas, R. and Malakauskas, K. (2016) 'Eosinophils enhance WNT-5a and TGF-beta1 genes

-
- expression in airway smooth muscle cells and promote their proliferation by increased extracellular matrix proteins production in asthma', *BMC pulmonary medicine*, 16(1), pp. 94-016-0254-9.
- Jendzjowsky, N.G. and Kelly, M.M. (2019) 'The Role of Airway Myofibroblasts in Asthma', *Chest*, 156(6), pp. 1254.
- Jenei, V., Sherwood, V., Howlin, J., Linnskog, R., Säfholm, A., Axelsson, L. and Andersson, T. (2009) 'A t-butylloxycarbonyl-modified Wnt5a-derived hexapeptide functions as a potent antagonist of Wnt5a-dependent melanoma cell invasion', *Proceedings of the National Academy of Sciences of the United States of America*, 106(46), pp. 19473-19478.
- Jetten, A.M., Shirley, J.E. and Stoner, G. (1986) 'Regulation of proliferation and differentiation of respiratory tract epithelial cells by TGF beta', *Experimental cell research*, 167(2), pp. 539-549.
- Jia, D., Underwood, J., Xu, Q. and Xie, Q. (2019) 'NOTCH2/NOTCH3/DLL3/MAML1/ADAM17 signaling network is associated with ovarian cancer', *Oncology letters*, 17(6), pp. 4914-4920.
- Jia, L., Miao, C., Cao, Y. and Duan, E.k. (2008) 'Effects of Wnt proteins on cell proliferation and apoptosis in HEK293 cells', *Cell biology international*, 32(7), pp. 807.
- Jiao, J., Wang, H., Lou, W., Jin, S., Fan, E., Li, Y., Han, D. and Zhang, L. (2011) 'Regulation of ciliary beat frequency by the nitric oxide signaling pathway in mouse nasal and tracheal epithelial cells', *Experimental cell research*, 317(17), pp. 2548-2553.
- Jin, Y.H., Kim, H., Ki, H., Yang, I., Yang, N., Lee, K.Y., Kim, N., Park, H.S. and Kim, K. (2009: A) 'Beta-catenin modulates the level and transcriptional activity of Notch1/NICD through its direct interaction', *Biochimica et biophysica acta*, 1793(2), pp. 290-299.
- Jin, Y.H., Kim, H., Oh, M., Ki, H. and Kim, K. (2009: B) 'Regulation of Notch1/NICD and Hes1 expressions by GSK-3alpha/beta', *Molecules and cells*, 27(1), pp. 15-19.
- Joskova, M., Mokry, J. and Franova, S. (2020) 'Respiratory Cilia as a Therapeutic Target of Phosphodiesterase Inhibitors', *Frontiers in Pharmacology*, 11, pp. 609.
- Jung, Y.S., Lee, H.Y., Kim, S.D., Park, J.S., Kim, J.K., Suh, P.G. and Bae, Y.S. (2013) 'Wnt5a stimulates chemotactic migration and chemokine production in human neutrophils', *Experimental & molecular medicine*, 45(6), pp. e27.
- Kalinina, E.P., Denisenko, Y.K., Vitkina, T.I., Lobanova, E.G., Novgorodtseva, T.P., Antonyuk, M.V., Gvozdenko, T.A., Knyshova, V.V. and Nazarenko, A.V. (2016) 'The Mechanisms of the Regulation of Immune Response in Patients with Comorbidity of Chronic Obstructive Pulmonary Disease and Asthma', *Canadian respiratory journal*, 2016, pp. 4503267.
- Kalluri, R. and Weinberg, R.A. (2009) 'The basics of epithelial-mesenchymal transition', *The Journal of clinical investigation*, 119(6), pp. 1420-1428.
- Kanaoka, Y. and Austen, K.F. (2019) 'Chapter Three - Roles of cysteinyl leukotrienes and their receptors in immune cell-related functions', in Frederick Alt (ed.) Academic Press, pp. 65.
- Kaplan, A. and Chang, K. (2020) 'Tiotropium in asthma – perspectives for the primary care physician', *Postgraduate medicine*, 0(ja), pp. nu.

-
- Katoh, M. and Katoh, M. (2009) 'Transcriptional mechanisms of WNT5A based on NF-kappaB, Hedgehog, TGFbeta, and Notch signaling cascades', *International journal of molecular medicine*, 23(6), pp. 763-769.
- Katsuno, Y., Meyer, D.S., Zhang, Z., Shokat, K.M., Akhurst, R.J., Miyazono, K. and Derynck, R. (2019) 'Chronic TGF- β exposure drives stabilized EMT, tumor stemness, and cancer drug resistance with vulnerability to bitopic mTOR inhibition', *Science Signaling*, 12(570), pp. eaau8544.
- Kaur, D., Chachi, L., Gomez, E., Sylvius, N., Singh, S.R., Ramsheh, M.Y., Saunders, R. and Brightling, C.E. (2020) 'ST2 expression and release by the bronchial epithelium is downregulated in asthma', *Allergy*, .
- Keller, L., Werner, S. and Pantel, K. (2019) 'Biology and clinical relevance of EpCAM', *Cell stress*, 3(6), pp. 165-180.
- Kelly, J.T. and Busse, W.W. (2008) 'Host immune responses to rhinovirus: mechanisms in asthma', *The Journal of allergy and clinical immunology*, 122(4), pp. 671-682.
- Khalil, N., O'Connor, R.N., Flanders, K.C. and Unruh, H. (1996) 'TGF-beta 1, but not TGF-beta 2 or TGF-beta 3, is differentially present in epithelial cells of advanced pulmonary fibrosis: an immunohistochemical study', *American journal of respiratory cell and molecular biology*, 14(2), pp. 131-138.
- Khalil, N., Parekh, T.V., O'Connor, R., Antman, N., Kepron, W., Yehaulaeshet, T., Xu, Y.D. and Gold, L.I. (2001) 'Regulation of the effects of TGF- β 1 by activation of latent TGF- β 1 and differential expression of TGF- β receptors (T β R-I and T β R-II) in idiopathic pulmonary fibrosis', *Thorax*, 56(12), pp. 907-915.
- Khalil, N., Xu, Y.D., O'Connor, R. and Duronio, V. (2005) 'Proliferation of pulmonary interstitial fibroblasts is mediated by transforming growth factor-beta1-induced release of extracellular fibroblast growth factor-2 and phosphorylation of p38 MAPK and JNK', *The Journal of biological chemistry*, 280(52), pp. 43000-43009.
- Khan, N.A., Willemarck, N., Talebi, A., Marchand, A., Binda, M.M., Dehairs, J., Rueda-Rincon, N., Daniels, V.W., Bagadi, M., Thimiri Govinda Raj, D.B., Vanderhoydonc, F., Munck, S., Chaltin, P. and Swinnen, J.V. (2016) 'Identification of drugs that restore primary cilium expression in cancer cells', *Oncotarget*, 7(9), pp. 9975-9992.
- Kikuchi, A., Yamamoto, H. and Sato, A. (2009) 'Selective activation mechanisms of Wnt signaling pathways', *Trends in cell biology*, 19(3), pp. 119-129.
- Kim, H., Yin, W., Nakamichi, Y., Panza, P., Grohmann, B., Buettner, C., Guenther, S., Ruppert, C., Kobayashi, Y., Guenther, A. and Stainier, D.Y.R. (2019) 'WNT/RYK signaling restricts goblet cell differentiation during lung development and repair', *Proceedings of the National Academy of Sciences*, 116(51), pp. 25697-25706.
- Kim, J., Kim, D.W., Chang, W., Choe, J., Kim, J., Park, C.S., Song, K. and Lee, I. (2012) 'Wnt5a is secreted by follicular dendritic cells to protect germinal center B cells via Wnt/Ca²⁺/NFAT/NF- κ B cell lymphoma 6 signaling', *Journal of immunology (Baltimore, Md.: 1950)*, 188(1), pp. 182-189.
- Kim, M.Y., Song, W.J. and Cho, S.H. (2016) 'Pharmacotherapy in the management of asthma in the elderly: a review of clinical studies', *Asia Pacific allergy*, 6(1), pp. 3-15.
- Knüppel, L., Ishikawa, Y., Aichler, M., Heinzelmann, K., Hatz, R., Behr, J., Walch, A., Bächinger, H.P., Eickelberg, O. and Staab-Weijnitz, C.A. (2017) 'A Novel Antifibrotic Mechanism of Nintedanib and Pirfenidone. Inhibition of Collagen Fibril Assembly', *American Journal of Respiratory Cell and Molecular Biology*, 57(1), pp. 77-90.

-
- Kogiso, H., Hosogi, S., Ikeuchi, Y., Tanaka, S., Shimamoto, C., Matsumura, H., Nakano, T., Sano, K.I., Inui, T., Marunaka, Y. and Nakahari, T. (2017) 'A low [Ca(2+)](i)-induced enhancement of cAMP-activated ciliary beating by PDE1A inhibition in mouse airway cilia', *Pflugers Archiv : European journal of physiology*, 469(9), pp. 1215-1227.
- Kolosova, I., Nethery, D. and Kern, J.A. (2011) 'Role of Smad2/3 and p38 MAP kinase in TGF- β 1-induced epithelial-mesenchymal transition of pulmonary epithelial cells', *Journal of cellular physiology*, 226(5), pp. 1248-1254.
- Königshoff, M., Balsara, N., Pfaff, E.M., Kramer, M., Chrobak, I., Seeger, W. and Eickelberg, O. (2008) 'Functional Wnt signaling is increased in idiopathic pulmonary fibrosis', *PLoS one*, 3(5), pp. e2142.
- Kony, S., Zureik, M., Driss, F., Neukirch, C., Leynaert, B. and Neukirch, F. (2004) 'Association of bronchial hyperresponsiveness and lung function with C-reactive protein (CRP): a population based study', *Thorax*, 59(10), pp. 892-896.
- Koopmans, T. and Gosens, R. (2018) 'Revisiting asthma therapeutics: focus on WNT signal transduction', *Drug discovery today*, 23(1), pp. 49-62.
- Kopan, R. and Ilagan, M.X. (2009) 'The canonical Notch signaling pathway: unfolding the activation mechanism', *Cell*, 137(2), pp. 216-233.
- Korol, A., Taiyab, A. and West-Mays, J.A. (2016) 'RhoA/ROCK signaling regulates TGF β -induced epithelial-mesenchymal transition of lens epithelial cells through MRTF-A', *Molecular medicine (Cambridge, Mass.)*, 22, pp. 713-723.
- Kovacs, T., Csongei, V., Feller, D., Ernszt, D., Smuk, G., Sarosi, V., Jakab, L., Kvell, K., Bartis, D. and Pongracz, J.E. (2014) 'Alteration in the Wnt microenvironment directly regulates molecular events leading to pulmonary senescence', *Aging cell*, 13(5), pp. 838-849.
- Krishnamurthy, A., Dasari, A., Noonan, A.M., Mehnert, J.M., Lockhart, A.C., Leong, S., Capasso, A., Stein, M.N., Sanoff, H.K., Lee, J.J., Hansen, A., Malhotra, U., Rippke, S., Gustafson, D.L., Pitts, T.M., Ellison, K., Davis, S.L., Messersmith, W.A., Eckhardt, S.G. and Lieu, C.H. (2018) 'Phase Ib Results of the Rational Combination of Selumetinib and Cyclosporin A in Advanced Solid Tumors with an Expansion Cohort in Metastatic Colorectal Cancer', *Cancer research*, 78(18), pp. 5398-5407.
- Krstić, J., Trivanović, D., Mojsilović, S. and Santibanez, J.F. (2015) 'Transforming Growth Factor-Beta and Oxidative Stress Interplay: Implications in Tumorigenesis and Cancer Progression', *Oxidative Medicine and Cellular Longevity*, 2015, pp. 654594.
- Kumawat, K. and Gosens, R. (2016) 'WNT-5A: signaling and functions in health and disease', *Cellular and molecular life sciences : CMLS*, 73(3), pp. 567-587.
- Kumawat, K., Menzen, M.H., Bos, I.S., Baarsma, H.A., Borger, P., Roth, M., Tamm, M., Halayko, A.J., Simoons, M., Prins, A., Postma, D.S., Schmidt, M. and Gosens, R. (2013) 'Noncanonical WNT-5A signaling regulates TGF-beta-induced extracellular matrix production by airway smooth muscle cells', *FASEB journal : official publication of the Federation of American Societies for Experimental Biology*, 27(4), pp. 1631-1643.
- Kumawat, K., Menzen, M.H., Slegtenhorst, R.M., Halayko, A.J., Schmidt, M. and Gosens, R. (2014) 'TGF-beta-activated kinase 1 (TAK1) signaling regulates TGF-beta-induced WNT-5A expression in airway smooth muscle cells via Sp1 and beta-catenin', *PLoS one*, 9(4), pp. e94801.
- Kuo, C.S., Pavlidis, S., Loza, M., Baribaud, F., Rowe, A., Pandis, I., Hoda, U., Rossios, C., Sousa, A., Wilson, S.J., Howarth, P., Dahlen, B., Dahlen, S., Chanez, P., Shaw, D., Krug, N., Sandström, T., De Meulder, B., Lefaudeux, D., Fowler, S., Fleming, L.,

-
- Corfield, J., Auffray, C., Sterk, P.J., Djukanovic, R., Guo, Y., Adcock, I.M., Chung, K.F. and U-BIOPRED Project Team † (2017: A) 'A Transcriptome-driven Analysis of Epithelial Brushings and Bronchial Biopsies to Define Asthma Phenotypes in U-BIOPRED', *American journal of respiratory and critical care medicine*, 195(4), pp. 443–455.
- Kuo, C.S., Pavlidis, S., Loza, M., Baribaud, F., Rowe, A., Pandis, I., Sousa, A., Corfield, J., Djukanovic, R., Lutter, R., Sterk, P.J., Auffray, C., Guo, Y., Adcock, I.M., Chung, K.F. and U-BIOPRED Study Group (2017: B) 'T-helper cell type 2 (Th2) and non-Th2 molecular phenotypes of asthma using sputum transcriptomics in U-BIOPRED', *The European respiratory journal*, 49(2), pp. 1602135. doi: 10.1183/13993003.02135-2016. Print 2017 Feb.
- Kurayoshi, M., Yamamoto, H., Izumi, S. and Kikuchi, A. (2007) 'Post-translational palmitoylation and glycosylation of Wnt-5a are necessary for its signalling', *The Biochemical journal*, 402(3), pp. 515-523.
- Kwak, H.J., Park, D.W., Seo, J.Y., Moon, J.Y., Kim, T.H., Sohn, J.W., Shin, D.H., Yoon, H.J., Park, S.S. and Kim, S.H. (2015) 'The Wnt/ β -catenin signaling pathway regulates the development of airway remodeling in patients with asthma', *Experimental & molecular medicine*, 47(12), pp. e198.
- Kwon, C., Cheng, P., King, I.N., Andersen, P., Shenje, L., Nigam, V. and Srivastava, D. (2011) 'Notch post-translationally regulates β -catenin protein in stem and progenitor cells', *Nature cell biology*, 13(10), pp. 1244-1251.
- Lachowicz-Scroggins, M.E., Yuan, S., Kerr, S.C., Dunican, E.M., Yu, M., Carrington, S.D. and Fahy, J.V. (2016) 'Abnormalities in MUC5AC and MUC5B Protein in Airway Mucus in Asthma', *American journal of respiratory and critical care medicine*, 194(10), pp. 1296-1299.
- Lackie, P.M., Baker, J.E., Günthert, U. and Holgate, S.T. (1997) 'Expression of CD44 isoforms is increased in the airway epithelium of asthmatic subjects.', *American Journal of Respiratory Cell and Molecular Biology*, 16(1), pp. 14-22.
- Lambrecht, B.N. and Hammad, H. (2015) 'The immunology of asthma', *Nature immunology*, 16(1), pp. 45-56.
- Lambrecht, B.N. and Hammad, H. (2012) 'The airway epithelium in asthma', *Nature medicine*, 18(5), pp. 684-692.
- Lange, P., Parner, J., Vestbo, J., Schnohr, P. and Jensen, G. (1998) 'A 15-year follow-up study of ventilatory function in adults with asthma', *The New England journal of medicine*, 339(17), pp. 1194-1200.
- Larsson, K., Kankaanranta, H., Janson, C., Lehtimäki, L., Ställberg, B., Løkke, A., Høines, K., Roslind, K. and Ulrik, C.S. (2020) 'Bringing asthma care into the twenty-first century', *NPJ primary care respiratory medicine*, 30(1), pp. 25-020-0182-2.
- Lawrence, D.A., Pircher, R. and Jullien, P. (1985) 'Conversion of a high molecular weight latent β -TGF from chicken embryo fibroblasts into a low molecular weight active β -TGF under acidic conditions', *Biochemical and biophysical research communications*, 133(3), pp. 1026.
- Lechapt-Zalcman, E., Prulière-Escabasse, V., Advenier, D., Galiacy, S., Charrière-Bertrand, C., Coste, A., Harf, A., d'Ortho, M.-. and Escudier, E. (2006) 'Transforming growth factor- β 1 increases airway wound repair via MMP-2 upregulation: a new pathway for epithelial wound repair?', *American Journal of Physiology-Lung Cellular and Molecular Physiology*, 290(6), pp. 1277-1282.

-
- Lee, J.H., Haselkorn, T., Borish, L., Rasouliyan, L., Chipps, B.E. and Wenzel, S.E. (2007) 'Risk factors associated with persistent airflow limitation in severe or difficult-to-treat asthma: insights from the TENOR study', *Chest*, 132(6), pp. 1882-1889.
- Lee, J.M., Kim, I.S., Kim, H., Lee, J.S., Kim, K., Yim, H.Y., Jeong, J., Kim, J.H., Kim, J.Y., Lee, H., Seo, S.B., Kim, H., Rosenfeld, M.G., Kim, K.I. and Baek, S.H. (2010) 'RORalpha attenuates Wnt/beta-catenin signaling by PKCalpha-dependent phosphorylation in colon cancer', *Molecular cell*, 37(2), pp. 183-195.
- Legrand, C., Gilles, C., Zahm, J.M., Polette, M., Buisson, A.C., Kaplan, H., Birembaut, P. and Tournier, J.M. (1999) 'Airway epithelial cell migration dynamics. MMP-9 role in cell-extracellular matrix remodeling', *The Journal of cell biology*, 146(2), pp. 517-529.
- Leir, S., Baker, J.E., Holgate, S.T. and Lackie, P.M. (2000) 'Increased CD44 expression in human bronchial epithelial repair after damage or plating at low cell densities', *American Journal of Physiology-Lung Cellular and Molecular Physiology*, 278(6), pp. 1129-1137.
- Lewis, B.W., Patial, S. and Saini, Y. (2019) 'Immunopathology of Airway Surface Liquid Dehydration Disease', *Journal of immunology research*, 2019, pp. 2180409.
- Li, C., Bellusci, S., Borok, Z. and Minoo, P. (2015) 'Non-canonical WNT signalling in the lung', *Journal of Biochemistry*, 158(5), pp. 355-365.
- Li, C., Xiao, J., Hormi, K., Borok, Z. and Minoo, P. (2002) 'Wnt5a participates in distal lung morphogenesis', *Developmental biology*, 248(1), pp. 68-81.
- Li, H., Romieu, I., Wu, H., Sienra-Monge, J., Ramírez-Aguilar, M., del Río-Navarro, B.E., del Lara-Sánchez, I.C., Kistner, E.O., Gjessing, H.K. and London, S.J. (2007) 'Genetic polymorphisms in transforming growth factor beta-1 (TGFB1) and childhood asthma and atopy', *Human genetics*, 121(5), pp. 529–538.
- Li, J., Zhang, N., Huang, X., Xu, J., Fernandes, J.C., Dai, K. and Zhang, X. (2013) 'Dexamethasone shifts bone marrow stromal cells from osteoblasts to adipocytes by C/EBPalpha promoter methylation', *Cell death & disease*, 4(10), pp. e832.
- Li, M., Wang, H., Huang, T., Wang, J., Ding, Y., Li, Z., Zhang, J. and Li, L. (2010) 'TAB2 scaffolds TAK1 and NLK in repressing canonical Wnt signaling', *The Journal of biological chemistry*, 285(18), pp. 13397-13404.
- Li, Y., Li, X., Zhou, W., Yu, Q. and Lu, Y. (2020) 'ORMDL3 modulates airway epithelial cell repair in children with asthma under glucocorticoid treatment via regulating IL-33', *Pulmonary pharmacology & therapeutics*, 64, pp. 101963.
- Ling, K., Sutanto, E.N., Iosifidis, T., Kicic-Starcevic, E., Looi, K., Garratt, L.W., Martinovich, K.M., Lannigan, F.J., Knight, D.A., Stick, S.M. and Kicic, A. (2016) 'Reduced transforming growth factor β 1 (TGF- β 1) in the repair of airway epithelial cells of children with asthma', *Respirology*, 21(7), pp. 1219-1226.
- Linke, F., Zaunig, S., Nietert, M.M., von Bonin, F., Lutz, S., Dullin, C., Janovská, P., Beissbarth, T., Alves, F., Klapper, W., Bryja, V., Pukrop, T., Trümper, L., Wilting, J. and Kube, D. (2017) 'WNT5A: a motility-promoting factor in Hodgkin lymphoma', *Oncogene*, 36(1), pp. 13-23.
- Liu, A., Chen, S., Cai, S., Dong, L., Liu, L., Yang, Y., Guo, F., Lu, X., He, H., Chen, Q., Hu, S. and Qiu, H. (2014) 'Wnt5a through noncanonical Wnt/JNK or Wnt/PKC signaling contributes to the differentiation of mesenchymal stem cells into type II alveolar epithelial cells in vitro', *PLoS one*, 9(3), pp. e90229.

-
- Liu, C., Xu, P., Lamouille, S., Xu, J. and Derynck, R. (2009) 'TACE-mediated ectodomain shedding of the type I TGF-beta receptor downregulates TGF-beta signaling', *Molecular cell*, 35(1), pp. 26-36.
- Liu, G., Betts, C., Cunoosamy, D.M., Åberg, P.M., Hornberg, J.J., Sivars, K.B. and Cohen, T.S. (2019: A) 'Use of precision cut lung slices as a translational model for the study of lung biology', *Respiratory research*, 20(1), pp. 162-019-1131-x.
- Liu, G., Cooley, M.A., Nair, P.M., Donovan, C., Hsu, A.C., Jarnicki, A.G., Haw, T.J., Hansbro, N.G., Ge, Q., Brown, A.C., Tay, H., Foster, P.S., Wark, P.A., Horvat, J.C., Bourke, J.E., Grainge, C.L., Argraves, W.S., Oliver, B.G., Knight, D.A., Burgess, J.K. and Hansbro, P.M. (2017) 'Airway remodelling and inflammation in asthma are dependent on the extracellular matrix protein fibulin-1c', *The Journal of pathology*, 243(4), pp. 510-523.
- Liu, J., Zhang, M., Niu, C., Luo, Z., Dai, J., Wang, L., Liu, E. and Fu, Z. (2013) 'Dexamethasone inhibits repair of human airway epithelial cells mediated by glucocorticoid-induced leucine zipper (GILZ)', *PloS one*, 8(4), pp. e60705.
- Liu, M., Zhao, Y., Wang, C., Luo, H., A, P. and Ye, L. (2019: B) 'Interleukin-17 plays a role in pulp inflammation partly by WNT5A protein induction', *Archives of Oral Biology*, 103, pp. 33.
- Liu, X., Ory, V., Chapman, S., Yuan, H., Albanese, C., Kallakury, B., Timofeeva, O.A., Nealon, C., Dakic, A., Simic, V., Haddad, B.R., Rhim, J.S., Dritschilo, A., Riegel, A., McBride, A. and Schlegel, R. (2012) 'ROCK inhibitor and feeder cells induce the conditional reprogramming of epithelial cells', *The American journal of pathology*, 180(2), pp. 599-607.
- Loeffler, M. and Roeder, I. (2002) 'Tissue stem cells: definition, plasticity, heterogeneity, self-organization and models--a conceptual approach', *Cells, tissues, organs*, 171(1), pp. 8-26.
- Loscertales, M., Mikels, A.J., Hu, J.K., Donahoe, P.K. and Roberts, D.J. (2008) 'Chick pulmonary Wnt5a directs airway and vascular tubulogenesis', *Development (Cambridge, England)*, 135(7), pp. 1365-1376.
- Lötvall, J., Akdis, C.A., Bacharier, L.B., Bjermer, L., Casale, T.B., Custovic, A., Lemanske, R.F., Jr, Wardlaw, A.J., Wenzel, S.E. and Greenberger, P.A. (2011) 'Asthma endotypes: a new approach to classification of disease entities within the asthma syndrome', *The Journal of allergy and clinical immunology*, 127(2), pp. 355-360.
- Loxham, M., Davies, D.E. and Blume, C. (2014) 'Epithelial function and dysfunction in asthma', *Clinical and experimental allergy : journal of the British Society for Allergy and Clinical Immunology*, 44(11), pp. 1299-1313.
- Loxham, M. and Davies, D.E. (2017) 'Phenotypic and genetic aspects of epithelial barrier function in asthmatic patients', *Journal of Allergy and Clinical Immunology*, 139(6), pp. 1736.
- Lu, B., Green, B.A., Farr, J.M., Lopes, F.C.M. and Van Raay, T.J. (2016) 'Wnt Drug Discovery: Weaving Through the Screens, Patents and Clinical Trials', *Cancers*, 8(9).
- Lu, C., Wang, X., Zhu, H., Feng, J., Ni, S. and Huang, J. (2015) 'Over-expression of ROR2 and Wnt5a cooperatively correlates with unfavorable prognosis in patients with non-small cell lung cancer', *Oncotarget*, 6(28), pp. 24912-24921.
- Lund, R.J., Osmala, M., Malonzo, M., Lukkarinen, M., Leino, A., Salmi, J., Vuorikoski, S., Turunen, R., Vuorinen, T., Akdis, C., Lähdesmäki, H., Lahesmaa, R. and Jartti, T. (2018) 'Atopic asthma after rhinovirus-induced wheezing is associated with DNA methylation change in the SMAD3 gene promoter', *Allergy*, 73(8), pp. 1735-1740.

-
- Lynch, K.R., O'Neill, G.P., Liu, Q., Im, D.S., Sawyer, N., Metters, K.M., Coulombe, N., Abramovitz, M., Figueroa, D.J., Zeng, Z., Connolly, B.M., Bai, C., Austin, C.P., Chateaufneuf, A., Stocco, R., Greig, G.M., Kargman, S., Hooks, S.B., Hosfield, E., Williams, D.L., Jr, Ford-Hutchinson, A.W., Caskey, C.T. and Evans, J.F. (1999) 'Characterization of the human cysteinyl leukotriene CysLT1 receptor', *Nature*, 399(6738), pp. 789-793.
- Maestre-Battle, D., Pena, O.M., Hirota, J.A., Gunawan, E., Rider, C.F., Sutherland, D., Alexis, N.E. and Carlsten, C. (2017) 'Novel flow cytometry approach to identify bronchial epithelial cells from healthy human airways', *Scientific reports*, 7, pp. 42214.
- Mak, J.C., Nishikawa, M. and Barnes, P.J. (1995) 'Glucocorticosteroids increase beta 2-adrenergic receptor transcription in human lung', *American Journal of Physiology-Lung Cellular and Molecular Physiology*, 268(1), pp. 41-46.
- Mak, J.C., Nishikawa, M., Shirasaki, H., Miyayasu, K. and Barnes, P.J. (1995) 'Protective effects of a glucocorticoid on downregulation of pulmonary beta 2-adrenergic receptors in vivo', *The Journal of clinical investigation*, 96(1), pp. 99-106.
- Makinde, T., Murphy, R.F. and Agrawal, D.K. (2007) 'The regulatory role of TGF-beta in airway remodeling in asthma', *Immunology and cell biology*, 85(5), pp. 348-356.
- Matsumoto, K., Taki, F., Miura, M., Matsuzaki, M. and Takagi, K. (1994) 'Serum levels of soluble IL-2R, IL-4, and soluble Fc epsilon RII in adult bronchial asthma', *Chest*, 105(3), pp. 681-686.
- Matsumoto, T., Yokoi, A., Hashimura, M., Oguri, Y., Akiya, M. and Saegusa, M. (2018) 'TGF- β -mediated LEFTY/Akt/GSK-3 β /Snail axis modulates epithelial-mesenchymal transition and cancer stem cell properties in ovarian clear cell carcinomas', *Molecular carcinogenesis*, 57(8), pp. 957-967.
- McGregor, M.C., Krings, J.G., Nair, P. and Castro, M. (2019) 'Role of Biologics in Asthma', *American journal of respiratory and critical care medicine*, 199(4), pp. 433-445.
- Mereness, J.A., Bhattacharya, S., Wang, Q., Ren, Y., Pryhuber, G.S. and Mariani, T.J. (2018) 'Type VI collagen promotes lung epithelial cell spreading and wound-closure', *PLoS one*, 13(12), pp. e0209095.
- Michalik, M., Wójcik-Pszczola, K., Paw, M., Wnuk, D., Koczurkiewicz, P., Sanak, M., Pękala, E. and Madeja, Z. (2018) 'Fibroblast-to-myofibroblast transition in bronchial asthma', *Cellular and molecular life sciences : CMLS*, 75(21), pp. 3943-3961.
- Mikels, A.J. and Nusse, R. (2006) 'Purified Wnt5a protein activates or inhibits beta-catenin-TCF signaling depending on receptor context', *PLoS biology*, 4(4), pp. e115.
- Milara, J., Mata, M., Serrano, A., Peiró, T., Morcillo, E.J. and Cortijo, J. (2010) 'Extracellular calcium-sensing receptor mediates human bronchial epithelial wound repair', *Biochemical pharmacology*, 80(2), pp. 236.
- Miller, M., Rosenthal, P., Beppu, A., Mueller, J.L., Hoffman, H.M., Tam, A.B., Doherty, T.A., McGeough, M.D., Pena, C.A., Suzukawa, M., Niwa, M. and Broide, D.H. (2014) 'ORMDL3 transgenic mice have increased airway remodeling and airway responsiveness characteristic of asthma', *Journal of immunology (Baltimore, Md. : 1950)*, 192(8), pp. 3475-3487.
- Mima, K., Okabe, H., Ishimoto, T., Hayashi, H., Nakagawa, S., Kuroki, H., Watanabe, M., Beppu, T., Tamada, M., Nagano, O., Saya, H. and Baba, H. (2012) 'CD44s regulates the TGF- β -mediated mesenchymal phenotype and is associated with poor prognosis in patients with hepatocellular carcinoma', *Cancer research*, 72(13), pp. 3414-3423.

-
- Minshall, E.M., Leung, D.Y.M., Martin, R.J., Song, Y.L., Cameron, L., Ernst, P. and Hamid, Q. (1997) 'Eosinophil-associated TGF- β 1 mRNA Expression and Airways Fibrosis in Bronchial Asthma', *American Journal of Respiratory Cell and Molecular Biology*, 17(3), pp. 326-333.
- Miyazawa, K. and Miyazono, K. (2017) 'Regulation of TGF- β Family Signaling by Inhibitory Smads', *Cold Spring Harbor perspectives in biology*, 9(3), pp. a022095. doi: 10.1101/cshperspect.a022095.
- Miyoshi, H., Ajima, R., Luo, C.T., Yamaguchi, T.P. and Stappenbeck, T.S. (2012) 'Wnt5a potentiates TGF-beta signaling to promote colonic crypt regeneration after tissue injury', *Science (New York, N.Y.)*, 338(6103), pp. 108-113.
- Modena, B.D., Tedrow, J.R., Milosevic, J., Bleecker, E.R., Meyers, D.A., Wu, W., Bar-Joseph, Z., Erzurum, S.C., Gaston, B.M., Busse, W.W., Jarjour, N.N., Kaminski, N. and Wenzel, S.E. (2014) 'Gene expression in relation to exhaled nitric oxide identifies novel asthma phenotypes with unique biomolecular pathways', *American journal of respiratory and critical care medicine*, 190(12), pp. 1363-1372.
- Moffatt, M.F., Gut, I.G., Demenais, F., Strachan, D.P., Bouzigon, E., Heath, S., von Mutius, E., Farrall, M., Lathrop, M., Cookson, W.O.C.M. and GABRIEL Consortium (2010) 'A large-scale, consortium-based genomewide association study of asthma', *The New England journal of medicine*, 363(13), pp. 1211-1221.
- Monadi, M., Firouzjahi, A., Hosseini, A., Javadian, Y., Sharbatdaran, M. and Heidari, B. (2016) 'Serum C-reactive protein in asthma and its ability in predicting asthma control, a case-control study', *Caspian journal of internal medicine*, 7(1), pp. 37–42.
- Montoro, D.T., Haber, A.L., Biton, M., Vinarsky, V., Lin, B., Birket, S.E., Yuan, F., Chen, S., Leung, H.M., Villoria, J., Rogel, N., Burgin, G., Tsankov, A.M., Waghray, A., Slyper, M., Waldman, J., Nguyen, L., Dionne, D., Rozenblatt-Rosen, O., Tata, P.R., Mou, H., Shivaraju, M., Bihler, H., Mense, M., Tearney, G.J., Rowe, S.M., Engelhardt, J.F., Regev, A. and Rajagopal, J. (2018) 'A revised airway epithelial hierarchy includes CFTR-expressing ionocytes', *Nature*, 560(7718), pp. 319-324.
- Moon, R.T. and Gough, N.R. (2016) 'Beyond canonical: The Wnt and β -catenin story', *Science signaling*, 9(422), pp. eg5.
- Moore, K.N., Gunderson, C.C., Sabbatini, P., McMeekin, D.S., Mantia-Smaldone, G., Burger, R.A., Morgan, M.A., Kapoun, A.M., Brachmann, R.K., Stagg, R., Farooki, A. and O'Ceirbhail, R.E. (2019) 'A phase 1b dose escalation study of ipafricept (OMP54F28) in combination with paclitaxel and carboplatin in patients with recurrent platinum-sensitive ovarian cancer', *Gynecologic oncology*, 154(2), pp. 294-301.
- Moore, W.C., Meyers, D.A., Wenzel, S.E., Teague, W.G., Li, H., Li, X., D'Agostino, R., Jr, Castro, M., Curran-Everett, D., Fitzpatrick, A.M., Gaston, B., Jarjour, N.N., Sorkness, R., Calhoun, W.J., Chung, K.F., Comhair, S.A., Dweik, R.A., Israel, E., Peters, S.P., Busse, W.W., Erzurum, S.C., Bleecker, E.R. and National Heart, Lung, and Blood Institute's Severe Asthma Research Program (2010) 'Identification of asthma phenotypes using cluster analysis in the Severe Asthma Research Program', *American journal of respiratory and critical care medicine*, 181(4), pp. 315-323.
- Mortensen, A., Cherrier, L. and Walia, R. (2018) 'Effect of pirfenidone on wound healing in lung transplant patients', *Multidisciplinary respiratory medicine*, 13, pp. 16-018-0129-4. eCollection 2018.
- Mu, Y., Sundar, R., Thakur, N., Ekman, M., Gudey, S.K., Yakymovych, M., Hermansson, A., Dimitriou, H., Bengoechea-Alonso, M.T., Ericsson, J., Heldin, C.H. and Landström, M. (2011) 'TRAF6 ubiquitinates TGF β 2 type I receptor to promote its cleavage and nuclear translocation in cancer', *Nature communications*, 2, pp. 330.

-
- Munye, M.M., Shoemark, A., Hirst, R.A., Delhove, J.M., Sharp, T.V., McKay, T.R., O'Callaghan, C., Baines, D.L., Howe, S.J. and Hart, S.L. (2017) 'BMI-1 extends proliferative potential of human bronchial epithelial cells while retaining their mucociliary differentiation capacity', *American journal of physiology.Lung cellular and molecular physiology*, 312(2), pp. L258-L267.
- tnerMurdoch, J.R. and Lloyd, C.M. (2010) 'Chronic inflammation and asthma', *Mutation research*, 690(1-2), pp. 24-39.
- Nakashima, N., Huang, C.L., Liu, D., Ueno, M. and Yokomise, H. (2010) 'Intratymoral Wnt1 expression affects survivin gene expression in non-small cell lung cancer', *International journal of oncology*, 37(3), pp. 687-694.
- Nelson, H.S., Weiss, S.T., Bleecker, E.R., Yancey, S.W., Dorinsky, P.M. and SMART Study Group (2006) 'The Salmeterol Multicenter Asthma Research Trial: a comparison of usual pharmacotherapy for asthma or usual pharmacotherapy plus salmeterol', *Chest*, 129(1), pp. 15-26.
- Neurohr, C., Nishimura, S.L. and Sheppard, D. (2006) 'Activation of transforming growth factor-beta by the integrin alphavbeta8 delays epithelial wound closure', *American journal of respiratory cell and molecular biology*, 35(2), pp. 252-259.
- Neveu, W.A., Allard, J.L., Raymond, D.M., Bourassa, L.M., Burns, S.M., Bunn, J.Y., Irvin, C.G., Kaminsky, D.A. and Rincon, M. (2010) 'Elevation of IL-6 in the allergic asthmatic airway is independent of inflammation but associates with loss of central airway function', *Respiratory Research*, 11(1), pp. 28.
- Newman, D.R., Sills, W.S., Hanrahan, K., Ziegler, A., Tidd, K.M., Cook, E. and Sannes, P.L. (2016) 'Expression of WNT5A in Idiopathic Pulmonary Fibrosis and Its Control by TGF-beta and WNT7B in Human Lung Fibroblasts', *The journal of histochemistry and cytochemistry : official journal of the Histochemistry Society*, 64(2), pp. 99-111.
- Ng-Blichfeldt, J., de Jong, T., Kortekaas, R.K., Wu, X., Lindner, M., Guryev, V., Hiemstra, P.S., Stolk, J., Königshoff, M. and Gosens, R. (2019) 'TGF-β activation impairs fibroblast ability to support adult lung epithelial progenitor cell organoid formation', *American Journal of Physiology-Lung Cellular and Molecular Physiology*, 317(1), pp. 14-28.
- Nguyen, H.M., Torres, J.A., Agrawal, S. and Agrawal, A. (2020) 'Nicotine Impairs the Response of Lung Epithelial Cells to IL-22', *Mediators of inflammation*, 2020, pp. 6705428.
- Niimi, A., Matsumoto, H., Amitani, R., Nakano, Y., Mishima, M., Minakuchi, M., Nishimura, K., Itoh, H. and Izumi, T. (2000) 'Airway Wall Thickness in Asthma Assessed by Computed Tomography', *American Journal of Respiratory and Critical Care Medicine*, 162(4), pp. 1518-1523.
- Nlandu-Khodo, S., Neelisetty, S., Phillips, M., Manolopoulou, M., Bhawe, G., May, L., Clark, P.E., Yang, H., Fogo, A.B., Harris, R.C., Taketo, M.M., Lee, E. and Gewin, L.S. (2017) 'Blocking TGF-β and β-Catenin Epithelial Crosstalk Exacerbates CKD', *Journal of the American Society of Nephrology : JASN*, 28(12), pp. 3490-3503.
- Noble, P.B., McFawn, P.K. and Mitchell, H.W. (2007) 'Responsiveness of the isolated airway during simulated deep inspirations: effect of airway smooth muscle stiffness and strain', *Journal of applied physiology*, 103(3), pp. 787-795.
- Nolte, M. and Margadant, C. (2020) 'Controlling Immunity and Inflammation through Integrin-Dependent Regulation of TGF-β', *Trends in cell biology*, 30(1), pp. 49.
- Nomachi, A., Nishita, M., Inaba, D., Enomoto, M., Hamasaki, M. and Minami, Y. (2008) 'Receptor tyrosine kinase Ror2 mediates Wnt5a-induced polarized cell migration by

-
- activating c-Jun N-terminal kinase via actin-binding protein filamin A', *The Journal of biological chemistry*, 283(41), pp. 27973-27981.
- Nunes, J.P.S. and Dias, A.A.M. (2017) 'ImageJ macros for the user-friendly analysis of soft-agar and wound-healing assays', *BioTechniques*, 62(4), pp. 175-179.
- O'Byrne, P., Fabbri, L.M., Pavord, I.D., Papi, A., Petruzzelli, S. and Lange, P. (2019) 'Asthma progression and mortality: the role of inhaled corticosteroids', *The European respiratory journal*, 54(1), pp. 1900491. doi: 10.1183/13993003.00491-2019. Print 2019 Jul.
- O'Hurley, G., Sjöstedt, E., Rahman, A., Li, B., Kampf, C., Pontén, F., Gallagher, W.M. and Lindskog, C. (2014) 'Garbage in, garbage out: a critical evaluation of strategies used for validation of immunohistochemical biomarkers', *Molecular oncology*, 8(4), pp. 783-798.
- Oishi, I., Suzuki, H., Onishi, N., Takada, R., Kani, S., Ohkawara, B., Koshida, I., Suzuki, K., Yamada, G., Schwabe, G.C., Mundlos, S., Shibuya, H., Takada, S. and Minami, Y. (2003) 'The receptor tyrosine kinase Ror2 is involved in non-canonical Wnt5a/JNK signalling pathway', *Genes to cells : devoted to molecular & cellular mechanisms*, 8(7), pp. 645-654.
- Okuchi, Y., Reeves, J., Ng, S.S., Doro, D.H., Junyent, S., Liu, K.J., El Haj, A.J. and Habib, S.J. (2020) 'Wnt-modified materials mediate asymmetric stem cell division to direct human osteogenic tissue formation for bone repair', *Nature Materials*, .
- Ornitz, D.M. and Itoh, N. (2015) 'The Fibroblast Growth Factor signaling pathway', *Wiley interdisciplinary reviews.Developmental biology*, 4(3), pp. 215-266.
- Osei, E.T., Booth, S. and Hackett, T.L. (2020) 'What Have In Vitro Co-Culture Models Taught Us about the Contribution of Epithelial-Mesenchymal Interactions to Airway Inflammation and Remodeling in Asthma?', *Cells*, 9(7), pp. 1694. doi: 10.3390/cells9071694.
- Ota, S., Ishitani, S., Shimizu, N., Matsumoto, K., Itoh, M. and Ishitani, T. (2012) 'NLK positively regulates Wnt/ β -catenin signalling by phosphorylating LEF1 in neural progenitor cells', *The EMBO journal*, 31(8), pp. 1904-1915.
- Padwal, M., Liu, L. and Margetts, P.J. (2020) 'The role of WNT5A and Ror2 in peritoneal membrane injury', *Journal of Cellular and Molecular Medicine*, 24(6), pp. 3481-3491.
- Palmer, C.N., Ismail, T., Lee, S.P., Terron-Kwiatkowski, A., Zhao, Y., Liao, H., Smith, F.J., McLean, W.H. and Mukhopadhyay, S. (2007) 'Filaggrin null mutations are associated with increased asthma severity in children and young adults', *The Journal of allergy and clinical immunology*, 120(1), pp. 64-68.
- Pan, J.H., Adair-Kirk, T.L., Patel, A.C., Huang, T., Yozamp, N.S., Xu, J., Reddy, E.P., Byers, D.E., Pierce, R.A., Holtzman, M.J. and Brody, S.L. (2014) 'Myb permits multilineage airway epithelial cell differentiation', *Stem cells (Dayton, Ohio)*, 32(12), pp. 3245-3256.
- Panigrahi, A. and Padhi, B.K. (2018) 'Chronic bronchitis and airflow obstruction is associated with household cooking fuel use among never-smoking women: a community-based cross-sectional study in Odisha, India', *BMC public health*, 18(1), pp. 924-018-5846-2.
- Pardo-Saganta, A., Law, B.M., Tata, P.R., Villoria, J., Saez, B., Mou, H., Zhao, R. and Rajagopal, J. (2015) 'Injury induces direct lineage segregation of functionally distinct airway basal stem/progenitor cell subpopulations', *Cell stem cell*, 16(2), pp. 184-197.
- Park, N.R., Cha, J.H., Jang, J.W., Bae, S.H., Jang, B., Kim, J., Hur, W., Choi, J.Y. and Yoon, S.K. (2016) 'Synergistic effects of CD44 and TGF- β 1 through AKT/GSK-3 β / β -catenin

-
- signaling during epithelial-mesenchymal transition in liver cancer cells', *Biochemical and biophysical research communications*, 477(4), pp. 568-574.
- Passantino, L., Muñoz, A.B. and Costa, M. (2013) 'Sodium metavanadate exhibits carcinogenic tendencies in vitro in immortalized human bronchial epithelial cells', *Metallomics : integrated biometal science*, 5(10), pp. 1357-1367.
- Pauwels, R.A., Pedersen, S., Busse, W.W., Tan, W.C., Chen, Y.Z., Ohlsson, S.V., Ullman, A., Lamm, C.J., O'Byrne, P.M. and START Investigators Group (2003) 'Early intervention with budesonide in mild persistent asthma: a randomised, double-blind trial', *Lancet (London, England)*, 361(9363), pp. 1071-1076.
- Payne, D.N., Rogers, A.V., Adelroth, E., Bandi, V., Guntupalli, K.K., Bush, A. and Jeffery, P.K. (2003) 'Early thickening of the reticular basement membrane in children with difficult asthma', *American journal of respiratory and critical care medicine*, 167(1), pp. 78-82.
- Pelletier, M., Maggi, L., Micheletti, A., Lazzeri, E., Tamassia, N., Costantini, C., Cosmi, L., Lunardi, C., Annunziato, F., Romagnani, S. and Cassatella, M.A. (2010) 'Evidence for a cross-talk between human neutrophils and Th17 cells', *Blood*, 115(2), pp. 335-343.
- Pembrey, L., Barreto, M.L., Douwes, J., Cooper, P., Henderson, J., Mpairwe, H., Ardura-Garcia, C., Chico, M., Brooks, C., Cruz, A.A., Elliott, A.M., Figueiredo, C.A., Langan, S.M., Nassanga, B., Ring, S., Rodrigues, L. and Pearce, N. (2018) 'Understanding asthma phenotypes: the World Asthma Phenotypes (WASP) international collaboration', *ERJ open research*, 4(3), pp. 00013-2018. doi: 10.1183/23120541.00013-2018. eCollection 2018 Jul.
- Peng, T., Frank, D.B., Kadzik, R.S., Morley, M.P., Rathi, K.S., Wang, T., Zhou, S., Cheng, L., Lu, M.M. and Morrisey, E.E. (2015) 'Hedgehog actively maintains adult lung quiescence and regulates repair and regeneration', *Nature*, 526(7574), pp. 578-582.
- Peters, M., Köhler-Bachmann, S., Lenz-Habijan, T. and Bufe, A. (2016) 'Influence of an Allergen-Specific Th17 Response on Remodeling of the Airways', *American journal of respiratory cell and molecular biology*, 54(3), pp. 350-358.
- Pittet, J.F., Griffiths, M.J., Geiser, T., Kaminski, N., Dalton, S.L., Huang, X., Brown, L.A., Gotwals, P.J., Koteliensky, V.E., Matthay, M.A. and Sheppard, D. (2001) 'TGF-beta is a critical mediator of acute lung injury', *The Journal of clinical investigation*, 107(12), pp. 1537-1544.
- Polimeni, M., Gulino, G.R., Gazzano, E., Kopecka, J., Marucco, A., Fenoglio, I., Cesano, F., Campagnolo, L., Magrini, A., Pietrojusti, A., Ghigo, D. and Aldieri, E. (2016) 'Multi-walled carbon nanotubes directly induce epithelial-mesenchymal transition in human bronchial epithelial cells via the TGF-beta-mediated Akt/GSK-3beta/SNAIL-1 signalling pathway', *Particle and fibre toxicology*, 13(1), pp. 27-016-0138-4.
- Pongracz, J.E. and Stockley, R.A. (2006) 'Wnt signalling in lung development and diseases', *Respiratory research*, 7, pp. 15-9921-7-15.
- Povinelli, B.J. and Nemeth, M.J. (2014) 'Wnt5a regulates hematopoietic stem cell proliferation and repopulation through the Ryk receptor', *Stem cells (Dayton, Ohio)*, 32(1), pp. 105-115.
- Prasad, C.P., Mohapatra, P. and Andersson, T. (2015) 'Therapy for BRAFi-Resistant Melanomas: Is WNT5A the Answer?', *Cancers*, 7(3), pp. 1900-1924.
- Prgomet, Z., Andersson, T. and Lindberg, P. (2017) 'Optimization, validation, and identification of two reliable antibodies for immunodetection of WNT5A', *Biotechnic &*

-
- histochemistry : official publication of the Biological Stain Commission*, 92(1), pp. 46-58.
- Puddicombe, S.M., Torres-Lozano, C., Richter, A., Bucchieri, F., Lordan, J.L., Howarth, P.H., Vrugt, B., Albers, R., Djukanovic, R., Holgate, S.T., Wilson, S.J. and Davies, D.E. (2003) 'Increased expression of p21(waf) cyclin-dependent kinase inhibitor in asthmatic bronchial epithelium', *American journal of respiratory cell and molecular biology*, 28(1), pp. 61-68.
- Ramezanpour, M., Smith, J.L.P., Ooi, M.L., Gouzos, M., Psaltis, A.J., Wormald, P.J. and Vreugde, S. (2019) 'Deferiprone has anti-inflammatory properties and reduces fibroblast migration in vitro', *Scientific reports*, 9(1), pp. 2378-019-38902-2.
- Rapp, J., Kiss, E., Meggyes, M., Szabo-Meleg, E., Feller, D., Smuk, G., Laszlo, T., Sarosi, V., Molnar, T.F., Kvell, K. and Pongracz, J.E. (2016) 'Increased Wnt5a in squamous cell lung carcinoma inhibits endothelial cell motility', *BMC cancer*, 16(1), pp. 915-016-2943-4.
- Ray, A., Oriss, T.B. and Wenzel, S.E. (2015) 'Emerging molecular phenotypes of asthma', *American journal of physiology. Lung cellular and molecular physiology*, 308(2), pp. L130-40.
- Reddel, H.K., Taylor, D.R., Bateman, E.D., Boulet, L.P., Boushey, H.A., Busse, W.W., Casale, T.B., Chanez, P., Enright, P.L., Gibson, P.G., de Jongste, J.C., Kerstjens, H.A., Lazarus, S.C., Levy, M.L., O'Byrne, P.M., Partridge, M.R., Pavord, I.D., Sears, M.R., Sterk, P.J., Stoloff, S.W., Sullivan, S.D., Szefer, S.J., Thomas, M.D., Wenzel, S.E. and American Thoracic Society/European Respiratory Society Task Force on Asthma Control and Exacerbations (2009) 'An official American Thoracic Society/European Respiratory Society statement: asthma control and exacerbations: standardizing endpoints for clinical asthma trials and clinical practice', *American journal of respiratory and critical care medicine*, 180(1), pp. 59-99.
- Redington, A.E., Roche, W.R., Holgate, S.T. and Howarth, P.H. (1998) 'Co-localization of immunoreactive transforming growth factor-beta 1 and decorin in bronchial biopsies from asthmatic and normal subjects', *The Journal of pathology*, 186(4), pp. 410-415.
- Ren, X. and MacKichan, J.K. (2014) 'Disease-associated Neisseria meningitidis isolates inhibit wound repair in respiratory epithelial cells in a type IV pilus-independent manner', *Infection and immunity*, 82(12), pp. 5023-5034.
- Restivo, G., Diener, J., Cheng, P.F., Kiowski, G., Bonalli, M., Biedermann, T., Reichmann, E., Levesque, M.P., Dummer, R. and Sommer, L. (2017) 'low neurotrophin receptor CD271 regulates phenotype switching in melanoma', *Nature communications*, 8(1), pp. 1988-017-01573-6.
- Reynolds, S.D., Brechbuhl, H.M., Smith, M.K., Smith, R.W. and Ghosh, M. (2012) 'Lung epithelial healing: a modified seed and soil concept', *Proceedings of the American Thoracic Society*, 9(2), pp. 27-37.
- Reynolds, S.D., Giangreco, A., Power, J.H. and Stripp, B.R. (2000) 'Neuroepithelial bodies of pulmonary airways serve as a reservoir of progenitor cells capable of epithelial regeneration', *The American journal of pathology*, 156(1), pp. 269-278.
- Reynolds, S.D., Rios, C., Wesolowska-Andersen, A., Zhuang, Y., Pinter, M., Happoldt, C., Hill, C.L., Lallier, S.W., Cosgrove, G.P., Solomon, G.M., Nichols, D.P. and Seibold, M.A. (2016) 'Airway Progenitor Clone Formation Is Enhanced by Y-27632-Dependent Changes in the Transcriptome', *American journal of respiratory cell and molecular biology*, 55(3), pp. 323-336.

-
- Riss, T.L., Moravec, R.A., Niles, A.L., Duellman, S., Benink, H.A., Worzella, T.J. and Minor, L. (2016) 'Cell Viability Assays', in Markossian, S., Grossman, A., Brimacombe, K., Arkin, M., Auld, D., Austin, C.P., Baell, J., Chung, T.D.Y., Coussens, N.P., Dahlin, J.L., Devanarayan, V., Foley, T.L., Glicksman, M., Hall, M.D., Haas, J.V., Hoare, S.R.J., Inglese, J., Iversen, P.W., Kales, S.C., Lal-Nag, M., Li, Z., McGee, J., McManus, O., Riss, T., Saradjian, P., Sittampalam, G.S., Tarselli, M., Trask, O.J., Jr, Wang, Y., Weidner, J.R., Wildey, M.J., Wilson, K., Xia, M. and Xu, X. (eds.) *Assay Guidance Manual*. Bethesda (MD) .
- Roane, B.M., Arend, R.C. and Birrer, M.J. (2019) 'Review: Targeting the Transforming Growth Factor-Beta Pathway in Ovarian Cancer', *Cancers*, 11(5), pp. 668. doi: 10.3390/cancers11050668.
- Roarty, K. and Serra, R. (2007) 'Wnt5a is required for proper mammary gland development and TGF-beta-mediated inhibition of ductal growth', *Development (Cambridge, England)*, 134(21), pp. 3929-3939.
- Roarty, K., Baxley, S.E., Crowley, M.R., Frost, A.R. and Serra, R. (2009) 'Loss of TGF-beta or Wnt5a results in an increase in Wnt/beta-catenin activity and redirects mammary tumour phenotype', *Breast cancer research : BCR*, 11(2), pp. R19.
- Robinson, D., Humbert, M., Buhl, R., Cruz, A.A., Inoue, H., Korom, S., Hanania, N.A. and Nair, P. (2017) 'Revisiting Type 2-high and Type 2-low airway inflammation in asthma: current knowledge and therapeutic implications', *Clinical and experimental allergy : journal of the British Society for Allergy and Clinical Immunology*, 47(2), pp. 161-175.
- Rock, J.R., Gao, X., Xue, Y., Randell, S.H., Kong, Y.Y. and Hogan, B.L. (2011) 'Notch-dependent differentiation of adult airway basal stem cells', *Cell stem cell*, 8(6), pp. 639-648.
- Rock, J.R., Onaitis, M.W., Rawlins, E.L., Lu, Y., Clark, C.P., Xue, Y., Randell, S.H. and Hogan, B.L. (2009) 'Basal cells as stem cells of the mouse trachea and human airway epithelium', *Proceedings of the National Academy of Sciences of the United States of America*, 106(31), pp. 12771-12775.
- Rodríguez, E., Baurecht, H., Herberich, E., Wagenpfeil, S., Brown, S.J., Cordell, H.J., Irvine, A.D. and Weidinger, S. (2009) 'Meta-analysis of filaggrin polymorphisms in eczema and asthma: robust risk factors in atopic disease', *The Journal of allergy and clinical immunology*, 123(6), pp. 1361-70.e7.
- Rout-Pitt, N., Farrow, N., Parsons, D. and Donnelley, M. (2018) 'Epithelial mesenchymal transition (EMT): a universal process in lung diseases with implications for cystic fibrosis pathophysiology', *Respiratory research*, 19(1), pp. 136-018-0834-8.
- Royal College of Physicians. (2014) *Why asthma still kills: the National Review of Asthma Deaths (NRAD) Confidential Enquiry report*, RCP, London.
- Sagar, S., Akbarshahi, H. and Uller, L. (2015) 'Translational value of animal models of asthma: Challenges and promises', *European journal of pharmacology*, 759, pp. 272.
- Sagara, H., Okada, T., Okumura, K., Ogawa, H., Ra, C., Fukuda, T. and Nakao, A. (2002) 'Activation of TGF- β /Smad2 signaling is associated with airway remodeling in asthma', *Journal of Allergy and Clinical Immunology*, 110(2), pp. 249-254.
- Saglani, S., Payne, D.N., Zhu, J., Wang, Z., Nicholson, A.G., Bush, A. and Jeffery, P.K. (2007) 'Early detection of airway wall remodeling and eosinophilic inflammation in preschool wheezers', *American journal of respiratory and critical care medicine*, 176(9), pp. 858-864.

-
- Saito, A., Horie, M. and Nagase, T. (2018) 'TGF- β Signaling in Lung Health and Disease', *International journal of molecular sciences*, 19(8), pp. 2460. doi: 10.3390/ijms19082460.
- Salpeter, S.R., Buckley, N.S., Ormiston, T.M. and Salpeter, E.E. (2006) 'Meta-analysis: effect of long-acting beta-agonists on severe asthma exacerbations and asthma-related deaths', *Annals of Internal Medicine*, 144(12), pp. 904-912.
- Sankpal, N.V., Fleming, T.P., Sharma, P.K., Wiedner, H.J. and Gillanders, W.E. (2017) 'A double-negative feedback loop between EpCAM and ERK contributes to the regulation of epithelial-mesenchymal transition in cancer', *Oncogene*, 36(26), pp. 3706-3717.
- Sato, Y. and Rifkin, D.B. (1989) 'Inhibition of endothelial cell movement by pericytes and smooth muscle cells: activation of a latent transforming growth factor-beta 1-like molecule by plasmin during co-culture', *The Journal of cell biology*, 109(1), pp. 309-315.
- Schagen, J., Sly, P.D. and Fantino, E. (2018) 'Characterizing well-differentiated culture of primary human nasal epithelial cells for use in wound healing assays', *Laboratory investigation; a journal of technical methods and pathology*, 98(11), pp. 1478-1486.
- Schamberger, A.C., Mise, N., Jia, J., Genoyer, E., Yildirim, A.Ö., Meiners, S. and Eickelberg, O. (2014) 'Cigarette smoke-induced disruption of bronchial epithelial tight junctions is prevented by transforming growth factor- β ', *American journal of respiratory cell and molecular biology*, 50(6), pp. 1040-1052.
- Schmid, A., Bai, G., Schmid, N., Zaccolo, M., Ostrowski, L.E., Conner, G.E., Fregien, N. and Salathe, M. (2006) 'Real-time analysis of cAMP-mediated regulation of ciliary motility in single primary human airway epithelial cells', *Journal of cell science*, 119(Pt 20), pp. 4176-4186.
- Schmid, A., Sailland, J., Novak, L., Baumlin, N., Fregien, N. and Salathe, M. (2017) 'Modulation of Wnt signaling is essential for the differentiation of ciliated epithelial cells in human airways', *FEBS letters*, 591(21), pp. 3493-3506.
- Schmid, A. and Salathe, M. (2011) 'Ciliary beat co-ordination by calcium', *Biology of the cell*, 103(4), pp. 159-169.
- Schnackenberg, B.J., Jones, S.M., Pate, C., Shank, B., Sessions, L., Pittman, L.M., Cornett, L.E. and Kurten, R.C. (2006) 'The beta-agonist isoproterenol attenuates EGF-stimulated wound closure in human airway epithelial cells', *American journal of physiology. Lung cellular and molecular physiology*, 290(3), pp. L485-91.
- Scottish Intercollegiate Guidelines Network/British Thoracic Society. (2019) British guideline on the management of asthma. Available at: www.sign.ac.uk
- Semenov, M.V., Habas, R., Macdonald, B.T. and He, X. (2007) 'SnapShot: Noncanonical Wnt Signaling Pathways', *Cell*, 131(7), pp. 1378.
- Semënov, M.V., Tamai, K., Brott, B.K., Kühl, M., Sokol, S. and He, X. (2001) 'Head inducer Dickkopf-1 is a ligand for Wnt coreceptor LRP6', *Current biology : CB*, 11(12), pp. 951-961.
- Semlali, A., Jacques, E., Rouabhia, M., Milot, J., Laviolette, M. and Chakir, J. (2010) 'Regulation of epithelial cell proliferation by bronchial fibroblasts obtained from mild asthmatic subjects', *Allergy*, 65(11), pp. 1438-1445.

-
- Shabana, M.A., Esawy, M.M., Ismail, N.A. and Said, A.M. (2019) 'Predictive role of IL-17A/IL-10 ratio in persistent asthmatic patients on vitamin D supplement', *Immunobiology*, 224(6), pp. 721-727.
- Shapiro, S.D. (2008) 'The use of transgenic mice for modeling airways disease', *Pulmonary pharmacology & therapeutics*, 21(5), pp. 699.
- Sharma, M. and Pruitt, K. (2020) 'Wnt Pathway: An Integral Hub for Developmental and Oncogenic Signaling Networks', *International journal of molecular sciences*, 21(21), pp. 8018. doi: 10.3390/ijms21218018.
- Sharma, S., Poon, A., Himes, B.E., Lasky-Su, J., Sordillo, J.E., Belanger, K., Milton, D.K., Bracken, M.B., Triche, E.W., Leaderer, B.P., Gold, D.R. and Litonjua, A.A. (2012) 'Association of variants in innate immune genes with asthma and eczema', *Pediatric allergy and immunology : official publication of the European Society of Pediatric Allergy and Immunology*, 23(4), pp. 315-323.
- Sharma, S., Raby, B.A., Hunninghake, G.M., Soto-Quirós, M., Avila, L., Murphy, A.J., Lasky-Su, J., Klanderman, B.J., Sylvia, J.S., Weiss, S.T. and Celedón, J.C. (2009) 'Variants in TGF β 1, dust mite exposure, and disease severity in children with asthma', *American journal of respiratory and critical care medicine*, 179(5), pp. 356-362.
- Shaw, D.E., Sousa, A.R., Fowler, S.J., Fleming, L.J., Roberts, G., Corfield, J., Pandis, I., Bansal, A.T., Bel, E.H., Auffray, C., Compton, C.H., Bisgaard, H., Bucchioni, E., Caruso, M., Chanez, P., Dahl\`en, B., Dahlen, S., Dyson, K., Frey, U., Geiser, T., Gerhardsson de Verdier, M., Gibeon, D., Guo, Y., Hashimoto, S., Hedlin, G., Jeyasingham, E., Hekking, P.W., Higenbottam, T., Horv\`ath, I., Knox, A.J., Krug, N., Erpenbeck, V.J., Larsson, L.X., Lazarinis, N., Matthews, J.G., Middelvel, R., Montuschi, P., Musial, J., Myles, D., Pahus, L., Sandstr\`om, T., Seibold, W., Singer, F., Strandberg, K., Vestbo, J., Vissing, N., von Garnier, C., Adcock, I.M., Wagers, S., Rowe, A., Howarth, P., Wagener, A.H., Djukanovic, R., Sterk, P.J. and Chung, K.F. (2015) 'Clinical and inflammatory characteristics of the European U-BIOPRED adult severe asthma cohort', *European Respiratory Journal*, 46(5), pp. 1308-1321.
- Sherwood, V., Chaurasiya, S.K., Ekström, E.J., Guilmain, W., Liu, Q., Koeck, T., Brown, K., Hansson, K., Agnarsson, M., Bergqvist, M., Jirström, K., Ponten, F., James, P. and Andersson, T. (2014) 'WNT5A-mediated β -catenin-independent signalling is a novel regulator of cancer cell metabolism', *Carcinogenesis*, 35(4), pp. 784-794.
- Shi, X., DiRenzo, D., Guo, L.W., Franco, S.R., Wang, B., Seedial, S. and Kent, K.C. (2014) 'TGF- β /Smad3 stimulates stem cell/developmental gene expression and vascular smooth muscle cell de-differentiation', *PLoS one*, 9(4), pp. e93995.
- Shi, Z., Xu, M., Chen, X., Wang, J., Zhao, T. and Zha, D. (2021) 'The regulatory role of SFRP5/WNT5A axis in allergic rhinitis through inhibiting JNK pathway activation and lowering mucin generation in human nasal epithelial cells', *Experimental and molecular pathology*, 118, pp. 104591.
- Shibata, A., Matsumoto, T., Uchida, M., Yamada, M., Miyamoto, Y., Inada, H., Eguchi, Y. and Toriumi, W. (2019) 'A Novel siRNA-Based Oligonucleotide, TRK-250, and Its Efficacy for Treatment of Idiopathic Pulmonary Fibrosis (IPF)', in Anonymous C64. *Pulmonary Fibrosis Models and Mechanistic Insights*. American Thoracic Society, pp. A5391-A5391.
- Shifren, A., Witt, C., Christie, C. and Castro, M. (2012) 'Mechanisms of remodeling in asthmatic airways', *Journal of allergy*, 2012, pp. 316049.
- Shrestha, J., Razavi Bazaz, S., Aboulkheyr Es, H., Yaghobian Azari, D., Thierry, B., Ebrahimi Warkiani, M. and Ghadiri, M. (2020) 'Lung-on-a-chip: the future of respiratory disease models and pharmacological studies', *Critical reviews in biotechnology*, 40(2), pp. 213-230.

-
- Shrine, N., Portelli, M.A., John, C., Soler Artigas, M., Bennett, N., Hall, R., Lewis, J., Henry, A.P., Billington, C.K., Ahmad, A., Packer, R.J., Shaw, D., Pogson, Z.E.K., Fogarty, A., McKeever, T.M., Singapuri, A., Heaney, L.G., Mansur, A.H., Chaudhuri, R., Thomson, N.C., Holloway, J.W., Lockett, G.A., Howarth, P.H., Djukanovic, R., Hankinson, J., Niven, R., Simpson, A., Chung, K.F., Sterk, P.J., Blakey, J.D., Adcock, I.M., Hu, S., Guo, Y., Obeidat, M., Sin, D.D., van den Berge, M., Nickle, D.C., Bossé, Y., Tobin, M.D., Hall, I.P., Brightling, C.E., Wain, L.V. and Sayers, I. (2019) 'Moderate-to-severe asthma in individuals of European ancestry: a genome-wide association study', *The Lancet.Respiratory medicine*, 7(1), pp. 20-34.
- Siddiqui, S., Gupta, S., Cruse, G., Haldar, P., Entwisle, J., McDonald, S., Whithers, P.J., Hainsworth, S.V., Coxson, H.O. and Brightling, C. (2009) 'Airway wall geometry in asthma and nonasthmatic eosinophilic bronchitis', *Allergy*, 64(6), pp. 951-958.
- Siddiqui, S., Sutcliffe, A., Shikotra, A., Woodman, L., Doe, C., McKenna, S., Wardlaw, A., Bradding, P., Pavord, I. and Brightling, C. (2007) 'Vascular remodeling is a feature of asthma and nonasthmatic eosinophilic bronchitis', *The Journal of allergy and clinical immunology*, 120(4), pp. 813-819.
- Silverman, E.S., Palmer, L.J., Subramaniam, V., Hallock, A., Mathew, S., Vallone, J., Faffe, D.S., Shikanai, T., Raby, B.A., Weiss, S.T. and Shore, S.A. (2004) 'Transforming growth factor-beta1 promoter polymorphism C-509T is associated with asthma', *American journal of respiratory and critical care medicine*, 169(2), pp. 214-219.
- Simons, B.D. and Clevers, H. (2011) 'Strategies for Homeostatic Stem Cell Self-Renewal in Adult Tissues', *Cell*, 145(6), pp. 851.
- Singhania, A., Rupani, H., Jayasekera, N., Lumb, S., Hales, P., Gozzard, N., Davies, D.E., Woelk, C.H. and Howarth, P.H. (2017) 'Altered Epithelial Gene Expression in Peripheral Airways of Severe Asthma', *PLoS one*, 12(1), pp. e0168680.
- Skronska-Wasek, W., Gosens, R., Königshoff, M. and Baarsma, H.A. (2018) 'WNT receptor signalling in lung physiology and pathology', *Pharmacology & therapeutics*, 187, pp. 150-166.
- Smeltz, R.B., Chen, J. and Shevach, E.M. (2005) 'Transforming growth factor-beta1 enhances the interferon-gamma-dependent, interleukin-12-independent pathway of T helper 1 cell differentiation', *Immunology*, 114(4), pp. 484-492.
- Smit, L., Baas, A., Kuipers, J., Korswagen, H., van de Wetering, M. and Clevers, H. (2004) 'Wnt activates the Tak1/Nemo-like kinase pathway', *The Journal of biological chemistry*, 279(17), pp. 17232-17240.
- Smith, C.M., Djakow, J., Free, R.C., Djakow, P., Lonnen, R., Williams, G., Pohunek, P., Hirst, R.A., Easton, A.J., Andrew, P.W. and O'Callaghan, C. (2012) 'ciliaFA: a research tool for automated, high-throughput measurement of ciliary beat frequency using freely available software', *Cilia*, 1(1), pp. 14.
- Snyder, R.J., Hussain, S., Tucker, C.J., Randell, S.H. and Garantziotis, S. (2017) 'Impaired Ciliogenesis in differentiating human bronchial epithelia exposed to non-Cytotoxic doses of multi-walled carbon Nanotubes', *Particle and fibre toxicology*, 14(1), pp. 44-017-0225-1.
- Spanjer, A.I., Baarsma, H.A., Oostenbrink, L.M., Jansen, S.R., Kuipers, C.C., Lindner, M., Postma, D.S., Meurs, H., Heijink, I.H., Gosens, R. and Königshoff, M. (2016) 'TGF- β -induced profibrotic signaling is regulated in part by the WNT receptor Frizzled-8', *FASEB journal : official publication of the Federation of American Societies for Experimental Biology*, 30(5), pp. 1823-1835.

-
- Spitzer, W.O., Suissa, S., Ernst, P., Horwitz, R.I., Habbick, B., Cockcroft, D., Boivin, J.F., McNutt, M., Buist, A.S. and Rebeck, A.S. (1992) 'The use of beta-agonists and the risk of death and near death from asthma', *The New England journal of medicine*, 326(8), pp. 501-506.
- Spurzem, J.R., Sacco, O., Rickard, K.A. and Rennard, S.I. (1993) 'Transforming growth factor-beta increases adhesion but not migration of bovine bronchial epithelial cells to matrix proteins', *The Journal of laboratory and clinical medicine*, 122(1), pp. 92-102.
- Spurzem, J.R., Gupta, J., Veys, T., Kneifl, K.R., Rennard, S.I. and Wyatt, T.A. (2002) 'Activation of protein kinase A accelerates bovine bronchial epithelial cell migration', *American Journal of Physiology-Lung Cellular and Molecular Physiology*, 282(5), pp. 1108-1116.
- Stevens, P.T., Kicic, A., Sutanto, E.N., Knight, D.A. and Stick, S.M. (2008) 'Dysregulated repair in asthmatic paediatric airway epithelial cells: the role of plasminogen activator inhibitor-1', *Clinical and experimental allergy : journal of the British Society for Allergy and Clinical Immunology*, 38(12), pp. 1901-1910.
- Stewart, C.E., Nijmeh, H.S., Brightling, C.E. and Sayers, I. (2012: A) 'uPAR regulates bronchial epithelial repair in vitro and is elevated in asthmatic epithelium', *Thorax*, 67(6), pp. 477-487.
- Stewart, C.E., Torr, E.E., Mohd Jamili, N.H., Bosquillon, C. and Sayers, I. (2012: B) 'Evaluation of differentiated human bronchial epithelial cell culture systems for asthma research', *Journal of allergy*, 2012, pp. 943982.
- Suissa, S., Ernst, P., Benayoun, S., Baltzan, M. and Cai, B. (2000) 'Low-dose inhaled corticosteroids and the prevention of death from asthma', *The New England journal of medicine*, 343(5), pp. 332-336.
- Sun, Q., Guo, S., Wang, C.C., Sun, X., Wang, D., Xu, N., Jin, S.F. and Li, K.Z. (2015) 'Cross-talk between TGF- β /Smad pathway and Wnt/ β -catenin pathway in pathological scar formation', *International journal of clinical and experimental pathology*, 8(6), pp. 7631-7639.
- Swarnkar, G., Karuppaiah, K., Mbalaviele, G., Chen, T.H. and Abu-Amer, Y. (2015) 'Osteopetrosis in TAK1-deficient mice owing to defective NF- κ B and NOTCH signaling', *Proceedings of the National Academy of Sciences of the United States of America*, 112(1), pp. 154-159.
- Swartz, M.A., Tschumperlin, D.J., Kamm, R.D. and Drazen, J.M. (2001) 'Mechanical stress is communicated between different cell types to elicit matrix remodeling', *Proceedings of the National Academy of Sciences of the United States of America*, 98(11), pp. 6180-6185.
- Syed, F., Huang, C.C., Li, K., Liu, V., Shang, T., Amegadzie, B.Y., Griswold, D.E., Song, X.Y. and Li, L. (2007) 'Identification of interleukin-13 related biomarkers using peripheral blood mononuclear cells', *Biomarkers : biochemical indicators of exposure, response, and susceptibility to chemicals*, 12(4), pp. 414-423.
- Takimoto, T., Wakabayashi, Y., Sekiya, T., Inoue, N., Morita, R., Ichiyama, K., Takahashi, R., Asakawa, M., Muto, G., Mori, T., Hasegawa, E., Saika, S., Hara, T., Nomura, M. and Yoshimura, A. (2010) 'Smad2 and Smad3 are redundantly essential for the TGF-beta-mediated regulation of regulatory T plasticity and Th1 development', *Journal of immunology (Baltimore, Md.: 1950)*, 185(2), pp. 842-855.
- Tanaka, S., Jiang, Y., Martinez, G.J., Tanaka, K., Yan, X., Kurosaki, T., Kaartinen, V., Feng, X.H., Tian, Q., Wang, X. and Dong, C. (2018) 'Trim33 mediates the proinflammatory function of Th17 cells', *The Journal of experimental medicine*, 215(7), pp. 1853-1868.

-
- Tang, Q., Chen, C., Zhang, Y., Dai, M., Jiang, Y., Wang, H., Yu, M., Jing, W. and Tian, W. (2018) 'Wnt5a regulates the cell proliferation and adipogenesis via MAPK-independent pathway in early stage of obesity', *Cell biology international*, 42(1), pp. 63-74.
- Teixeira, V.H., Nadarajan, P., Graham, T.A., Pipinikas, C.P., Brown, J.M., Falzon, M., Nye, E., Poulson, R., Lawrence, D., Wright, N.A., McDonald, S., Giangreco, A., Simons, B.D. and Janes, S.M. (2013) 'Stochastic homeostasis in human airway epithelium is achieved by neutral competition of basal cell progenitors', *eLife*, 2, pp. e00966.
- Telford, W.G., Babin, S.A., Khorev, S.V. and Rowe, S.H. (2009) 'Green fiber lasers: an alternative to traditional DPSS green lasers for flow cytometry', *Cytometry.Part A : the journal of the International Society for Analytical Cytology*, 75(12), pp. 1031-1039.
- Tenghao, S., Ning, C., Shenghai, W., Qinlong, S., Jiaqian, W., Kuo, W., Zhanbiao, Y. and Xigang, M. (2020) 'Keratinocyte Growth Factor-2 Reduces Inflammatory Response to Acute Lung Injury Induced by Oleic Acid in Rats by Regulating Key Proteins of the Wnt/ β -Catenin Signaling Pathway', *Evidence-based complementary and alternative medicine : eCAM*, 2020, pp. 8350579.
- The Human Protein Atlas. (n.d.) *WNT5A*. Available at: <https://www.proteinatlas.org/ENSG00000114251-WNT5A/tissue> (Accessed: 02 July 2020).
- Thomas, B., Rutman, A., Hirst, R.A., Haldar, P., Wardlaw, A.J., Bankart, J., Brightling, C.E. and O'Callaghan, C. (2010) 'Ciliary dysfunction and ultrastructural abnormalities are features of severe asthma', *The Journal of allergy and clinical immunology*, 126(4), pp. 722-729.e2.
- Thompson, H.G.R., Mih, J.D., Krasieva, T.B., Tromberg, B.J. and George, S.C. (2006) 'Epithelial-derived TGF- β 2 modulates basal and wound-healing subepithelial matrix homeostasis', *American Journal of Physiology-Lung Cellular and Molecular Physiology*, 291(6), pp. 1277-1285.
- Tian, F., Mauro, T.M. and Li, Z. (2019) 'The pathological role of Wnt5a in psoriasis and psoriatic arthritis', *Journal of Cellular and Molecular Medicine*, 23(9), pp. 5876-5883.
- Tilley, A.E., Walters, M.S., Shaykhiev, R. and Crystal, R.G. (2015) 'Cilia dysfunction in lung disease', *Annual Review of Physiology*, 77, pp. 379-406.
- Tomiita, M., Campos-Alberto, E., Shima, M., Namiki, M., Sugimoto, K., Kojima, H., Watanabe, H., Sekine, K., Nishimuta, T., Kohno, Y. and Shimojo, N. (2015) 'Interleukin-10 and interleukin-5 balance in patients with active asthma, those in remission, and healthy controls', *Asia Pacific allergy*, 5(4), pp. 210-215.
- Torgerson, D.G., Ampleford, E.J., Chiu, G.Y., Gauderman, W.J., Gignoux, C.R., Graves, P.E., Himes, B.E., Levin, A.M., Mathias, R.A., Hancock, D.B., Baurley, J.W., Eng, C., Stern, D.A., Celedón, J.C., Rafaels, N., Capurso, D., Conti, D.V., Roth, L.A., Soto-Quiros, M., Togiias, A., Li, X., Myers, R.A., Romieu, I., Van Den Berg, D.J., Hu, D., Hansel, N.N., Hernandez, R.D., Israel, E., Salam, M.T., Galanter, J., Avila, P.C., Avila, L., Rodriguez-Santana, J.R., Chapelala, R., Rodriguez-Cintron, W., Diette, G.B., Adkinson, N.F., Abel, R.A., Ross, K.D., Shi, M., Faruque, M.U., Dunston, G.M., Watson, H.R., Mantese, V.J., Ezurum, S.C., Liang, L., Ruczinski, I., Ford, J.G., Huntsman, S., Chung, K.F., Vora, H., Li, X., Calhoun, W.J., Castro, M., Sienna-Monge, J.J., del Rio-Navarro, B., Deichmann, K.A., Heinzmann, A., Wenzel, S.E., Busse, W.W., Gern, J.E., Lemanske, R.F., Jr, Beaty, T.H., Bleeker, E.R., Raby, B.A., Meyers, D.A., London, S.J., Mexico City Childhood Asthma Study (MCAAS), Gilliland, F.D., Children's Health Study (CHS) and HARBORS study, Burchard, E.G., Genetics of Asthma in Latino Americans (GALA) Study, Study of Genes-Environment and Admixture in Latino Americans (GALA2) and Study of African Americans, Asthma, Genes & Environments (SAGE), Martinez, F.D., Childhood Asthma Research and Education (CARE) Network, Weiss, S.T., Childhood Asthma Management

-
- Program (CAMP), Williams, L.K., Study of Asthma Phenotypes and Pharmacogenomic Interactions by Race-Ethnicity (SAPPHIRE), Barnes, K.C., Genetic Research on Asthma in African Diaspora (GRAAD) Study, Ober, C. and Nicolae, D.L. (2011) 'Meta-analysis of genome-wide association studies of asthma in ethnically diverse North American populations', *Nature genetics*, 43(9), pp. 887-892.
- Toskala, E., Smiley-Jewell, S.M., Wong, V.J., King, D. and Plopper, C.G. (2005) 'Temporal and spatial distribution of ciliogenesis in the tracheobronchial airways of mice', *American journal of physiology. Lung cellular and molecular physiology*, 289(3), pp. L454-9.
- Totzke, J., Gurbani, D., Raphemot, R., Hughes, P.F., Bodoor, K., Carlson, D.A., Loisel, D.R., Bera, A.K., Eibschutz, L.S., Perkins, M.M., Eubanks, A.L., Campbell, P.L., Fox, D.A., Westover, K.D., Haystead, T.A.J. and Derbyshire, E.R. (2017) 'Takinib, a Selective TAK1 Inhibitor, Broadens the Therapeutic Efficacy of TNF- α Inhibition for Cancer and Autoimmune Disease', *Cell chemical biology*, 24(8), pp. 1029-1039.e7.
- Trifunović, J., Miller, L., Debeljak, Ž. and Horvat, V. (2015) 'Pathologic patterns of interleukin 10 expression--a review', *Biochemia medica*, 25(1), pp. 36-48.
- Tyler, S.R. and Bunyavanich, S. (2019) 'Leveraging -omics for asthma endotyping', *The Journal of allergy and clinical immunology*, 144(1), pp. 13-23.
- Uhlen, M., Bandrowski, A., Carr, S., Edwards, A., Ellenberg, J., Lundberg, E., Rimm, D.L., Rodriguez, H., Hiltke, T., Snyder, M. and Yamamoto, T. (2016) 'A proposal for validation of antibodies', *Nature Methods*, 13(10), pp. 823-827.
- van Amerongen, R. and Nusse, R. (2009) 'Towards an integrated view of Wnt signaling in development', *Development*, 136(19), pp. 3205-3214.
- van Caam, A., Madej, W., Garcia de Vinuesa, A., Goumans, M.J., Ten Dijke, P., Blaney Davidson, E. and van der Kraan, P. (2017) 'TGF β 1-induced SMAD2/3 and SMAD1/5 phosphorylation are both ALK5-kinase-dependent in primary chondrocytes and mediated by TAK1 kinase activity', *Arthritis research & therapy*, 19(1), pp. 112-017-1302-4.
- Van de Laar, E., Clifford, M., Hasenoeder, S., Kim, B.R., Wang, D., Lee, S., Paterson, J., Vu, N.M., Waddell, T.K., Keshavjee, S., Tsao, M.S., Ailles, L. and Moghal, N. (2014) 'Cell surface marker profiling of human tracheal basal cells reveals distinct subpopulations, identifies MST1/MSP as a mitogenic signal, and identifies new biomarkers for lung squamous cell carcinomas', *Respiratory research*, 15, pp. 160-014-0160-8.
- Van Gassen, G., De Jonghe, C., Nishimura, M., Yu, G., Kuhn, S., St George-Hyslop, P. and Van Broeckhoven, C. (2000) 'Evidence that the beta-catenin nuclear translocation assay allows for measuring presenilin 1 dysfunction', *Molecular medicine (Cambridge, Mass.)*, 6(7), pp. 570-580.
- Vanaki, S.M., Holmes, D., Saha, S.C., Chen, J., Brown, R.J. and Jayatilake, P.G. (2020) 'Muco-ciliary clearance: A review of modelling techniques', *Journal of Biomechanics*, 99, pp. 109578.
- Veerati, P.C., Mitchel, J.A., Reid, A.T., Knight, D.A., Bartlett, N.W., Park, J. and Grainge, C.L. (2020) 'Airway mechanical compression: its role in asthma pathogenesis and progression', *European Respiratory Review*, 29(157).
- Vesel, M., Rapp, J., Feller, D., Kiss, E., Jaromi, L., Meggyes, M., Miskei, G., Duga, B., Smuk, G., Laszlo, T., Karner, I. and Pongracz, J.E. (2017) 'ABCB1 and ABCG2 drug transporters are differentially expressed in non-small cell lung cancers (NSCLC) and expression is modified by cisplatin treatment via altered Wnt signaling', *Respiratory research*, 18(1), pp. 52-017-0537-6.

-
- Vignola, A.M., Chanez, P., Chiappara, G., Merendino, A., Pace, E., Rizzo, A., la Rocca, A.M., Bellia, V., Bonsignore, G. and Bousquet, J. (1997) 'Transforming growth factor-beta expression in mucosal biopsies in asthma and chronic bronchitis', *American journal of respiratory and critical care medicine*, 156(2 Pt 1), pp. 591-599.
- Vignola, A., Riccobono, L., Mirabella, A., Profita, M., Chanez, P., Bellia, V., Mautino, G., D'Accardi, P., Bousquet, J. and Bonsignore, G. (1998) 'Sputum Metalloproteinase-9/Tissue Inhibitor of Metalloproteinase-1 Ratio Correlates with Airflow Obstruction in Asthma and Chronic Bronchitis', *American Journal of Respiratory and Critical Care Medicine*, 158(6), pp. 1945-1950.
- Villar, J., Cabrera, N.E., Casula, M., Valladares, F., Flores, C., López-Aguilar, J., Blanch, L., Zhang, H., Kacmarek, R.M. and Slutsky, A.S. (2011: A) 'WNT/ β -catenin signaling is modulated by mechanical ventilation in an experimental model of acute lung injury', *Intensive care medicine*, 37(7), pp. 1201-1209.
- Villar, J., Cabrera, N.E., Valladares, F., Casula, M., Flores, C., Blanch, L., Quilez, M.E., Santana-Rodríguez, N., Kacmarek, R.M. and Slutsky, A.S. (2011: B) 'Activation of the Wnt/ β -catenin signaling pathway by mechanical ventilation is associated with ventilator-induced pulmonary fibrosis in healthy lungs', *PLoS one*, 6(9), pp. e23914.
- Villar, J., Cabrera-Benítez, N.E., Ramos-Nuez, A., Flores, C., García-Hernández, S., Valladares, F., López-Aguilar, J., Blanch, L. and Slutsky, A.S. (2014) 'Early activation of pro-fibrotic WNT5A in sepsis-induced acute lung injury', *Critical Care (London, England)*, 18(5), pp. 568-014-0568-z.
- Viñals, F. and Pouyssegur, J. (2001) 'Transforming growth factor beta1 (TGF-beta1) promotes endothelial cell survival during in vitro angiogenesis via an autocrine mechanism implicating TGF-alpha signaling', *Molecular and cellular biology*, 21(21), pp. 7218-7230.
- Vink, P.M., Smout, W.M., Driessen-Engels, L.J., de Bruin, A.M., Delsing, D., Krajnc-Franken, M.A., Jansen, A.J., Rovers, E.F., van Puijenbroek, A.A., Kaptein, A., Nolte, M.A., Garritsen, A. and van Eenennaam, H. (2013) 'In vivo knockdown of TAK1 accelerates bone marrow proliferation/differentiation and induces systemic inflammation', *PLoS one*, 8(3), pp. e57348.
- Vladar, E.K. and Königshoff, M. (2020) 'Noncanonical Wnt planar cell polarity signaling in lung development and disease', *Biochemical Society transactions*, 48(1), pp. 231-243.
- Wadsworth, S.J., Nijmeh, H.S. and Hall, I.P. (2006) 'Glucocorticoids increase repair potential in a novel in vitro human airway epithelial wounding model', *Journal of clinical immunology*, 26(4), pp. 376-387.
- Waljee, A.K., Rogers, M.A., Lin, P., Singal, A.G., Stein, J.D., Marks, R.M., Ayanian, J.Z. and Nallamothu, B.K. (2017) 'Short term use of oral corticosteroids and related harms among adults in the United States: population based cohort study', *BMJ (Clinical research ed.)*, 357, pp. j1415.
- Wallingford, J.B. and Mitchell, B. (2011) 'Strange as it may seem: the many links between Wnt signaling, planar cell polarity, and cilia', *Genes & development*, 25(3), pp. 201-213.
- Wan, H., Winton, H.L., Soeller, C., Stewart, G.A., Thompson, P.J., Gruenert, D.C., Cannell, M.B., Garrod, D.R. and Robinson, C. (2000) 'Tight junction properties of the immortalized human bronchial epithelial cell lines Calu-3 and 16HBE14o-', *The European respiratory journal*, 15(6), pp. 1058-1068.
- Wan, W.Y., Hollins, F., Haste, L., Woodman, L., Hirst, R.A., Bolton, S., Gomez, E., Sutcliffe, A., Desai, D., Chachi, L., Mistry, V., Szyndralewicz, C., Wardlaw, A., Saunders, R., O'Callaghan, C., Andrew, P.W. and Brightling, C.E. (2016) 'NADPH Oxidase-4

-
- Overexpression Is Associated With Epithelial Ciliary Dysfunction in Neutrophilic Asthma', *Chest*, 149(6), pp. 1445-1459.
- Wang, B., Tang, Z., Gong, H., Zhu, L. and Liu, X. (2017) 'Wnt5a promotes epithelial-to-mesenchymal transition and metastasis in non-small-cell lung cancer', *Bioscience reports*, 37(6), pp. 10.1042/BSR20171092. Print 2017 Dec 22.
- Wang, C., Cassandras, M. and Peng, T. (2019) 'The Role of Hedgehog Signaling in Adult Lung Regeneration and Maintenance', *Journal of developmental biology*, 7(3), pp. 14. doi: 10.3390/jdb7030014.
- Wang, C., Zhao, Y., Su, Y., Li, R., Lin, Y., Zhou, X. and Ye, L. (2013) 'C-Jun N-terminal kinase (JNK) mediates Wnt5a-induced cell motility dependent or independent of RhoA pathway in human dental papilla cells', *PLoS one*, 8(7), pp. e69440.
- Wang, P., Henning, S.M. and Heber, D. (2010) 'Limitations of MTT and MTS-based assays for measurement of antiproliferative activity of green tea polyphenols', *PLoS one*, 5(4), pp. e10202.
- Wawrzyniak, P., Wawrzyniak, M., Wanke, K., Sokolowska, M., Bendelja, K., Rückert, B., Globinska, A., Jakiela, B., Kast, J.I., Idzko, M., Akdis, M., Sanak, M. and Akdis, C.A. (2017) 'Regulation of bronchial epithelial barrier integrity by type 2 cytokines and histone deacetylases in asthmatic patients', *Journal of Allergy and Clinical Immunology*, 139(1), pp. 93.
- Weeden, C.E., Chen, Y., Ma, S.B., Hu, Y., Ramm, G., Sutherland, K.D., Smyth, G.K. and Asselin-Labat, M.L. (2017) 'Lung Basal Stem Cells Rapidly Repair DNA Damage Using the Error-Prone Nonhomologous End-Joining Pathway', *PLoS biology*, 15(1), pp. e2000731.
- Wells, R.G. (2013) 'Tissue mechanics and fibrosis', *Biochimica et Biophysica Acta (BBA) - Molecular Basis of Disease*, 1832(7), pp. 884.
- Wenzel, S.E. (2012) 'Asthma phenotypes: the evolution from clinical to molecular approaches', *Nature medicine*, 18(5), pp. 716-725.
- Wenzel, S.E. (2006) 'Asthma: defining of the persistent adult phenotypes', *Lancet (London, England)*, 368(9537), pp. 804-813.
- Whitsett, J.A. (2018) 'Airway Epithelial Differentiation and Mucociliary Clearance', *Annals of the American Thoracic Society*, 15(Suppl 3), pp. S143-S148.
- Winn, R.A., Marek, L., Han, S., Rodriguez, K., Rodriguez, N., Hammond, M., Van Scoyk, M., Acosta, H., Mirus, J., Barry, N., Bren-Mattison, Y., Van Raay, T.J., Nemenoff, R.A. and Heasley, L.E. (2005) 'Restoration of Wnt-7a expression reverses non-small cell lung cancer cellular transformation through frizzled-9-mediated growth inhibition and promotion of cell differentiation', *The Journal of biological chemistry*, 280(20), pp. 19625–19634.
- WNTresearch. (n.d.) BOX-5. Available at: <https://www.wntresearch.com/box-5/?lang=en> (Accessed: 30 October 2020).
- Wolsk, H.M., Harshfield, B.J., Laranjo, N., Carey, V.J., O'Connor, G., Sandel, M., Strunk, R.C., Bacharier, L.B., Zeiger, R.S., Schatz, M., Hollis, B.W., Weiss, S.T. and Litonjua, A.A. (2017) 'Vitamin D supplementation in pregnancy, prenatal 25(OH)D levels, race, and subsequent asthma or recurrent wheeze in offspring: Secondary analyses from the Vitamin D Antenatal Asthma Reduction Trial', *The Journal of allergy and clinical immunology*, 140(5), pp. 1423-1429.e5.

-
- Worthington, J.J., Klementowicz, J.E. and Travis, M.A. (2011) 'TGFbeta: a sleeping giant awoken by integrins', *Trends in biochemical sciences*, 36(1), pp. 47-54.
- Xiao, C., Puddicombe, S.M., Field, S., Haywood, J., Broughton-Head, V., Puxeddu, I., Haitchi, H.M., Vernon-Wilson, E., Sammut, D., Bedke, N., Cremin, C., Sones, J., Djukanovic, R., Howarth, P.H., Collins, J.E., Holgate, S.T., Monk, P. and Davies, D.E. (2011) 'Defective epithelial barrier function in asthma', *The Journal of allergy and clinical immunology*, 128(3), pp. 549-56.e1-12.
- Xiao, L., Du, Y., Shen, Y., He, Y., Zhao, H. and Li, Z. (2012) 'TGF-beta 1 induced fibroblast proliferation is mediated by the FGF-2/ERK pathway', *Frontiers in bioscience (Landmark edition)*, 17, pp. 2667-2674.
- Xie, M., Mustovich, A.T., Jiang, Y., Trudeau, J.B., Ray, A., Ray, P., Hu, H., Holguin, F., Freeman, B. and Wenzel, S.E. (2015) 'IL-27 and type 2 immunity in asthmatic patients: association with severity, CXCL9, and signal transducer and activator of transcription signaling', *The Journal of allergy and clinical immunology*, 135(2), pp. 386-394.
- Xiong, W.J., Hu, L.J., Jian, Y.C., Wang, L.J., Jiang, M., Li, W. and He, Y. (2012) 'Wnt5a participates in hepatic stellate cell activation observed by gene expression profile and functional assays', *World journal of gastroenterology*, 18(15), pp. 1745-1752.
- Xu, J., Lamouille, S. and Derynck, R. (2009) 'TGF-beta-induced epithelial to mesenchymal transition', *Cell research*, 19(2), pp. 156-172.
- Xu, W., Xu, B., Zhao, Y., Yang, N., Liu, C., Wen, G. and Zhang, B. (2015) 'Wnt5a reverses the inhibitory effect of hyperoxia on transdifferentiation of alveolar epithelial type II cells to type I cells', *Journal of physiology and biochemistry*, 71(4), pp. 823-838.
- Yamamizu, K., Matsunaga, T., Uosaki, H., Fukushima, H., Katayama, S., Hiraoka-Kanie, M., Mitani, K. and Yamashita, J.K. (2010) 'Convergence of Notch and beta-catenin signaling induces arterial fate in vascular progenitors', *The Journal of cell biology*, 189(2), pp. 325-338.
- Yang, G., Zhou, J., Teng, Y., Xie, J., Lin, J., Guo, X., Gao, Y., He, M., Yang, X. and Wang, S. (2014) 'Mesenchymal TGF- β Signaling Orchestrates Dental Epithelial Stem Cell Homeostasis Through Wnt Signaling', *Stem cells*, 32(11), pp. 2939-2948.
- Yang, L., Qiu, C.X., Ludlow, A., Ferguson, M.W. and Brunner, G. (1999) 'Active transforming growth factor-beta in wound repair: determination using a new assay', *The American journal of pathology*, 154(1), pp. 105-111.
- Yang, X., Li, H., Ma, Q., Zhang, Q. and Wang, C. (2018) 'Neutrophilic Asthma Is Associated with Increased Airway Bacterial Burden and Disordered Community Composition', *BioMed Research International*, 2018, pp. 9230234.
- Yao, L., Sun, B., Zhao, X., Zhao, X., Gu, Q., Dong, X., Zheng, Y., Sun, J., Cheng, R., Qi, H. and An, J. (2014) 'Overexpression of Wnt5a promotes angiogenesis in NSCLC', *BioMed research international*, 2014, pp. 832562.
- Yao, Y., Chang, W., He, L., Jin, Y. and Li, C. (2016) 'An updated meta-analysis of transforming growth factor- β 1 gene: Three well-characterized polymorphisms with asthma', *Human immunology*, 77(12), pp. 1291.
- Ye, H., Cai, P., Zhou, Q. and Ma, W. (2011) 'Transforming growth factor- β 1 suppresses the up-regulation of matrix metalloproteinase-2 by lung fibroblasts in response to tumor necrosis factor- α ', *Wound Repair and Regeneration*, 19(3), pp. 392-399.

-
- Yu, B., Jiang, K. and Zhang, J. (2018) 'MicroRNA-124 suppresses growth and aggressiveness of osteosarcoma and inhibits TGF- β -mediated AKT/GSK-3 β /SNAIL-1 signaling', *Molecular medicine reports*, 17(5), pp. 6736-6744.
- Yu, Q. and Stamenkovic, I. (2000) 'Cell surface-localized matrix metalloproteinase-9 proteolytically activates TGF-beta and promotes tumor invasion and angiogenesis', *Genes & development*, 14(2), pp. 163-176.
- Yu, Z., Jiang, Y. and Sun, C. (2020) 'Glucocorticoids inhibits the repair of airway epithelial cells via the activation of wnt pathway', *Respiratory Physiology & Neurobiology*, 271, pp. 103283.
- Yuan, S.B., Ji, G., Li, B., Andersson, T., Neugebauer, V. and Tang, S.J. (2015) 'A Wnt5a signaling pathway in the pathogenesis of HIV-1 gp120-induced pain', *Pain*, 156(7), pp. 1311-1319.
- Zhang, Y., Zhang, J., Huang, J., Li, X., He, C., Tian, C., Peng, C., Guo, L., Xiao, Y. and Fan, H. (2010) 'Polymorphisms in the transforming growth factor-beta1 gene and the risk of asthma: A meta-analysis', *Respirology (Carlton, Vic.)*, 15(4), pp. 643-650.
- Zhang, Y.E. (2017) 'Non-Smad Signaling Pathways of the TGF- β Family', *Cold Spring Harbor perspectives in biology*, 9(2), pp. a022129. doi: 10.1101/cshperspect.a022129.
- Zhao, J., Bu, D., Lee, M., Slavkin, H.C., Hall, F.L. and Warburton, D. (1996) 'Abrogation of transforming growth factor-beta type II receptor stimulates embryonic mouse lung branching morphogenesis in culture', *Developmental biology*, 180(1), pp. 242-257.
- Zheng, L. and Conner, S.D. (2018) 'Glycogen synthase kinase 3beta inhibition enhances Notch1 recycling', *Molecular biology of the cell*, 29(4), pp. 389-395.
- Zhou, S., Eid, K. and Glowacki, J. (2004) 'Cooperation between TGF-beta and Wnt pathways during chondrocyte and adipocyte differentiation of human marrow stromal cells', *Journal of bone and mineral research : the official journal of the American Society for Bone and Mineral Research*, 19(3), pp. 463-470.
- Zhou, X., Hu, H., Huynh, M.L., Kotaru, C., Balzar, S., Trudeau, J.B. and Wenzel, S.E. (2007) 'Mechanisms of tissue inhibitor of metalloproteinase 1 augmentation by IL-13 on TGF-beta 1-stimulated primary human fibroblasts', *The Journal of allergy and clinical immunology*, 119(6), pp. 1388-1397.
- Zhu, M., Li, J.S., Tian, D., Ma, Y., Li, N.P. and Wu, R.L. (2007) 'Spatial-temporal distribution of glycogen synthase kinase 3beta and adenomatous polyposis coli protein are involved in the injury and repair of airway epithelial cells induced by scratching', *Sheng li xue bao : [Acta physiologica Sinica]*, 59(2), pp. 197-203.
- Zhu, S., Liu, L., Korzh, V., Gong, Z. and Low, B.C. (2006) 'RhoA acts downstream of Wnt5 and Wnt11 to regulate convergence and extension movements by involving effectors Rho Kinase and Diaphanous: Use of zebrafish as an in vivo model for GTPase signaling', *Cellular signalling*, 18(3), pp. 359.